

University of Mississippi

eGrove

Electronic Theses and Dissertations

Graduate School

1-1-2020

Chemical And Biological Evaluations Of Asimina Triloba And Rollinia Mucosa.

Taghreed Ali Majrashi

Follow this and additional works at: <https://egrove.olemiss.edu/etd>

Recommended Citation

Majrashi, Taghreed Ali, "Chemical And Biological Evaluations Of Asimina Triloba And Rollinia Mucosa." (2020). *Electronic Theses and Dissertations*. 1815.

<https://egrove.olemiss.edu/etd/1815>

This Dissertation is brought to you for free and open access by the Graduate School at eGrove. It has been accepted for inclusion in Electronic Theses and Dissertations by an authorized administrator of eGrove. For more information, please contact egrove@olemiss.edu.

CHEMICAL AND BIOLOGICAL EVALUATIONS OF *ASIMINA TRILOBA* AND *ROLLINIA*
MUCOSA

A Dissertation
presented in partial fulfillment of requirements
for the degree of Doctor of Philosophy in Pharmaceutical Sciences
Department of BioMolecular Sciences, Division of Pharmacognosy
The University of Mississippi

by

Taghreed Ali Jobran Majrashi

May 2020

Copyright © 2020 by Taghreed A. Majrashi

All rights reserve

ABSTRACT

Studies have shown the potential risks of neurodegeneration associated with chronic consumption of plants of the Annonaceae family, which emphasize the need for further studies to identify the neurotoxic compounds in the edible annonaceous plants and compare their risk to their benefits in defeating cancer. Our study is focused on the alkaloidal constituents of two plants from the Annonaceae family, *Asimina triloba* and *Rollinia mocusa*. This study was carried out to explore the anticancer and neurotoxic constituents of the plants with the intention that separating neurotoxic constituents would help in reducing the undesirable effects of the plants if it is used as an alternative therapy.

Chapter II describes the phytochemical investigation of the alkaloids from *Asimina triloba* twigs that yielded one new aporphine glycoside, (-)-anolobine-9-O- β -D-glucopyranoside **1**, along with seven known isoquinoline alkaloids, anolobine **2**, nornuciferine **3**, norushinsunine **4**, liriodenine **5**, lysicamine **6**, stepharine **7**, and coclaurine **8**. Alkaloids **3** and **6-8** are reported for the first time from this plant.

In chapter III, the structural characteristics of eight alkaloids from methanolic extracts of dried twigs of *Asimina triloba* have been studied using UHPLC-QToF-MS in positive ion mode. This study described an investigation of the fragmentation pathways leading to the identification of key diagnostic fragment ions for the annonaceous alkaloids.

Chapter IV demonstrates the anticancer potential and the neurotoxicity of the isolated alkaloids from *Asimina triloba* twigs. Six alkaloids (anolobine-9-O- β -D-glucopyranoside, anolobine, norushinsunine, liriodenine, squamolone and coclaurine) were evaluated for their anticancer potential in four human solid tumor cell lines (SK-MEL, KB, BT-549, and SK-OV-3). The potential for neurotoxicity was determined using rat cortical neurons. Three extracts, namely crude methanolic extract, alkaloids rich extract, and acetogenins rich extract, were also included in the study to explore how the presence and the absence of the alkaloids or acetogenins will affect the anticancer activity and neurotoxicity of this plant. This is the first report of anticancer activity and the neurotoxic effect of the alkaloidal constituents of *Asimina triloba*.

Finally, chapter V describes the total synthesis of (\pm) anonaine, 3,4-methylenedioxy-1-phenanthreneethylamine, (\pm) romucosine, and [2-(3,4-methylenedioxy-1-phenanthrenyl)ethyl]-methylcarbamate by using direct arylation reactions with 3,4-methylenedioxyphenethylamine **1** and 2-bromophenylacetic acid **2** in the preparation of aporphine analogues. The presence of the synthesized compounds in *Rollinia mucosa* seeds and fruits was verified through the analytical technique using UHPLC-QToF-MS. All synthesized compounds were subjected to the biological evaluation to understand how they induce or reduce the cytotoxicity as well as neurotoxicity.

Improved accuracy and precision of the bioactive marker compounds and natural toxins in the edible plants, dietary supplement, and natural health products will be helpful to the regulatory agencies.

DEDICATION

This dissertation is dedicated in memory of my father, Ali Majrashi, who always believed in me and always told me that I'm capable of doing anything I set my mind to.

LIST OF ABBREVIATIONS

THF	Tetrahydrofuran
ACGs	Acetogenins
NADH	Nicotinamide Adenine Dinucleotide (NAD) + hydrogen (H)
ATP	Adenosine triphosphate
HRESI-MS	High Resolution Electrospray Ionization Mass Spectroscopy
NMR	Nuclear Magnetic Resonance
DEPT	Distortionless Enhancement by Polarization Transfer
HMBC	Heteronuclear Multiple Bond Correlation
CD	Circular Dichroism
CE	Cotton Effect
TLC	Thin Layer Chromatography
UV/Vis	Ultraviolet–visible
IR	Infrared Spectroscopy
UHPLC-QToF	Ultra-High-Performance Liquid Chromatography- Quadrupole Time-of-Flight Mass Spectrometry
QToF-MS	Quad Time-of-Flight Mass Spectrometry
ESI	Electrospray Ionization
<i>m/z</i>	Mass-to-Charge Ratio

Da	Dalton
mL	Milliliter
TFA	Trifluoroacetic Acid
RMFM	<i>Rollinia mucosa</i> Fruits Methanolic Extract
Non-ALK-F	Non-Alkaloids Fruits Extract
ALK-F	Fruits Alkaloidal Extract
RMSM	<i>Rollinia mucosa</i> Seeds Methanolic Extract
Non-ALK-S	Non-Alkaloids Seeds Extract
ALK-S	Seeds Alkaloidal Extract
°C	Degrees Celsius
µg	Microgram
IC ₅₀	Inhibitory Concentration, 50%

ACKNOWLEDGEMENTS

I am grateful to all of those with whom I have had the pleasure to work during my time at the University of Mississippi. I would like to thank my amazing advisor, Dr. Ikhlas Khan, Director of the National Center for Natural Products Research, Distinguished Professor of Pharmacognosy, for his invaluable guidance, encouragement, and for giving me the wonderful opportunity to work in his group.

I am thankful for the members of my Dissertation Committee, Dr. Samir Ross, Dr. David Colby, and Dr. Cole Stevens, who provided me extensive personal and professional guidance. I would like to express my sincere appreciation to Dr. Amar Chittiboyina and Dr. Zulfiqar Ali for their support, guidance, and constant help in my research work.

I am genuinely thankful to Dr. Shabana Khan for her kindness, support, guidance, and for the friendly and welcoming atmosphere that she created around her. I would like to thank her for running the anticancer assays and for being available all the time I needed to discuss data with her.

Special thanks to Dr. Nicole Ashpole and Dr. Bharathi Avula for their contributions, time, and effort, who added more value to this work by their scientific collaborations.

I also present my appreciation to my friends and my colleagues who have been part of my life and who have supported and encouraged me during my studies.

Most importantly, I wish to thank my loving and supportive husband, Abdullah, and my amazing daughter, Tulin, who have always faith in me and provide unending inspiration. I could not have achieved what I have without their love and support.

My sincere appreciation goes to my mom and my siblings, who have provided me with unquestionable love and encouragement for the whole of my life. Their prayers and wishes were always warm my heart and gave me the strength to persevere.

A special appreciation to the Saudi Arabian Cultural Mission (SACM) and King Khalid University for the scholarship that I received and the grant I was awarded, which allowed me to pursue this research.

TABLE OF CONTENTS

ABSTRACT.....	II
DEDICATION.....	IV
LIST OF ABBREVIATIONS.....	V
ACKNOWLEDGEMENTS.....	VII
TABLE OF CONTENTS.....	IX
LIST OF FIGURES.....	XIV
LIST OF SCHEMES.....	XVII
LIST OF TABLES.....	XVIII
CHAPTER I.....	1
INTRODUCTION.....	1
1. MAGNOLIALES.....	1
2. THE FAMILY ANNONACEAE.....	3
3. ANNOACEOUS ACETOGENINS.....	4

4. ANNONACEOUS ALKALOIDS	6
5. OVERALL AIMS.....	8
CHAPTER II.....	13
ISOQUINOLINE ALKALOIDS FROM <i>ASIMINA TRILOBA</i>	13
1. INTRODUCTION.....	13
2. RESULTS AND DISCUSSION	15
3. EXPERIMENTAL	19
3.1. Apparatus and reagents	19
3.2. Plant material	19
3.3. Extraction and Isolation	19
4. CONCLUSION.....	24
CHAPTER II COPYRIGHT.....	25
CHAPTER III	26
TARGETED ANALYSIS OF ANNONACEOUS ALKALOIDS FROM <i>ASIMINA TRILOBA</i> USING UHPLC-QTOF-MS.....	26
1. INTRODUCTION.....	26
2. EXPERIMENTAL APPROACH	28
3. PLANT MATERIALS	29

4. STANDARDS AND PLANT SAMPLE PREPARATION	29
5. INSTRUMENTATION AND ANALYTICAL CONDITIONS	30
5.1. Ultra-High-Performance Liquid Chromatography-Quadrupole Time of Flight-Mass Spectrometry (UHPLC/QToF-MS)	30
5.2. Data analysis.....	32
6. RESULTS AND DISCUSSION	32
6.1. BENZYLISOQUINOLINE ALKALOIDS	35
6.2. PROAPORPHINE ALKALOIDS	37
6.3. APORPHINE ALKALOIDS	38
6.4. OXOAPORPHINE ALKALOIDS	41
7. CONCLUSION.....	49
CHAPTER III COPYRIGHT	50
CHAPTER IV	51
CYTOTOXIC AND NEUROTOXIC POTENTIAL OF ALKALOIDAL CONSTITUENTS OF <i>ASIMINA TRILOBA</i>	51
1. INTRODUCTION.....	51
2. MATERIALS AND METHODS	53
2.1. PLANT MATERIAL	53
2.2. CYTOTOXICITY ASSAY	54
2.3. NEURONS ISOLATION.....	55

2.4. NEUROTOXICITY ASSAY	56
2.5. STATISTICAL ANALYSIS	56
3. RESULTS.....	56
3.1. CYTOTOXICITY	56
3.2. NEUROTOXICITY	59
4. DISCUSSION.....	64
5. CONCLUSION.....	65
CHAPTER V	67
SYNTHESIS OF SOME ALKALOIDS REPORTED FROM <i>ROLLINIA MUCOSA</i> AND EVALUATION OF THEIR BIOLOGICAL ACTIVITIES	67
1. INTRODUCTION.....	67
2. RESULT AND DISCUSSION.....	69
2.1. SYNTHESIS	69
2.2. ESI-QToF-MS OF REFERENCE STANDARDS	73
2.3. TARGETED ANALYSIS OF <i>ROLLINIA MUCOSA</i> USING UHPLC-QToF-MS	74
2.4. ANTICANCER	76
2.5. NEUROTOXICITY	80
3. MATERIALS AND METHODS	85
3.1. GENERAL EXPERIMENTAL PROCEDURES OF THE SYNTHESIS	85

3.2. ULTRA-HIGH-PERFORMANCE LIQUID CHROMATOGRAPHY-QUADRUPOLE TIME OF FLIGHT- MASS SPECTROMETRY (UHPLC/QToF-MS)	85
3.3. Mass Data analysis	87
3.4. PLANT MATERIAL	88
3.5. ALKALOIDS EXTRACTION	88
3.6. ANTICANCER ASSAY.....	88
3.7. NEUROTOXICITY ASSAY	89
3.8. STATISTICAL ANALYSIS	90
4. EXPERIMENTAL	90
4.1. SYNTHESIS OF COMPOUNDS 3-9.....	90
4.2. ENANTIOMERS RESOLUTION	95
4.2.1. <i>THE RECYCLING PROCESS OF RESOLUTION USING DIBENZOYL TARTARIC ACID.</i>	95
4.2.2. <i>THE ENANTIOMERS RESOLUTION WITH (-)(1R)-MENTHYL CHLOROFORMATE.</i>	96
5. CONCLUSION.....	97
 BIBLIOGRAPHY.....	 99
 APPENDIX.....	 114
 VITA.....	 185

LIST OF FIGURES

Figure 1-1 The six families of Magnoliales order and their genus and species.....	2
Figure 1- 2 Core units for classification of Annonaceous acetogenins (Alali et al., 1999)	5
Figure 1- 3 The chemical structure of uvaricin.....	6
Figure 1- 4 A) simple isoquinolines, B) bisbenzylisoquinolines,.....	7
Figure 1- 5 Previously reported alkaloids from <i>Asimina triloba</i>	10
Figure 2- 1 Structures of isolated alkaloids from <i>Asimina triloba</i>	14
Figure 2- 2 Key HMBC (\rightarrow) and COSY (\blackrightarrow) correlations of 1	16
Figure 2- 3 CD spectra of anolobine-9- <i>O</i> - β -D-glucopyranoside 1 and its aglycone (anolobine 2)	17
Figure 2- 4 CD spectrum of stepharine (7)	18
Figure 2- 5 CD spectrum of coclaurine (8).....	18
Figure 2- 6 Anolobine-9- <i>O</i> - β -D-glucopyranoside (1)	21
Figure 3- 1 ESI-MS _n spectrum of coclaurine.....	36
Figure 3- 2 Tentative fragmentation pathways of the coclaurine	36
Figure 3- 3 ESI-MS _n spectrum of stepharine	37
Figure 3- 4 Tentative fragmentation pathways of the stepharine.	38
Figure 3- 5 ESI-MS _n spectrum of nornuciferine.....	39

Figure 3- 6 Tentative fragmentation pathways of the nornuciferine	39
Figure 3- 7 ESI-MS _n spectrum of lysicamine	40
Figure 3- 8 Tentative fragmentation pathways of the lysicamine.....	41
Figure 3- 9 ESI-MS _n spectrum of liriodenine	42
Figure 3- 10 Tentative fragmentation pathways of the liriodenine.....	43
Figure 3- 11 ESI-MS _n spectrum of norushinsunine	43
Figure 3- 12 Tentative fragmentation pathways of the norushinsunine	44
Figure 3- 13 ESI-MS _n spectrum of anolobine.....	44
Figure 3- 14 Tentative fragmentation pathways of the anolobine	45
Figure 3- 15 ESI-MS _n spectrum of anolobine-9- <i>O</i> -β-D-glucopyranoside.....	46
Figure 3- 16 Tentative fragmentation pathways of the anolobine-9- <i>O</i> -β-D-glucopyranoside	47
Figure 4- 1 Chemical structures of alkaloids from <i>Asimina triloba</i>	54
Figure 4- 2 Effect of the MeOH extract, ACG extract and ALK extract on neuronal cell viability.	60
Figure 4- 3 Effect of anolobine-9- <i>O</i> -β-D-glucopyranoside, anolobine and coclaurine on neuronal cell viability.	61
Figure 4- 4 Effect of norushinsunine, liriodenine and squamolone on neuronal cell viability.....	62
Figure 4- 5 Effect of Extracts and pure compounds on cell viability at 10 μg/mL. Asterisks designate statistically significant decreases in cell viability compared to vehicle control.	63

Figure 5- 1 Synthesized alkaloids from <i>Rollinia mucosa</i>	76
Figure 5- 2 Effect of RMSM, Non-ALK-S, and ALK-S extracts on neuronal cell viability.....	81
Figure 5- 3 Effect of RMFM, Non-ALK-F, and ALK-F extracts on neuronal cell viability.....	82
Figure 5- 4 Effect of compounds 6-9 on neuronal cell viability.....	83
Figure 5- 5 Effect of extracts and synthesized compounds 6-9 on cell viability at 20 µg/mL. Asterisks designate statistically significant decreases in cell viability compared to vehicle control.	84

LIST OF SCHEMES

Scheme 1. <i>Bischler-Napieralski</i> reaction, and Boc protection reaction.	70
Scheme 2. Direct intramolecular arylation, and Boc deprotection.	70
Scheme 3. Preparation of romucosine and [2-(3,4-methylenedioxy-1-phenanthrenyl)ethyl]- methylcarbamate.	71
Scheme 4. The enantiomers resolution of 3 with (-) (1 <i>R</i>)-menthyl chloroformate.....	72

LIST OF TABLES

Table 2- 1 ¹ H and ¹³ C NMR data of anolobine-9- <i>O</i> - β -D-glucoopyranoside (1) (DMSO-d ₆ , 500 MHz/150 MHz).....	22
Table 3- 1 Accurate mass data, fragment ions for the alkaloids of Annonaceae family using UHPLC Q-ToF.....	33
Table 3- 2 Accurate mass data, fragment ions for the alkaloids of Annonaceae family using UHPLC Q-ToF.....	34
Table 3- 3 Targeted analysis of <i>As. triloba</i> plant parts using UHPLC-QToF-MS	48
Table 4- 1 Anti-cell proliferative activity of extracts and compounds against a panel of cell lines.	58
Table 5- 1 Accurate mass data, fragment ions for compounds 6-9 using UHPLC Q-ToF.....	74
Table 5- 2 Targeted analysis of <i>R. mucosa</i> fruits and seeds extracts using UHPLC-QToF-MS ..	75
Table 5- 3 Anti-cell proliferative effects of compounds 6-9.	77
Table 5- 4 Anti-cell proliferative activity of <i>Rollinia mucosa</i> extracts against a panel of cell lines.	79

CHAPTER I

INTRODUCTION

1. Magnoliales

The order Magnoliales consists of six families (Annonaceae, Eupomatiaceae, Degeneriaceae, Himantandraceae, Magnoliaceae, and Myristicaceae) (Soltis et al., 2004) (**Figure 1-1**). Among all the six families, the Annonaceae and Magnoliaceae are the most studied families. The family of Eupomatiaceae consists of the single genus, *Eupomatia*, with three species (*Eupomatia bennettii* F. Muell., *Eupomatia laurina* R. Br., and *Eupomatia barbata* Jessup) of shrubs and trees occurring in tropical to temperate rainforests of Australia and New Guinea (Kim et al., 2005). The family of Degeneriaceae has a single genus *Degeneria*, which is endemic to Fiji (Cambie et al., 1992). Himantandraceae family also consists of a single genus, with one species, called *Galbulimima* F.M. Bailey, which is found in Australia, New Guinea, and Indonesia (Brophy et al., 2005). The family Myristicaceae is comprised of 20 genera and nearly 500 species, which are a medium-sized family of angiosperm trees with a wide pan-tropical distribution (Sauquet 2003). The family Magnoliaceae consists of 12 genera and about 220 species of woody trees and shrubs. The genera *Magnolia* (incl. *Talauma*), *Liriodendron*, *Michelia*, and *Aromadendron* have been used in traditional folk medicine in Asia and North America (Schühly et al., 2001). The Magnoliaceae contain secondary metabolites such as phenolic compounds, sesquiterpene lactones, monoterpenes, and alkaloids, some with considerable *in vitro* bioactivities (Kelm and Nair 2000; Son et al. 2000; Talapatra et al. 1982).

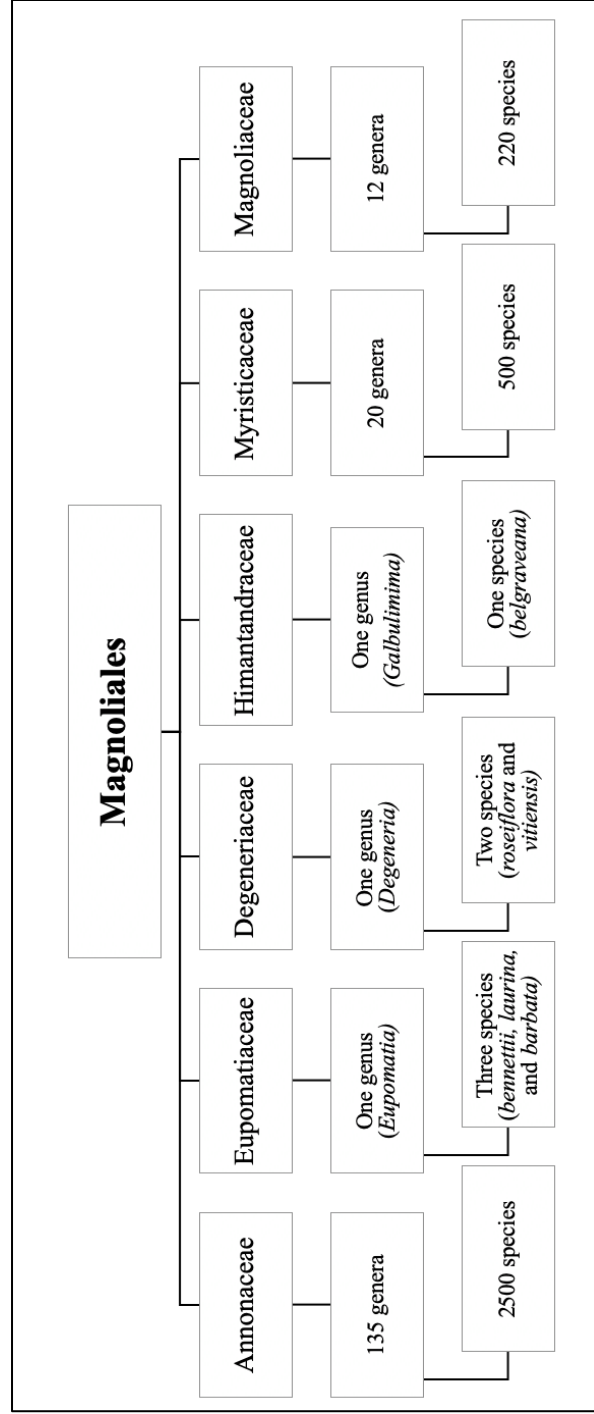


Figure 1-1 The six families of Magnoliales order and their genus and species.

2. The family Annonaceae

The Annonaceae, also called the custard apple family, is the largest family in the Magnoliales order. This family comprises of 135 genera and nearly 2500 species. Annonaceae are predominantly grown in tropical and subtropical forests, except the *Asimina* genus that extends into temperate regions. (Rabêlo et al. 2014). Some of the Annonaceae species are important in folk medicine in treating various tumors and cancers. Also, many of them have valuable economic importance as a source of large and pulpy edible fruits, such as pawpaw (*Asimina triloba*), *Annona cherimolia*, *Annona squamosa*, *Annona muricata*, and *Rollinia mucosa* that are cultivated in many countries (Rasai et al., 1995).

Furthermore, several Annonaceae plants are marketed as dietary supplements that promote overall health. Among the dietary supplements, products that contain twig extracts of pawpaw (*Asimina triloba* L. Dunal), e.g., Pawpaw Cell-Reg, or graviola (*Annona muricata*) are reported to exhibited antitumor efficacy both in animal models and some clinical studies (McLaughlin et al. 2003).

Annonaceae plants contain a broad spectrum of biologically active acetogenins that have been used for the treatment of different medical conditions. The acetogenins give Annonaceae plants unique characteristics as anticancer, antioxidant, and anti-HIV agents at very low concentrations with fewer side effects (Bermejo et al., 2005; McLaughlin 2008; Moghadamtousi et al., 2015). Also, Annonaceae plants contain different alkaloids that are derived from isoquinoline class including, benzyl-tetrahydroisoquinolines, protoberberines, proaporphines, aporphines, oxoaporphines, and other miscellaneous alkaloids. Annonaceae alkaloids play critical roles in folk treatments, and they possess anticancer, anti-bacterial, anti-inflammatory, and anti-protozoal activities (Lúcio et al., 2015).

Furthermore, other different compounds have been isolated from Annonaceae plants, including a number of flavonoids, some with the antioxidant activities (Gonda et al., 2000; Ouattara et al., 2011). However, most of the literature are mainly focusing on the annonaceous acetogenins and alkaloids, which have displayed a broad array of pharmacological effects and are being clinically evaluated for the treatment of different diseases.

3. Annonaceous acetogenins

Annonaceous acetogenins are long-chain fatty acids (C32 or C34) that have been combined with a terminal aliphatic side chain connecting to some hydrophilic functional groups, such as one to three THF rings and several hydroxy groups. Biogenetically, they are derived from the polyketide pathway. Annonaceous acetogenins were previously classified in terms of two major structural factors, the terminal γ -lactone ring and the substituents on the long aliphatic chain into: linear ACGs, epoxy ACGs, mono-tetrahydrofuran ACGs, *bis*-tetrahydrofuran and other miscellaneous ACGs (**Figure 1-2**) (Alali et al., 1999; Zafra-Polo et al., 1998).

In 1982, the first discovery of the acetogenins, uvaricin, which was isolated from the root of *Uvaria accuminata* by a group of scientists at the University of Arizona. Uvaricin (**Figure 1-3**) demonstrated significant activity toward the P-388 lymphocytic leukemia in mice (Jolad et al., 1982). Since then, ACGs have attracted significant scientific interest and more than 500 ACGs isolated and identified from different Annonaceae plants.

The Annonaceous acetogenins are potent inhibitors of complex I (NADH: ubiquinone oxidoreductase) of the mitochondrial electron transport systems, and they are potent inhibitors of NADH oxidase of the plasma membranes of cancer cells. Complex I plays an essential role in the maintenance of the bioenergetic function of the cell by driving the adenosine triphosphate (ATP)

synthesis from the mitochondrial reducing equivalents produced in the central metabolic oxidative pathways, which induces tumor cell apoptosis (programmed cell death) (Degli et al., 1994).

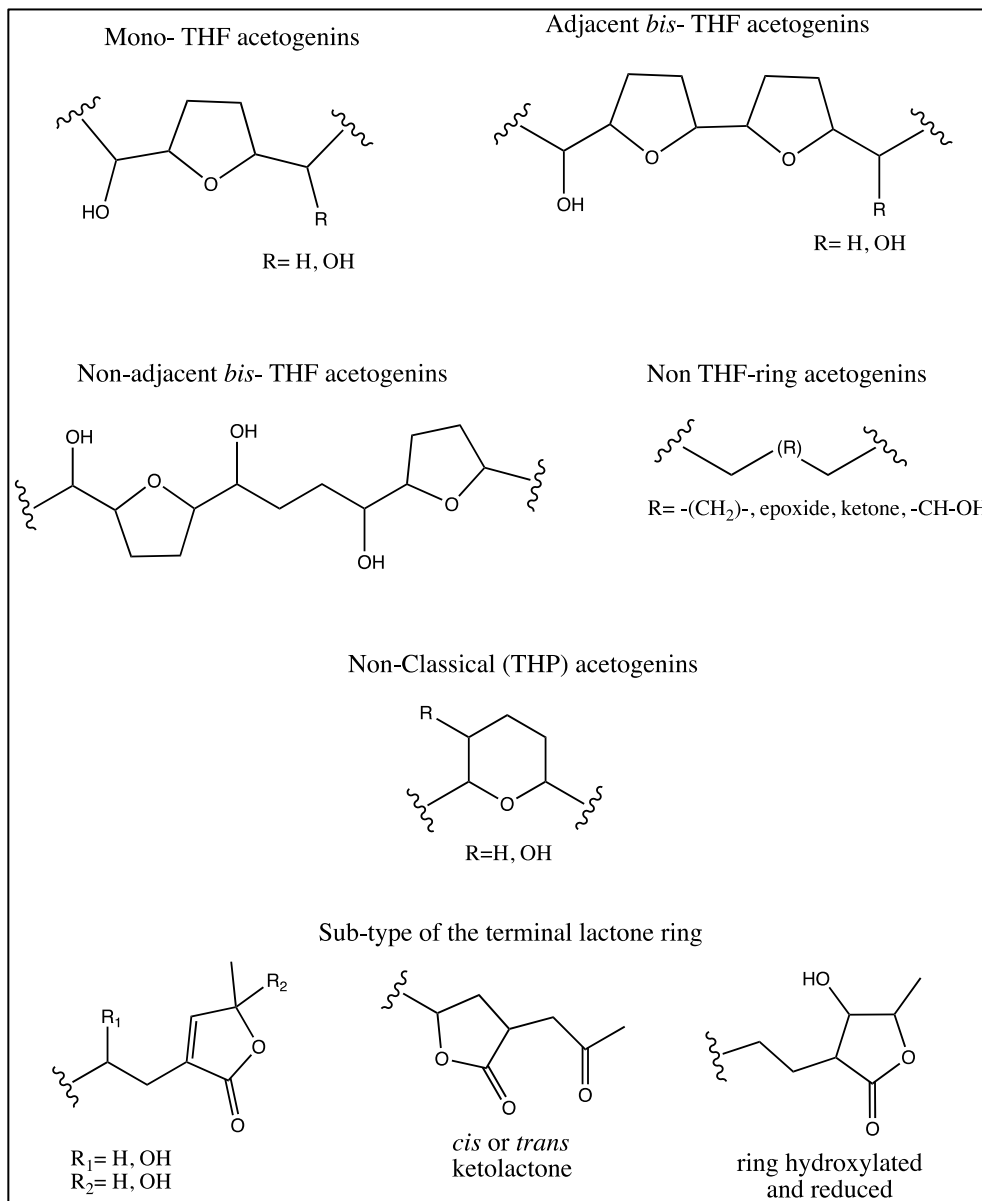


Figure 1- 2 Core units for classification of Annonaceous acetogenins (Alali et al., 1999)

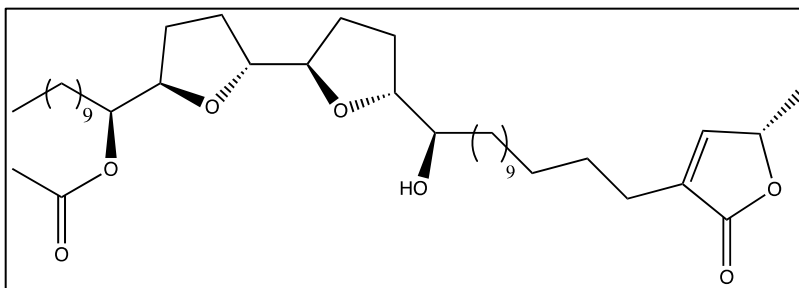


Figure 1- 3 The chemical structure of uvaricin

Annonaceous acetogenins have been found to display a broad range of biological activities, such as antitumor, antimalarial, anthelmintic, pesticidal, antiviral, and antimicrobial effects (Alali et al., 1998; Coothankandaswamy et al., 2010; McLaughlin 2008; Pomper et al., 2009). Among the broad array of biological activities reported in the biomedical literature for the AGEs, their antitumor and cytotoxic effects have received the most attention.

4. Annonaceous alkaloids

Annonaceae plants contain Approximately 800 alkaloids that derived from isoquinoline class, including simple isoquinolines, benzyltetrahydroisoquinolines, bisbenzylisoquinolines, protoberberines, proaporphines, aporphinoids, oxoaporphines, phenanthrenes, and other miscellaneous isoquinoline-type alkaloids (Lúcio et al., 2015) (**Figure 1-4**). The isoquinoline alkaloids are a large group of important secondary metabolites that have significant pharmacological importance. Many have been used extensively in folk medicine.

Annonaceous alkaloids possess diverse biological activities such as cytotoxicity (Wu et al., 1995), antiplatelet aggregation activity (Chen et al., 1996), cardiovascular activity (Lin et al., 1994) and antimicrobial activity (Ko et al., 1993).

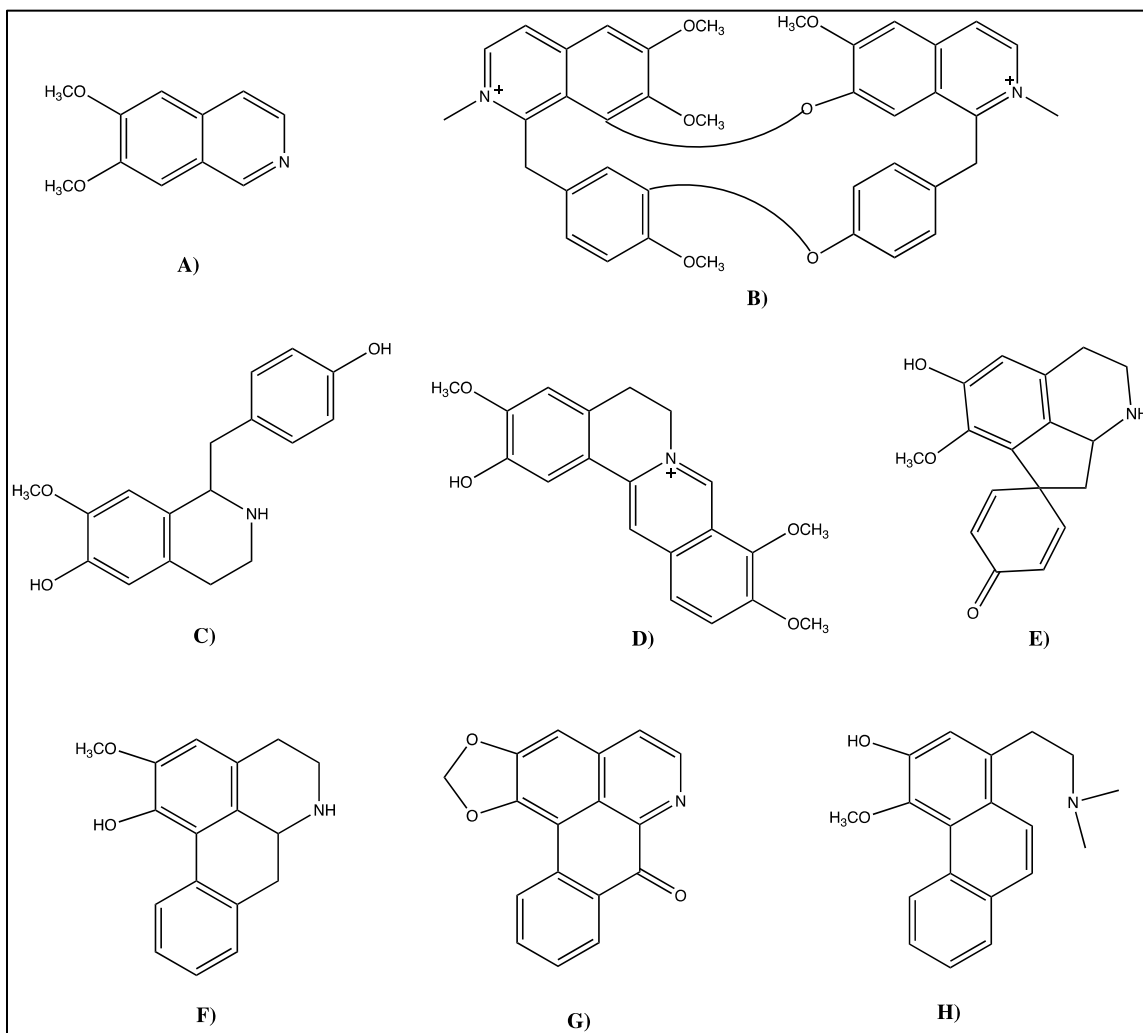


Figure 1- 4 A) simple isoquinolines, B) bisbenzylisoquinolines,
 C) benzyltetrahydroisoquinolines, D) protoberberines, E) proaporphines,
 F) aporphinoids, G) oxoaporphines, and H) phenanthrenes

The anticancer effects of isoquinoline alkaloids are mainly related to their effect on cell cycle arrest and DNA damage. Anonaine, an aporphine alkaloids, was reported to cause DNA damage associated with increased intracellular nitric oxide, ROS, glutathione (GSH) depletion, disruptive mitochondrial transmembrane potential, activation caspase 3, 7, 8 & 9 and poly ADP ribose polymerase cleavage in human cervical cancer cell (HeLa) (Chen et al., 2008). Furthermore, this alkaloid up-regulates the protein expression of p53 and Bax (Chen et al., 2008).

Also, studies have shown that liriodenine, an oxoaporphines, has induced apoptosis in CAOV-3 cells via the mitochondrial signaling pathway by the involvement of caspase-3 and caspase-9, inhibiting the proliferation of CAOV-3 cells (Nordin et al., 2015). Annonamine, asimilobine, isolaureline, and (s)-narcorydine are aporphine alkaloids that have isolated from Annonaceae plants and have demonstrated anticancer activities as well (Coria-Téllez et al., 2018). Therefore, isoquinoline alkaloids, especially the aporphine type, are a promising potential drug candidate for the treatment of cancer.

5. Overall aims

In spite of the success of some Annonaceae plants in the anticancer activity further environmental lipophilic complex I inhibitors have been studied in different Annonaceae plants and were found to cause decreased ATP levels in neuronal cell and redistribution of phosphorylated tau protein from axons to the cell body, causing neuronal cell death (Paul et al., 2013). Epidemiological studies have linked the consumption of Annonaceae plants to a high prevalence of atypical parkinsonism in Guadeloupe (Stamelou et al., 2010; Escobar-Khondiker et al., 2007). The potential risks of neurodegeneration associated with chronic consumption of the fruits and tea leaves from Annonaceae plants emphasize the need for further studies to determine

and identify the neurotoxic compounds in the edible annonaceous plants and compare their risk to their benefits in defeating cancer.

Among the annonaceous plants, *Asimina triloba* (pawpaw) is one of the most efficient Annonaceae plant species that can specifically interrupt the biochemistry of cancer cells, and its extract has been found to be the most potent of more than 3000 species of higher plants screened for bioactive compounds (McLaughlin 2008). It is the only species of Annonaceae with edible fruits that grow in the temperate region and are native to North America (Brannan et al., 2018). Pawpaw and many other Annonaceae plants are mainly consumed either as fresh fruits or processed into ice creams, juices, liquors, and many other products. Moreover, its extract has shown effective pesticidal and anticancer properties (Callaway et al., 1992). It is also currently marketed as a dietary supplement for its potential use in alternative anticancer medicine.

This study focused on *Asimina triloba* specifically on its alkaloids constituents due to the lack of studies on the isolation and identification of the alkaloids in this plant, only eight alkaloids have previously reported from *Asimina triloba* (**Figure 1-5**) (Tomita et al. 1965; Zhao et al. 1993).

Moreover, our study concentrated on the alkaloidal constituents of *Rollinia mucosa* by synthesizing some of its characteristic alkaloids and identify their biological benefits and safety. Our central hypothesis is that the alkaloidal extract and pure alkaloids contribute to the cytotoxicity of the *Asimina triloba* and *Rollinia mucosa*, and their presence would be a reason for the neurotoxicity of these plants.

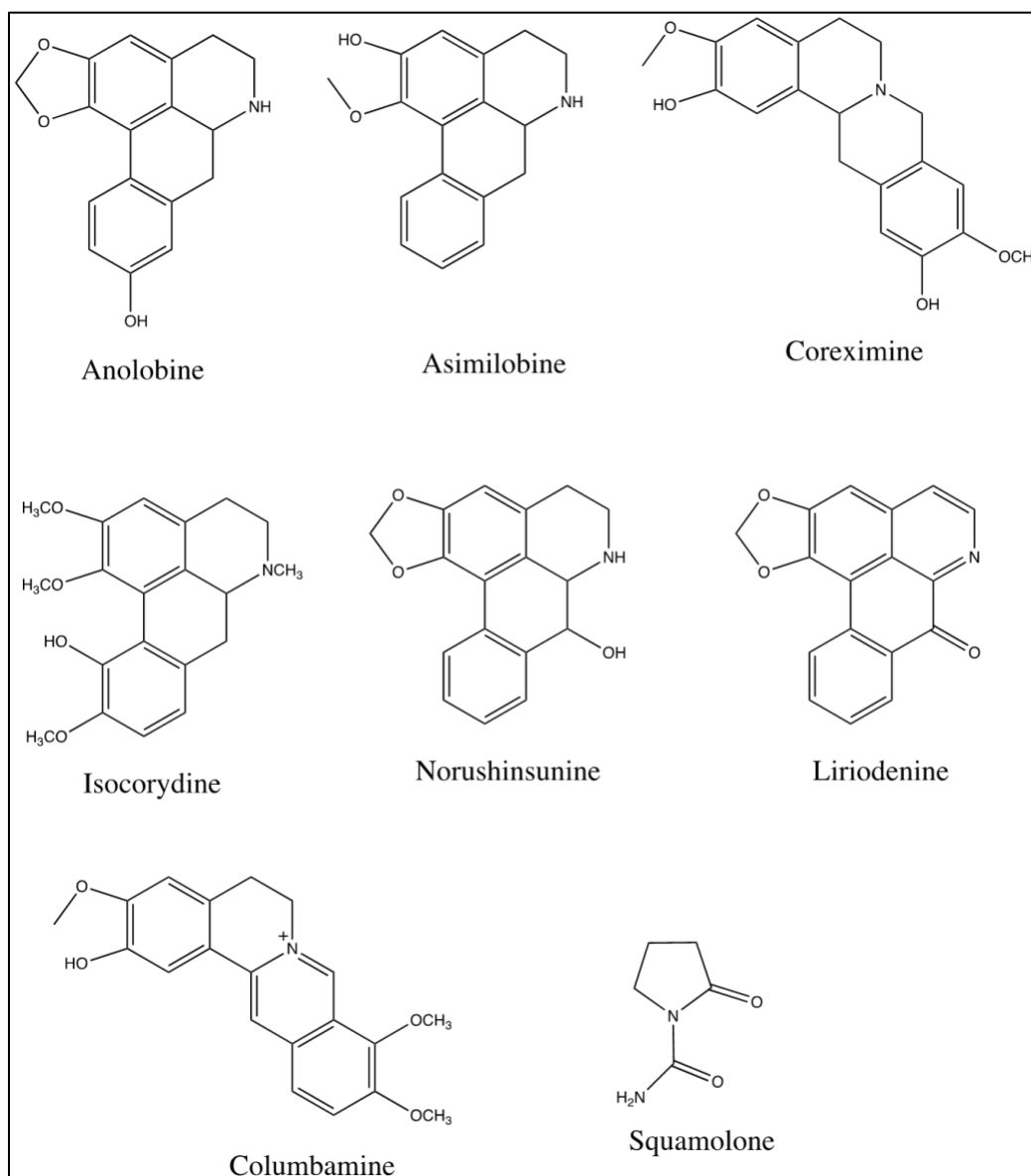


Figure 1- 5 Previously reported alkaloids from *Asimina triloba*

The study and identification of the neurotoxic extracts and pure compounds would help in the development of dietary supplements by choosing the plant extract that has the minimum amount of the neurotoxin to reduce the possibility of undesirable side effects.

To render the cytotoxic and neurotoxicity effects of *Asimina triloba* (chapter iv) and *Rollinia mucosa* (chapter v), different plant extracts and pure compounds were screened against different cancer cell lines and cortical neurons. The twigs of *Asimina triloba*, which known to be the most active part of this plant and has been used in the preparation of different dietary supplements, were subjected to extraction with methanol to get the crude extract (rich with alkaloids and acetogenins) followed by acid-base extraction to obtain alkaloidal rich extract and alkaloids free extract (mainly contain acetogenins).

In chapter ii, the alkaloids rich extract was subjected to different column chromatography to isolate and purify the alkaloids followed by structural elucidation and characterization by 1D and 2D NMR spectroscopic and HRESI-MS spectrometric analysis. The isolated alkaloids from *Asimina triloba* twigs were subjected to targeted analysis study using UHPLC-QToF in positive ion mode to get their accurate MS and MS/MS experiments. Then, they were used as standards for the analysis of two *Asimina* species (*Asimina triloba* and *Asimina parviflora*) and one dietary supplement containing twigs of *Asimina triloba*, as described in chapter iii.

Alkaloids from *Rollinia mucosa* were obtained by the total synthesis of some of their previously reported alkaloids (chapter v). Moreover, the presence of the synthesized compounds in *Rollinia mucosa* seeds and fruits were verified through the analytical technique using UHPLC-QToF-MS. The synthesized alkaloids were screened against different cancer cell lines and cortical neurons to evaluate their biological activities.

To address our hypothesis, two aims will be executed: aim 1: chemical and biological evaluations of *Asimina triloba*, and aim 2: synthesis of some alkaloids from *Rollinia mucosa* and understanding their structure-activity relationships. The details of each aim are demonstrated in chapter ii - v.

CHAPTER II
ISOQUINOLINE ALKALOIDS FROM *ASIMINA TRILOBA*

1. Introduction

Pawpaw (*Asimina triloba* [L.] Dunal) is native to the eastern United States (Galli et al. 2007). It belongs to the Annonaceae family, which is a large family of tropical and subtropical trees and shrubs comprising about 129 genera and more than 2000 species (Rabêlo et al. 2014). Pawpaw is mainly distributed in temperate forests of 26 states in the eastern United States, extending from northern Florida to southern Ontario and as far west as eastern Nebraska (Galli et al. 2007).

Previous phytochemical studies of pawpaw have led to the isolation of more than 50 bioactive compounds called acetogenins (McLaughlin 2008) that displayed antitumor, antimalarial, anthelmintic, piscicidal, antiviral, and antimicrobial activities (Alali et al. 1998; McLaughlin 2008; Pomper et al. 2009; Coothankandaswamy et al. 2010). Only a few alkaloids have been reported from this plant, including coreximine, asimilobine, isocorydine, squamolone, anolobine, liriodenine, norushinsunine and squamolone (Tomita et al. 1965; Zhao et al. 1993).

In the present study, a phytochemical investigation of *Asimina triloba* twigs was undertaken to explore their alkaloidal constituent. Eight aporphine alkaloids including a new aporphine glycoside, (-)-anolobine-9-*O*- β -D-glucopyranoside (**1**), were isolated, and their structures (**Figure 2- 1**) were determined by 1D and 2D NMR spectroscopic and HRESI-MS spectrometric analysis.

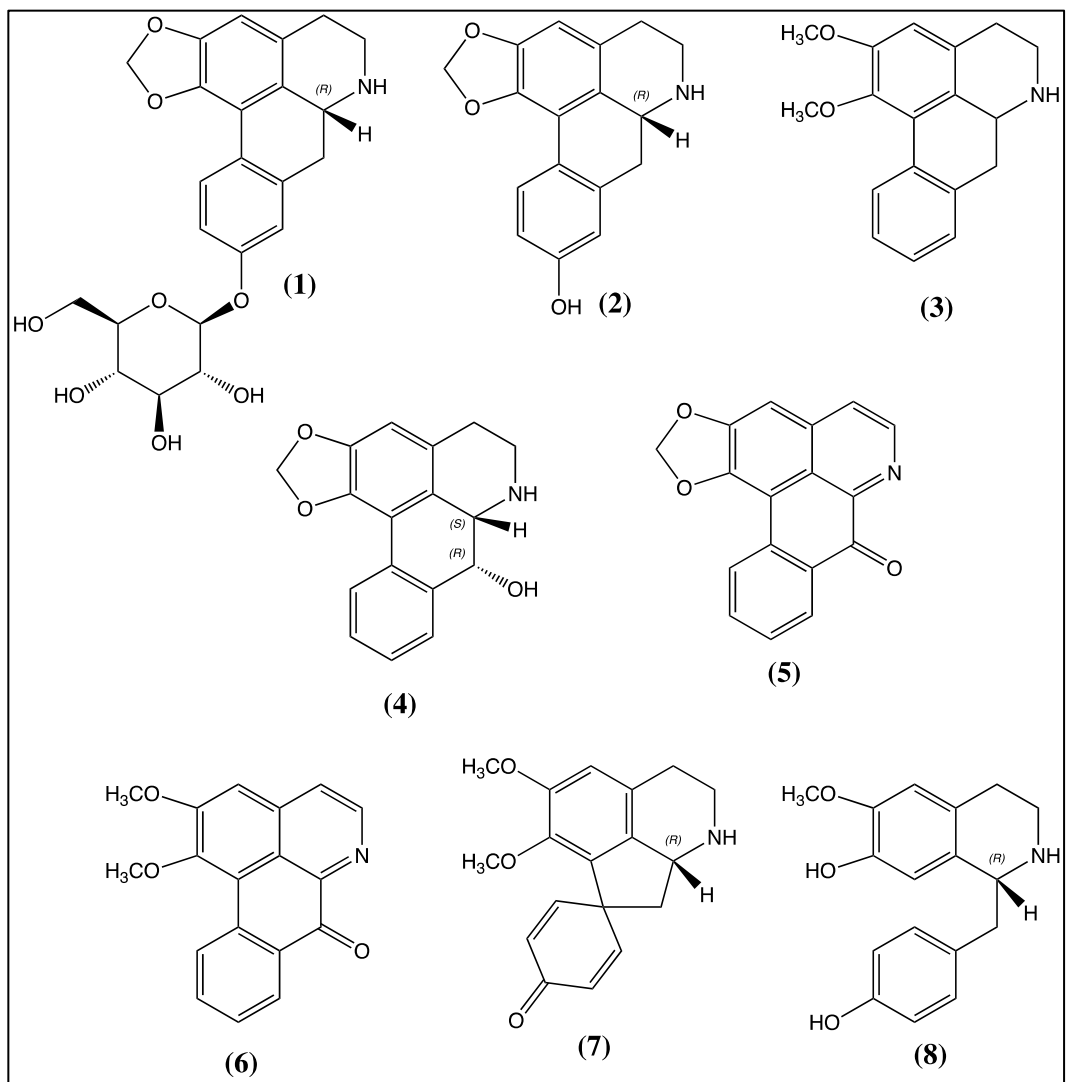


Figure 2- 1 Structures of isolated alkaloids from *Asimina triloba*

2. Results and discussion

Compound **1** was obtained as a yellowish-brown amorphous powder. The HRESIMS (m/z 444.1655 [M+H]⁺, calcd 444.1658) established the molecular formula as C₂₃H₂₅NO₈, indicating 12 degrees of unsaturation. The UV spectrum of **1** showed absorption (λ_{max}) at 275 nm. The IR spectrum showed band for secondary amine that overlapped with a hydroxyl group at 3358 cm⁻¹. The decoupled ¹³C NMR spectrum of **1** exhibited 23 resonances, which were differentiated by DEPT NMR spectrum as five methylenes, ten methines, and eight non-protonated carbons.

The ¹H and ¹³C NMR spectra exhibited characteristic resonances for the methylenedioxy group [$\delta_{\text{H}}/\delta_{\text{C}}$ 5.96 (brd. s, 1H), 6.09 (brd. s, 1H)/100.8], four aromatic methines [$\delta_{\text{H}}/\delta_{\text{C}}$ 6.60 (s)/107.7 (CH-3), 6.97 (d, $J = 2.3$ Hz)/116.3 (CH-8), 6.98 (dd, $J = 9.4, 2.3$ Hz)/115.6 (CH-10), 7.90 (d, $J = 9.4$ Hz)/128.1 (CH-11)], and a glucopyranose [$\delta_{\text{H}}/\delta_{\text{C}}$ 4.90 (d, $J = 7.5$ Hz)/100.9 (CH-1'), δ_{C} 73.7 (C-2'), 77.1 (C-3'), 70.2 (C-4'), 77.6 (C-5'), and 61.1 (C-6')] (**Table 2- 1**). The glucose unit was located at C-9 due to the correlation of anomeric proton (H-1') with C-9 (δ_{C} 157.1) in the HMBC spectrum.

The HMBC correlations of methylenedioxy protons with C-1 (δ_{C} 141.7) and C-2 (δ_{C} 146.5) confirmed its position at C-1 and C-2 (**Figure 2- 2**). The absolute configuration at the stereogenic center C-6a of compound **1** and its aglycone, anolobine (**2**), were determined as *R* from their characteristic negative cotton effect (CE) at 237 and 235 nm respectively, (**Figure 2- 3**) (Ringdahl et al. 1981).

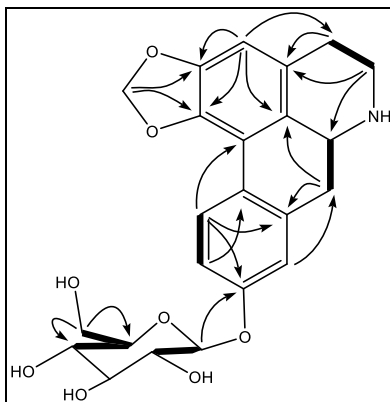


Figure 2- 2 Key HMBC (\rightarrow) and COSY (—) correlations of **1**

The NMR data of the aglycone part of **1** was in agreement with those of anolobine (Chen et al. 1997; Guo et al. 2011; Costa et al. 2015). Therefore, the structure of **1** was elucidated as (-)-anolobine-9-*O*- β -D-glucopyranoside. Aporphine glycosides are rare alkaloids. So far, only seven aporphine glycosides have been reported (Dary et al. 2017; Dembitsky VM. 2005), and anolobine-9-*O*- β -D-glucopyranoside **1** is the first aporphine glycoside with anolobine **2** as the aglycone. Known alkaloids were identified as anolobine (**2**), norruciferine (**3**), norushinsunine (**4**), liriodenine (**5**), lysicamine (**6**), stepharine (**7**) and coclaurine (**8**) by analyzing their NMR and mass data (**Figure 1- 1**). Compounds **3** and **6-8** are reported for the first time from this plant.

The assignment of the absolute configurations at C-6a of the proaporphine alkaloid, stepharine **7**, and the tetrahydrobenzylisoquinoline alkaloid, coclaurine **8**, were determined by CD experiment. Stephanine (**7**) showed negative CE at 225 and 295 nm (**Figure 2- 4**) in contrast to the previously reported (*S*)-(+)-stepharine, which has positive CE at 266 and 293 nm, suggesting *R* configuration at C-6a (Snatzke et al. 1966).

The hypsochromic shift at 220 of stepharine indicated that it afforded the conformation of type D(b) proaporphine alkaloids in which there is no overlap between the π -system of the dienone group and the oxygen *p*-orbital of 1-OMe group, and the bathochromic shift of the (*S*)-(+)-

stepharine at 266 is due to overlapping between the π -system and the oxygen p -orbital (Snatzke et al. 1966).

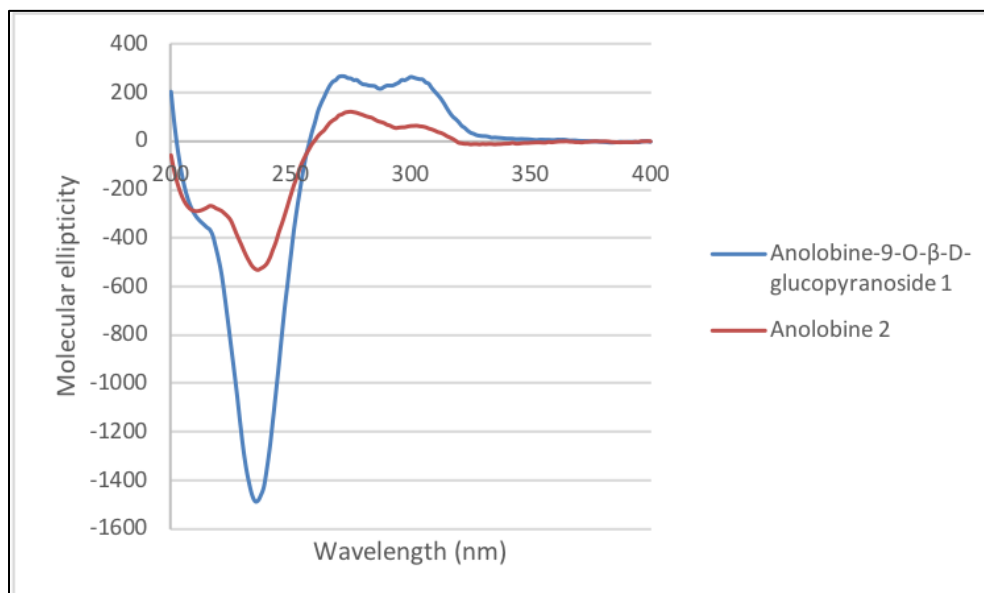


Figure 2- 3 CD spectra of anolobine-9-*O*- β -D-glucopyranoside **1** and its aglycone (anolobine **2**)

Coclaurine (**8**) demonstrated negative CE at 220 and 293 (**Figure 2- 5**), resembled to (*R*)-(+)-isotembetarine perchlorate (negative CE at 236 and 285) (Moriyasu et al. 1997) instead of (*S*)-(+)-reticuline (positive CE at 240 and 290) (Nishiyama et al. 2000), supporting *R* configuration at C-6a of coclaurine. The stereochemistry of stepharine and coclaurine at C-6a was further supported by comparing their optical rotation values $[\alpha]_{25D} -110$ (Chen et al. 1997) and $[\alpha]_{25D} +16$ (Stadler et al. 1988), respectively, with the reported optical rotation values.

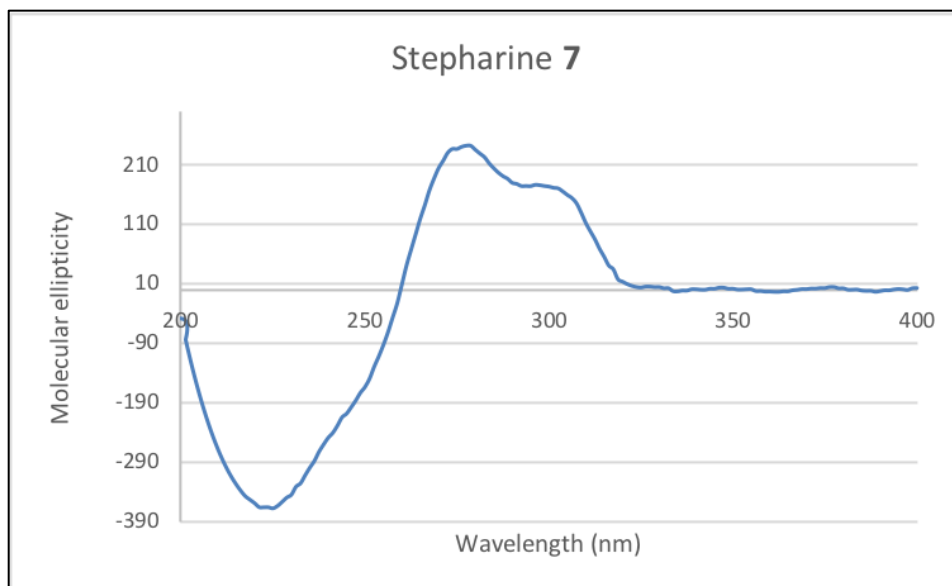


Figure 2- 4 CD spectrum of stepharine (7)

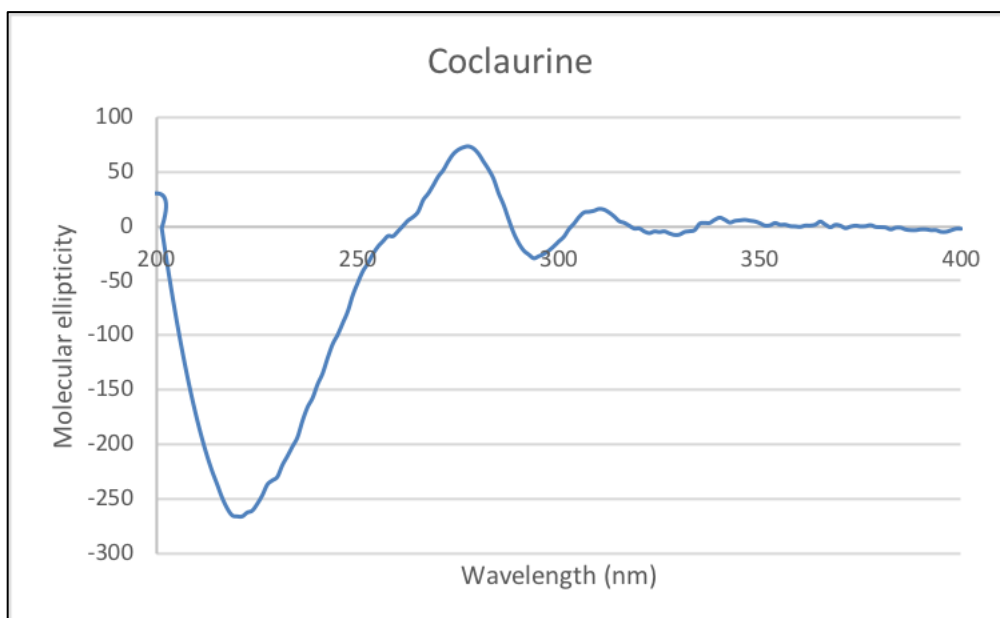


Figure 2- 5 CD spectrum of coclaurine (8)

3. Experimental

3.1. Apparatus and reagents

Circular Dichroism data are obtained from Olis DSM 20 CD digital subtractive method circular dichrometer with a deza subtractive double grating monochromator. Rudolph Research Analytical Autopol IV automatic polarimeter was used to obtain the specific rotations. IR spectra were recorded on an Agilent Technologies Cary 630 FTIR. UV spectrum was acquired on a Varian Cary 50 Bio UV-visible spectrophotometer. NMR spectra were obtained on Bruker AU III 400 or 500 MHz NMR spectrometers using DMSO-*d*₆, CD₃OD, or CDCl₃ solvents. An Agilent Technologies 6200 series mass spectrometer was used to record mass spectra. Column chromatography was carried out using flash silica gel (40 μm, 60 Å, J. T. Baker). TLC was performed on aluminum-backed plates, pre-coated with silica gel F254 (200 μm, 60 Å, (Merck). Spots were detected at UV-254 nm. Visualization was attained by spraying with Dragendorff's reagent or with 1% vanillin solution (prepared with 5% H₂SO₄ in EtOH) followed by heating. Preparative-TLC plates (20 cm × 20 cm, 500 μm) were utilized for the purification.

3.2. Plant material

Asimina triloba twigs were received from Dr. Jerry McLaughlin (Tippecanoe County, Indiana). Voucher specimens (#17328) were deposited at the National Centre for Natural Products Research, University of Mississippi, USA.

3.3. Extraction and Isolation

The plant material was finely powdered (1 kg) and extracted with methanol to obtain 25 g of extract. An aliquot of MeOH extract (20 g) was subjected to usual acid-base alkaloidal

extraction. The extract was suspended in 2% HCl (500 mL) and extracted with EtOAc (3 × 500 mL) in a separating funnel. After separating the EtOAc layers, the resulting aqueous acidic layer's pH was adjusted to 9–10 with ammonia solution and subsequently extracted again with EtOAc (3 × 500 mL). The combined EtOAc layers from basified solution were dried to give an alkaloidal extract (1.3 g), which was fractionated by column chromatography (CC) (115 cm × 3 cm) using silica gel and eluted with following solvents systems: CHCl₃ (1L), CHCl₃- CH₃OH [9:1 (2 L)], and EtOAc-CHCl₃- CH₃OH-H₂O [15:8:2:0.5 (2 L) and 6:4:4:1 (2 L)] to give 5 fractions (Frs. 1-5) and one pure compound [anolobine-9-*O*-β-D-glucopyranoside 1 (16 mg)]. Fr. 1 (66.8 mg) was subjected to CC over silica gel [(84 cm × 1.3 cm), EtOAc-CHCl₃-CH₃OH-H₂O (6:4:4:1)], followed by preparative thin layer chromatography (PTLC) [EtOAc-CHCl₃- CH₃OH-H₂O (6:4:4:1)] to give stepharine (3.5 mg). Fr. 2 (46.6 mg) was subjected to PTLC [silica gel, CHCl₃-CH₃OH (30:1)], which yielded a mixture of liriodenine and nornuciferine (23%:66%, 4.3 mg) and another mixture of lysicamine and liriodenine (60%:40%, 1.4 mg). Fr. 3 (93.2 mg) was chromatographed over silica gel [(85 cm × 2 cm), EtOAc-CHCl₃-CH₃OH-H₂O (10:6:4:1)] followed by PTLC [EtOAc-CHCl₃-CH₃OH-H₂O (10:6:4:1)] to purify norushinsunine (2.4 mg). Fr. 4 (201.0 mg) was subjected to CC over silica gel [(98 cm × 2.4 cm), CHCl₃-CH₃OH (17:3), followed by PTLC [CHCl₃-CH₃OH-H₂O (8:2:0.5)] to afford anolobine (2.0 mg). Coclaurine (2.6 mg) was purified from Fr. 5 (80.1 mg) by CC [silica gel (84 cm × 1.3 cm), CHCl₃-CH₃OH-H₂O (8:2:0.25)], followed by PTLC [CHCl₃-CH₃OH-H₂O (8:2:0.25)].

3.3.1. (*R*)-(-)-anolobine-9-*O*-β-D-glucopyranoside (1)

Yellowish brown amorphous powder; HRESIMS m/z 444.1655 [M+H]⁺ (calcd. for [C₂₃H₂₅NO₈ + H], 444.1658); IR (KBr) ν_{\max} 3358, 3329, 2920, 2849, 1608, 1228, 1045 cm⁻¹; [α]_{25D}

: -15 ($c = 0.5$, CH_3OH); UV/Vis λ_{max} (CH_3OH) nm ($\log \epsilon$): 210 (3.8), 275 (3.6); ^1H NMR (500 MHz, DMSO-d_6): δ 7.90 (1H, d, $J = 9.4$ Hz, H-11), 6.98 (1H, dd, $J = 9.4, 2.3$ Hz, H-10), 6.97 (1H, d, $J = 2.3$ Hz, H-8), 6.60 (1H, s, H-3), 5.96 and 6.09 (each 1H, brd. s, $-\text{OCH}_2\text{O}-$), 4.90 (1H, d, $J = 7.5$ Hz, H-1'), 3.69 (2H, overlapped, H-6a and H-6'), 3.48 (1H, dd, $J = 11.9, 5.8$ Hz, H-6'), 3.35 (1H, ddd, $J = 9.1, 5.8, 2.1$ Hz, H-5'), 3.23 - 3.31 (2H, overlapped, H-2' and H-3'), 3.18 (1H, t, $J = 9.1$ Hz, H-4'), 3.15 (1H, m, H-5), 2.83 (1H, dd, $J = 14.5, 4.8$ Hz, H-7 β), 2.79 (1H, m, H-4), 2.77 (1H, m, H-5), 2.57 (1H, t, $J = 14.5$, H-7 α), and 2.53 (1H, m, H-4). ^{13}C NMR (125 MHz, DMSO-d_6): δ 157.1 (C-9), 146.5 (C-2), 141.7 (C-1), 137.7 (C-7a), 128.5 (C-11c), 128.1 (C-11), 127.6 (C-3a), 125.0 (C-11a), 116.3 (C-8), 115.6 (C-10), 115.0 (C-11b), 107.7 (C-3), 100.9 (C-1'), 100.8 ($-\text{OCH}_2\text{O}-$), 77.6 (C-5'), 77.1 (C-3'), 73.7 (C-2'), 70.2 (C-4'), 61.1 (C-6'), 53.5 (C-6a), 43.3 (C-5), 37.1 (C-7), and 29.5 (C-4) (**Table 2- 1, Figure 2- 6**).

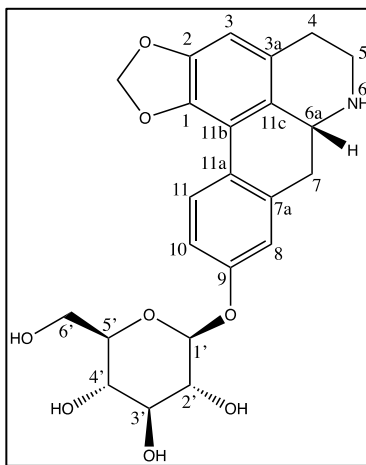


Figure 2- 6 Anolobine-9-*O*- β -D-glucopyranoside (**1**)

Table 2- 1 ¹H and ¹³C NMR data of anolobine-9-*O*-β-D-glucopyranoside (**1**) (DMSO-d₆, 500 MHz/150 MHz)

No.	Mult.	δ ¹³ C [ppm]	δ ¹ H [ppm]
1	C	141.72	-
2	C	146.49	-
3	CH	107.65	6.597 (s)
3a	C	127.63	
4	CH ₂	29.46	2.532 (m) 2.790 (m)
5	CH ₂	43.29	2.772 (m) 3.151 (m)
6a	CH	53.53	3.699 (overlapped)
7	CH ₂	37.12	2.570 (t, J = 14.5, H-7α), 2.832 (dd, J = 14.5, 4.8 Hz, H-7β)
7a	C	137.71	-
8	CH	116.35	6.972 (d, J = 2.3 Hz)
9	C	157.09	-
10	CH	115.61	6.981 (dd, J = 9.4, 2.3 Hz)
11	CH	128.14	7.905 (d, J = 9.4 Hz)
11a	C	125.01	-
11b	C	114.99	-
11c	C	128.53	-
OCH ₂ O	CH ₂	100.83	5.963, 6.089 (each brd. s)
1'	CH	100.86	4.901 (d, J = 7.5 Hz)
2'	CH	73.72	3.234 - 3.312 (overlapped)
3'	CH	77.12	3.234 - 3.312 (overlapped)
4'	CH	70.19	3.180 (t, J = 9.1 Hz)
5'	CH	77.57	3.353 (ddd, J = 9.1, 5.8, 2.1 Hz)
6'	CH ₂	61.14	3.699 (overlapped) 3.487 (dd, J = 11.9, 5.8 Hz)

3.3.2. (*R*)-(-)-Anolobine (2)

Light yellow powder; HRESIMS m/z 282.1133 $[M+H]^+$ (calcd. for $[C_{17}H_{15}NO_3 + H]$, 282.1130); $[\alpha]_{25D}$: -22 ($c = 0.5$, CH_3OH); 1H and ^{13}C NMR data matched with the literature (Chen et al. 1997; Guo et al. 2011; Costa et al. 2015).

3.3.3. Nornuciferine (3)

Yellow amorphous powder; HRESIMS m/z (282.1486) $[M+H]^+$ (calcd. for $[C_{18}H_{19}NO_2 + H]$, 282.1494). 1H and ^{13}C NMR data matched with literature (Hasrat et al. 1997; Hsieh et al. 1999).

3.3.4. (-)-Norushinsunine (4)

Light brown solid mass; HRESIMS m/z 282.1123 $[M+H]^+$ (calcd. for $[C_{17}H_{15}NO_3 + H]$, 282.1130); $[\alpha]_{25D}$: -40 ($c = 0.1$, CH_3OH); 1H NMR data matched with the literature (Chen et al. 1997; Hsieh et al. 1999).

3.3.5. Liriodenine (5)

Yellow amorphous powder (in mixture form with nornuciferine); HRESIMS m/z (276.0656) $[M+H]^+$ (calcd. for $[C_{17}H_9NO_3 + H]$, 276.0661). 1H and ^{13}C NMR data matched with literature (Chen et al. 1997; Guo et al. 2011).

3.3.6. Lysicamine (6)

Yellow powder; HRESIMS m/z 292.0968 $[M+H]^+$ (calcd. for $[C_{18}H_{13}NO_3 + H]$, 292.0974); 1H and ^{13}C NMR data matched with literature (Chen et al. 1997; Rabêlo et al. 2015).

3.3.7. (R)-(-)-Stepharine (7)

Dark brown solid mass; HRESIMS m/z 298.1439 $[M+H]^+$ (calcd. for $[C_{18}H_{19}NO_3 + H]$, 298.1443); $[\alpha]_{25D}$: -110 ($c = 0.1$, $CHCl_3$); 1H and ^{13}C NMR data matched with the literature (Chen et al. 1997; Costa et al. 2015; Rabêlo et al. 2015).

3.3.8. (R)-(+)-Coclaurine (8)

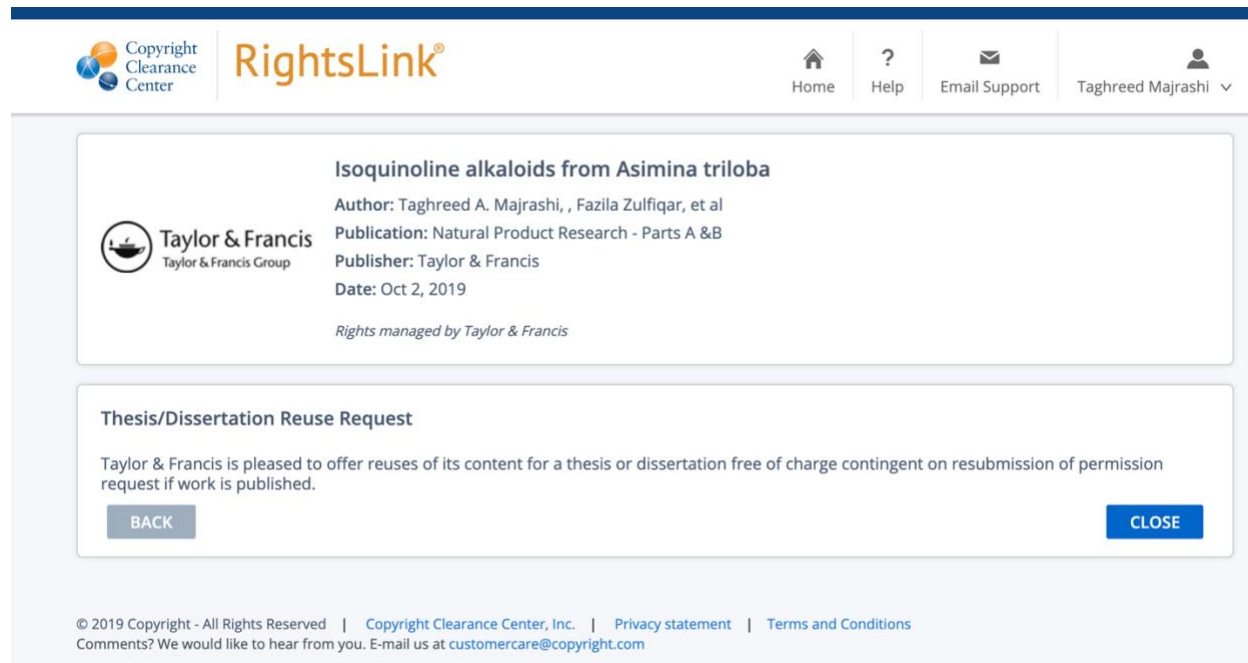
Colorless prisms (CH_3OH); HRESIMS m/z 286.1437 $[M+H]^+$ (calcd. for $[C_{17}H_{19}NO_3 + H]$, 286.1443); $[\alpha]_{25D} +16$ ($c = 0.25$, CH_3OH); 1H and ^{13}C NMR data matched with the literature (Costa et al. 2015).

4. Conclusion

The phytochemical investigation of the alkaloids from *Asimina triloba* twigs yielded one new aporphine glycoside, (-)-anolobine-9-*O*- β -D-glucopyranoside (**1**), along with seven known isoquinoline alkaloids, anolobine (**2**), nornuciferine (**3**), norushinsunine (**4**), liriodenine (**5**), lysicamine (**6**), stepharine (**7**) and coclaurine (**8**). Alkaloids **3** and **6-8** are reported for the first time from this plant.

Chapter II Copyright

The content of chapter ii has been published in the Natural Product Research. The journal offers reuse of the articles by the author for thesis or dissertation free of charge as shown below.



The screenshot displays the RightsLink interface. At the top left, there are logos for the Copyright Clearance Center and RightsLink. The top right navigation bar includes links for Home, Help, Email Support, and a user profile for Taghreed Majrashi. The main content area features a card for the article "Isoquinoline alkaloids from Asimina triloba" by Taghreed A. Majrashi, et al., published in Natural Product Research - Parts A & B by Taylor & Francis on October 2, 2019. Below this, a "Thesis/Dissertation Reuse Request" notification states that Taylor & Francis offers free reuse for theses or dissertations upon request. The notification includes "BACK" and "CLOSE" buttons. The footer contains copyright information and contact details for the Copyright Clearance Center.

Copyright Clearance Center | RightsLink®

Home | Help | Email Support | Taghreed Majrashi

Isoquinoline alkaloids from Asimina triloba
Author: Taghreed A. Majrashi, , Fazila Zulfiqar, et al
Publication: Natural Product Research - Parts A & B
Publisher: Taylor & Francis
Date: Oct 2, 2019
Rights managed by Taylor & Francis

Thesis/Dissertation Reuse Request
Taylor & Francis is pleased to offer reuses of its content for a thesis or dissertation free of charge contingent on resubmission of permission request if work is published.

BACK | CLOSE

© 2019 Copyright - All Rights Reserved | Copyright Clearance Center, Inc. | Privacy statement | Terms and Conditions
Comments? We would like to hear from you. E-mail us at customer care@copyright.com

CHAPTER III
TARGETED ANALYSIS OF ANNONACEOUS ALKALOIDS FROM *ASIMINA TRILOBA*
USING UHPLC-QTOF-MS

1. Introduction

Standardization of botanical supplements is an essential tool in the formulation of high-quality dietary supplements. The development of an analytical method to characterize and quantify the biomarkers and chemical markers would be valuable not only for herbal identification and quality control but would also enhance understanding of the botanicals' biological activity and their benefits or potential risk to human health.

Phytochemical and pharmacological investigations on *Asimina* species revealed the presence of several bioactive compounds, including alkaloids, acetogenins, phenolic compounds, terpenes, and essential oils (Leboeuf et al., 1980). Chemical studies of the plant (family Annonaceae) have increased in the last two decades due to the presence of annonaceous molecules (e.g., isoquinoline alkaloids and acetogenins) with pharmacological uses (González-Esquinca et al., 2014). Approximately 500 alkaloids have been identified in 138 Annonaceae species in 43 genera.

Most of these alkaloids present in Annonaceae possess isoquinoline derived structures including benzyltetrahydroisoquinolines (coclaurine, higenamine), protoberberines (coreximine, jatrorrhizine, berberine, corydaline, tetrahydropalmatine), proaporphines (pronuciferine, stepharine), aporphines (anonaine, asimilobine, glaucine, magnoflorine, isocorydine, norisocorydine, norcorydine, lysicamine, nornuciferine), and oxoaporphines (liriodenine, anolobine, norushinsunine, lanuginosine) (Leboeuf et al., 1980). The aporphinoids are the largest group of compounds occurring in the Annonaceae plants (Leboeuf et al., 1980).

The presence of acetogenins was investigated in the *Asimina triloba* fruits using different analysis techniques, including HPLC-MS (Pomper et al., 2009) and HPLC-DAD (Donno et al., 2014). A quantitative liquid chromatography/tandem mass spectrometry (LC/MS/MS) method was established for the quality control of the acetogenins in the extracts of the pawpaw tree (*Asimina triloba*). The concentrations of the three major compounds (bullatacin, asimicin, and trilobacin) were evaluated (Gu et al., 1999). A droplet-liquid microjunction-surface sampling probe coupled to UPLC-PDA-HRMS/MS system was used to detect acetogenins in situ from *Asimina triloba* (Sica et al., 2016).

The alkaloid liriodenine was analyzed by the TLC image analysis and HPLC-DAD method from twenty-eight plant materials of Magnoliaceae, Annonaceae and Nelumbonaceae in Thailand (Mongkolrat et al., 2013). The levels of reticuline, norreticuline, and N-methylcoclaurine were determined in three *Annona* species (*A. reticulata*, *A. squamosa*, *A. muricata*) (Kotake et al., 2004). Previous studies have evaluated the analysis to a specific type of plant or acetogenins or alkaloids from *Annona* or *Asimina* species (Donno et al., 2014; Mongkolrat et al., 2013; Pomper et al., 2009; Ratnayake et al., 1992; Yang et al., 2009).

Most of the previous work was focused on target acetogenins or alkaloids with limited information on alkaloids from *Asimina triloba* samples. In this regard, metabolomics provides an efficient tool for investigating the alkaloids in a single analysis, including health promoting compounds.

Utilizing the high chromatographic resolution and separation capabilities of UHPLC with QToF-MS provides the structural characterization from accurate mass measurement for both MS and MS-MS experiments. This technique offers a significant advantage for the rapid screening of compounds in complex matrices. In the present study, the structural characteristics of 8 alkaloids from methanolic extracts of dried twigs of *Asimina triloba* have been studied using UHPLC-QToF-MS in positive ion mode.

Herein, this study described an investigation of the fragmentation pathways leading to the identification of key diagnostic fragment ions for the annonaceous alkaloids. MS-MS experiments lessen the ambiguities in the identification of compounds. Because of the many isomers, even accurate mass MS/MS is insufficient for complete identification, requiring chromatographic separation and comparison of standards. Alkaloids were characterized and confirmed from their retention times obtained from standard compounds.

2. Experimental approach

The high chromatographic resolution and separation capabilities of the UHPLC with QToF-MS have been applied to the identification and characterization of isolated alkaloids (anolobine-9-*O*- β -D-glucopyranoside, anolobine, nornuciferine, norushinsunine, liriodenine, and lysicamine, stepharine, and coclaurine) from *Asimina triloba* (Majrashi et al., 2018).

The standard compounds were characterized and detected from methanolic extracts of different parts of *Asimina triloba*, *Asimina parviflora*, and one dietary supplement claiming to contain pawpaw (*Asimina triloba*) and identified by comparing the retention times and the MS and MS/MS data with reference standards. No previous phytochemical work has been reported with species of *Asimina parviflora* except for one paper where five bioactive compounds (asimicilone, 6-cis-docosenamide, asimicin, (+)-syringaresinol, and β -sitosterol- β -D-glucopyranoside) were isolated and identified (Ratnayake et al., 1992). Herein, the standard compounds have been used to distinguish between the two *Asimina* species, *triloba* and *parviflora*.

3. Plant materials

Dried seed (NCNPR code # 17325), twigs (NCNPR code # 17328), bark (NCNPR code # 17326), and twigs with bark (NCNPR code # 17327) of *Asimina triloba* were obtained by Dr. Jerry McLaughlin at Purdue University's School of Pharmacy (West Lafayette, IN). Leaf (NCNPR code # 19098), stem (NCNPR code # 19099), root (NCNPR code # 19100) of *Asimina parviflora*, were provided by David Ellis (Botanist, Purdue University, West Lafayette, Indiana). Dietary supplement (#18447) claiming to contain pawpaw (*Asimina triloba* twigs extract) was purchased online. Specimens of all samples were deposited at the NCNPR's botanical repository at the University of Mississippi.

4. Standards and plant sample preparation

All standards were prepared at a concentration of 10 μ g/mL. Dry plant samples (0.5 g) or an adequate amount of capsule contents (average weight of dosage form) or 25 mg of extracts were sonicated in 2.5 mL of methanol for 30 min, followed by centrifugation for 15 min at $959 \times g$. The

supernatant was transferred to a 10 mL volumetric flask. The procedure was repeated three more times, and the respective supernatants were combined. The final volume was adjusted to 10 mL with methanol and mixed thoroughly. Prior to injection, an adequate volume (*ca.* 2 mL) was passed through a 0.45 μ m PTFE membrane filter. The first 1.0 mL was discarded, and the remaining volume was collected in an LC sample vial.

5. Instrumentation and analytical conditions

5.1. Ultra-High-Performance Liquid Chromatography-Quadrupole Time of Flight-Mass Spectrometry (UHPLC/QToF-MS)

The liquid chromatographic system was an Agilent Series 1290 comprised of the following modular components: binary pump, a vacuum solvent microdegasser, an autosampler with a 100-well tray and a thermostatically controlled column compartment. The separation was achieved on an Agilent Poroshell 120 EC-18 (2.1 \times 100 mm, 2.7 μ) column. The mobile phase consisted of water with 0.1% formic acid (A) and acetonitrile with 0.1% formic acid (B) at a flow rate of 0.23 mL/min, with the following gradient: 0 min, 2% B in next 20 min to 10% B, for next 30 min 20% B, for next 20 min 50% B, for next 20 min 70% B, for next 20 min 90% B and to 100% B in next 10 min. Each run was followed by a 5 min wash with 100% B and an equilibration period of 5 min with 2% B. Two microliters of sample were injected. The column temperature was set at 40 $^{\circ}$ C, and UV spectra were recorded from 190-400 nm.

The mass spectrometric analysis was performed with a QToF-MS/MS (Model #G6530A, Agilent Technologies, Palo Alto, CA, USA) equipped with an ESI source with Jet Stream technology using the following parameters: drying gas (N₂) flow rate, 11.0 L/min; drying gas temperature, 325 $^{\circ}$ C; nebulizer, 30 psig, sheath gas temperature, 325 $^{\circ}$ C; sheath gas flow, 11

L/min; capillary, 3000V; skimmer, 65V; Oct RF V, 750V; fragmentor voltage, 100V. The sample collision energy was set at 55eV. All the operations, acquisition, and analysis of data were controlled by Agilent MassHunter Acquisition Software Ver. A.05.00 and processed with MassHunter Qualitative Analysis software Ver. B.07.00. Each sample was analyzed in a positive mode in the range of $m/z = 100-1700$.

Accurate mass measurements were obtained by means of ion correction techniques using reference masses at m/z 121.0509 (protonated purine) and 922.0098 [protonated hexakis (1H, 1H, 3H-tetrafluoropropoxy) phosphazine or HP-921] in positive ion mode. The compounds were confirmed in each spectrum. For this purpose, the reference solution was introduced into the ESI source via a T-junction using an Agilent Series 1200 isocratic pump (Agilent Technologies, Santa Clara, CA, USA) using a 100:1 splitter set at a flow rate of 20 $\mu\text{L}/\text{min}$. For recording ToF-MS spectra, the quadrupole was set to pass all ions (Rf only mode), and all ions were transmitted into the pusher region of the time-of-flight analyzer where they were mass-analyzed with a 1 s integration time up to m/z 1000. For the ESI-MS/MS CID experiments, ions of interest were mass-selected by the quadrupole mass filter. The selected ions then collided with nitrogen in a high-pressure collision cell, and the collision energy was optimized to afford good product ion signals that were subsequently mass measured with the ToF analyzer.

Analysis was performed in the reflectron mode with a resolving power of about 10,000 at m/z 922. The instrument was set to extended dynamic range (up to 10^5 with lower resolving power). MS/MS spectra were recorded simultaneously at a rate 2.0 spectra s^{-1} . In order to filter selected precursor ions and their isotopes for MS/MS, an isolation window of 1.3 m/z was set for the quadrupole.

5.2. Data analysis

MassHunter Workstation software, including Qualitative Analysis (version B.07.00), was used for processing both raw MS and MS/MS data, including molecular feature extraction, background subtraction, data filtering, and molecular formula estimation (using accurate mass of all isotopes, their relative abundances, and all detected adducts with their measured isotopes).

To perform subtraction of molecular features (MFs) originating from the background, analysis of a blank sample (methanol) was carried out under identical instrument settings, and background MFs were removed. This method involved the use of the $[M+H]^+$ and $[M+Na]^+$ ions in the positive ion mode, found in the extracted ion chromatogram (EIC).

6. Results and discussion

In order to determine the optimal ionization method for analytes, positive and negative ion modes were investigated with the same UHPLC mobile phase at a flow rate of 0.23 mL/min. All compounds showed good detection in positive ion mode. Identification or elucidation of these compounds using UHPLC-QToF-MS can be performed with the assistance of reference standards (**Table 3- 1**). Some chromatographic peaks contained the same protonated molecules in the MS spectra and similar product ions in MS/MS spectra but had different retention behaviors, which were helpful for their identification.

Table 3- 1 Accurate mass data, fragment ions for the alkaloids of Annonaceae family using UHPLC Q-ToF						
Name	Retention Time (min)	Molecular formula	m/z Calculated	m/z Experimental [M+H] ⁺ / [M+Na] ⁺	Error (mDa)	Fragment Ions (30V)
Anolobine-9- <i>O</i> -β-D-glucopyranoside	27.3	C ₂₃ H ₂₅ NO ₈	444.1653 [M+H] ⁺	444.1653	0.0	427.1312 [M+H-NH ₃] ⁺ 265.0820 [M+H-NH ₃ -Glu] ⁺ 247.0759 [M+H-NH ₃ -Glu-H ₂ O] ⁺ 235.0712 [M+H-NH ₃ -Glu-CH ₂ O] ⁺ 217.0656 [M+H-NH ₃ -Glc-H ₂ O-CH ₂ O] ⁺ 207.0775 [M+H-NH ₃ -Glc-CH ₂ O-CO] ⁺ 179.0842 [M+H-NH ₃ -Glc-CH ₂ O-2CO] ⁺
Anolobine	39.5	C ₁₇ H ₁₅ NO ₃	282.1125 [M+H] ⁺	282.1123	-0.2	265.0839 [M+H-NH ₃] ⁺ 247.0731 [M+H-NH ₃ -H ₂ O] ⁺ 235.0730 [M+H-NH ₃ -CH ₂ O] ⁺ 217.0635 [M+H-NH ₃ -H ₂ O-CH ₂ O] ⁺ 207.079 [M+H-NH ₃ -CH ₂ O-CO] ⁺ 179.0828 [M+H-NH ₃ -CH ₂ O-2CO] ⁺ 189.0694 [M+H-NH ₃ -CH ₂ O-CO-H ₂ O] ⁺
Nornuciferine	36.3	C ₁₈ H ₁₉ NO ₂	282.1489 [M+H] ⁺	282.1487	-0.2	251.1048 [M+H-CH ₃ NH ₂] ⁺ 236.0817 [M+H-CH ₃ NH ₂ -CH ₃] ⁺ 219.0791 [M+H-CH ₃ NH ₂ -CH ₃ OH] ⁺ 191.0844 [M+H-CH ₃ NH ₂ -CH ₃ OH-CO] ⁺
Norushinsunine	39.0	C ₁₇ H ₁₅ NO ₃	282.1125 [M+H] ⁺	282.1125	0.0	264.1014 [M+H-H ₂ O] + 234.0902 [M+H-H ₂ O-CH ₂ O] + 206.0952 [M+H-H ₂ O-CH ₂ O-CO] + 179.0845 [M+H-H ₂ O-CH ₂ O-CO-NH ₃] +
Liriodenine	48.2	C ₁₇ H ₉ NO ₃	276.0655 [M+H] ⁺	276.0656	+0.1	248.0694 [M+H-CO] ⁺ 220.0743 [M+H-2CO] ⁺ 218.0591 [M+H-CO-2CH ₃] ⁺ , 190.0643 [M+H-2CO -2CH ₃] ⁺

Table 3- 2 Accurate mass data, fragment ions for the alkaloids of Annonaceae family using UHPLC Q-ToF						
Name	Retention Time (min)	Molecular formula	m/z Calculated	m/z Experimental [M+H]⁺/ [M+Na]⁺	Error (mDa)	Fragment Ions (30V)
Lysicamine	59.1	C ₁₈ H ₁₃ NO ₃	292.0968 [M+H] ⁺	292.0965	+0.3	277.0719 [M+H-CH ₃] ⁺ 260.0695 [M+H-CH ₃ -17] ⁺ 248.0692 [M+H-CH ₄ -CO] ⁺ 231.0654 [M+H-CH ₄ -CO-17] ⁺ 219.0664 [M+H-CH ₄ -CO-29] ⁺
Stepharine	23.7	C ₁₈ H ₁₉ NO ₃	298.1438 [M+H] ⁺	298.1439	+0.1	281.1122 [M+H-NH ₃] ⁺ 269.1140 [M+H-CO] ⁺ 254.0896 [M+H-CO-CH ₃] ⁺ 238.0946 [M+H-CO-OCH ₃] ⁺ 223.0733 [M+H-CO-CH ₃ -OCH ₃] ⁺ 192.0992 [M+H-CO-CH ₃ -2OCH ₃] ⁺ 161.0811 [M+H-CO-CH ₃ -3OCH ₃] ⁺ 146.0577 [M-CO-2CH ₃ -3OCH ₃] ⁺
Coclaurine	23.1	C ₁₇ H ₁₉ NO ₃	286.1438 [M+H] ⁺	286.1439	+0.1	269.1155 [M+H-NH ₃] ⁺ 254.0933 [M+H-CH ₃ OH] ⁺ 175.0747 [M+H-C ₆ H ₈ NO] ⁺ 143.0483 [M+H-C ₇ H ₁₀ NO-H ₂ O] ⁺ 107.0493 [M+H-C ₁₀ H ₁₂ O] ⁺

Alkaloids isolated from *Asimina triloba* twigs have a secondary amine, and they are composed of three-four rings with different skeletons. The ESI mass spectra of these alkaloids showed abundant $[M+H]^+$ ions due to the strong basicity of the secondary amine group. The data were obtained in positive electrospray ionization mode at collision energies 30eV. Only singly charged positive $[M+H]^+$ were used to produce targeted MS-MS spectra. The alkaloids of the aporphine, oxoaporphine, and benzyloquinolines type represent the predominant group in this genus. The alkaloidal skeleton was determined from the UV absorption spectra and mass spectrometry fragmentation.

6.1. Benzyloquinoline alkaloids

The prototype molecule of coclaurine was identified based on exact mass measurement and comparison with the standard compound. According to the structural characteristics, elution of benzyloquinolines was achieved before that of the other class of alkaloids. Major characteristics ions were formed by inductive cleavage and α -cleavage at the nitrogen of the tyramine moiety (Jeong et al., 2012; Schmidt et al., 2005) (**Figure 3- 1, 3- 2**). Coclaurine (m/z 286.1439 $[M+H]^+$) produced product ions at m/z 269.1155 $[M+H-NH_3]^+$, 254.0933 $[M+H-CH_3OH]^+$, 237.0905 $[M+H-NH_3-H_2O]^+$, 209.0951, 194.0717, 143.0483, 115.054 and major fragment ion 107.0493 (**Table 3- 1, Figure 3- 1, 3- 2**). The UV absorption maxima of this compound were 200, 227, 283 nm.

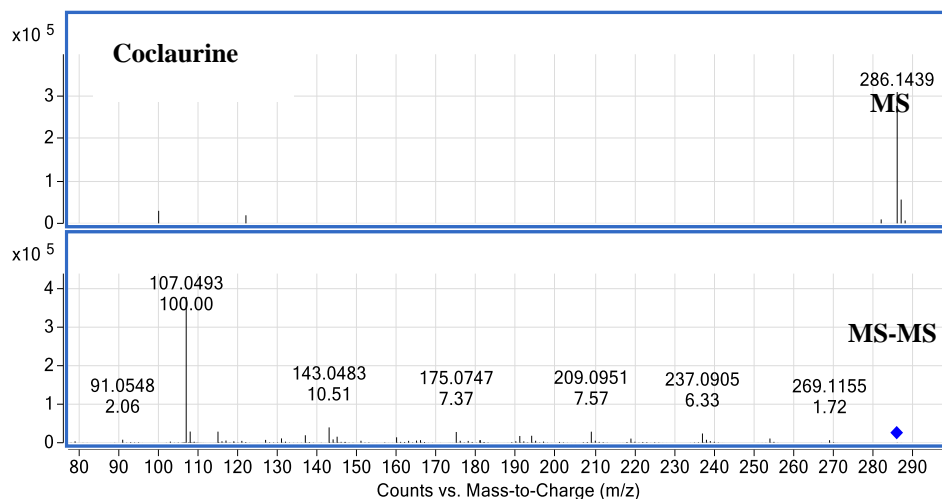


Figure 3- 1 ESI-MS_n spectrum of coclaurine

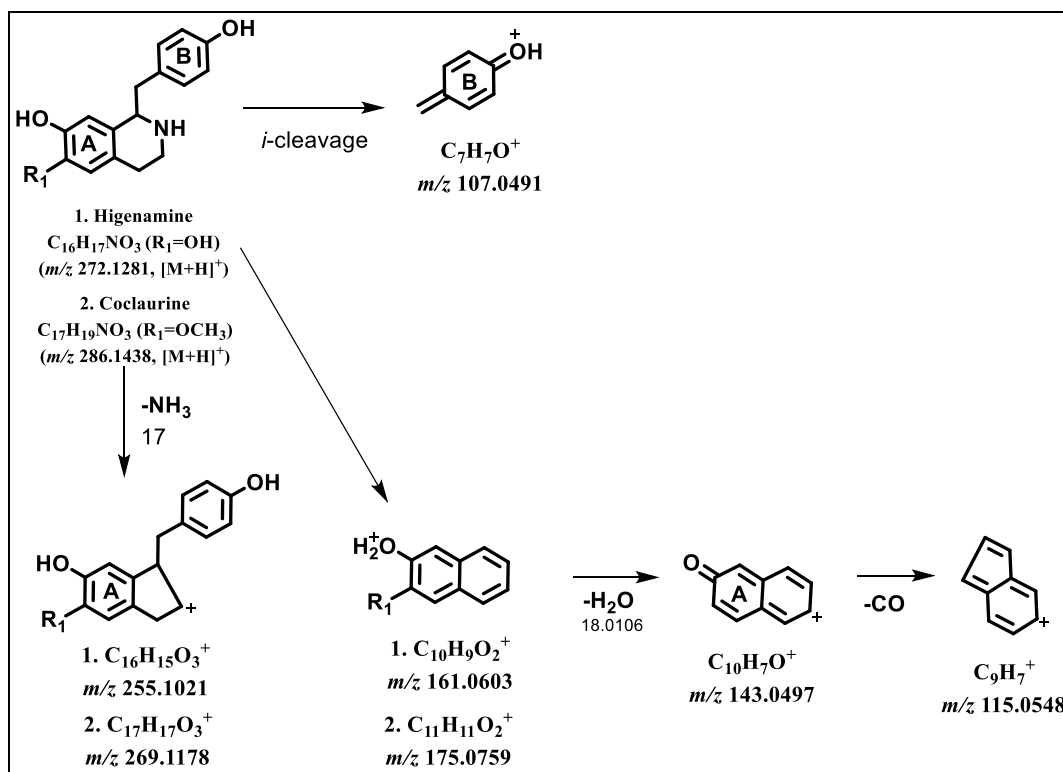


Figure 3- 2 Tentative fragmentation pathways of the coclaurine

6.2. Proaporphine Alkaloids

Proaporphine Alkaloids, such as stepharine with the *p*-cyclohexadienone moiety, are the precursor of aporphine alkaloids (Dai et al. 2012; Jeong et al., 2012; Tomita et al. 1965). The mass spectrum showed the molecular ion peak at m/z 298.1439 $[M+H]^+$, thus indicating a molecular formula of $C_{13}H_{19}NO_3$. The fragmentation peaks were observed at m/z 281.1122 $[M+H-NH_3]^+$, m/z 269.1140 $[M+H-CO]^+$ attributed to the loss of amino and carbonyl groups from the dienone type fragment. Additional peaks at m/z 254.0896 $[M+H-CO-CH_3]^+$, 238.0946 $[M+H-CO-OCH_3]^+$, 223.0733 $[M+H-CO-CH_3-OCH_3]^+$, 192.0992 $[M+H-CO-CH_3-2OCH_3]^+$, 161.0811 $[M+H-CO-CH_3-3OCH_3]^+$ and 146.0577 $[M+H-CO-2CH_3-3OCH_3]^+$ were observed.

The molecular ion is decomposed by RDA (retro-diels-alder) reaction of the tetrahydroisoquinoline ring, and the process is similar to the fragmentation of aporphine alkaloids (Table 3- 1, Figure 3- 3, 3- 4). The UV absorption spectrum, measured in methanol showed at 210, 234, and 285 nm.

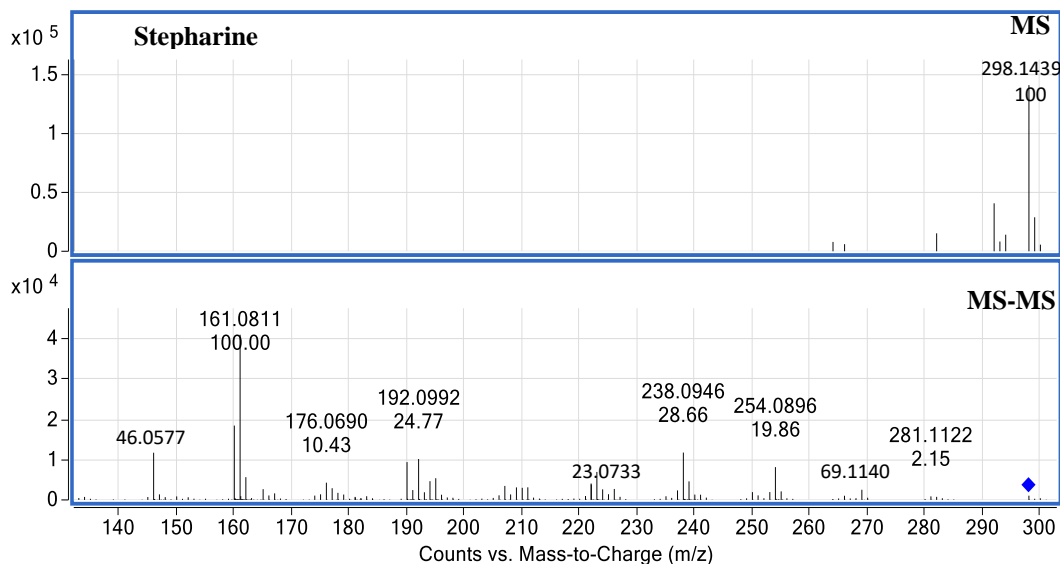


Figure 3- 3 ESI-MS n spectrum of stepharine

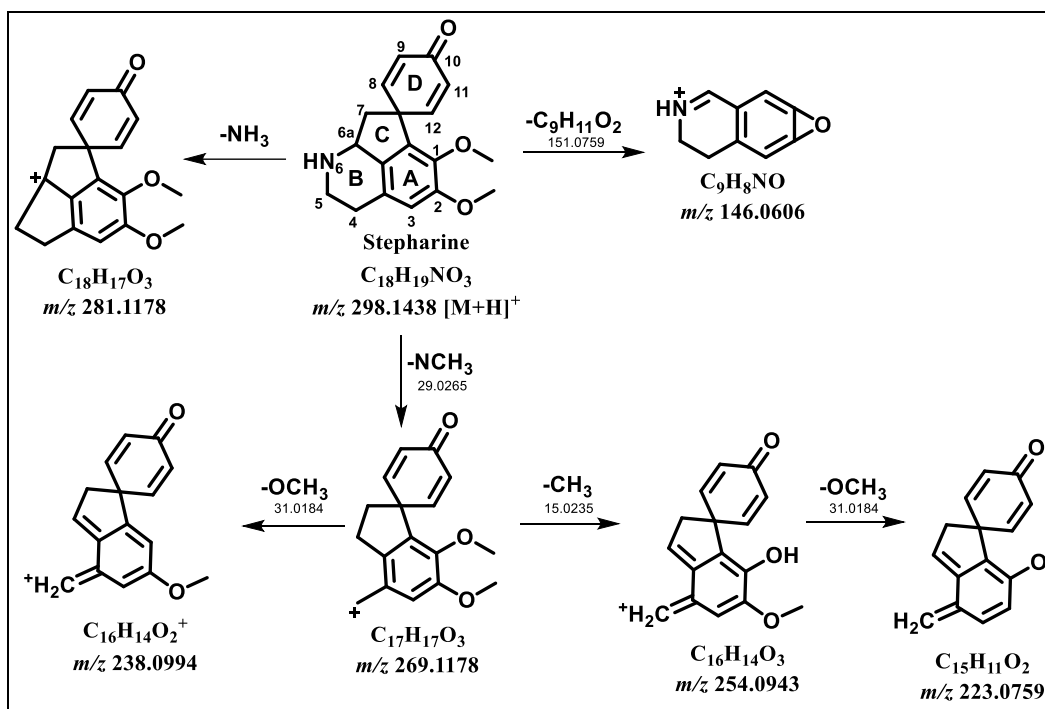


Figure 3- 4 Tentative fragmentation pathways of the stepharine.

6.3. Aporphine Alkaloids

Aporphine alkaloids are the largest group of isoquinoline alkaloids and due to their rigid structures, the mass spectra are characterized by loss of small molecules such as water, CO, or CO₂ with cation radicals fragment ions frequently present. The degree of substitution on the nitrogen can be identified on the loss of ammonia (secondary nitrogen), methylamine (tertiary nitrogen) or dimethylamine (quaternary nitrogen) (Sangster and Stuart 1965; Shamma et al. 1971; Singh et al., 2017; Tang et al., 2014; Tian et al. 2014).

Nornuciferine showed a protonated molecule [M+H]⁺ at *m/z* 282.1487 and the fragmentation was due successive loss of methylamine group (–CH₃NH₂ [M+H–31]⁺), methyl group (–CH₃ group [M+H–15]⁺), –CH₃OH moiety, –CO molecule produced ions at *m/z* 267.0906,

251.1048, 236.0817, 219.0791, major fragment ion m/z 191.0844 (Table 3-1, Figure 3-5, 3-6) and UV absorption spectra at 215, 270 and 310 nm.

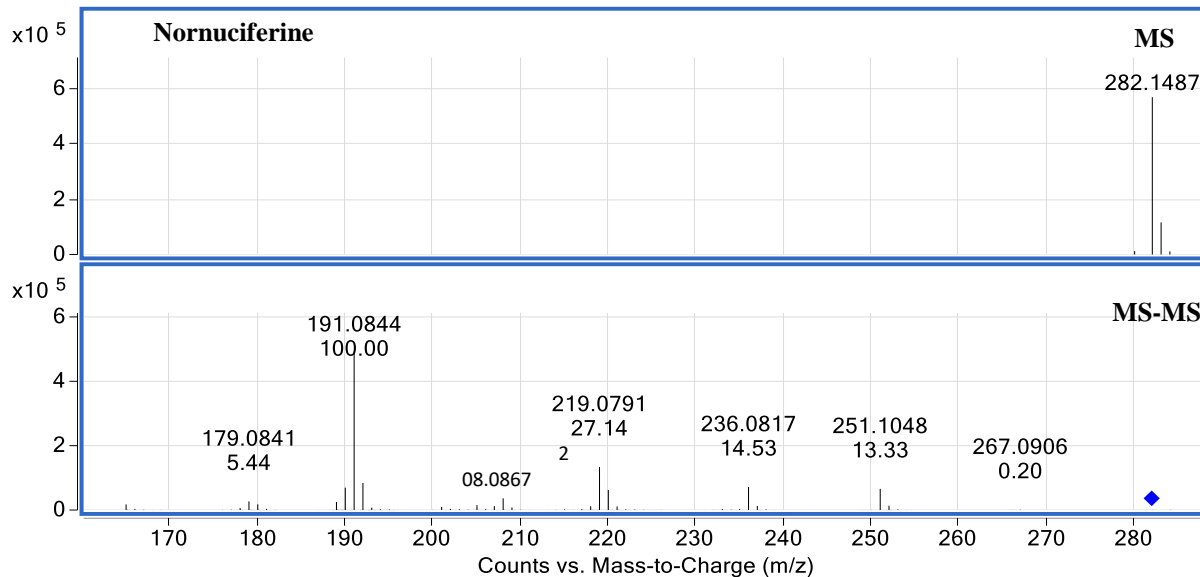


Figure 3- 5 ESI-MS_n spectrum of nornuciferine.

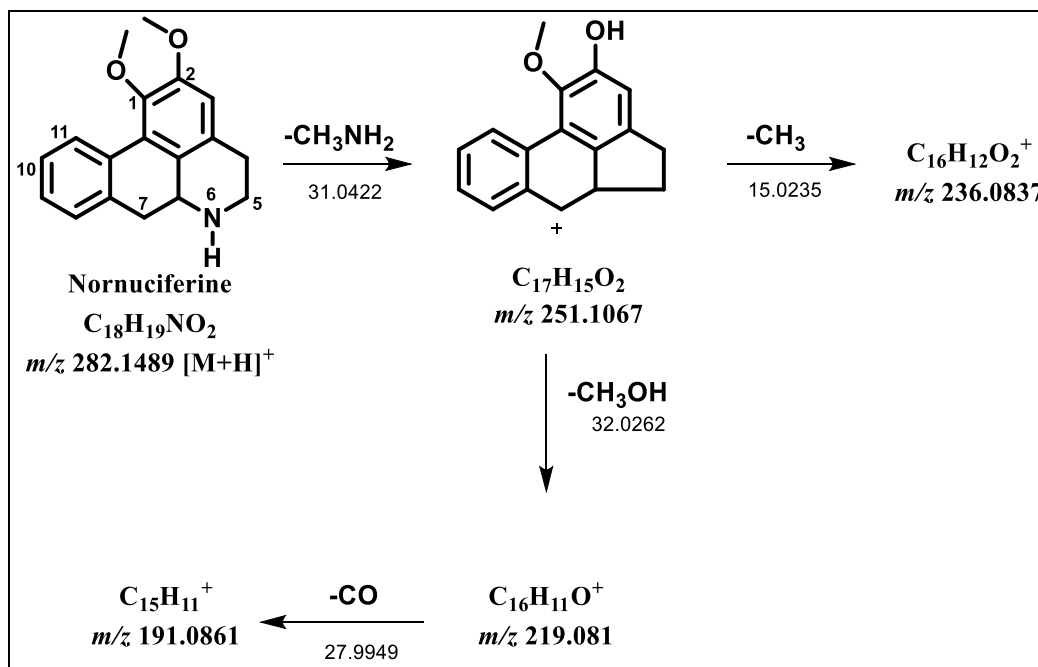


Figure 3- 6 Tentative fragmentation pathways of the nornuciferine

Similar the case with lysicamine where it showed a protonated molecule $[M+H]^+$ at m/z 292.0965 and the fragmentation was due to successive loss of methyl group ($-CH_3$ group $[M+H-15]^+$), $-CH_4-CO$ moiety, CO molecule produced ions at m/z 277.0719 (major), 260.0695, 248.0692 (major), 191.0705 (Table 3- 1, Figure 3- 7, 3- 8) and UV absorption spectra at 215, 275 and 310 nm.

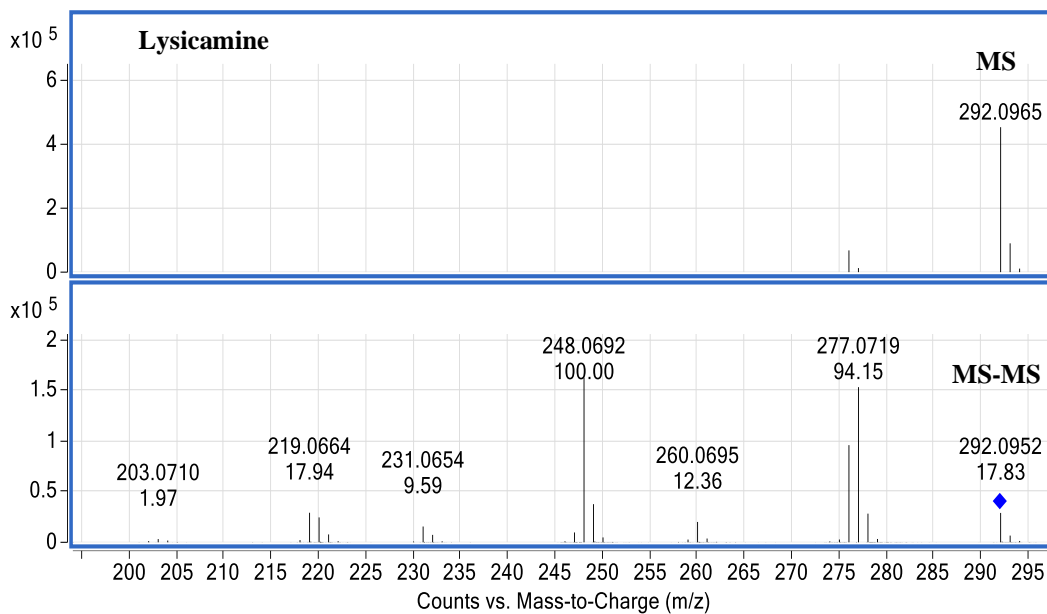


Figure 3- 7 ESI- MS_n spectrum of lysicamine

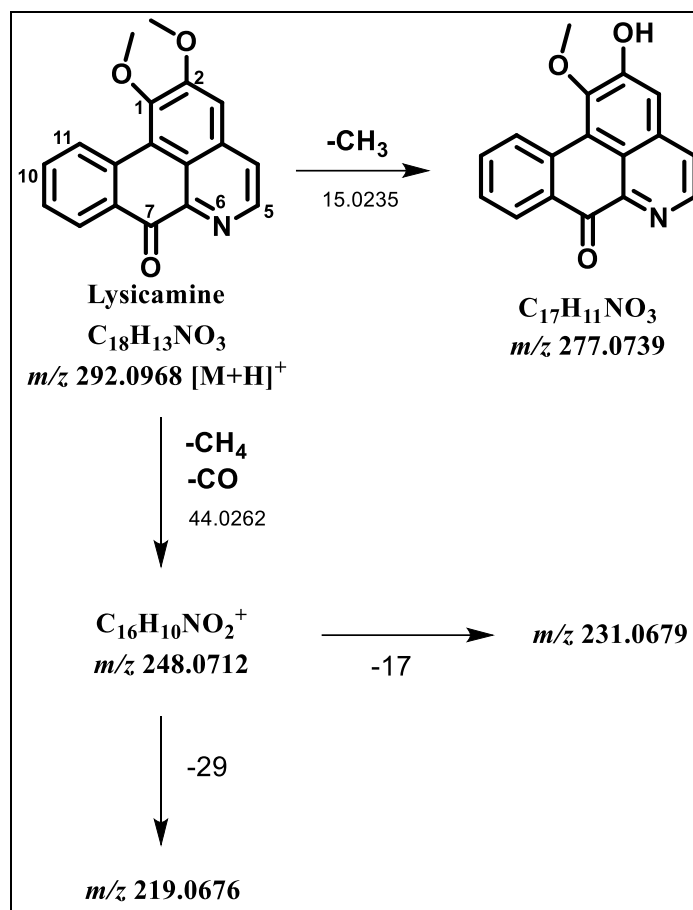


Figure 3- 8 Tentative fragmentation pathways of the lysicamine

6.4. Oxoaporphine Alkaloids

Liriodenine, norushinsinine, anolobine, and anolobine-9-*O*- β -D-glucopyranoside of this group of alkaloids were identified based on comparison with standard compounds. The mass spectrum of these compounds revealed molecular ions at 276.0656, 282.1125, 282.1123 and 444.1653, respectively, corresponding to protonated molecule $[M+H]^+$. The fragmentation of the protonated molecular ion of liriodenine led to product ions of m/z 248.0694, 220.0743, 218.0591, 190.0643.

The product ion at m/z 248 and m/z 220 were formed by successive losses of $-CO$ from the molecular ion at m/z 276. The more abundant product ion at m/z 190.0649 was formed by the loss of a carbonyl and $-CH_3$ groups (Table 3- 1, Figure 3- 9, 3- 10). The UV absorption maximum found to be 200, 255, 277, 330, and 399 nm, corresponds with the oxoaporphine skeleton.

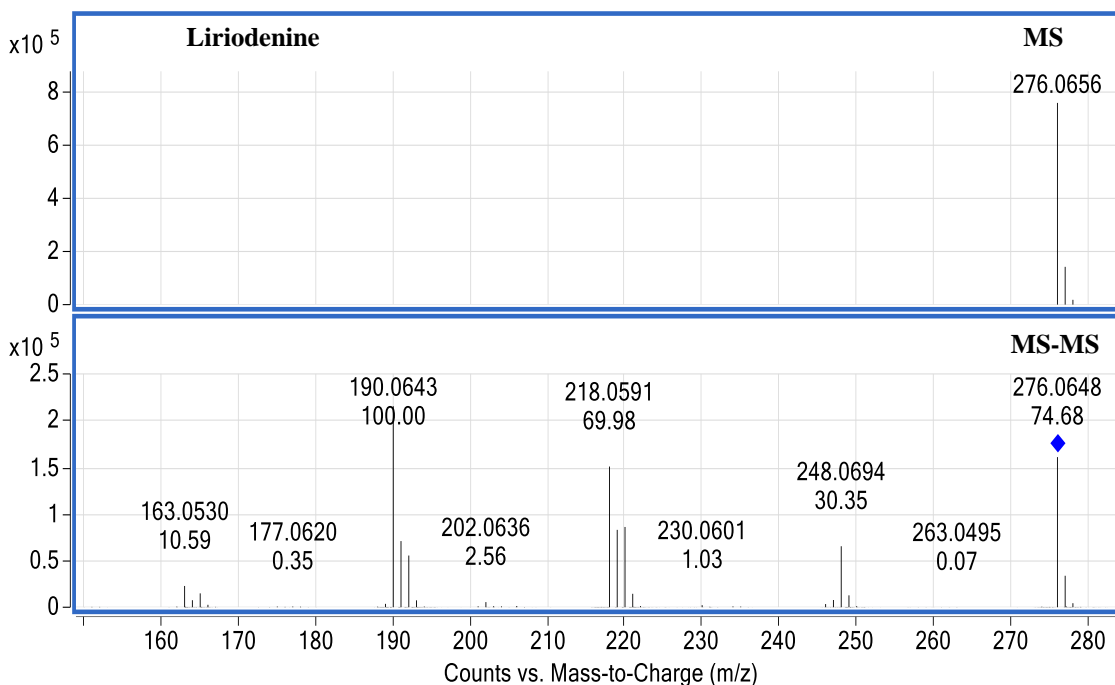


Figure 3- 9 ESI- MS_n spectrum of liriodenine

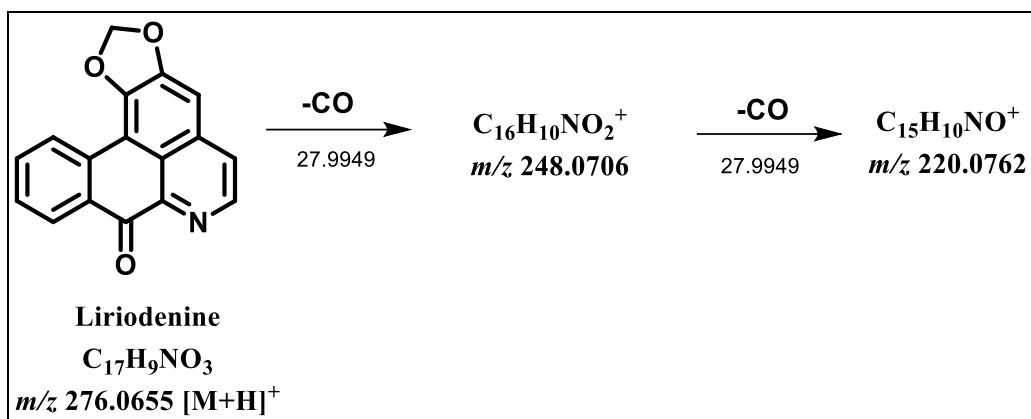


Figure 3- 10 Tentative fragmentation pathways of the liriodenine

Norushinsinine, the fragmentation of the protonated molecular ion at m/z 282.1125 led to successive losses of 18, 30, and 28 Da, which indicate losses of water, $-CH_2O$ and $-CO$ corresponding to product ions of m/z 264.1014, 234.0902, 206.0952, and 179.0845. The more abundant product ion was m/z 206.0952 (**Table 3- 1, Figure 3- 11, 3- 12**). The UV absorption maximum found to be 205, 235, 245, 271, 280, and 318 nm.

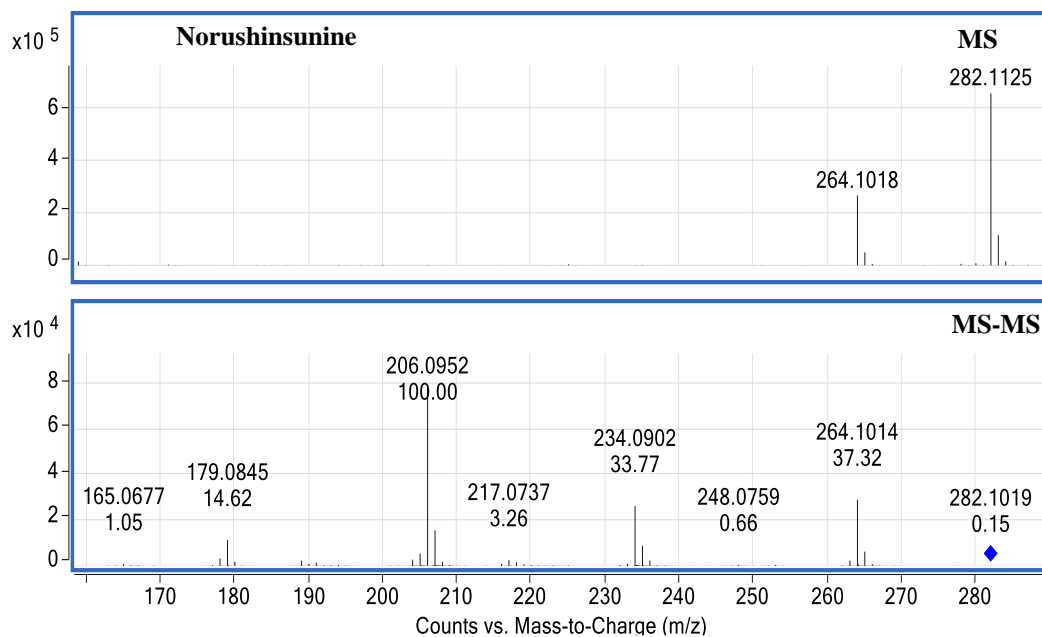


Figure 3- 11 ESI- MS_n spectrum of norushinsinine

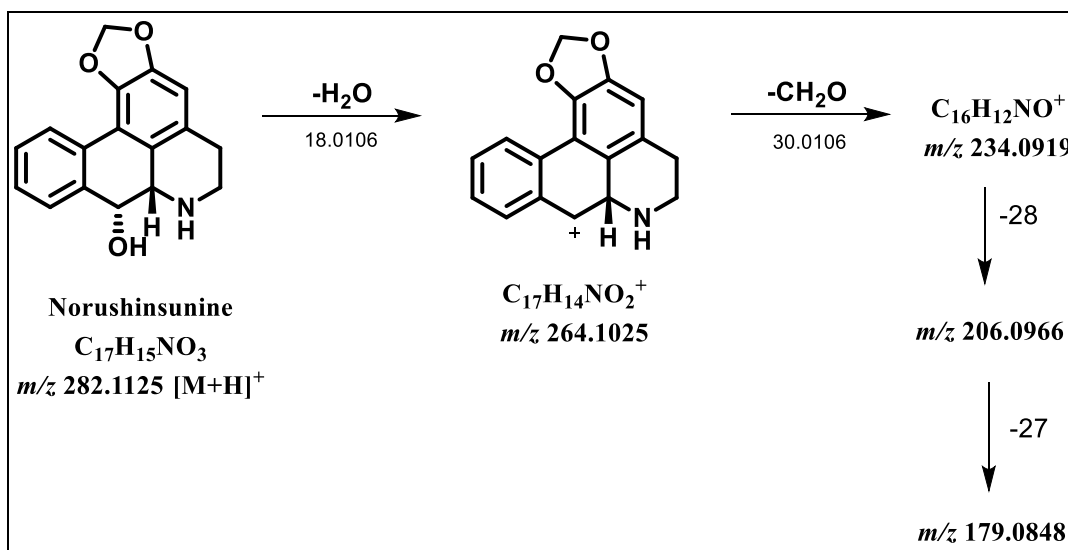


Figure 3- 12 Tentative fragmentation pathways of the norushinsinine

The protonated molecule at m/z 282.1123 (anolobine) presented mass fragment ions at m/z 265.0839, 247.0731, 235.0730, 219.0778, 217.0635, 207.079, 189.0694, and 179.0828 with losses of 17, 18, 28, and 30 Da, corresponding to NH_3 , H_2O , CO , and CH_2O (**Table 3- 1, Figure 3- 13, 3- 14**).

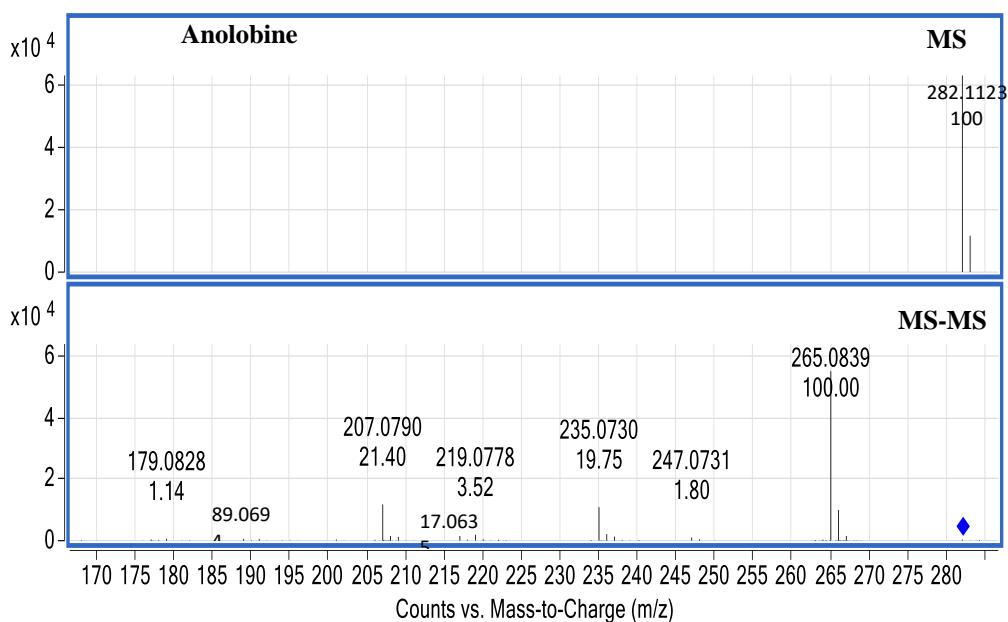


Figure 3- 13 ESI- MS_n spectrum of anolobine

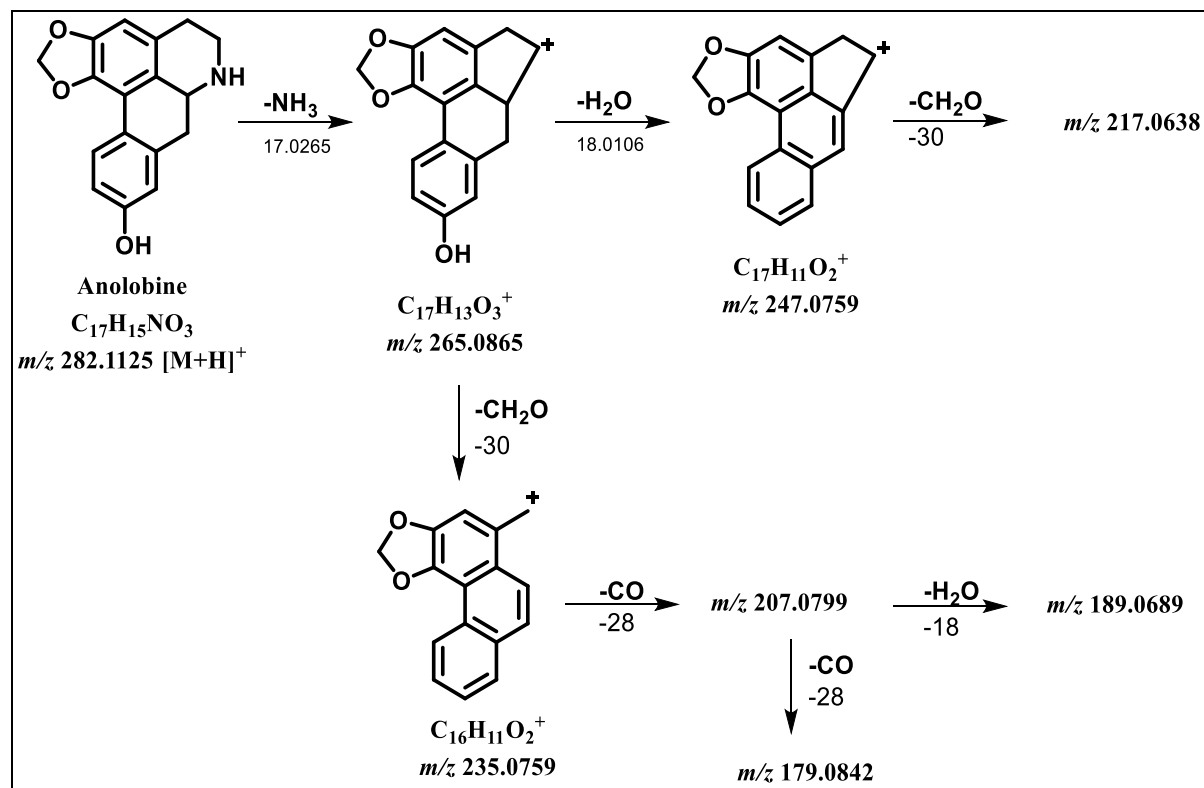


Figure 3- 14 Tentative fragmentation pathways of the anolobine

Anolobine-9-*O*- β -D-glucopyranoside exhibited a protonated molecular ion at m/z 444.1655 ($C_{23}H_{25}NO_8$). The parent ion showed fragment ions at m/z 427.1312 $[M+H-NH_3]^+$ and the ion at m/z 265.0820 $[M+H-NH_3\text{-glucose}]$ indicating a loss of dehydrated hexose ($C_6H_{10}O_5$) moiety. The UV absorption maximum found to be 213, 230, 276, 285, and 320 nm (**Table 3- 1, Figure 3- 15, 3- 16**).

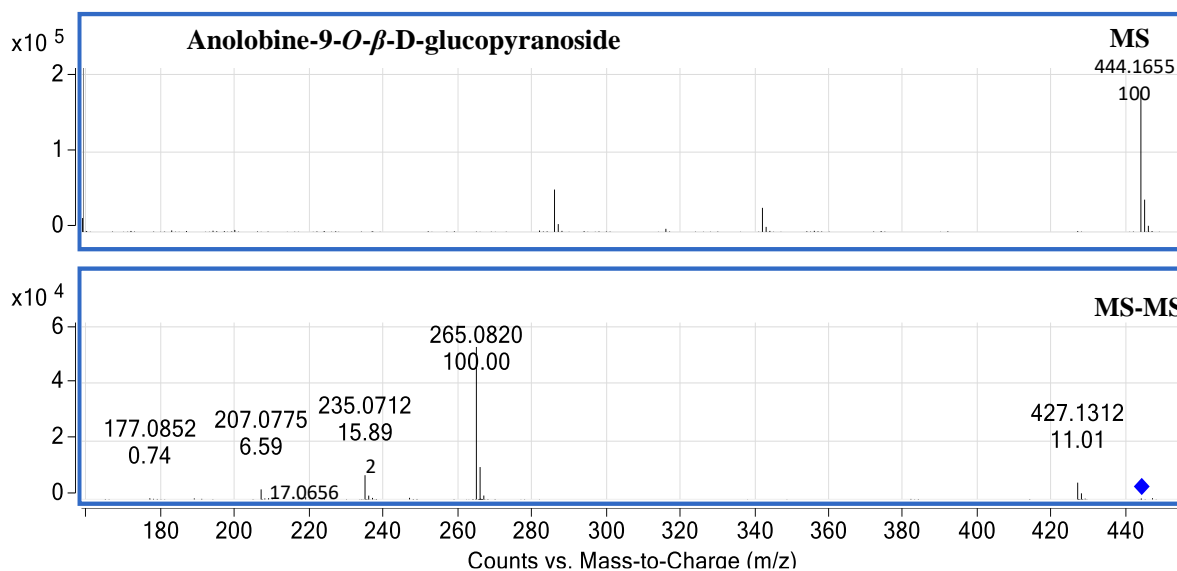


Figure 3- 15 ESI- MS_n spectrum of anolobine-9-*O*- β -D-glucopyranoside

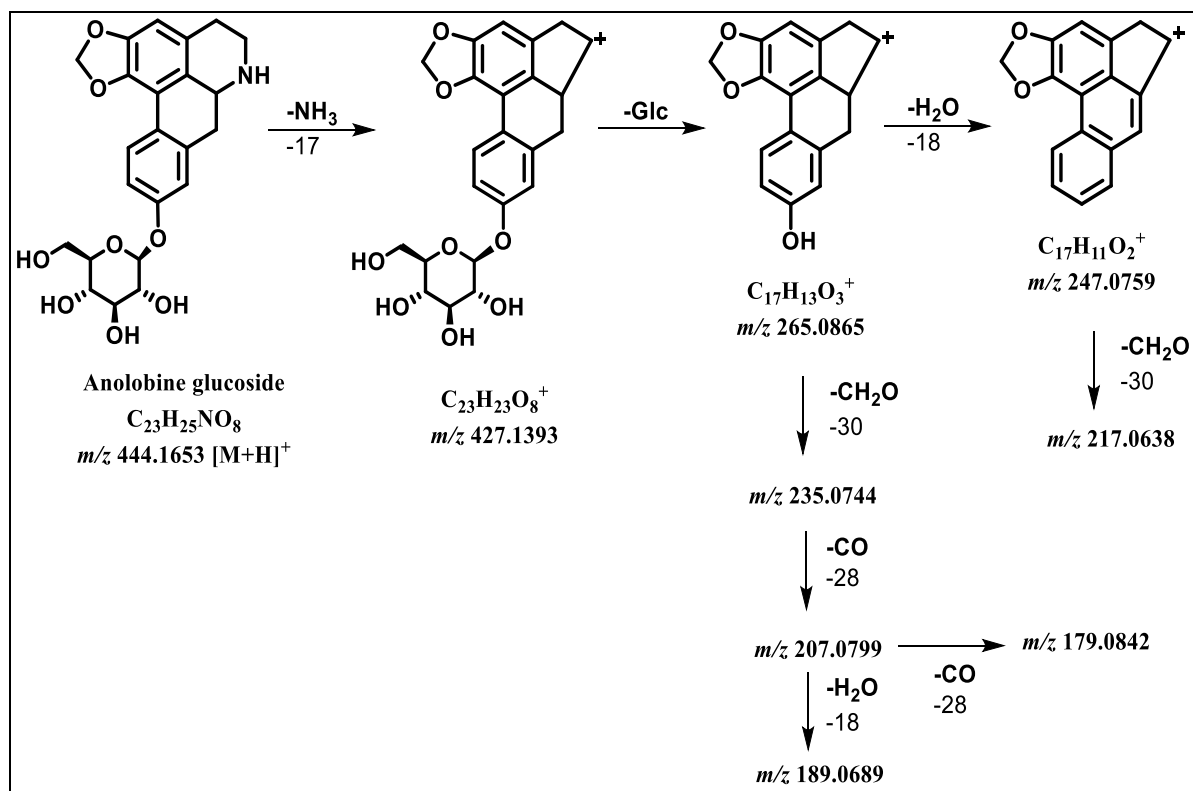


Figure 3- 16 Tentative fragmentation pathways of the anolobine-9-*O*-β-D-glucopyranoside

Twigs and bark of *Asimina triloba* indicated the presence of all eight reference compounds (Table 3- 1, 3- 2). Leaf, stem, and root of *As. parviflora* showed for the presence of six standards. However, anolobine and lysicamine were not detected. Liriodenine, coclaurine, norushinsunine, and stepharine were common to all samples analyzed.

#	Name	<i>Asimina triloba</i> Plant Part						<i>Asimina parviflora</i> Plant Part			
		Mixed	Seed	Bark	Twig/ Bark	Twig	Prod.	Leaf	Stem	Root	
1	Anolobine-9- <i>O</i> - β - D-glucopyranoside	+	+	+	+	+	+	ND	+	ND	
2	Anolobine	+	ND	+	+	+	+	ND	ND	ND	
3	Nornuciferine	+	+	+	+	+	+	ND	+	ND	
4	Norushinsunine	+	+	+	+	+	+	+	+	+	
5	Liriodenine	+	+	+	+	+	+	+	+	+	
6	Lysicamine	ND	ND	+	+	+	+	ND	ND	ND	
7	Stepharine	+	+	+	+	+	+	+	+	+	
8	Coclaurine	+	+	+	+	+	+	+	+	+	

The MS-MS of eight standards were investigated using UV spectra and ESI-MS-MS technique to determine diagnostic ions based on the structural characteristics of alkaloids in *Asimina* species. On the basis of the fragmentation patterns of the secondary, tertiary, and quaternary alkaloids, the alkaloids extracted from *As. triloba* were tentatively identified and characterized using the UHPLC-QToF technique. These compounds comprising of benzyloisoquinoline, aporphine, oxoaporphine, and proaporphine were identified by interpreting the MS-MS spectra based on different alkaloidal structures. Several pharmacological activities for these compounds were previously observed, including anti-acetylcholinesterase, antioxidant, antidepressant, antiepileptic, antimicrobial, antileishmanial, antitrypanosomal, antiplasmodial, antiproliferative, antibacterial, antifungal, antiulcer, cytotoxic, immune-stimulant, and anxiolytic-like (Egydio-Brandão et al., 2017).

7. Conclusion

UHPLC-QToF-MS has been applied to the identification and characterization of alkaloids from *Asimina triloba* and *Asimina parviflora*. The standard compounds were characterized and detected from methanolic extracts of the two *Asimina* species. The compounds were identified by comparing the retention times and the MS and MS/MS data with reference standards. Finally, because of the simple sample preparation and high reproducibility, the developed analytical method would be valuable not only for herbal identification and quality control but would also enhance understanding of the biological activity and their benefits to human health.

Chapter III Copyright

The content of chapter iii has been published in the Journal of Pharmaceutical and Biomedical Analysis. The journal offers reuse of the articles by the author for thesis or dissertation, the permission is not required as shown below.



 **RightsLink**[®] Home ? Help ✉ Email Support Taghreed Majrashi ▼

 **Targeted and non-targeted analysis of annonaceous alkaloids and acetogenins from Asimina and Annona species using UHPLC-QToF-MS**

Author:
Bharathi Avula, Ji-Yeong Bae, Taghreed Majrashi, Tung-Ying Wu, Yan-Hong Wang, Mei Wang, Zulfiqar Ali, Yang-Chang Wu, Ikhlas A. Khan

Publication: Journal of Pharmaceutical and Biomedical Analysis

Publisher: Elsevier

Date: 10 September 2018

© 2018 Elsevier B.V. All rights reserved.

Please note that, as the author of this Elsevier article, you retain the right to include it in a thesis or dissertation, provided it is not published commercially. Permission is not required, but please ensure that you reference the journal as the original source. For more information on this and on your other retained rights, please visit: <https://www.elsevier.com/about/our-business/policies/copyright#Author-rights>

BACK CLOSE WINDOW

© 2019 Copyright - All Rights Reserved | [Copyright Clearance Center, Inc.](#) | [Privacy statement](#) | [Terms and Conditions](#)
Comments? We would like to hear from you. E-mail us at customer-care@copyright.com

The reference of the full article is:

Avula B, Bae J, Majrashi T, et al. Targeted and non-targeted analysis of annonaceous alkaloids and acetogenins from Asimina and Annona species using UHPLC-QToF-MS. *Journal of Pharmaceutical and Biomedical Analysis*. 2018;159:548-566.

CHAPTER IV
CYTOTOXIC AND NEUROTOXIC POTENTIAL OF ALKALOIDAL CONSTITUENTS OF
ASIMINA TRILOBA

1. Introduction

Annonaceae is the largest plant family of the magnoliales, which has over 120 genera and about 2,100 species (Aminimoghadamfarouj et al., 2011; Brannan et al., 2018). Plants belonging to the Annonaceae family are found mainly in the tropics or subtropics (Leboeuf et al., 1980), except the *Asimina* genus that extends into temperate regions (Hormaza, 2014). Some of the Annonaceae species are important in folk medicine. They have been used to treat various cancers (Quílez et al., 2018), and many of them have valuable economic importance as a source of large and pulpy edible fruits, such as pawpaw (*Asimina triloba*), custard apple (*Annona cherimola*), sugar apple (*Annona squamosa*), graviola (*Annona muricata*) and biriba (*Rollinia mucosa*) (Rasai et al., 1995).

Annonaceae plants contain a broad spectrum of biologically active acetogenins that have displayed antitumor, antimalarial, anthelmintic, pesticidal, antiviral, and antimicrobial effects (Alali et al., 1998; Coothankandaswamy et al., 2010; McLaughlin, 2008; Pomper et al., 2009) and have been used for the treatment of various medical conditions. Also, Annonaceae plants contain different sub-classes of alkaloids that are derived from isoquinoline class, including, benzyl-tetrahydroisoquinolines, protoberberines, proaporphines, aporphines, oxoaporphines, and other miscellaneous isoquinolines (Cave, 1985).

The popularity of the Annonaceae plants and their potential health effects (especially their anticancer activities) has grown in recent years, despite studies that have shown the development of atypical parkinsonism in people who consume large amounts of annonaceous products (McLaughlin, 2008; Stamelou et al., 2010). The underlying neurotoxicity related to chronic consumption has been linked to some acetogenins (e.g., annonacin) and alkaloids (e.g., coreximine and reticuline) found in different Annonaceae plants such as *Annona muricata* (Lannuzel et al., 2002; Potts et al., 2012). Annonacin, the most abundant acetogenin in *A. muricata*, has been shown to cause neuronal loss and accumulation of phosphorylated tau protein in cultured neurons (Escobar-Khondiker et al., 2007; Hollerhage et al., 2009).

Some isoquinoline alkaloids, obtained from various species of Annonaceae, show dopamine receptor antagonistic activity as well as neuronal cell death (Zhang et al., 2007). The potential risks of neurodegeneration associated with chronic consumption of the fruits and leaves from Annonaceae plants emphasized the need for further studies to determine and identify the neurotoxic compounds in these edible plants and compare their risk to their benefits in defeating cancer.

The present investigation is focused on *Asimina triloba*, commonly known as pawpaw. This is one of the Annonaceae plant species that is attributed to treating cancer, and its extract has been found to be the most potent of 3,500 species of higher plants screened for bioactive compounds (McLaughlin, 2008). It is native to North America, and it is the only species of Annonaceae with edible fruits that grows in the temperate regions. Pawpaw and many other plants of this species are consumed either as fresh fruits or processed into ice creams, juices, liquors, and many other products. It is also currently marketed as a dietary supplement for its potential use in alternative cancer treatment (Coothankandaswamy et al., 2010).

This study was carried out to explore the cytotoxic and neurotoxic constituents of the plant with the intention that separating the neurotoxic constituents would help in reducing the adverse/undesirable effects of the plant if it is used as an alternative therapy. Although much effort has been directed in the past towards the acetogenins constituents, and it has been well-established that cytotoxic potential of this plant is due to the presence of acetogenins. However, the alkaloidal constituents of *Asimina triloba* have not been explored in terms of cytotoxicity and neurotoxicity. Therefore, we focused on determining the cytotoxicity and neurotoxicity of three different extracts of *A. triloba*: a crude methanolic extract (MeOH), an acetogenin-rich extract (ACG), and the alkaloid-rich extract (ALK). Additionally, we explored six alkaloids isolated from ALK extract to understand how the presence and the absence of the alkaloids and acetogenins will affect the biological properties of this plant.

2. Materials and methods

2.1. Plant material

The three extracts (MeOH extract, ALK extract, and ACG extract) were prepared as reported before (Majrashi et al., 2018). Briefly, the plant material was extracted with methanol and then subjected to the acid-base alkaloidal extraction. In brief, the MeOH extract was suspended in 2% HCl and extracted with ethyl acetate (EtOAc). After separating the EtOAc layers, the pH of the resulting aqueous acidic layer was basified with ammonia solution and subsequently extracted again with EtOAc. The combined EtOAc layers were dried to give an alkaloidal rich extract, which was fractionated by column chromatography to obtain the pure alkaloids. The structures of the alkaloids (anolobine-9-O- β -D-glucopyranoside, anolobine, norushinsunine, liriodenine, squamolone and coclaurine) isolated from alkaloid rich fraction are shown in **Figure 4- 1**.

The identity and purity of these alkaloids were confirmed by chromatographic (TLC, HPLC) methods and by the analysis of the spectral data (IR, 1D- and 2D-NMR, ESI-HRMS). A detailed description has been reported by us earlier (Majrashi et al., 2018; Avula et al., 2018).

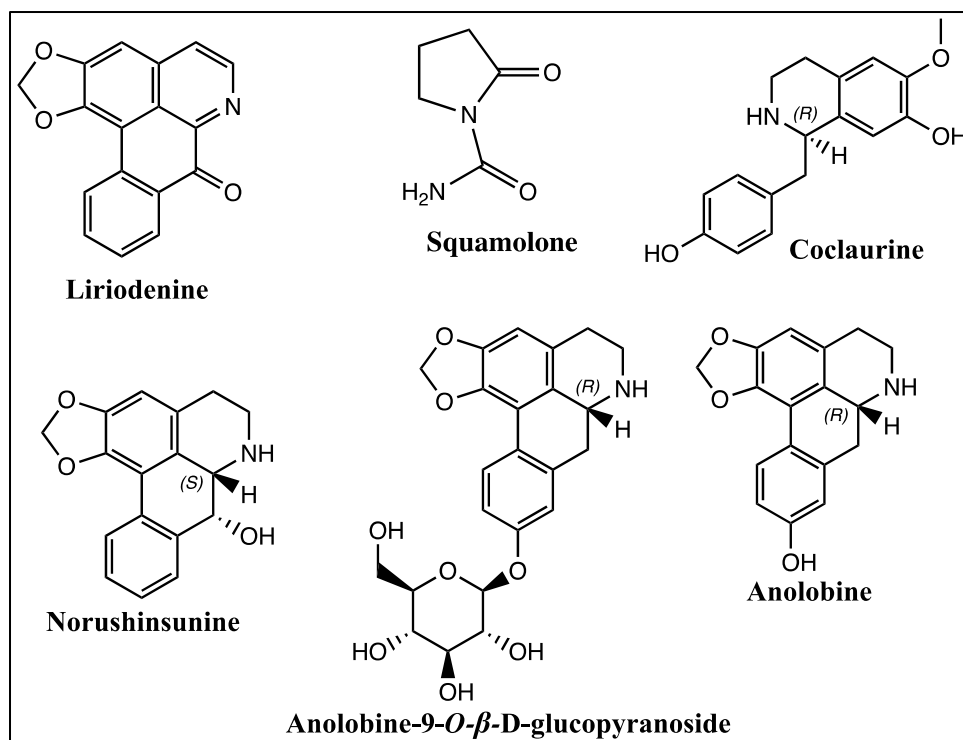


Figure 4- 1 Chemical structures of alkaloids from *Asimina triloba*

2.2. Cytotoxicity assay

The cytotoxic activity of the various extracts and pure compounds was determined towards a panel of four human solid tumor cell lines: melanoma (SK-MEL), epidermal carcinoma (KB), breast carcinoma (BT-549), and ovarian carcinoma (SK-OV-3). Moreover, non-cancer kidney cell lines (LLC-PK1 and VERO) were also employed to determine if the anti-cell proliferative activity of these extracts and compounds was selective for the tested tumor cell lines.

All cell lines were obtained from the American Type Culture Collection (ATCC, Rockville, MD). The cells were seeded in 96-well plates (10,000 cells/well) and incubated for 24 h. The three extracts and six pure alkaloids from *Asimina triloba* were dissolved in DMSO, diluted in media, and added to the cells at concentrations of 50, 25, 12.5, 6.25, 3.125 $\mu\text{g}/\text{mL}$. After incubating for 48 hrs, cell viability was determined by using a tetrazolium dye WST-8, which is converted to a water-soluble formazan product in the presence of 1-methoxy PMS by the activity of cellular enzymes. The color of the formazan product was measured at 450 nm on a plate reader. Doxorubicin was used as a positive control for cytotoxicity assay, and DMSO (0.25%) was used as the vehicle control. The IC₅₀ values were obtained from concentration-response curves. The values are represented as mean \pm standard deviation (n = 3).

2.3. Neurons isolation

Primary cortical neurons were isolated from embryonic day 18-19 Sprague Dawley male and female rats and were cultured as previously described (Ashpole et al., 2011). Briefly, cortical cells were dissected and mechanically and enzymatically dissociated with trituration and papain, respectively. The cells were suspended in a neurobasal media with serum and plated on poly-lysine coated 24-well or 96-well plates. The total number of neurons used was 125,000 per well. After 24 hours, the media was replaced with neurobasal media supplemented with B27 and penicillin and streptomycin. The cultured neurons were maintained in an incubator at 37 °C and were treated following 8–10 days in culture. All experiments were overseen and approved by the University of Mississippi IACUC (protocol 16-024).

2.4. Neurotoxicity assay

The neurotoxicity evaluation was performed in 8-10 day old rat cortical neurons. The extracts and compounds were added to neuronal growth media (neurobasal, B27, penicillin, and streptomycin) in the following range of concentrations (10, 5, 1, and 0.1 $\mu\text{g/mL}$) and incubated for 24 hrs. DMSO (0.1%) was used as vehicle control. The MTS assay was used to assess the toxicity of the extracts and compounds. MTS Aqueous One Solution Reagent was added after incubating the extracts, compounds, and the control for 24 hrs. Once the MTS was administered to the wells, the plates were put back into the incubator for 1-2 hrs. The formazan dye produced by viable cells was quantified by measuring the absorbance at 490 nm. LIVE/DEAD viability stains (Invitrogen) was used to verify living and cytotoxic cells in a controlled study. Stained cells were quantified by the Nikon Elements software following image acquisition on the Nikon HCA inverted fluorescent microscope (100x) in a single field per well, chosen at random by the software.

2.5. Statistical analysis

A one-way ANOVA was used to perform statistical analysis followed by Dunnett's post hoc test to examine the significant difference against the control at $p < 0.05$ for each dose of a compound or extract.

3. Results

3.1. Cytotoxicity

The cytotoxic potential of the three extracts and six alkaloids (**Figure 4- 1**) was evaluated in terms of their anti-cell proliferative activities in a panel of cell lines, as shown in **Table 4- 1**. Among the three extracts, the acetogenin-rich extract (ACG) showed the most potent anti-

proliferative activity towards melanoma (SK-MEL), epidermal carcinoma (KB), and breast ductal carcinoma (BT-549) cells with IC50 values of 0.09, 0.11, and 0.11 $\mu\text{g/mL}$, respectively. The extract was equally potent towards both non-cancer kidney cell lines (LLC-PK1 and VERO) with IC50 values of 0.12 and 0.31 $\mu\text{g/mL}$. The extract rich in alkaloids (ALK) also showed cytotoxic activity towards SK-MEL, KB, and BT-549 cells, and the IC50 values were 1.9, 2.6, and 1.7 $\mu\text{g/mL}$, respectively. The ALK extract was comparatively less toxic (14 X) to VERO cells (IC50 4.25 $\mu\text{g/mL}$) than the ACG extract. This is the first report of the anti-cell proliferative activity of the ALK extract from *Asimina triloba*. Interestingly, the MeOH extract was more potent than ALK extract towards KB and BT-549 cells (IC50 = 0.6 and 0.55 $\mu\text{g/mL}$, respectively), but less potent than ALK extract towards SK-MEL cells (IC50 = 7.1 $\mu\text{g/mL}$). It was worth noting that MeOH extract was much less potent than ACG extract towards all the cell lines. Both MeOH and ALK extracts were much less toxic to VERO cells in comparison to ACG extract. None of the extracts were effective towards ovarian cancer cells (SK-OV-3), indicating selectivity of cytotoxic potential among various cancers.

Among the alkaloids, liriodenine was the most effective towards all cancer cells with IC50 of 2.15, 6.3, 9.5, and 4.75 $\mu\text{g/mL}$ for SK-MEL, KB, BT-549, and SK-OV-3 cells, respectively. Another alkaloid, norushinsunine, also demonstrated activity against all cancer cells with IC50 values in the range of 9.75 – 23 $\mu\text{g/mL}$. This is the first report of the cytotoxic activity of this compound. This compound was much less toxic to VERO cells in comparison to liriodenine. Anolobine-9-O- β -D-glucopyranoside, which is a newly isolated alkaloid from *Asimina triloba* (Majrashi et al., 2018), was also effective against SK-MEL and KB cell lines with IC50 values of 31.5 and 47.5 $\mu\text{g/mL}$. However, the activity was weaker than the other two alkaloids.

Anolobine, squamolone, and coclaurine were not active to any of the cancer cells at the highest tested concentration of 50 µg/mL.

Table 4- 1 Anti-cell proliferative activity of extracts and compounds against a panel of cell lines.						
	IC50 µg/mL					
Sample Name	Cancer Cell Lines				Non-cancer Kidney Cell Lines	
	SK-MEL	KB	BT-549	SK-OV-3	LLC-PK ₁	Vero
MeOH extract	7.1 ± 1.25	0.6 ± 0.0	0.55 ± 0.05	NA	0.2 ± 0.06	19.0 ± 1.0
ACG extract	0.09 ± 0.01	0.11 ± 0.01	0.11 ± 0.02	NA	0.12 ± 0.04	0.31 ± 0.01
ALK extract	1.9 ± 0.1	2.6 ± 0.1	1.7 ± 0.3	NA	1.5 ± 0.3	4.25 ± 0.25
Norushinsunine	16.0 ± 1.0	9.75 ± 2.25	19.5 ± 0.5	23.0 ± 2.0	7.75 ± 0.25	>25
Squamolone	NA	NA	NA	NA	NA	NA
Coclaurine	NA	NA	NA	NA	NA	NA
Anolobine-9-O-β-D-glucopyranoside	31.5 ± 6.5	47.5 ± 2.5	>50	>50	NA	NA
Anolobine	NA	NA	>50	NA	NA	NA
Liriodenine	2.15 ± 0.15	6.3 ± 0.4	9.5 ± 0.5	4.75 ± 1.05	6.0 ± 1.0	8.1 ± 0.1
Doxorubicin	1.3 ± 0.5	1.7 ± 0.42	1.4 ± 0.40	1.7 ± 0.47	0.4 ± 0.56	>5

NA= no activity at the highest test concentration (50 µg/mL).

3.2. Neurotoxicity

Among the three extracts of *A. triloba*, the MeOH extract and ACG extract showed toxicity to neuronal cells at 10 µg/mL causing a 40% and a 20% decrease in cell viability, respectively (**Figure 4- 2A-B, and 4- 5**). The alkaloidal extract was not toxic at the highest tested concentration of 10 µg/mL but showed a 20% decrease in viability at lower concentrations (**Figure 4- 2C**). Four alkaloids, namely norushinsunine, liriodenine, anolobine, and anolobine-9-*O*-β-D-glucopyranoside, decreased cell viability significantly at 10 µg/mL, as shown in **Figure 4- 5**. Anolobine-9-*O*-β-D-glucopyranoside demonstrated a strong effect at 1 µg/mL, and no further reduction in cell viability was noticed with higher concentrations of 5 and 10 µg/mL, as shown in **Figure 4- 3A**.

However, Anolobine (the aglycone) was less effective in reducing cell viability of neuronal cells (**Figure 4- 3B**). Norushinsunine exhibited significant toxicity at 10 µg/mL (**Figure 4- 4A**). On the other hand, Liriodenine demonstrated a dose-dependent reduction in the cell viability in the concentration range of 1 – 10 µg/mL, as shown in **Figure 4- 4B**. Coclaurine and squamolone did not show a significant decrease in cell viability (**Figure 4- 3C and 4C**). To summarize the data, all of the extracts and alkaloids were combined in a bar graph to display their effects at the highest tested concentration of 10 µg/mL (**Figure 4- 5**).

Figure 4- 2 Effect of the MeOH extract, ACG extract and ALK extract on neuronal cell viability.

MeOH extract (**A**) and ACG extract (**B**) showed a significant concentration-dependent decrease in cell viability. ALK (**C**) extract did not show a significant reduction in cell viability with the increasing concentrations.

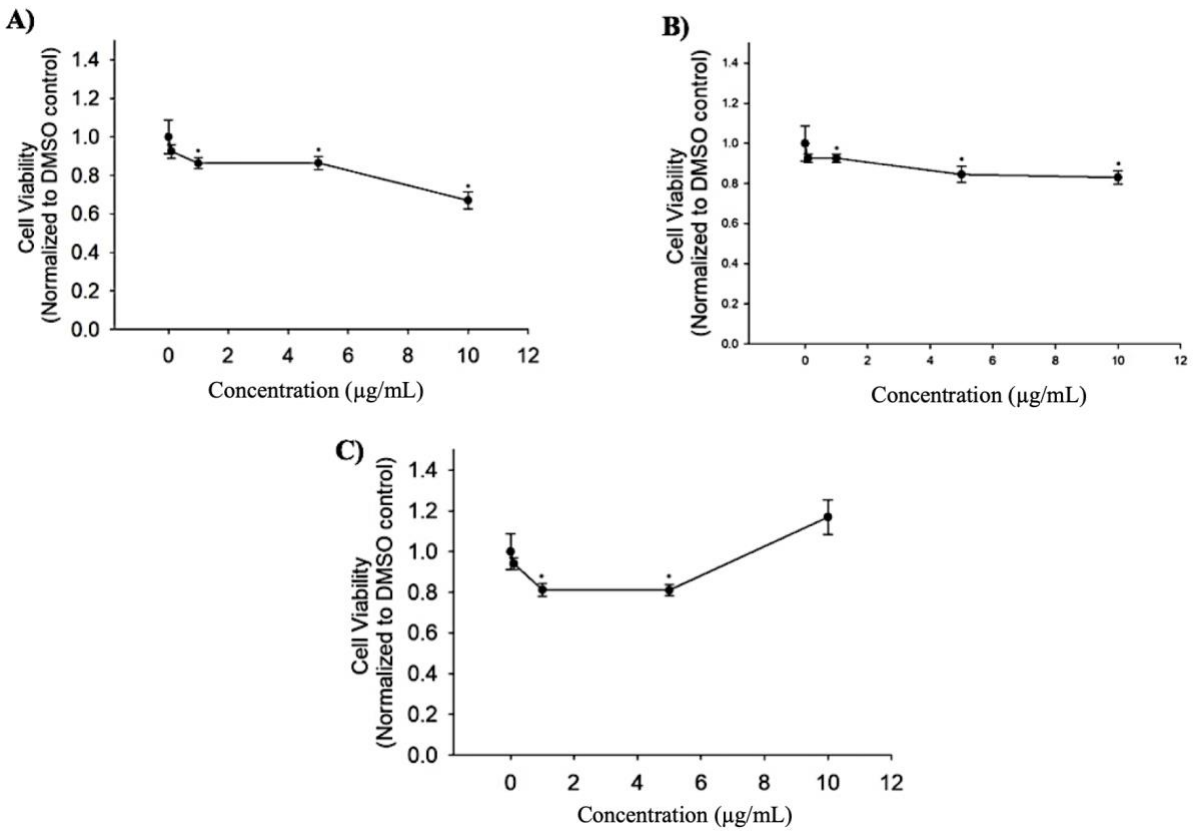


Figure 4- 3 Effect of anolobine-9-*O*- β -D-glucopyranoside, anolobine and coclaurine on neuronal cell viability.

Anolobine-9-*O*- β -D-glucopyranoside (**A**) and Anolobine (**B**) demonstrated a significant concentration-dependent reduction in cell viability. Coclaurine (**C**) did not show a significant concentration-dependent decrease in cell viability.

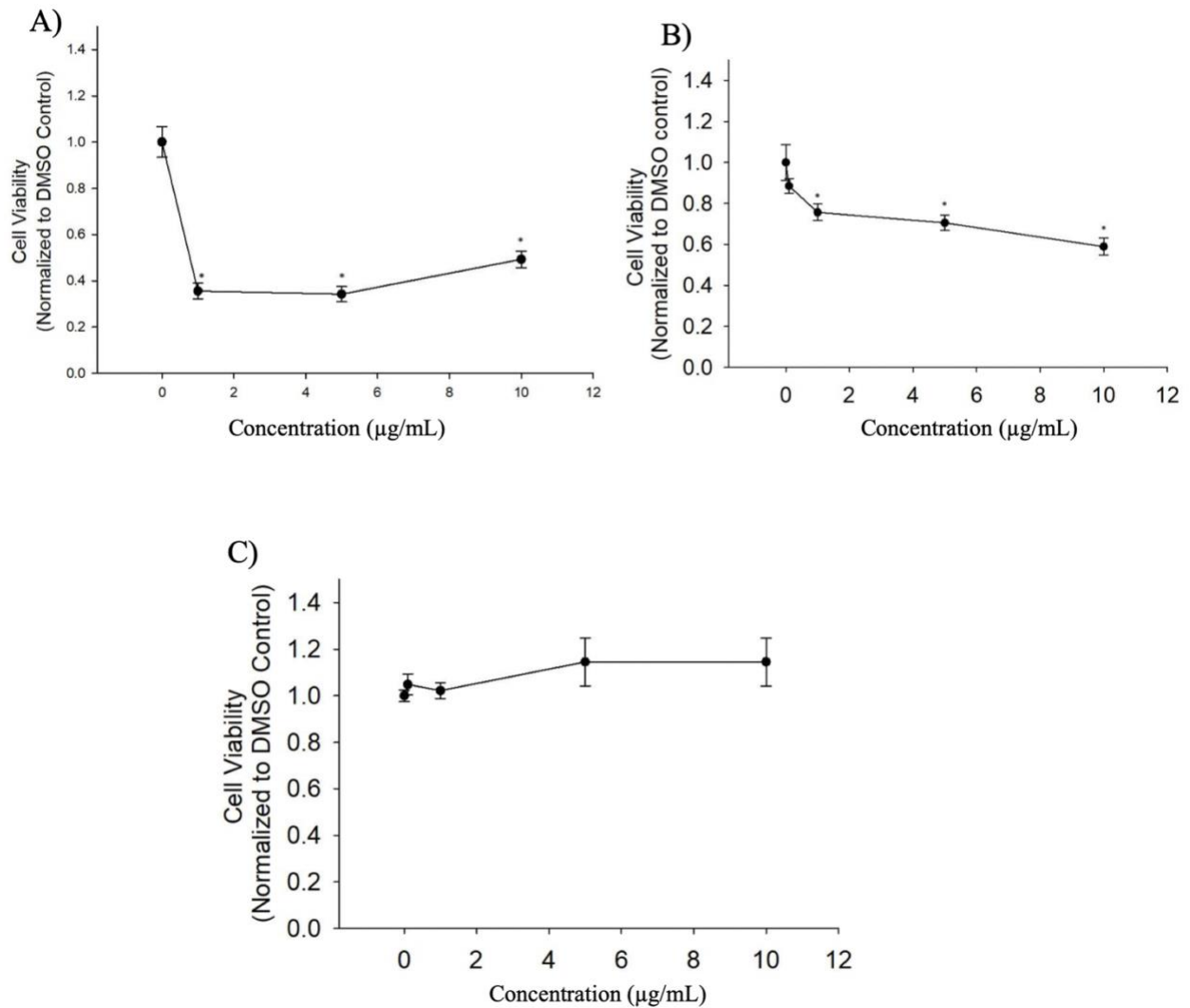


Figure 4- 4 Effect of norushinsunine, liriodenine and squamolone on neuronal cell viability.

Norushinsunine (**A**) and Liriodenine (**B**) displayed a significant reduction in cell viability with increasing concentration. However, Squamolone (**C**) did not show a significant concentration-dependent decrease in cell viability.

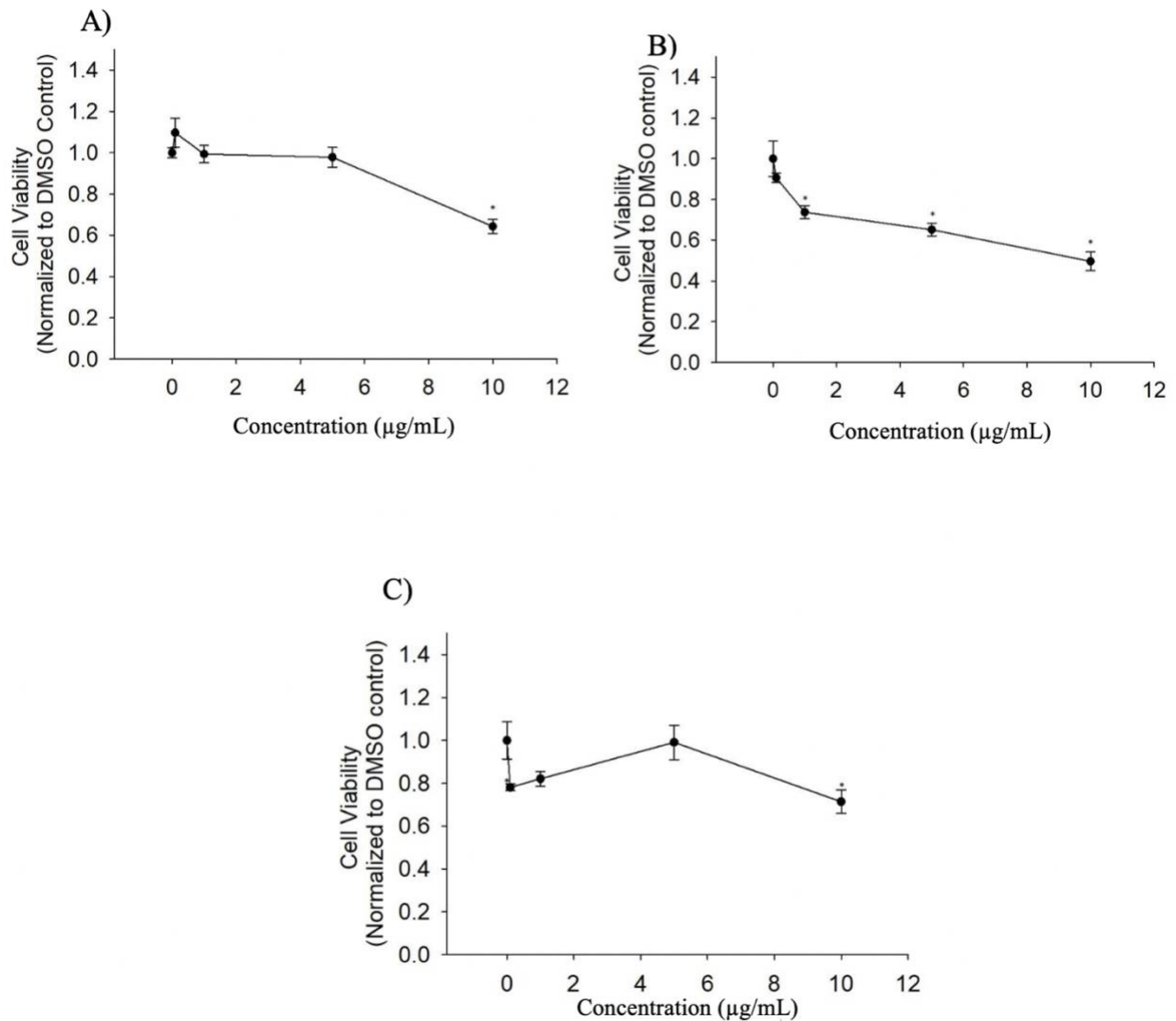
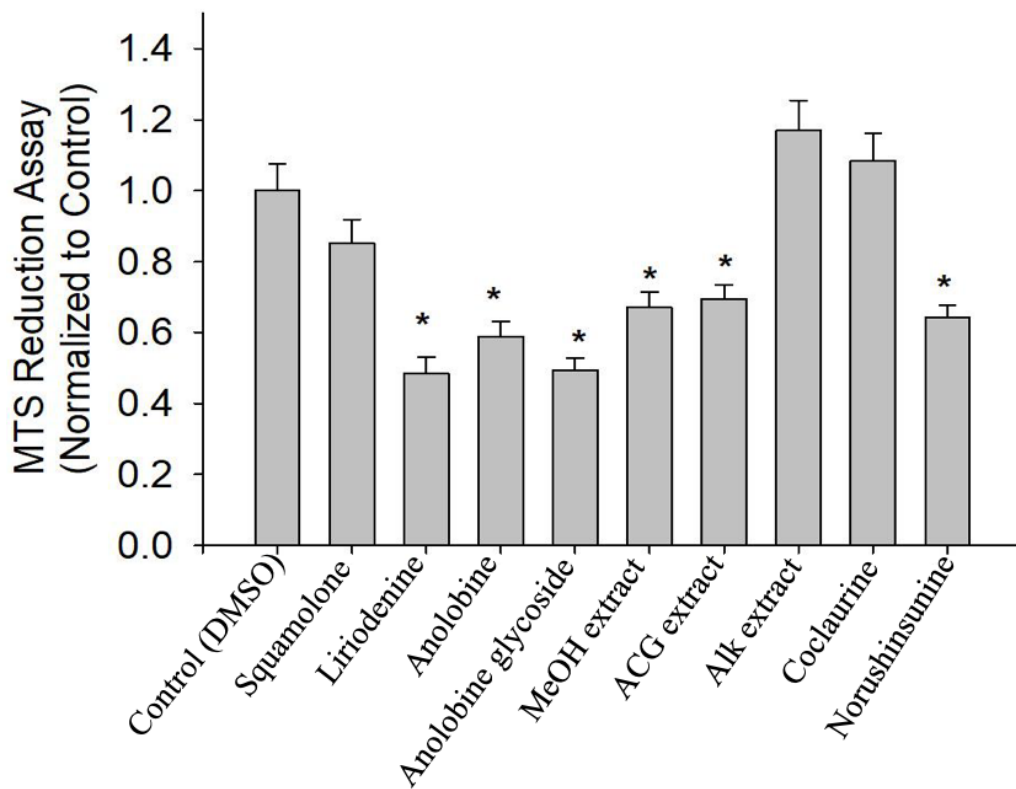


Figure 4- 5 Effect of Extracts and pure compounds on cell viability at 10 $\mu\text{g}/\text{mL}$. Asterisks designate statistically significant decreases in cell viability compared to vehicle control.



4. Discussion

Among all tested extracts, the ACG extract was the most potent in inhibiting cell proliferation of all cell lines, except SK-OV-3. However, the same extract was found to be significantly toxic to the neurons as well, which might affect its benefit in treating cancer. Interestingly, the ALK extract showed cytotoxicity that has not been reported before towards SK-MEL, KB, and BT-549 cells with IC50 values in a lower concentration range (1.7-2.6 $\mu\text{g/mL}$).

Regardless, the toxic effects of some of the pure alkaloids on the neurons, our study showed that ALK extract did not show a significant decrease in cell viability at 10 $\mu\text{g/mL}$, which might be a result of an antagonistic effect of combined alkaloids in which the combination of the alkaloids shows less effect than the individual compound. Almost all of the previous studies in *A. triloba* have focused on the acetogenins and their potential effects in cancer treatment. Acetogenins from *A. triloba* have shown different biological activities, including antibacterial, antifungal, anticancer, and insecticidal effects (Cuendet et al., 2008).

The acetogenins are known for their potent inhibitory effect of mitochondrial (complex I) and cytoplasmic (anaerobic) production of adenosine triphosphate (ATP), induces tumor cell apoptosis, programmed cell death (McLaughlin, 2008). Annonacin, an acetogenin with a monotetrahydrofuran ring, has been reported to inhibit the growth estrogen receptor- α (ER α)-positive breast cancer cell line (MCF-7) (Ko et al., 2011; Yuan et al., 2003). Moreover, many studies have illustrated the anti-tumor effect of other acetogenins as well such as bullatacin, asimicin, and trilobacin against various cancers including gastric cancer (Liet al., 2017), colon cancer (Zhao et al., 1994), prostate cancer and pancreatic cancer (Zhao et al., 1996).

The biological evaluation of the alkaloidal constituents of *A. triloba* has not been taken into consideration before. Nonetheless, the alkaloids are one of the most important secondary

metabolites that are known to possess therapeutic properties that one cannot ignore. Some of the isoquinoline alkaloids from other Annonaceae plants have been reported for significant anticancer activities. For example, the oxoaporphine alkaloid liriodenine has manifested cytotoxic effects in several cancer cell lines, including the adenocarcinoma of the liver (Hsieh et al., 2005), colon cancer (Chen et al., 2012), and human lung adenocarcinoma (Chang et al., 2004). In our study, liriodenine illustrated interesting cytotoxicity towards all of the tested cancer cell lines (including SK-OV-3), with greater activity towards the human melanoma (SK-MEL) cell line with an IC₅₀ of 2.15 µg/mL.

A previous study has reported that squamolone showed significant cytotoxicity towards hepatocarcinoma cell lines (Hsieh et al., 2001). However, this alkaloid did not display any activity towards any of the cancer cell lines in our study, indicating specificity for a particular cell line. To the best of our knowledge, the cytotoxicity and neurotoxicity evaluations of the alkaloidal extract of *A. triloba* twigs and the pure alkaloids (anolobine-9-O-β-D-glucopyranoside, anolobine, norushinsunine, and coclaurine) have not been reported before.

The previous neurotoxicity studies of *A. triloba* have focused on the neurotoxic acetogenin (annonacin), which has been found to induce nigral neuron death (Escobar-Khondiker et al., 2007; Lannuzel et al., 2002; Lannuzel et al., 2003). Furthermore, one study has reported that annonacin (30.07 µg/mL) and crude EtOAc extract of *Asimina triloba* fruit pulp (47.96 µg/mL) induced 50% death of cortical neurons (Potts et al., 2012).

5. Conclusion

Our study highlighted the contribution of the alkaloidal constituents in the neurotoxicity of *A. triloba*. However, our results are not conclusive on the neurotoxicity of *A. triloba* alkaloids.

Further studies are warranted, such as addressing the bioavailability of neurotoxic compounds *in vivo*. Moreover, the effects of these extracts and compounds on neuronal tumors of the central nervous system have not been reported. This estimation would be insightful for future studies, which suggests that the neurotoxic compounds and extracts from *A. triloba* might be beneficial in the fight against neuronal-based cancer.

CHAPTER V

SYNTHESIS OF SOME ALKALOIDS REPORTED FROM *ROLLINIA MUCOSA* AND EVALUATION OF THEIR BIOLOGICAL ACTIVITIES

1. Introduction

Rollinia mucosa is a tropical fruit tree belonging to the Annonaceae family and known as biriba. *Rollinia* fruit has been used traditionally in the West Indies and Indonesia for the treatment of tumors (Hartwell 1982) as well as for nutritious purposes (Shi et al. 1997). In Brazil, the alkaloidal extract of *Rollinia mucosa* exhibited antimicrobial and antifungal activities (Caetano and Dabun, 1987). In Brazil and Peru, the lignans isolated from this species were reported to be effective in enhancing the toxicity of a wide variety of insecticides (Paulo et al., 1991).

Rollinia mucosa is native to the western Amazon region of Peru and Brazil in South America. *Rollinia mucosa*'s seeds from Brazil were sent to the United States and the Philippines in the early 1900s., and now they are mostly found in Indonesia (Love and Paull 2011). Its chemical composition and pharmacological activities have been described previously (Caetano and Dabun, 1987; Chen et al. 1996; Liaw et al., 1999; Paulo et al. 1991). This species contains a wide range of compounds including, acetogenins, aporphine alkaloids, steroids, lignans, tryptamine and fatty acid derivatives, which have been isolated and identified from different parts of this plant (Chen et al. 1996; Liaw et al., 1999; Paulo et al. 1991).

The phytochemical investigations of the alkaloidal constituents of *Rollinia mucosa* have revealed several aporphine alkaloids, including N-methoxycarbonyl aporphines that exhibited significant inhibition of collagen, arachidonic acid, and platelet activating factor-induced platelet aggregation (Kuo et al. 2001).

A previous study indicated that *Rollinia mucosa* fruit pulp has similar neurotoxicity to graviola, although it has a significantly less amount of the neurotoxic acetogenins that are found in graviola (Höllerhage et al. 2015). The study highlighted that the neurotoxicity of *Rollinia mucosa* fruit could be linked to other not quantified toxins. We hypothesize that the N-methoxycarbonyl aporphine alkaloids, which have been isolated from *Rollinia mucosa*, have cytotoxic effects and may also be responsible for the neurotoxicity that has been reported from the ethyl acetate extract taken from the fruits and seeds of *Rollinia mucosa* (Höllerhage et al. 2015).

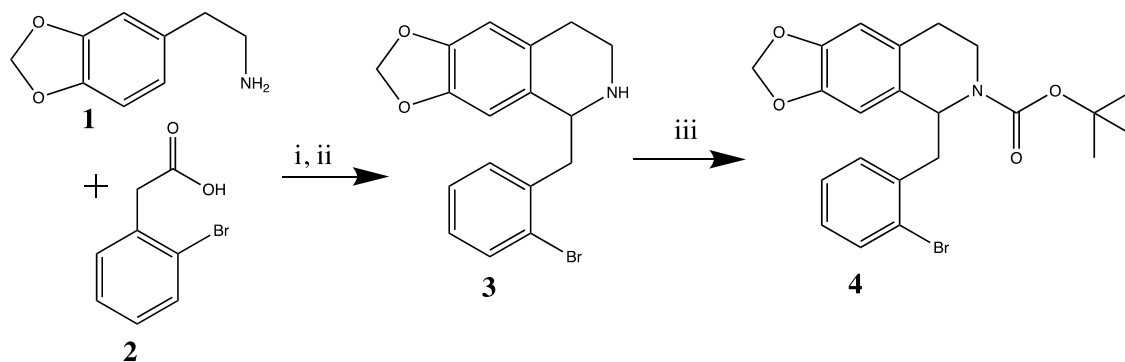
The cytotoxicity and the neurotoxicity of these alkaloids have not been reported before. Therefore, our study aims to understand how they contribute to the biological activities of this plant. (R, S) (\pm) Romucosine, N-methoxycarbonyl aporphine alkaloid (Chen et al. 1996), and other relative compounds will be obtained through the total synthesis in order to get a better yield because this type of alkaloid is usually isolated in meager amounts. That will allow us to gain enough quantities of the desired compounds that will be subjected to different biological screening, including cytotoxicity and neurotoxicity, to identify their biological properties and safety. Herein, we describe the total synthesis of (\pm) anonaine, 3,4-methylenedioxy-1-phenanthreneethylamine, (\pm) romucosine, and [2-(3,4-methylenedioxy-1-phenanthrenyl)ethyl]-methylcarbamate by using direct arylation reactions with 3,4-methylenedioxyphenethylamine **1** and 2-bromophenylacetic acid **2** in the preparation of these alkaloids.

We also describe the separation of the enantiomers using different resolution reactions. Only the resolution with (-)-menthyl chloroformate succeeded in separating the enantiomers, but we were not able to remove the menthyl chloroformate moiety using different reactions and conditions. Finally, the presence of the synthesized alkaloids in *Rollinia mucosa* was studied by using a targeted analysis of *Rollinia mucosa* fruits and seeds extracts using UHPLC-QToF-MS. Moreover, all synthesized compounds were subjected to the biological evaluation in order to understand how different alkaloid derivatives induced or reduced the cytotoxicity, as well as neurotoxicity.

2. Result and Discussion

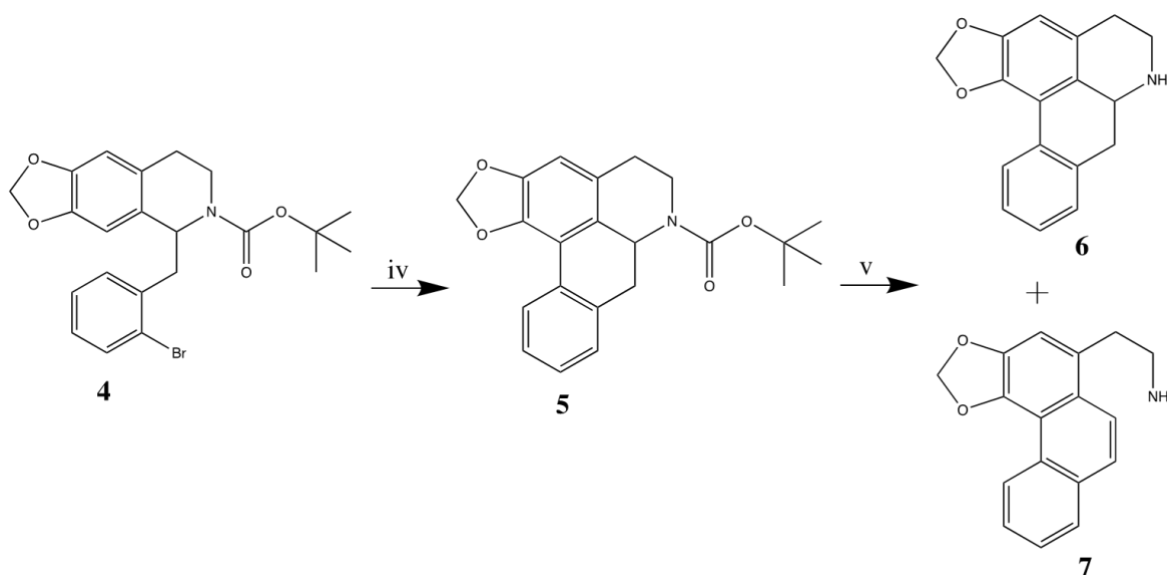
2.1. Synthesis

Total synthesis of **6**, **7**, **8**, and **9** was carried out by *Bischler-Napieralski* reaction (Huang et al. 2004) with 3,4-methylenedioxyphenethylamine **1**, 2-bromophenylacetic acid **2**, and an excess of the reagent POCl₃, followed by NaBH₄ reduction without further purification due to the air sensitivity of the produced amine to give compound **3** in 55% yield (**Scheme 1**). The resulted tetrahydroisoquinolines **3** was protected with Boc (tert-butyl carbamate group) to produce **4** in 70% yield (**Scheme 1**), which was subjected to palladium-catalyzed direct intramolecular arylation of aryl bromides reported before (Lafrance et al. 2007) to afford compound **5** in 64% yield (**Scheme 2**). The deprotection of the tert-butyl carbamate group was carried out under acidic conditions using either TFA or 4M HCL/dioxane (**Scheme 2**). The deprotection of the amine gives two products: air sensitive amine, (R, S) (±) anonaine **6**, as a minor product in 10% yield, and an aromatic stabilized new compound 3,4-methylenedioxy-1-phenanthreneethylamine **7** as a major product in 40% yield.



Scheme 1. *Bischler-Napieralski* reaction, and Boc protection reaction.

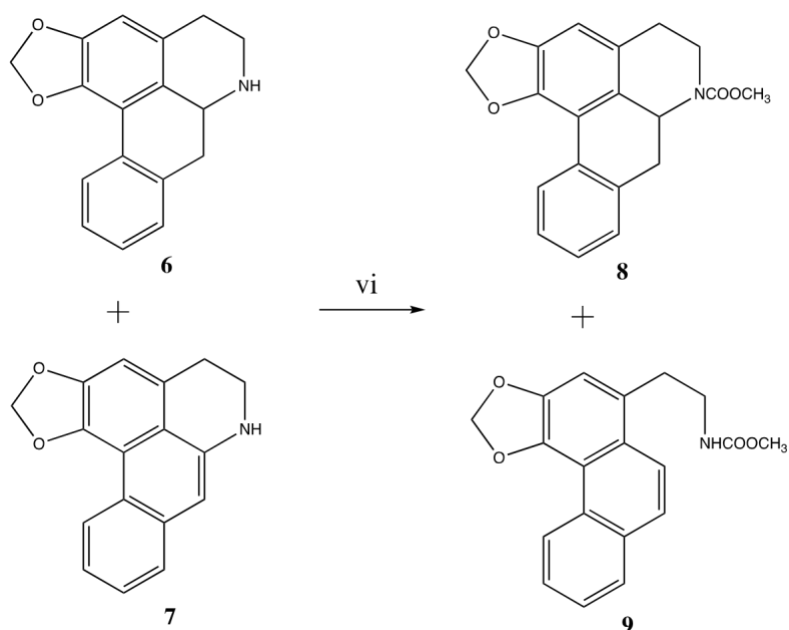
Reaction conditions: (i) *Bischler-Napieralski*: POCl₃, PhMe, r.t. to 120 °C, 3.5 h. (ii) Reduction: NaBH₄, MeOH, r.t., 2.5 h. (iii) Boc protection: (ROC)₂O, DMAP (cat.), iPr₂EtN, CH₂Cl₂. Overnight, r.t.



Scheme 2. Direct intramolecular arylation, and Boc deprotection.

Reaction conditions: (iv) Pd (OAc)₂, ligand (2 equiv. to Pd), K₂CO₃ (2 equiv.), DMA (0.2 M). (v) involves two methods: **Method A**: TFA, DCM, room temp., 1 h. **Method B**: 4M HCl/dioxane, 0°C, 1 h.

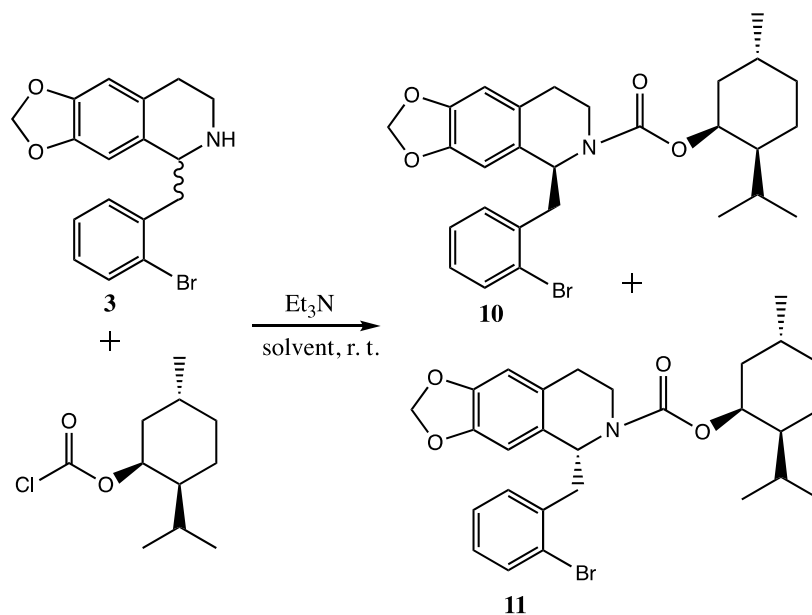
A mixture of (R, S) (\pm) anonaine **6** and 3,4-methylenedioxy-1-phenanthreneethylamine **7** was treated with methyl chloroformate (Kohnen et al. 2007) to afford (R, S) (\pm) romucosine **8** in 70 % yield and another new compound [2-(3,4-methylenedioxy-1-phenanthrenyl)ethyl]-methylcarbamate **9** in 17% yield (**Scheme 3**). In order to get (R)-anonaine, (S)-anonaine, (R)-romucosine, and (S)-romucosine, the racemic mixture of (\pm) tetrahydroisoquinolines **3** (more stable than anonaine) was underwent two different resolution reactions to separate the R and S enantiomers, which are the recycle process of resolution using (+)-dibenzoyl tartaric acid (Shi et al. 2006), and the resolution with (-)-menthyl chloroformate.



Scheme 3. Preparation of romucosine and [2-(3,4-methylenedioxy-1-phenanthrenyl)ethyl]-methylcarbamate.

Reaction conditions: (vi) ClCO₂Me, CH₂Cl₂, 0 °C.

The resolution with (+)-dibenzoyl tartaric acid has been reported to be efficient in the preparation of (R)-(-)-apomorphine and (R)-(-)-aporphine analogs from their racemic mixtures (Shi et al. 2006). However, we were not able to resolve the racemic compound (\pm) tetrahydroisoquinolines **3** using the (+)-dibenzoyl tartaric acid; no salt precipitated was noticed in several solvents tried. On the other hand, the resolution with (-)-menthyl chloroformate succeeded in separating the enantiomers (**Scheme 4**). The treatment of (\pm) tetrahydroisoquinolines **3** with (-)-menthyl chloroformate selectively gives diastereomeric carbamates that are resolvable on the normal phase column chromatography. The optical rotation analysis revealed $[\alpha]_{25D} - 47$ ($c = 0.3$, CHCl_3) for (-) tetrahydroisoquinolines **10**, and $[\alpha]_{25D} + 42$ ($c = 0.28$, CHCl_3) for (+) tetrahydroisoquinolines **11**, which prove the successful separation of the enantiomers. However, the cleavage of the carbamates in compounds **10** and **11** was challenging.



Scheme 4. The enantiomers resolution of **3** with (-) (1*R*)-menthyl chloroformate.

Different reactions and conditions were performed to remove the menthyl moiety after the enantiomeric separation, and none of them have worked. Treatment of **10** and **11** with 4M HCl/dioxane at 0 °C for 3 hrs, then at r.t for overnight afforded unreacted starting material with many other spots on the TLC. The use of different concentrations of TFA in dichloromethane at r.t. for 48 hrs afforded unreacted starting material as well with other impurities. Also, the attempted hydrolysis of menthyl carbamates in a pressure glass container at 110 °C in TFA for 6 hrs and basify with 10 M sodium hydroxide solution led to the disappearance of starting material, but the desired product was not detected. The hydrolysis with 5M lithium hydroxide or 5M sodium hydroxide in THF at r.t. for 2 hrs, then by heating (60 °C) under reflux for overnight afforded unreacted starting material with other impurities. Finally, the treatment of **10** and **11** with LiAlH₄ in dry THF at r.t. for 24 hrs afforded only recovered starting material.

2.2. ESI-QToF-MS of reference standards

Compounds **6-9** were analyzed using LC-ESI-QToF-MS to find the specificity of MS-MS spectral patterns based on their structures (**Table 5- 1**). Compounds **6** and **7** chromatographic peaks contained the same protonated molecules in the MS spectra ($[M+H]^+$ 266.1176) and similar product ions in MS/MS spectra (191.0850) but had different retention behaviors (6.03 min and 6.6min for compounds **6** and **7**; respectively). Similarly, compounds **8** and **9** showed the same protonated molecules in the MS spectra ($[M+H]^+$ 324.123) and similar product ions in MS/MS spectra (249.0926) with different retention behaviors (10.85 min and 10.25 for compounds **8** and **9**; respectively).

Table 5- 1 Accurate mass data, fragment ions for compounds **6-9** using UHPLC Q-ToF.

Sample name	Rt (min)	Molecular Formula	[M+H] ⁺	Fragments
Compound 6	6.03	C ₁₇ H ₁₅ NO ₂	266.1176	191.0850
Compound 7	6.6	C ₁₇ H ₁₃ NO ₂	266.1176	249.0876, 191.0866
Compound 8	10.85	C ₁₉ H ₁₇ NO ₄	324.123	249.0898, 191.0840
Compound 9	10.25	C ₁₉ H ₁₅ NO ₄	324.123	249.0926

2.3. Targeted analysis of *Rollinia mucosa* using UHPLC-QToF-MS

The high chromatographic resolution and separation capabilities of the UHPLC with QToF-MS have been applied to the identification and characterization of synthesized alkaloids (compound **6-9**) (**Table 5- 2**). Three of the standard compounds (compound **7-9**) were not detected from methanolic extracts (RMFM and RMSM) or the alkaloidal extracts of the fruits and seeds of *Rollinia mucosa*. Anonaine (compound **6**) is the only compound that was detected from methanolic extract (RMSM) and alkaloidal extract (ALK-S) of the seeds, and a tiny amount was also detected in the fruits methanolic extract (RMFM) (**Table 5- 2**).

The presence of anonaine in *Rollinia mucosa* extracts was identified by comparing the retention time and the MS and MS/MS data with a reference standard (compound **6**). Anonaine and romucosine (compound **9**) have been reported previously from the fruits of *Rollinia mucosa* (Chen et al., 1996). Herein, we confirm the presence of anonaine in the *Rollinia mucosa* fruits and seeds (**Table 5- 2**).

However, we were not able to detect the presence of romucosine (compound **9**) in *Rollinia mucosa* fruits or seeds, which indicate that romucosine would be an artifact formed during the

acid-base extraction of alkaloids. Therefore, it is not clear whether the N-(methoxycarbonyl) alkaloids isolated from *Rollinia mucosa* earlier (Chen et al., 1996; Kuo et al., 2001; Kuo et al., 2004) are “natural products” or artifacts formed during the alkaloidal extraction process. The use of conventional acid-base extraction to isolate the N-(methoxycarbonyl) alkaloids from *Rollinia mucosa* should be revised because it can lead to the formation of artifacts (Maltese et al., 2009). It is also possible that *Rollinia mucosa* species have several subspecies or chemotypes, which might produce different types of compounds, including the N-(methoxycarbonyl) alkaloids.

Table 5- 2 Targeted analysis of *R. mucosa* fruits and seeds extracts using UHPLC-QToF-MS

#	Sample	Compound 6	Compound 7	Compound 8	Compound 9
	Rt	6.03	6.6	10.85	10.25
	<i>m/z</i>	266.1176	266.1176	324.123	324.123
1	RMFM	Tiny (t)	ND	ND	ND
2	RMSM	+	ND	ND	ND
3	ALK-F	ND	ND	ND	ND
4	ALK-S	+	ND	ND	ND

2.4. Anticancer

The anticancer potential of the synthesized alkaloids (**Figure 5-1**) and extracts was evaluated in terms of their anti-cell proliferative activities in a panel of cancer cell lines, as shown in **Table 5- 3** and **Table 5- 4**.

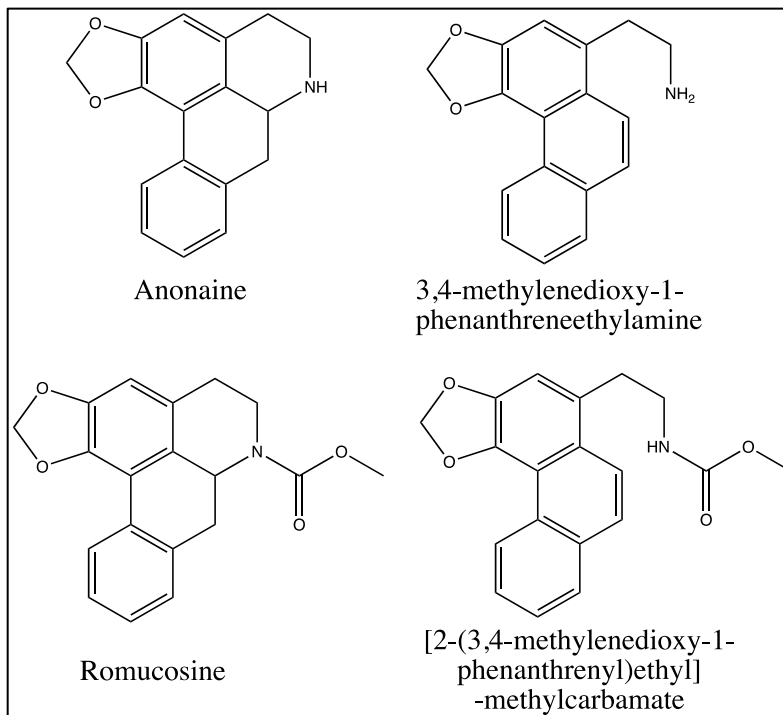


Figure 5- 1 Synthesized alkaloids from *Rollinia mucosa*

Anonaine (compound **6**) was effective towards all cancer cells with IC_{50} of 5.9, 18.5, 16.0, and 10.5 $\mu\text{g/mL}$ for SK-MEL, KB, BT-549, and SK-OV-3 cells, respectively. 3, 4-Methylenedioxy-1-phenanthreneethylamine (compound **7**) was also effective towards all cancer cells and was more effective than anonaine towards KB, and SK-OV-3 cells with IC_{50} of 11.5 and 8.9 $\mu\text{g/mL}$, and it has almost similar activities to anonaine towards BT-549 with IC_{50} of 17.5 $\mu\text{g/mL}$.

3, 4-Methylenedioxy-1-phenanthreneethylamine was less active than anonaine towards SK-MEL with IC₅₀ of 11.5 µg/mL. Moreover, 3, 4-methylenedioxy-1-phenanthreneethylamine was less toxic to LLC-PK1 and VERO cells in comparison to anonaine. Romucosine (compound **8**) demonstrated selective anticancer activities towards SK-MEL with IC₅₀ of 15.2 µg/mL. [2-(3, 4-methylenedioxy-1-phenanthrenyl)ethyl]-methylcarbamate (compound **9**) also has selective activities towards SK-MEL and SK-OV-3 with IC₅₀ of 18.5 and 17.5 µg/mL. Romucosine and [2-(3,4-methylenedioxy-1-phenanthrenyl)ethyl]-methylcarbamate were not toxic towards LLC-PK1 and VERO cells comparing to anonaine and 3, 4-Methylenedioxy-1-phenanthreneethylamine, as shown in **Table 5- 3**.

Table 5- 3 Anti-cell proliferative effects of compounds **6-9**.

Sample Code	SK-MEL	KB	BT-549	SK-OV-3	LLC-PK1	Vero
	IC ₅₀ µg/mL	IC ₅₀ µg/mL	IC ₅₀ µg/mL	IC ₅₀ µg/mL	IC ₅₀ µg/mL	IC ₅₀ µg/mL
Compound (6)	5.9 ± 0.4	18.5 ± 1.5	16.0 ± 1.0	10.5 ± 0.5	9.2 ± 0.7	9.0 ± 1.0
Compound (7)	11.5 ± 0.5	11.5 ± 0.5	17.5 ± 0.5	8.9 ± 0.2	11.5 ± 0.5	16.5 ± 0.5
Compound (8)	15.2 ± 2.7	43.0 ± 7.0	29.0 ± 1.0	32.5 ± 2.5	46.5 ± 1.5	50.0 ± 0.0
Compound (9)	18.5 ± 0.5	28.0 ± 4.0	37.0 ± 2.0	17.5 ± 0.5	32.5 ± 7.5	29.5 ± 0.5
Doxorubicin	0.7 ± 0.0	1.1 ± 0.1	1.3 ± 0.1	0.9 ± 0.2	0.8 ± 0.02	>5

Several studies have been conducted on the anticancer activities of (-) anonaine on different cancer cell lines including a study reported that (-) anonaine showed a significant cytotoxic effect against three cell cultures (rat hepatocytes, HepG2 and HeLa) with IC₅₀ values of 70.3, 33.5, and 24.8 µg/mL, respectively (Correché et al., 2008). Another study has indicated that (-) anonaine displayed significant cytotoxicity against AGS (human gastric cancer cell), DLD1 (human colon cancer cell), HA59T (human hepatoma cell), and HepG2 (human hepatoma cell) cancer cell lines with AGS cells being the most susceptible (Chen et al., 2000). Also, it was reported to cause DNA damage associated with increased intracellular nitric oxide, ROS, glutathione (GSH) depletion, disruptive mitochondrial transmembrane potential, activation caspase 3, 7, 8 & 9 and poly ADP ribose polymerase cleavage in human cervical cancer cell (HeLa) (Chen et al., 2008).

Herein, we reported that anonaine showed a significant effect in all cancer cell lines tested in this study with IC₅₀ range 5.9-18.5 µg/mL. Romucosine has been tested before on three cancer cell lines, Human MCF-7 cells (breast cancer), NCI-H460 cells (lung cancer), and SF-268 cells (central nervous cancer), and it showed no cytotoxic activities (Liu et al., 2008). In our study, romucosine displayed selective anticancer activities toward SK-MEL 15.2 µg/mL. 3, 4-Methylenedioxy-1-phenanthreneethylamine and [2-(3,4-methylenedioxy-1-phenanthrenyl)ethyl]-methylcarbamate are new compounds that have not synthesized or isolated previously. The anticancer activities of 3, 4-methylenedioxy-1-phenanthreneethylamine and [2-(3,4-methylenedioxy-1-phenanthrenyl)ethyl]-methylcarbamate have not been reported before, and our study indicated interesting anticancer activities of these compounds.

Rollinia mucosa fruits extracts (RMFM, Non-ALK-F, and ALK-F) and seeds extracts (RMSM, Non-ALK-S, and ALK-S) anti-cell proliferative results are shown in **Table 5- 4**. Surprisingly, all extracts are toxic to all cancer cell lines with very low concentrations. The extent

of toxicity to KB cells is very similar to LLCPK1 cells for all the extracts. Furthermore, the extracts are more toxic to SKMEL, BT-549, and SK-OV3 cells compared to KB and LLCPK1 cells. The toxicity to Vero cells is lower compared to the other cell lines included in the assay. This pattern is similar to Doxorubicin. In general, seed extracts are more toxic than the fruit extracts toward all cell lines. These findings are conflicting with neurotoxicity results, which showed that all extracts (except ALK-S) are not toxic to the neurons up to 20 µg/mL. However, we would suggest that these extracts cause extreme toxicities to the cancer cell lines and the non-cancer kidney cell lines due to their ability to penetrate those cells but not able to penetrate the neuron cells. Therefore, further future studies are needed to understand these results.

Table 5- 4 Anti-cell proliferative activity of *Rollinia mucosa* extracts against a panel of cell lines.

Sample Code	Cancer Cell Lines				Non-cancer Kidney Cell Lines	
	SK-MEL	KB	BT-549	SK-OV-3	LLC-PK1	Vero
	IC50 µg/mL	IC50 µg/mL	IC50 µg/mL	IC50 µg/mL	IC50 µg/mL	IC50 µg/mL
RMFM	0.027	0.092	0.03	0.034	0.09	0.35
RMSM	<0.016	<0.016	<0.016	<0.016	<0.016	0.038
Non-ALK-F	0.026	0.088	0.037	0.038	0.096	0.37
Non-ALK-S	<0.016	<0.016	<0.016	<0.016	<0.016	0.033
ALK-F	0.075	0.2	0.092	0.088	0.2	>0.5
ALK-S	<0.016	<0.016	<0.016	<0.016	<0.016	0.16
Doxorubicin	0.5	0.6	0.72	0.34	0.3	>5

2.5. Neurotoxicity

Among the six extracts (RMSM, non-ALK-S, ALK-S, RMFM, non-ALK-F, and ALK-F), the alkaloidal extract from the seeds of *Rollinia mucosa* (ALK-S) showed a significant dose-dependent decrease in cell viability at 10 and 20 $\mu\text{g/mL}$ (**Fig. 5- 2C**). All other extracts (RMSM, non-ALK-S, RMFM, non-ALK-F, and ALK-F) were not toxic at the highest tested concentration of 20 $\mu\text{g/mL}$ (**Fig. 5- 2A-B** and **Fig. 5- 3A-C**). The alkaloid anonaine (compound **6**) exhibited significant toxicity at 5 $\mu\text{g/mL}$, and no further reduction in cell viability was noticed with higher concentrations of 10 and 20 $\mu\text{g/mL}$, as shown in **Fig 5- 4A**.

The rest of the alkaloids [3, 4-methylenedioxy-1-phenanthreneethylamine (compound **7**), romucosine (compound **8**), and [2-(3,4-methylenedioxy-1-phenanthrenyl)ethyl]-methylcarbamate (compound **9**)] did not show a significant decrease in cell viability (**Fig. 5- 4B-D**). To summarize the data, all of the extracts and alkaloids were combined in a bar graph to display their effects at the highest tested concentration of 20 $\mu\text{g/mL}$ (**Fig. 5- 5**).

Figure 5- 2 Effect of RMSM, Non-ALK-S, and ALK-S extracts on neuronal cell viability.

A) MeOH extract (RMSM) and **B)** non-alkaloid seeds extract (Non-ALK-S) from the seeds of *Rollinia mucosa* did not show a significant reduction in cell viability with the increasing concentrations. **C)** The alkaloid extract (ALK-S) showed a significant concentration-dependent decrease in cell viability.

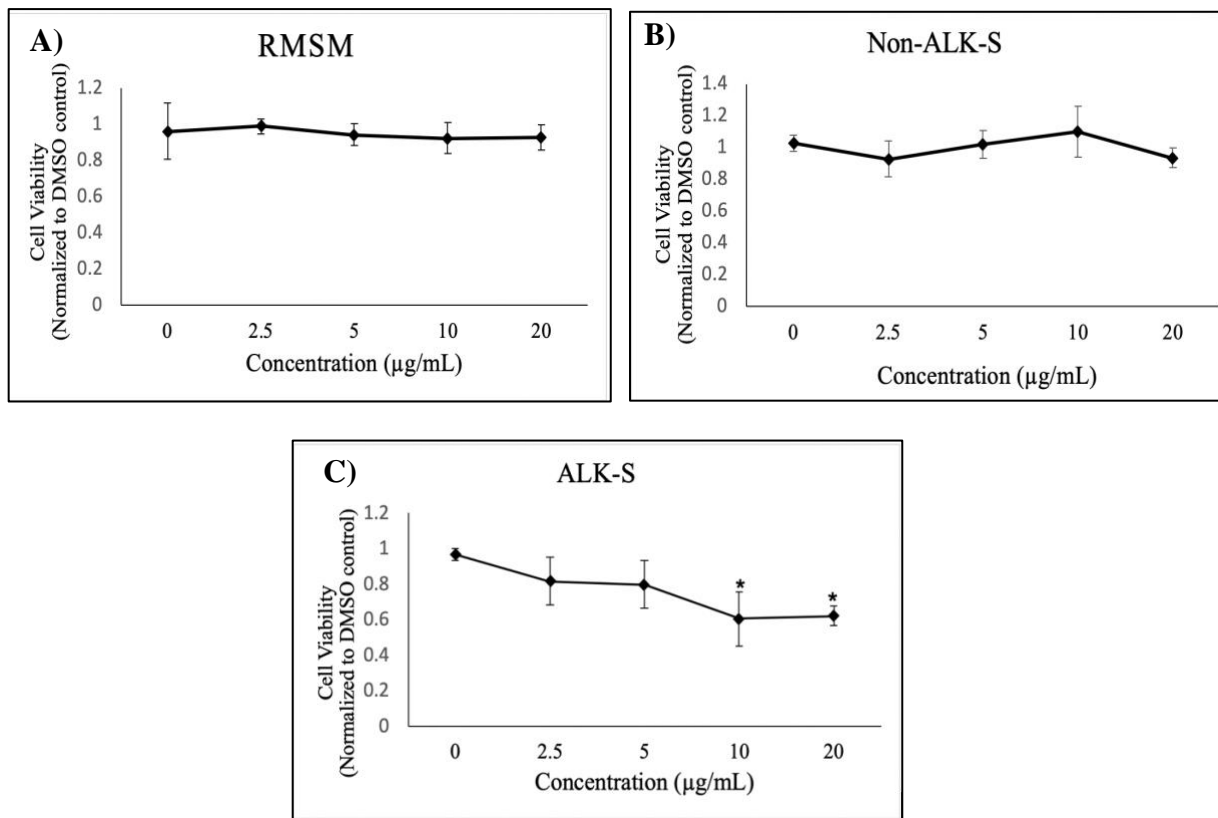


Figure 5- 3 Effect of RMFM, Non-ALK-F, and ALK-F extracts on neuronal cell viability. All of the three extracts [MeOH extract (RMFM), non-alkaloid extract (Non-ALK-F) and alkaloid extract (ALK-F)] of *Rollinia mucosa*'s fruits did not show a significant concentration-dependent decrease in cell viability.

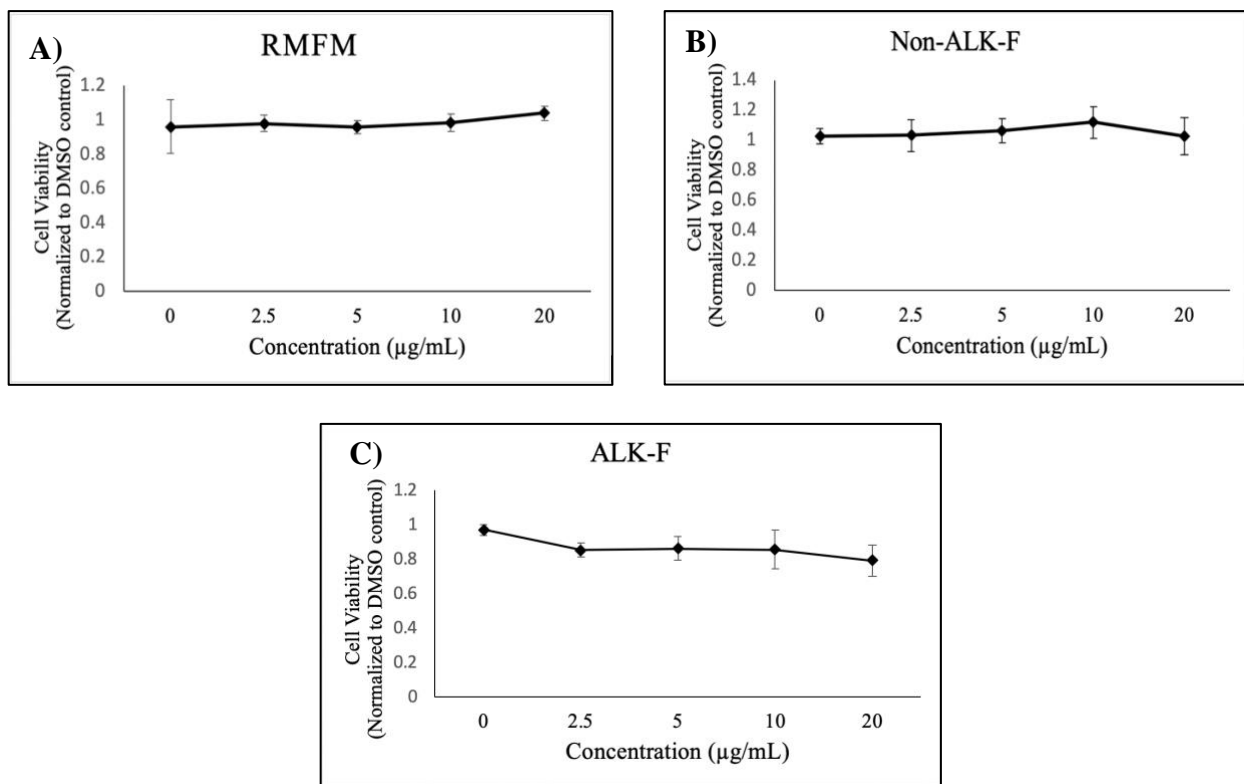


Figure 5- 4 Effect of compounds **6-9** on neuronal cell viability.

A) Anonaine (Compound **6**) demonstrated a significant reduction in cell viability at 5 $\mu\text{g/mL}$. **B)**, **C)**, and **D)** Compounds **7-9** did not show a significant concentration-dependent decrease in cell viability.

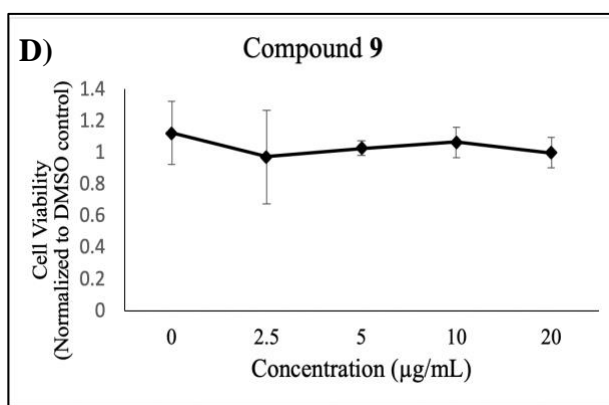
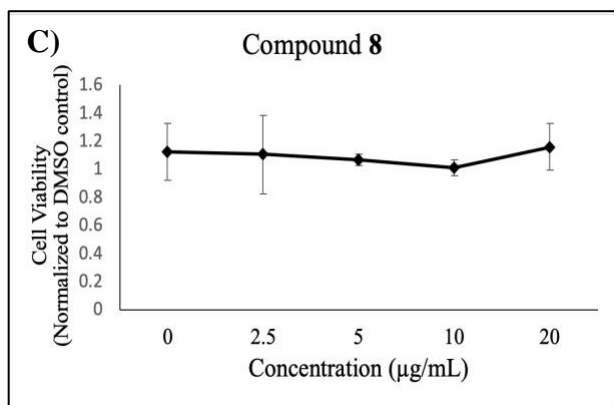
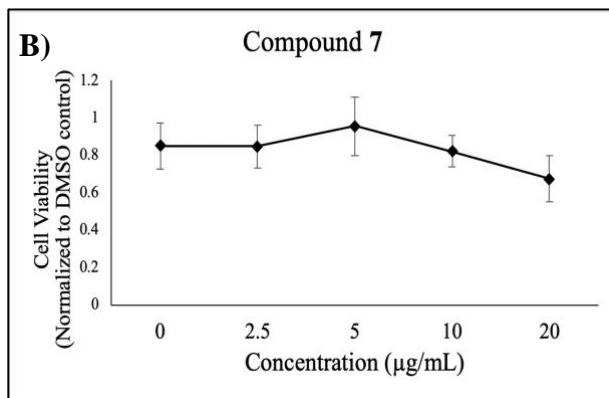
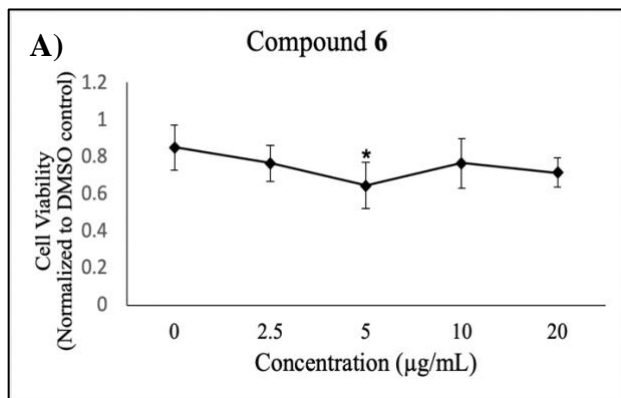
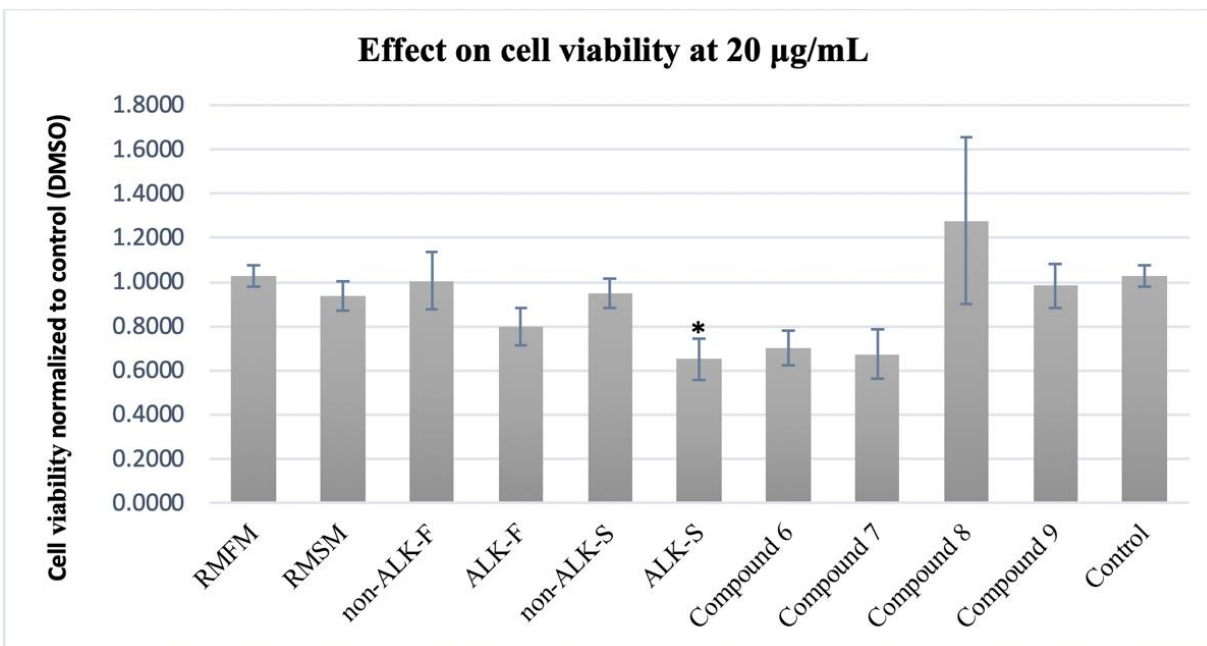


Figure 5- 5 Effect of extracts and synthesized compounds **6-9** on cell viability at 20 $\mu\text{g/mL}$. Asterisks designate statistically significant decreases in cell viability compared to vehicle control.



3. Materials and methods

3.1. General experimental procedures of the synthesis

Reactions were performed under argon atmosphere in oven-dried glassware with magnetic stirring. Solvents were distilled under an argon atmosphere before use. All reagents obtained commercially were used without further purification. The reaction progress was monitored on aluminum-backed plates, pre-coated with silica gel F254 (200 μm , 60 \AA , (Merck) thin-layer chromatography (TLC) plates. Spots were detected at UV-254 nm. Visualization was attained by dipping the TLC plate into a solution of phosphomolybdic acid (PMA), 10 g of phosphomolybdic acid in 100 mL of absolute ethanol, followed by heating with a heat gun. Column chromatography was carried out using flash silica gel (40 μm , 60 \AA , J. T. Baker). NMR spectra were obtained on Bruker AU III 400 or 500 MHz NMR spectrometers using, CD_3OD or CDCl_3 solvents. IR spectra were recorded on an Agilent Technologies Cary 630 FTIR. Rudolph Research Analytical Autopol IV automatic polarimeter was used to obtain the specific rotations. High-resolution mass spectra were recorded on an Agilent electrospray ionization quadrupole time-of-flight (ESI-QTOF) instrument.

3.2. Ultra-High-Performance Liquid Chromatography-Quadrupole Time of Flight-Mass Spectrometry (UHPLC/QToF-MS)

The liquid chromatographic system was an Agilent Series 1290 comprised of the following modular components: binary pump, a vacuum solvent microdegasser, an autosampler with a 100-well tray, and a thermostatically controlled column compartment. The separation was achieved on an Agilent Poroshell 120 EC-18 (2.1 \times 100 mm, 2.7 μ) column.

The mobile phase consisted of water with 0.1% formic acid (A) and acetonitrile with 0.1% formic acid (B) at a flow rate of 0.23 mL/min, with the following gradient: 0 min, 2% B in next 20 min to 10% B, for next 30 min 20% B, for next 20 min 50% B, for next 20 min 70% B, for next 20 min 90% B and to 100% B in next 10 min. Each run was followed by a 5 min wash with 100% B and an equilibration period of 5 min with 2% B. Two microliters of sample were injected.

The column temperature was set at 40 °C, and UV spectra were recorded from 190-400 nm. The mass spectrometric analysis was performed with a QToF-MS/MS (Model #G6530A, Agilent Technologies, Palo Alto, CA, USA) equipped with an ESI source with Jet Stream technology using the following parameters: drying gas (N₂) flow rate, 8.0 L/min; drying gas temperature, 300 °C; nebulizer, 27 psig, sheath gas temperature, 300 °C; sheath gas flow, 8.0 L/min; capillary, 3500V; skimmer, 65V; Oct RF V, 750V; fragmentor voltage, 100V. The sample collision energy was set at 55eV. All the operations' acquisition and analysis of data were controlled by Agilent MassHunter Acquisition Software Ver. A.05.00 and processed with MassHunter Qualitative Analysis software Ver. B.07.00. Each sample was analyzed in a positive mode in the range of $m/z = 100-1700$.

Accurate mass measurements were obtained using ion correction techniques using reference masses at m/z 121.0509 (protonated purine) and 922.0098 [protonated hexakis (1H, 1H, 3H-tetrafluoropropoxy) phosphazine or HP-921] in positive ion mode. The compounds were confirmed in each spectrum. For this purpose, the reference solution was introduced into the ESI source via a T-junction using an Agilent Series 1200 isocratic pump (Agilent Technologies, Santa Clara, CA, USA) using a 100:1 splitter set at a flow rate of 20 μ L/min.

For recording ToF-MS spectra, the quadrupole was set to pass all ions (Rf only mode), and all ions were transmitted into the pusher region of the time-of-flight analyzer where they were

mass-analyzed with a 1 s integration time up to m/z 1000. For the ESI-MS/MS CID experiments, ions of interest were mass-selected by the quadrupole mass filter. The selected ions then collided with nitrogen in a high-pressure collision cell, and the collision energy was optimized to afford good product ion signals that were subsequently mass measured with the ToF analyzer.

The analysis was performed in the reflectron mode with a resolving power of about 10,000 at m/z 922. The instrument was set to an extended dynamic range (up to 10^5 with lower resolving power). MS/MS spectra were recorded simultaneously at a rate of 2.0 spectra s^{-1} . In order to filter selected precursor ions and their isotopes for MS/MS, an isolation window of 1.3 m/z was set for the quadrupole.

3.3. Mass Data analysis

MassHunter Workstation software, including Qualitative Analysis (version B.07.00), was used for processing both raw MS and MS/MS data, including molecular feature extraction, background subtraction, data filtering, and molecular formula estimation (using accurate mass of all isotopes, their relative abundances, and all detected adducts with their measured isotopes). To perform subtraction of molecular features (MFs) originating from the background, analysis of a blank sample (methanol) was carried out under identical instrument settings, and background MFs were removed. This method involved the use of the $[M+H]^+$ and $[M+Na]^+$ ions in the positive ion mode, found in the extracted ion chromatogram (EIC).

3.4. Plant Material

Rollinia mucosa fruits and seeds methanol extract were received from Dr. Yang-Chang Wu, Chair Professor Graduate Institute of Integrated Medicine Director (Chinese Medicine R&D Center (CMUH), China Medical University).

3.5. Alkaloids extraction

Dried *Rollinia mucosa* fruits (212.128 g) and seeds (67.374 g) were finely powdered and extracted separately with methanol to obtain (6.603 g) of fruit extract (RMFM) and (5.776 g) of seeds extract (RMSM). An aliquot of MeOH extract (1.250 g of fruits and 1.380 of seeds) was subjected separately to the acid-base alkaloidal extraction. The extract was suspended in 3% HCl (75 mL) and extracted with CHCl₃ (3 × 75 mL) in a separating funnel. After separating the CHCl₃ layers, the resulting aqueous acidic layer's pH was adjusted to 9–10 with ammonia solution and subsequently extracted again with CHCl₃ (3 × 75 mL). The combined CHCl₃ layers from the basified solution were dried to give an alkaloidal extract (19 mg) from fruit extract (ALK-F) and (7 mg) from seeds extract (ALK-S).

3.6. Anticancer assay

The anticancer activity of the various extracts and pure compounds was determined towards a panel of four human solid tumor cell lines: melanoma (SK-MEL), epidermal carcinoma (KB), breast carcinoma (BT-549), and ovarian carcinoma (SK-OV-3). Moreover, non-cancer kidney cell lines (LLC-PK₁ and VERO) were also employed to determine if the anti-cell proliferative activity of these extracts and compounds was selective for the tested tumor cell lines. All cell lines were obtained from the American Type Culture Collection (ATCC, Rockville, MD).

The cells were seeded in 96-well plates (10,000 cells/well) and incubated for 24 h. The extracts and pure alkaloids were dissolved in DMSO, diluted in media, and added to the cells at concentrations of 50, 25, 12.5, 6.25, 3.125 $\mu\text{g/mL}$. After incubating for 48 hrs, cell viability was determined by using a tetrazolium dye WST-8, which is converted to a water-soluble formazan product in the presence of 1-methoxy PMS by the activity of cellular enzymes. The color of the formazan product was measured at 450 nm on a plate reader. Doxorubicin was used as a positive control for anticancer assay, and DMSO (0.25%) was used as the vehicle control. The IC_{50} values were obtained from concentration-response curves. The values are represented as mean \pm average deviation ($n = 2$).

3.7. Neurotoxicity assay

The neurotoxicity evaluation was performed in 8-10 day old rat cortical neurons. The extracts and compounds were added to neuronal growth media (neurobasal, B27, penicillin, and streptomycin) in the following range of concentrations (10, 5, 1, and 0.1 $\mu\text{g/mL}$) and incubated for 24 hrs. DMSO (0.1%) was used as vehicle control. The MTS assay was used to assess the toxicity of the extracts and compounds. MTS Aqueous One Solution Reagent was added after incubating the extracts, compounds, and the control for 24 hrs. Once the MTS was administered to the wells, the plates were put back into the incubator for 1-2 hrs. The formazan dye produced by viable cells was quantified by measuring the absorbance at 490 nm. LIVE/DEAD viability stains (Invitrogen) were used to verify living and cytotoxic cells in a controlled study. Stained cells were quantified by the Nikon Elements software following image acquisition on the Nikon HCA inverted fluorescent microscope (100x) in a single field per well, chosen at random by the software.

3.8. Statistical analysis

A one-way ANOVA was used to perform statistical analysis followed by Dunnett's post hoc test to examine the significant difference against the control at $p < 0.05$ for each dose of a compound or extract.

4. Experimental

4.1. Synthesis of compounds 3-9

5-(2-Bromobenzyl)-5,6,7,8-tetrahydro[1,3dioxolo[4,5-g]isoquinoline (3):

To a mixture of 2-bromophenylacetic acid (10.00 mmol) and 3,4-methylenedioxyphenethylamine (1.81 g, 10.00 mmol), POCl_3 (4 ml, 43.92 mmol) was added dropwise. After 1 h stirring at r.t., toluene (10 ml) was added and the mixture heated under reflux for 3.5 h. Then the mixture was evaporated, the residue dissolved in MeOH (5 ml), and the soln. poured into ice. The aq. phase was basified with 25% NH_4OH soln. and extracted with CH_2Cl_2 (3x 50 ml), the combined org. phase washed with H_2O (100 ml), dried (Na_2SO_4), and evaporated, and the residue dissolved in MeOH (30 ml). To this soln., NaBH_4 (946 mg, 25.00 mmol) was added portion-wise for 30 min while stirring. After 24 h, the soln. was evaporated, the residue suspended in CH_2Cl_2 (50 ml) and washed with H_2O (50 ml), the org. phase dried (Na_2SO_4), evaporated (2.00 g), and (1.00 g) of the residue purified by CC (Al_2O_3) using [hexane: EtOAc (9:1), hexane: EtOAc (8:2), hexane: EtOAc (7:3), hexane: EtOAc (6:4), and EtOAc. The product didn't come out with all of the solvent systems mentioned above; therefore, we used acetone: H_2O (9:1) to afford 500 mg white crystal of compound **3**.

^1H (400 MHz, DMSO- d_6): δ = 2.90 (dt, J = 16.8, 6.01 Hz, 1 H), 3.12 (dt, J = 16.5, 6.04 Hz, 1 H), 3.16–3.25 (m, 1 H), 3.38–3.5 (m, 3 H), 4.65 (t, J = 7.25 Hz, 1 H), 5.97 (d, J = 1.32 Hz, 1 H), 5.99 (d, J = 1.2 Hz, 1 H), 6.45 (d, J = 1.38 Hz, 1 H), 6.83 (d, J = 1.38 Hz, 1 H), 7.28 (tt, J = 7.58, 1.66 Hz, 1 H), 7.39 (tt, J = 7.47, 1.45 Hz, 1 H), 7.58 (dt, J = 7.62, 1.65 Hz, 1 H), 7.68 (dt, J = 7.94, 1.43 Hz, 1 H) ppm.

^{13}C NMR (100 MHz, DMSO- d_6): δ = 25.3, 39.06, 39.9, 54.1, 101.5, 106.6, 108.9, 125.14, 125.16, 126.5, 128.5, 129.9, 133.1, 133.3, 135.6, 146.3, 147.3 ppm. HRESI-MS calcd. for $[\text{C}_{17}\text{H}_{16}\text{BrNO}_2 + \text{H}]$ (M^{++}H): 346.044; found: 346.051.

tert-Butyl 5-(2-Bromobenzyl)-7,8-dihydro-[1,3]dioxolo[4,5-*g*]isoquinoline-6(5H)-carboxylate

(**4**):

To a solution of the bromo-tetrahydrobenzylisoquinoline (**3**) (1.0 equiv.), diisopropylethylamine (3.0 equiv.) and 1–3 mg of 4-(dimethylamino) pyridine in DCM (0.2 M) was added slowly di-*tert*-butyl dicarbonate (2.0 equiv.) and the resulting mixture was stirred overnight at 23 °C. The reaction was then quenched by adding a solution of NH_4Cl and was extracted with DCM. The crude reaction mixture was then purified by column chromatography on silica gel using hexane/ EtOAc mixtures to afford 0.7 g of (**4**).

^1H NMR and ^{13}C NMR analysis revealed the presence of two amide rotamers present in a 4:1 ratio. ^1H NMR (400 MHz, CDCl_3 , major rotamer): δ = 1.10 (s, 9 H), 2.66 (ddd, J = 16.16, 4.28, 2.14 Hz, 1 H), 2.86–2.94 (m, 1 H), 2.98 (dd, J = 13.83, 11.13 Hz, 1 H), 3.29 (ddd, J = 13.85, 9.64, 3.65 Hz, 2 H), 4.32–4.42 (m, 1 H), 5.38 (dd, J = 11.11, 3.13 Hz, 1 H), 5.94 (d, J = 1.45 Hz, 1H), 5.95 (d, J = 1.40 Hz, 1H), 6.62 (s, 1 H), 6.90 (s, 1 H), 7.10 (dd, J = 7.46, 1.81 Hz, 1 H), 7.15 (td, J = 7.66, 1.8 Hz, 1 H), 7.24 (m, 1 H), 7.59 (dd, J = 7.95, 1.28 Hz, 1 H).

^{13}C NMR (100 MHz, CDCl_3 , major rotamer): $\delta = 27.8, 28.6, 36.1, 42.7, 53.9, 79.4, 100.9, 106.8, 108.6, 125.3, 127.4, 127.6, 128.2, 130.2, 131.8, 132.5, 138.1, 146.1, 146.4, 154.1$ ppm. HRESI-MS calcd. for $[\text{C}_{17}\text{H}_{16}\text{BrNO}_2 + \text{CH}_3\text{OH} + \text{H}] (\text{M}^+ + \text{CH}_3\text{OH} + \text{H})$: 478.1229; found 478.1085.

tert-Butyl 5,6,7a,8-Tetrahydrobenzo[*g*][1,3]dioxolo[4',5':4,5]-benzo[1,2,3-*de*]quinoline-7-carboxylate (**5**):

General Procedure for the intramolecular direct arylation.

To (0.3g, 1 equiv.) of the aryl halide (**4**) in a round-bottomed flask with a magnetic stir bar, K_2CO_3 (2 equiv.), ligand (Di-*tert*-butyl(methyl)phosphonium tetrafluoroborate) (0.1 equiv.), and $\text{Pd}(\text{OAc})_2$ (0.05 equiv.) were added. The flask is purged with argon. Anhydrous DMA (N,N-dimethylacetamide) is then added (0.2 M), and the resulting mixture is heated to 130 °C overnight. The reaction mixture is then concentrated and loaded onto a silica gel column for chromatography using hexane/EtOAc mixtures to afford 0.193g of (**5**).

^1H NMR (400 MHz, CDCl_3): $\delta = 1.53$ (s, 9 H), 2.63 (dt, $J = 15.4, 2.25$ Hz, 1 H), 2.79 – 2.98 (m, 3 H), 3.06 (dd, $J = 13.8, 4.3$ Hz, 1 H), 4.42 (d, $J = 12.4$ Hz, 1 H), 4.83 (d, $J = 12.8$ Hz, 1 H), 5.98 (d, $J = 1.41$ Hz, 1 H), 6.11 (d, $J = 1.4$ Hz, 1 H), 6.62 (s, 1 H), 7.24–7.36 (m, 3 H), 8.13 (d, $J = 7.66$ Hz, 1 H) ppm.

^{13}C NMR (100 MHz, CDCl_3): $\delta = 28.5, 29.7, 30.4, 34.9, 51.6, 79.9, 100.8, 107.5, 117.2, 126.0, 126.9, 126.9, 127.0, 127.7, 127.9, 128.4, 130.7, 136.0, 142.9, 146.7, 154.5$ ppm. HRESI-MS calcd. for $[\text{C}_{17}\text{H}_{15}\text{NO}_2] (\text{M}^+)$: 365.1627; found: 365.2474.

6,7,7a,8-tetrahydro-5H-[1,3]dioxolo[4',5':4,5]benzo[1,2,3-de]benzo[g]quinoline [(±)Anonaine (**6**)], and 6,7-dihydro-5H-[1,3]dioxolo[4',5':4,5]benzo[1,2,3-de]benzo[g]quinoline [3,4-methylenedioxy-1-phenanthreneethylamine (**7**)]:

Method A:

Trifluoroacetic acid (0.34 mL, 13.0 equiv.) was added dropwise to a solution of (**5**) (0.122 g, 1.0 equiv.) in dichloromethane (3 mL) and the resulting mixture was stirred at room temperature for 1 h. The solution was removed under reduced pressure, and saturated NaHCO₃ was added to the residue. The mixture was extracted with EtOAc, dried with MgSO₄, filtered, evaporated and then purified by chromatography on column using hexane/EtOAc mixture as the eluent to afford 10 mg of (±) anonaine **6** and 40 mg of 3, 4-methylenedioxy-1-phenanthreneethylamine **7**.

Method B:

A solution of 4M HCl/dioxane was added to the carbamate (**5**) in a round-bottom flask with a magnetic stir-bar at 0 °C. The reaction was completed within 45 mins. TLC indicated the formation of (±) anonaine **6** and 3,4-methylenedioxy-1-phenanthreneethylamine **7**. Then, the solvent was removed by rotary evaporation under high vacuum at room temperature to afford a mixture of **6** and **7** in a salt form that was stored without further purification for the preparation of compounds **8** and **9**.

¹H NMR for (±)Anonaine **6** (400 MHz, CD₃OD): δ = 2.66–2.74 (m, 1 H), 2.79 (t, J = 14.16 Hz, 1 H), 2.95–3.11 (m, 3 H), 3.35–3.49 (m, 1 H), 3.96 (dd, J = 14.05, 4.91 Hz, 1 H), 5.91 (d, J = 1.14 Hz, 1 H), 6.06 (d, J = 1.17 Hz, 1 H), 6.59 (s, 1 H), 7.20–7.32 (m, 3 H), 8.13 (d, J = 7.64 Hz, 1 H) ppm.

¹³C NMR (100 MHz, CD₃OD): δ = 27.1, 34.9, 42.1, 52.9, 100.8, 107.3, 109.9, 115.7, 125.0, 125.6, 126.8, 127.4, 127.7, 130.6, 133.8, 142.7, 147.5 ppm. HRESI-MS calcd. for [C₁₇H₁₅NO₂ + H] (M⁺⁺H) 266.118; found: 266.122.

¹H NMR for 3,4-methylenedioxy-1-phenanthreneethylamine **7** (500 MHz, CD₃OD): δ = 3.24 (dd, J = 9.33, 6.51 Hz, 2 H), 3.41 (dd, J = 9.14, 6.72 Hz, 2 H), 6.25 (s, 2H), 7.22 (s, 1 H), 7.60 (dt, J = 6.22, 3.52 Hz, 2 H), 7.66 (d, J = 9.27 Hz, 1H), 7.80–7.92 (m, 2 H), 9.06 (dd, J = 6.09, 3.45 Hz, 1 H) ppm.

¹³C NMR (125 MHz, CD₃OD): δ = 30.8, 40.2, 101.3, 110.5, 116.8, 121.6, 125.4, 125.8, 126.0, 126.6, 126.9, 127.0, 127.4, 128.4, 131.9, 142.9, 145.1 ppm. HRESI-MS calcd. For [C₁₇H₁₅NO₂ + H] (M⁺⁺H) 266.118; found: 266.123.

*Methyl 5,6,7a,8-tetrahydro-7H-[1,3]dioxolo[4',5':4,5]benzo[1,2,3-de]benzo[g]quinoline-7-carboxylate, (\pm) romucosine (**8**), and methyl 5,6-dihydro-7H-[1,3]dioxolo[4',5':4,5] benzo[1,2,3-de]benzo[g]quinoline-7-carboxylate, [2-(3,4-methylenedioxy-1-phenanthrenyl)ethyl]-methylcarbamate (**9**):*

The salt mixture of **6** and **7** (89 mg) in dry CH₂Cl₂ (40 mL) was treated with triethylamine (6.00 equiv.) in a round-bottom flask with a magnetic stir-bar at 0 °C for 10 min, then methyl chlorocarbonate (8.08 mL) was slowly added. The reaction mixture was stirred for 1 hr, and H₂O was added to quench excess reagent. The mixture was partitioned with CHCl₃ and dried with MgSO₄, filtered, evaporated and then purified by chromatography on column using hexane/EtOAc mixtures as the eluent to afford 64 mg of (\pm) romucosine **8** and 16 mg of [2-(3,4-methylenedioxy-1-phenanthrenyl)ethyl]-methylcarbamate **9**.

^1H NMR of (\pm) romucosine **8** (500 MHz, CDCl_3): δ = 2.64 (dt, J = 15.48, 2.37 Hz, 1 H), 2.77–3.13 (m, 4 H), , 3.79 (s, 3 H), 4.45 (brs, 1 H), 4.88 (d, J = 13.54 Hz, 1 H), 5.99 (d, J = 1.49 Hz, 1 H), 6.12 (d, J = 1.5 Hz, 1 H), 6.632 (s, 1 H), 7.27–7.31 (m, 2 H), 7.35 (td, J = 7.55, 2.04 Hz, 1 H), 8.13 (dd, J = 7.71, 1.16 Hz, 1 H) ppm.

^{13}C NMR (125 MHz, CDCl_3): δ = 29.7, 30.3, 39.1, 51.6, 52.6, 100.9, 107.6, 117.4, 125.5, 127.0, 127.1, 127.8, 127.8, 128.6, 130.7, 135.7, 143.0, 146.8, 155.4 ppm. HRESI-MS calcd. For $[\text{C}_{19}\text{H}_{17}\text{NO}_4 + \text{H}_+]$ ($\text{M} + \text{H}_+$) 324.124 found: 324.128.

^1H NMR of [2-(3,4-methylenedioxy-1-phenanthrenyl)ethyl]-methylcarbamate **9** (500 MHz, CDCl_3): δ = 3.26 (t, J = 7.28 Hz, 2 H), 3.52 (q, J = 6.95 Hz, 2 H), 3.71 (s, 3 H), 6.23 (s, 2 H), 7.11 (s, 1 H), 7.54–7.67 (m, 3 H), 7.77–7.96 (m, 2 H), 9.10 (dd, J = 7.41, 1.9 Hz, 1 H) ppm.

^{13}C NMR (125 MHz, CDCl_3): δ = 33.9, 42.2, 52.1, 101.1, 110.7, 117.1, 122.5, 125.3, 126.1, 126.3, 126.8, 127.3, 127.6, 128.6, 129.4, 131.9, 142.4, 144.9, 157.1 ppm. HRESI-MS calcd. For $[\text{C}_{19}\text{H}_{17}\text{NO}_4 + \text{H}]$ ($\text{M} + \text{H}$) 324.123 found: 324.128.

4.2. Enantiomers resolution

4.2.1. *The recycling process of resolution using dibenzoyl tartaric acid.*

At 0 °C, 10 mg of (\pm) bromo-tetrahydrobenzylisoquinoline **3** was dissolved in 1 mL of ethyl acetate in a two-necked flask. Then, 10.35 mg of dibenzoyl tartaric acid was dissolved with 1 ml of ethyl acetate and was added to the alkaloid mixture and stirred for 10 min at room temp. After that isopropanol (1.4 mL) was added and the mixture was heated at reflux (85 °C) Refluxing was continued for 5 hrs, and the mixture was allowed to cool to room temperature and then to 0 °C in an ice bath, no precipitate was notice, and a lot of TLC spots have shown. We were not able to separate the enantiomers using this reaction.

4.2.2. *The enantiomers resolution with (-)(1R)-menthyl chloroformate.*

(5R)-2-isopropyl-5-methylcyclohexyl (5S)-5-(2-bromobenzyl)-7,8-dihydro-[1,3]dioxolo[4,5-g]isoquinoline-6(5H)-carboxylate (**10**), and (5R)-2-isopropyl-5-methylcyclohexyl (5R)-5-(2-bromobenzyl)-7,8-dihydro-[1,3]dioxolo[4,5-g]isoquinoline-6(5H)-carboxylate (**11**):

(±) Bromo-tetrahydrobenzylisoquinoline **3** was dissolved in acetonitrile (10 mL), and (1.2 mL) of triethylamine was added, followed by (0.76 mL) of (-)(1R)-menthyl chloroformate dropwise. The mixture was reacted for 30 minutes at room temperature. Then, the mixture was concentrated and then purified by chromatography on column using hexane/EtOAc mixtures as the eluent to afford 94 mg of **10** and 40 mg of **11**.

¹H NMR and ¹³C NMR analysis of compound **10** revealed the presence of two amide rotamers present in a 1:1 ratio. ¹H NMR of compound **10** (500 MHz, CDCl₃): δ = 0.5 (d, J = 6.8 Hz, 1 H), 0.71 (d, J = 6.9 Hz, 1 H), 0.79 (d, J = 7.02 Hz, 2 H), 0.82–1.93 (m, 14 H), 2.63–2.69 (m, 1H), 2.72–2.99 (m, 1 H), 3.06 (ddd, J = 13.22, 9.83, 2.88 Hz, 1 H), 3.29 (dd, J = 13.62, 4.71 Hz, 1 H), 3.35–3.51 (m, 1 H), 4.27 (ddd, J = 13.34, 6.07, 2.90 Hz, 1 H), 4.41 (qd, J = 11.03, 4.29 Hz, 1 H), 5.37 (dd, J = 10.0, 4.46 Hz, 1 H), 5.92 (s, 1H), 5.94 (s, 1H), 6.60 (d, J = 9.33 Hz, 1 H), 6.68 (d, J = 3.08 Hz, 1 H), 7.04–7.14 (m, 2 H), 7.20 (t, J = 7.3 Hz, 1 H), 7.55 (dd, J = 7.96, 1.17 Hz, 1 H) ppm.

¹³C NMR (125 MHz, CDCl₃): δ = 16.7, 20.6, 21.4, 22.6, 24.8, 26.5, 29.0, 31.3, 34.3, 38.2, 42.6, 47.0, 54.4, 75.2, 100.8, 107.0, 108.6, 125.4, 127.3, 127.5, 128.2, 130.0, 131.4, 132.6, 137.7, 146.0, 146.4, 155.4 ppm. . HRESI-MS calcd. For [C₂₈H₃₄BrNO₄ +H⁺] (M+H⁺): 528.175 found: 528.181.

^1H NMR and ^{13}C NMR analysis of compound **11** as well revealed the presence of two amide rotamers present in a 2:1 ratio. ^1H NMR of compound **11** (500 MHz, CDCl_3): δ = 0.66 (d, J = 6.9 Hz, 1 H), 0.79 (d, J = 6.4 Hz, 1 H), 0.84 (d, J = 7.52 Hz, 2 H), 0.84–1.45 (m, 14 H), 2.65–2.71 (m, 1H), 2.87–2.97 (m, 1 H), 3.01 (dd, J = 13.8, 10.7 Hz, 1 H), 3.25 (dd, J = 13.8, 3.6 Hz, 1 H), 3.36 (ddd, J = 13.3, 10.3, 4.3 Hz, 1 H), 4.24 (td, J = 10.8, 4.3 Hz, 1 H), 4.31–4.34 (m, 1 H), 5.47 (dd, J = 10.7, 3.5 Hz, 1 H), 5.94 (d, J = 1.6 Hz, 1H), 5.95 (d, J = 1.4 Hz, 1H), 6.62 (s, 1 H), 6.68 (s, 1 H), 7.05–7.12 (m, 2 H), 7.21 (td, J = 7.4, 1.2 Hz, 1 H), 7.57 (dd, J = 7.56, 1.18 Hz, 1 H) ppm.

^{13}C NMR (125 MHz, CDCl_3): δ = 16.6, 20.7, 23.5, 26.5, 28.5, 29.7, 31.0, 34.2, 36.9, 40.0, 42.9, 46.9, 53.5, 74.9, 100.9, 106.9, 108.6 125.3, 127.08, 127.5, 128.4, 130.0, 131.3, 132.6, 137.8, 146.0, 146.4, 155.9 ppm. HRESI-MS calcd. For $[\text{C}_{28}\text{H}_{34}\text{BrNO}_4 + \text{H}]$ (M^{++}H): 528.175 found: 528.181.

5. Conclusion

This study described the total synthesis of (\pm) anonaine, 3, 4-methylenedioxy-1-phenanthreneethylamine, (\pm) romucosine, and [2-(3,4-methylenedioxy-1-phenanthrenyl)ethyl]-methylcarbamate by using of direct arylation reactions with 3,4-methylenedioxyphenethylamine **1** and 2-bromophenylacetic acid **2** in the preparation of aporphine analogs.

We also described the separation of the enantiomers using different resolution reactions. The resolution with (–)-menthyl chloroformate succeeded in separating the enantiomers. However, the cleavage of menthyl chloroformate moiety proves difficulties.

Anonaine, 3, 4-methylenedioxy-1-phenanthreneethylamine, romucosine, and [2-(3,4-methylenedioxy-1-phenanthrenyl)ethyl]-methylcarbamate have subjected to the biological

evaluation to understand how they would induce or reduce the cytotoxicity as well as the neurotoxicity. Several studies have indicated the anticancer activities of anonaine, and it showed an interesting anticancer effective towards all cancer cell lines in our study. The anticancer activities of 3, 4-methylenedioxy-1-phenanthreneethylamine, romucosine, and [2-(3,4-methylenedioxy-1-phenanthrenyl)ethyl]-methylcarbamate were reported here for the first time.

Anonaine (compound **6**) was significantly toxic to the neurons at 5 µg/mL. Also, the alkaloidal extract significantly decreased the viability of the neurons with increasing concentration. All other extracts and synthesized compounds did not have a significant decrease in neuron cells viability according to statistical analysis. However, all extracts were extremely toxic to all tested cancer and normal cell lines, so further studies are needed to understand these conflicting results.

Lastly, the presence of the synthesized alkaloids in *Rollinia mucosa* was studied by using a targeted analysis of *Rollinia mucosa* fruits and seeds extracts using UHPLC-QToF-MS. Only anonaine was detected from *Rollinia mucosa* fruits and seeds methanolic extracts and *Rollinia mucosa* seeds alkaloidal extract.

We were not able to detect the presence of romucosine, which has been reported to be isolated from *Rollinia mucosa* fruits. Our study suggested that romucosine and other N-methoxycarbonyl alkaloids reported previously from *Rollinia mucosa* could be artifacts formed during the acid-base extraction, or they might be found in different sub-species of *Rollinia mucosa*.

BIBLIOGRAPHY

- Alali FQ, Kaakeh W, Bennett GW, McLaughlin JL. Annonaceous acetogenins as natural pesticides: potent toxicity against insecticide-susceptible and -resistant German cockroaches (Dictyoptera: Blattellidae). *Journal of economic entomology*. 1998;91:641.
- Alali FQ, Liu X, McLaughlin JL. Annonaceous acetogenins: Recent progress. *Journal of Natural Products*. 1999;62:504-540.
- Aminimoghadamfarouj N, Nematollahi A, Wiart C. Annonaceae: bio-resource for tomorrow's drug discovery. *Journal of Asian Natural Products Research*. 2011;13:465-476.
- Ashpole NM, Hudmon A. 2011. Excitotoxic neuroprotection and vulnerability with CaMKII inhibition. *Mol Cell Neurosci*. 46:720-730.
- Avula B, Bae J, Majrashi T, Wu T, Wang Y, Wang M, Ali Z, Wu Y, Khan IA. Targeted and non-targeted analysis of annonaceous alkaloids and acetogenins from *Asimina* and *Annona* species using UHPLC-QToF-MS. *Journal of Pharmaceutical and Biomedical Analysis*. 2018;159:548-566.
- Bermejo A, Figadere B, Zafra-Polo M, Barrachina I, Estornell E, Cortes D. Acetogenins from Annonaceae: recent progress in isolation, synthesis and mechanisms of action. *Natural Product Reports*. 2005;22:269.
- Brannan RG, Peters TE, Black KJ, Kukor BJ. Valorization of underutilized north American pawpaw (*Asimina triloba*): Investigation as a lipid oxidation inhibitor in turkey homogenate model system. *Journal of the Science of Food and Agriculture*. 2018;98:2210.

- Brophy JJ, Goldsack RJ, Forster PI. The Leaf Essential Oil of *Galbulimima baccata* (Himantandraceae) from Queensland, Australia. *Journal of Essential Oil Research*. 2005;17:536-538.
- Caetano LC, Dadoun H. Pallidine and Aporphinoid Alkaloids from *Rollinia mucosa*. *Journal of Natural Products*. 1987;50:330-330.
- Callaway MB. Current Research for the Commercial Development of Pawpaw [*Asimina triloba* (L.) Dunal]. *HortScience*. 1992;27:90-191.
- Cambie RC, Lal AR, Pausler MG. Constituents of *Degeneria vitiensis* Heartwood. *Biochemical Systematics and Ecology*. 1992;20:265-265.
- Carmen Zafra-Polo M, Figadère B, Gallardo T, Tormo J, Cortes D. Natural acetogenins from annonaceae, synthesis and mechanisms of action. *Phytochemistry. Elsevier Ltd*; 1998;48:1087-1117.
- Cave A. Annonaceae Alkaloids. The chemistry and biology of isoquinoline alkaloids. *West Berlin*. 1985;pp 79-101.
- Chang F, Chang H, Wu Y, Lai Y. Anti-Cancer Effect of Liriodenine on Human Lung Cancer Cells. *Kaohsiung Journal of Medical Sciences*. 2004;20:365-371.
- Chen C, Chen C, Chen C, et al. (-)-Anonaine induces apoptosis through Bax- and caspase-dependent pathways in human cervical cancer (HeLa) cells. *Food and Chemical Toxicology*. 2008;46:2694-2702.
- Chen KS, Ko FN, Teng CM, Wu YC. Antiplatelet and vasorelaxing actions of some aporphinoids. *Planta medica*. 1996;62:133.
- Chen C, Chang F, Shih Y, et al. Cytotoxic constituents of *Polyalthia longifolia* var. *pendula*. *Journal of Natural Products*. 2000;63:1475-1478.

- Chen C, Chang F, Wu Y. The constituents from the stems of *Annona cherimola*. *Journal of The Chinese Chemical Society*. 1997;44:313-319.
- Chen C, Chen S, Chen C. Liriodenine induces G1/S cell cycle arrest in human colon cancer cells via nitric oxide- and p53-mediated pathway. *Process Biochemistry*. 2012;47:1460-1468.
- Chen YY, Chang FR, Wu YC. Isoquinoline Alkaloids and Lignans from *Rollinia mucosa*. *Journal of Natural Products*. 1996;59:904-906.
- Chen Y, Chang F, Yen H, Wu Y. Epomusenins A and B, two acetogenins from fruits of *Rollinia mucosa*. *Phytochemistry*. 1996;42:1081-1083.
- Coothankandaswamy V, Liu Y, Mao S, et al. The alternative medicine pawpaw and its acetogenin constituents suppress tumor angiogenesis via the HIF-1/VEGF pathway. *Journal of Natural Products*. 2010;73:956-961.
- Coria-Télliz AV, Montalvo-González E, Yahia EM, Obledo-Vázquez EN. *Annona muricata*: A comprehensive review on its traditional medicinal uses, phytochemicals, pharmacological activities, mechanisms of action and toxicity. *Arabian Journal of Chemistry*. 2018;11:662-691.
- Correché ER, Andujar SA, Kurdelas RR, Lechón MJG, Freile ML, Enriz RD. Antioxidant and cytotoxic activities of canadine: Biological effects and structural aspects. *Bioorganic & Medicinal Chemistry*. 2008;16:3641-3651.
- Costa EV, Marília Fernanda Chaves Sampaio, Salvador MJ, Nepel A, Barison A. CHEMICAL CONSTITUENTS FROM THE STEM BARK OF *Annona pickelii* (Annonaceae). *Química Nova*. 2015;38:769-776.

- Cuendet M, Oteham CP, Moon RC, Keller WJ, Peaden PA, Pezzuto JM. Dietary administration of *Asimina triloba* (pawpaw) extract increases tumor latency in N-methyl-N-nitrosourea-treated rats. *Pharmaceutical Biology*. 2008;46: 3-7.
- Dai X, Hu R, Sun C, Pan Y. Comprehensive separation and analysis of alkaloids from *Stephania yunnanensis* by counter-current chromatography coupled with liquid chromatography tandem mass spectrometry analysis. *Journal of Chromatography A*. 2012;1226:18-23.
- Dary C, Bun S, Herbette G, Mabrouki F, Bun H, Kim S, Jabbour F, Hul S, Baghdikian B, Ollivier E. Chemical profiling of the tuber of *Stephania cambodica* gagnep. (menispermaceae) and analytical control by UHPLC-DAD. *Natural Product Research*. 2017;31:802-809.
- Degli Esposti M, Ghelli A, Ratta M, Cortes D, Estornell E. Natural substances (acetogenins) from the family Annonaceae are powerful inhibitors of mitochondrial NADH dehydrogenase (Complex I). *Biochemical Journal*. 1994;301:161-167.
- Dembitsky VM. Astonishing diversity of natural surfactants: 6. Biologically active marine and terrestrial alkaloid glycosides. *Lipids*. 2005;40:1081.
- Donno D, Beccaro GL, Mellano MG, Cerutti AK, Bounous G. Chemical fingerprinting as nutraceutical quality differentiation tool in *Asimina triloba* L. fruit pulp at different ripening stages: An old species for new health needs. *Journal of Food and Nutrition Research*. 2014;53:81-95.
- Egydio-Brandão APM, Novaes P, Santos DYAC. Alkaloids from *Annona*: Review from 2005 to 2016. *JSM Biochemistry & Molecular Biology*. 2017;4:1031.

- Escobar-Khondiker M, Hollerhage M, Muriel M, et al. Annonacin, a Natural Mitochondrial Complex I Inhibitor, Causes Tau Pathology in Cultured Neurons. *Journal of Neuroscience*. 2007;27:7827-7837.
- Galli F, Archbold DD, Pomper KW. Pawpaw: An old fruit for new needs. *Acta Horticulturae*. 2007;744:461-466.
- Gonda R, Takeda T, Akiyama T. Studies on the constituents of *Anaxagorea luzonensis* A. GRAY. *Chemical and Pharmaceutical Bulletin*. 2000;48:1219-1222.
- González-Esquinca AR, De-La-Cruz-Chacón I, Castro-Moreno M, Orozco-Castillo JA, Riley-Saldaña CA. Alkaloids and acetogenins in Annonaceae development: biological considerations. *Revista Brasileira de Fruticultura*. 2014;36:1-16.
- Gu Z, Zhou D, Lewis NJ, et al. Quantitative evaluation of Annonaceous acetogenins in monthly samples of paw paw (*Asimina triloba*) twigs by liquid chromatography/electrospray ionization/tandem mass spectrometry. *Phytochemical Analysis*. 1999;10:32-38.
- Guo Z, Wang J, Wang X, Luo J, Luo J, Kong L. A novel aporphine alkaloid from *Magnolia officinalis*. *Fitoterapia*. 2011;82:637-641.
- Hartwell JL. *Plants Used Against Cancer*. Quarterman Publications Inc, Lawrence, MA. 1982;P 379.
- Hasrat JA, Pieters L, De Backer J-, Vauquelin G, Vlietinck AJ. Screening of medicinal plants from Suriname for 5-HT1A ligands: Bioactive isoquinoline alkaloids from the fruit of *Annona muricata*. *Phytomedicine*. 1997;4:133-140.
- Höllerhage M, Matusch A, Champy P, et al. Natural lipophilic inhibitors of mitochondrial complex I are candidate toxins for sporadic neurodegenerative tau pathologies. *Experimental Neurology*. 2009;220:133-142.

- Höllerhage M, Rösler TW, Berjas M, et al. Neurotoxicity of Dietary Supplements from Annonaceae Species. *International Journal of Toxicology*. 2015;34:543.
- Hormaza JI. The pawpaw, a forgotten north American fruit tree Arnold Arboretum of Harvard University. 2014.
- Huang W, Singh OV, Chen C, Lee S. Synthesis of (\pm)-glaucine and (\pm)-neospirodienone via a one-pot Bischler-Napieralski reaction and oxidative coupling by a hypervalent iodine reagent. *Cheminformatics*. 2004;35:25.
- Hsieh P, Hsieh T, Liu T, et al. Liriodenine inhibits the proliferation of human hepatoma cell lines by blocking cell cycle progression and nitric oxide-mediated activation of p53 expression. *Food and Chemical Toxicology*. 2005;43:1117-1126.
- Hsieh T, Chang F, Wu Y. The constituents of *Cananga odorata*. *Journal of The Chinese Chemical Society*. 1999;46:607-611.
- Hsieh TJ, Chang FR, Chia YC, et al. The alkaloids of *Artabotrys uncinatus*. *Journal of Natural Products*. 2001;64:1157-1161.
- Jeong E, Lee SY, Yu SM, et al. Identification of structurally diverse Alkaloids in *Corydalis* species by liquid chromatography/electrospray ionization tandem mass spectrometry. *Rapid Communications in Mass Spectrometry*. 2012;26:1661-1674.
- Jolad SD, Hoffmann JJ, Schram KH, Cole JR, Tempesta MS, Kriek GR, Bates RBJ. Uvaricin, a new antitumor agent from *Uvaria accuminata* (Annonaceae). *The Journal of Organic Chemistry*. 1982;47:3151-3153.
- Kelm MA, Nair MG. A brief summary of biologically active compounds from *Magnolia* spp. *Natural Products Chemistry*. 2000;24:845.

- Kim S, Koh J, Ma H, et al. Sequence and Expression Studies of A-, B-, and E-Class MADS-Box Homologues in Eupomatia (Eupomatiaceae): Support for the Bracteate Origin of the Calyptra. *International Journal of Plant Sciences*. 2005;166:185-198.
- Ko F, Yu S, Su M, Wu Y, Teng C. Pharmacological activity of (-)-discretamine, a novel vascular α -adrenoceptor and 5-hydroxytryptamine receptor antagonist, isolated from *Fissistigma glaucescens*. *British Journal of Pharmacology*. 1993;110:882-888.
- Ko Y, Wu Y, Wu T, Chang F, Guh J, Chuang L. Annonacin induces cell cycle-dependent growth arrest and apoptosis in estrogen receptor- α -related pathways in MCF-7 cells. *Journal of Ethnopharmacology*. 2011;137:1283-1290.
- Kohnen AL, Dunetz JR, Danheiser RL. Synthesis of ynamides by n-alkynylation of amine derivatives. preparation of n-allyl-n-(methoxycarbonyl)-1,3-decadiynylamine. *Organic Syntheses*. 2007;84:88-101.
- Kotake Y, Okuda K, Kamizono M, et al. Detection and determination of reticuline and N-methylcoculaurine in the Annonaceae family using liquid chromatography-tandem mass spectrometry. *Journal of Chromatography B*. 2004;806:75-78.
- Kuo R, Chen C, Lin A, Chang F, Wu Y. A New Phenanthrene Alkaloid, Romucosine I, from *Rollinia mucosa* Baill. *Zeitschrift für Naturforschung*. 2004;59:334-336.
- Kuo R, Chang F, Chen C, Teng C, Yen H, Wu Y. Antiplatelet activity of N-methoxycarbonyl aporphines from *Rollinia mucosa*. *Phytochemistry*. 2001;57:421-425.
- Lafrance M, Blaquiere N, Fagnou K. Aporphine Alkaloid Synthesis and Diversification via Direct Arylation. *European Journal of Organic Chemistry*. 2007;2007:811-825.

- Lannuzel A, Michel PP, Caparros-Lefebvre D, Abaul J, Hocquemiller R, Ruberg M. Toxicity of Annonaceae for dopaminergic neurons: potential role in atypical parkinsonism in Guadeloupe. *Movement Disorders*. 2002;17:84-90.
- Lannuzel A, Michel PP, Höglinger GU, et al. The mitochondrial complex I inhibitor annonacin is toxic to mesencephalic dopaminergic neurons by impairment of energy metabolism. *Neuroscience*. 2003;121:287-296.
- Leboeuf M, Cavé A, Bhaumik PK, Mukherjee R, Mukherjee B. The phytochemistry of the annonaceae. *Phytochemistry*. 1980;21:2783-2813.
- Li Y, Ye J, Chen Z, et al. Annonaceous acetogenins mediated up-regulation of Notch2 exerts growth inhibition in human gastric cancer cells in vitro. *Oncotarget*. 2017;8:21140-21152.
- Liaw CC, Chang FR, Chen YY, Chiu HF, Wu MJ, Wu YC. New annonaceous acetogenins from *Rollinia mucosa*. *Journal of Natural Products*. 1999;62:1613-1617.
- Lin C, Yang C, Ko F, Wu Y, Teng C. Antimuscarinic action of liriodenine, isolated from *Fissistigma glaucescens*, in canine tracheal smooth muscle. *British Journal of Pharmacology*. 1994;113:1464-1470.
- Liu C, Chen Y, Cheng M, Lee S, Abd El-razek MH, Chang W, Chen Y, Chen I. Cytotoxic constituents from the root wood of formosan *Michelia compressa*. *Journal of the Chilean Chemical Society*. 2008;53.
- Lúcio, Ana Silvia Suassuna Carneiro, Almeida, Jackson Roberto Guedes da Silva, Da-Cunha EVL, Tavares JF, Barbosa Filho JM. Alkaloids of the Annonaceae: occurrence and a compilation of their biological activities. *The Alkaloids. Chemistry and Biology*. 2015;74:233.

- Love K, Paull RE. Rollinia. *The College of Tropical Agriculture and Human Resources*. 2011.
- Majrashi TA, Zulfiqar F, Chittiboyina AG, Ali Z, Khan IA. Isoquinoline alkaloids from *Asimina triloba*. *Natural Product Research*. 2018;33:2823-2829.
- Maltese F, van der Kooy F, Verpoorte R. Solvent derived artifacts in natural products chemistry. *Natural Product Communications*. 2009;4:447.
- McLaughlin JL. Paw paw and cancer: annonaceous acetogenins from discovery to commercial products. *Journal of Natural Products*. 2008;71:1311-1321.
- McLaughlin JL, Benson GB, Forsythe JW. A novel mechanism for the control of clinical cancer: Inhibition of the production of adenosine triphosphate (ATP) with a standardized extract of paw paw. 2003.
- Moghadamtousi SZ, Fadaeinasab M, Nikzad S, Mohan G, Ali HM, Kadir HA. *Annona muricata* (Annonaceae): A Review of Its Traditional Uses, Isolated Acetogenins and Biological Activities. *International Journal of Molecular Sciences*. 2015;16:15625-15658.
- Mongkolrat S, Palanuvej C, Ruangrunsi N. Quality assessment and lirioidenine quantification of *Nelumbo nucifera* dried leaf in Thailand. *Pharmacognosy Journal*. 2012;4:24-28.
- Moriyasu M, Ichimaru M, Nishiyama Y, Kato A, Wang J, Zhang H, Lu GB. (R)-(+)-Isotembetarine, a Quaternary Alkaloid from *Zanthoxylum nitidium*. *Journal of Natural Products*. 1997;60:299-301.
- Nishiyama Y, Moriyasu M, Ichimaru M, Iwasa K, Kato A, Mathenge SG, Mutiso PBC, Juma FD. Secondary and tertiary isoquinoline alkaloids from *Monodora junodii*. *Nature Medicine*. 2000;54:338-341.

- Nordin N, Majid NA, Hashim NM, Rahman MA, Hassan Z, Ali HM. Liriodenine, an aporphine alkaloid from *Enicosanthellum pulchrum*, inhibits proliferation of human ovarian cancer cells through induction of apoptosis via the mitochondrial signaling pathway and blocking cell cycle progression. *Drug Design, Development and Therapy*. 2015;9:1437-1448.
- Paul J, Gnanam R, Jayadeepa RM, Arul L. Anti cancer activity on Graviola, an exciting medicinal plant extract vs various cancer cell lines and a detailed computational study on its potent anti-cancerous leads. *Current topics in medicinal chemistry*. 2013;13:1666.
- Paulo MD, Kaplan MA, Laprevote O, Roblot F, Hocquemiller R, Cave A. Lignans and other non-alkaloidal constituents from *Rollinia mucosa*. *Fitoterapia*. 1991;62:150-152.
- Pomper KW, Lowe JD, Crabtree SB, Keller W. Identification of annonaceous acetogenins in the ripe fruit of the North American pawpaw (*Asimina triloba*). *Journal of Agricultural and Food Chemistry*. 2009;57:8339-8343.
- Potts LF, Luzzio FA, Smith SC, Hetman M, Champy P, Litvan I. Annonacin in *Asimina triloba* fruit: Implication for neurotoxicity. *Neurotoxicology*. 2012;33:53-58.
- Ouattara Z A, Boti JB, Ahibo AC, Tomi F, Bighelli A. *Artabotrys oliganthus* Engl. & Diels from Ivory Coast: composition of leaf, stem bark and fruit oils. *Journal of Essential Oil Bearing Plants*. 2011;14.
- Quílez AM, Fernández-Arche MA, García-Giménez MD, De la Puerta R. Potential therapeutic applications of the genus *Annona*: Local and traditional uses and pharmacology. *Journal of Ethnopharmacology*. 2018;225:244-270.

- Rabêlo SV, Araújo CD, Costa VCD, Tavares JF, Da Silva MS, Filho JM, Almeida JRGD. Occurrence of alkaloids in species of the genus *Annona* L. (Annonaceae): A review. *Nutraceuticals Functional Foods*. 2014;1:41-60.
- Rabêlo SV, Costa EV, Barison A, et al. Alkaloids isolated from the leaves of atemoya (*Annona cherimola* × *Annona squamosa*). *Revista Brasileira de Farmacognosia*. 2015;25:419-421.
- Rasai S, George AP, Kantharajah AS. Tissue culture of *Annona spp.* (cherimoya, atemoya, sugar apple and soursop): A review. *Scientia Horticulturae. Elsevier B.V.* 1995;62:1-14.
- Ratnayake S, Fang X, Anderson JE, McLaughlin JL, Evert DR. Bioactive constituents from the twigs of *Asimina parviflora*. *Journal of Natural Products*. 1992;55:1462-1467.
- Ringdahl B, Chan RPK, Craig JC, Cava MP, Shamma M. Circular Dichroism of Aporphines. *Journal of Natural Products*. 1981;44:80-85.
- Sangster AW, Stuart KL. Ultraviolet Spectra of Alkaloids. *Chemical Reviews*. 1965;65:69-130.
- Sauquet H. Androecium diversity and evolution in Myristicaceae (Magnoliales), with a description of a new Malagasy genus, *Doyleanthus* gen. nov. *American Journal of Botany*. 2003;90:1293-1305.
- Schmidt J, Raith K, Boettcher C, Zenk MH. Analysis of benzyloquinoline-type alkaloids by electrospray tandem mass spectrometry and atmospheric pressure photoionization. *European Journal of Mass Spectrometry*. 2005;11:325-333.
- Schühly W, Khan I, Fischer N. The Ethnomedicinal Uses of Magnoliaceae from the Southeastern United States as Leads in Drug Discovery. *Pharmaceutical Biology*. 2001;39:63-69.
- Shamma M, Shamma M, Shamma M, et al. The Ultraviolet Spectra of Phenolic Aporphines in Basic Solution. *Journal of Organic Chemistry*. 1971;36:3253-3254.

- Shi G, MacDougal JM, McLaughlin JL. Bioactive annonaceous acetogenins from *Rollinia mucosa*. *Phytochemistry*. 1997;45:719-723.
- Shi X, Ni F, Shang H, Yan M, Su J. Racemization of (S)-(+)-10,11-dimethoxyaporphine and (S)-(+)-aporphine: efficient preparations of (R)-(-)-apomorphine and (R)-(-)-aporphine via a recycle process of resolution. *Tetrahedron: Asymmetry*. 2006;17:2210-2215.
- Sica VP, El-Elimat T, Oberlies NH. In situ analysis of *Asimina triloba* (pawpaw) plant tissues for acetogenins via the droplet-liquid microjunction-surface sampling probe coupled to UHPLC-PDA-HRMS/MS. *Analytical Methods*. 2016;8:6143-6149.
- Singh A, Bajpai V, Kumar S, Singh Rawat AK, Kumar B. Analysis of isoquinoline alkaloids from *Mahonia leschenaultia* and *Mahonia napaulensis* roots using UHPLC-Orbitrap-MS and UHPLC-QqQ LIT -MS/MS. *Journal of Pharmaceutical Analysis*. 2017;7:77-86.
- Snatzke G, Wollenberg G. Alkaloids from *Croton* species. Part V. Configuration of linearisine and circular dichroism of proaporphine-type alkaloids. *Journal of the Chemical Society C: Organic*. 1966:1681.
- Soltis PS, Soltis DE. The origin and diversification of angiosperms. *American Journal of Botany*. 2004;91:1614-1626.
- Son HJ, Lee HJ, Yun-Choi HS, Ryu J. Inhibitors of Nitric Oxide Synthesis and TNF- α Expression from *Magnolia obovata* in Activated Macrophages. *Planta Medica*. 2000;66:469-471.
- Stadler R, Loeffler S, Cassels BK, Zenk MH. Bisbenzylisoquinoline biosynthesis in *Berberis stolonifera* cell cultures. *Phytochemistry*. 1988;27:2557-2565.
- Stamelou M, de Silva R, Arias-Carrión O, et al. Rational therapeutic approaches to progressive supranuclear palsy. *Brain: a journal of neurology*. 2010;133:1578-1590.

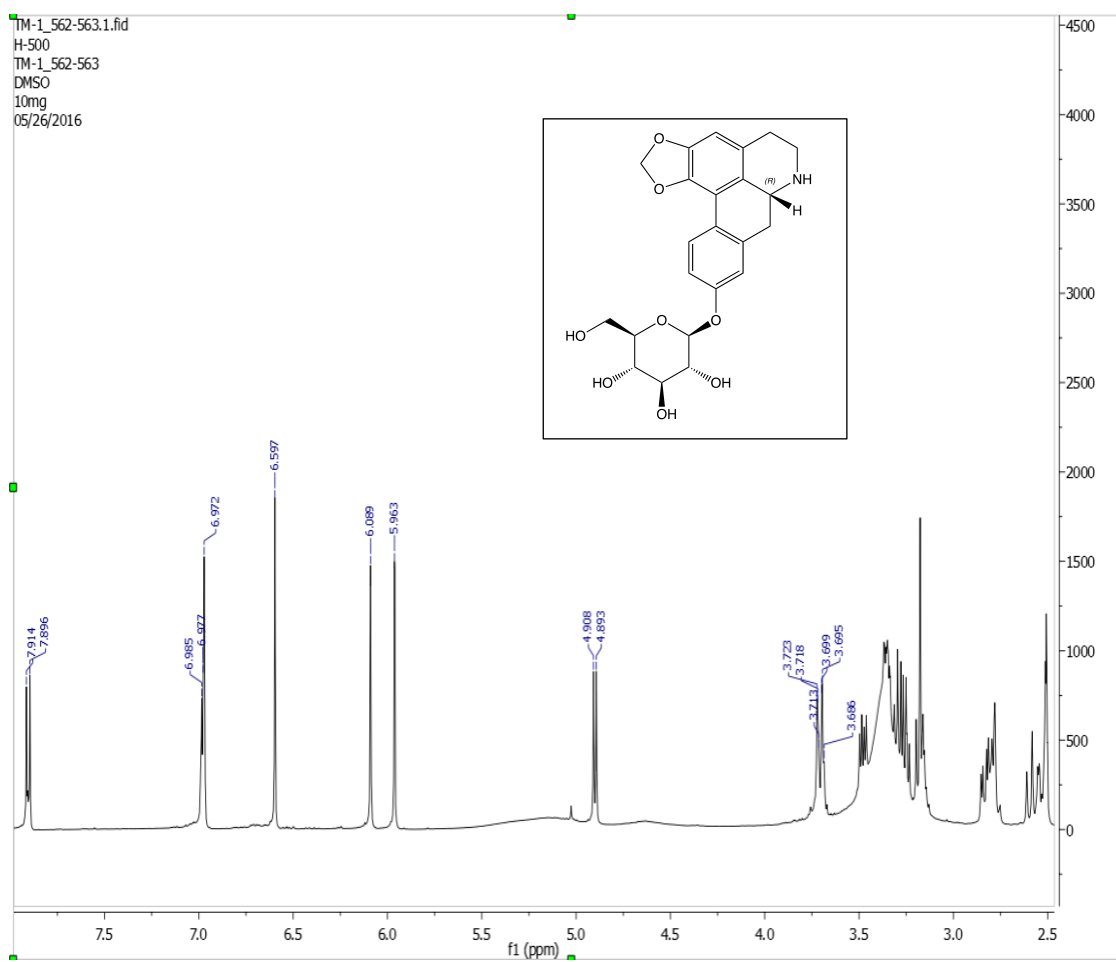
- Stévigny C, Jiwan JH, Rozenberg R, De Hoffmann E, Quetin-Leclercq J. Key fragmentation patterns of aporphine alkaloids by electrospray ionization with multistage mass spectrometry. *Rapid Communications in Mass Spectrometry*. 2004;18:523-528.
- Talapatra SK, Talapatra B, Chaudhuri PK. (-)-Maglifloenone, a novel spirocyclohexadienone neolignan and other constituents from *Magnolia liliflora*. *Phytochemistry*. 1982;21:747-750.
- Tang DQ, Zheng XX, Chen X, Yang DZ, Du Q. Quantitative and qualitative analysis of common peaks in chemical fingerprint of Yuanhu Zhitong tablet by HPLC-DAD-MS/MS. *Journal of Pharmaceutical Analysis*. 2014;4:96-106.
- Tian X, Li Z, Lin Y, Chen M, Pan G, Huang C. Study on the PK profiles of magnoflorine and its potential interaction in Cortex phellodendri decoction by LC-MS/MS. *Analytical and Bioanalytical Chemistry*. 2014;406:841-849.
- Tomita M, Kato A, Ibuka T, Furukawa H, Kozuka M. Mass spectra of pronuciferine and stepharine. *Tetrahedron Letters*. 1965;6:2825-2829.
- Tomita M, Kozuka M. Alkaloids of *Asimina triloba* dunal. *Yakugaku Zasshi*. 1965;85:77-82.
- Wu YC, Chang GY, Ko FN, Teng CM. Bioactive constituents from the stems of *Annona montana*. *Planta Medica*. 1995;61:146.
- Yang H, Li X, Tang Y, Zhang N, Chen J, Cai B. Supercritical fluid CO₂ extraction and simultaneous determination of eight annonaceous acetogenins in *Annona* genus plant seeds by HPLC-DAD method. *Journal of Pharmaceutical and Biomedical Analysis*. 2009;49:140-144.

- Yuan SF, Chang H, Chen H, et al. Annonacin, a mono-tetrahydrofuran acetogenin, arrests cancer cells at the G1 phase and causes cytotoxicity in a Bax- and caspase-3-related pathway. *Life Sciences*. 2003;72:2853-2861.
- Zhang A, Zhang Y, Branfman AR, Baldessarini RJ, Neumeyer JL. Advances in development of dopaminergic aporphinoids. *Journal of Medicinal Chemistry*. 2007;50:171-181.
- Zhao G, Chao J, Zeng L, Rieser MJ, McLaughlin JL. The absolute configuration of adjacent bis-THF acetogenins and asiminocin, a novel highly potent asimicin isomer from *Asimina triloba*. *Bioorganic & Medicinal Chemistry*. 1996;4:25-32.
- Zhao G-, Rieser MJ, Hui Y-, Miesbauer LR, Smith DL, McLaughlin JL. Biologically active acetogenins from stem bark of *Asimina triloba*. *Phytochemistry*. 1993;33:1065-1073.
- Zhao GX, Miesbauer LR, Smith DL, McLaughlin JL. Asimin, asiminacin, and asiminecin: novel highly cytotoxic asimicin isomers from *Asimina triloba*. *Journal of Medicinal Chemistry*. 1994;37:1971-1976.

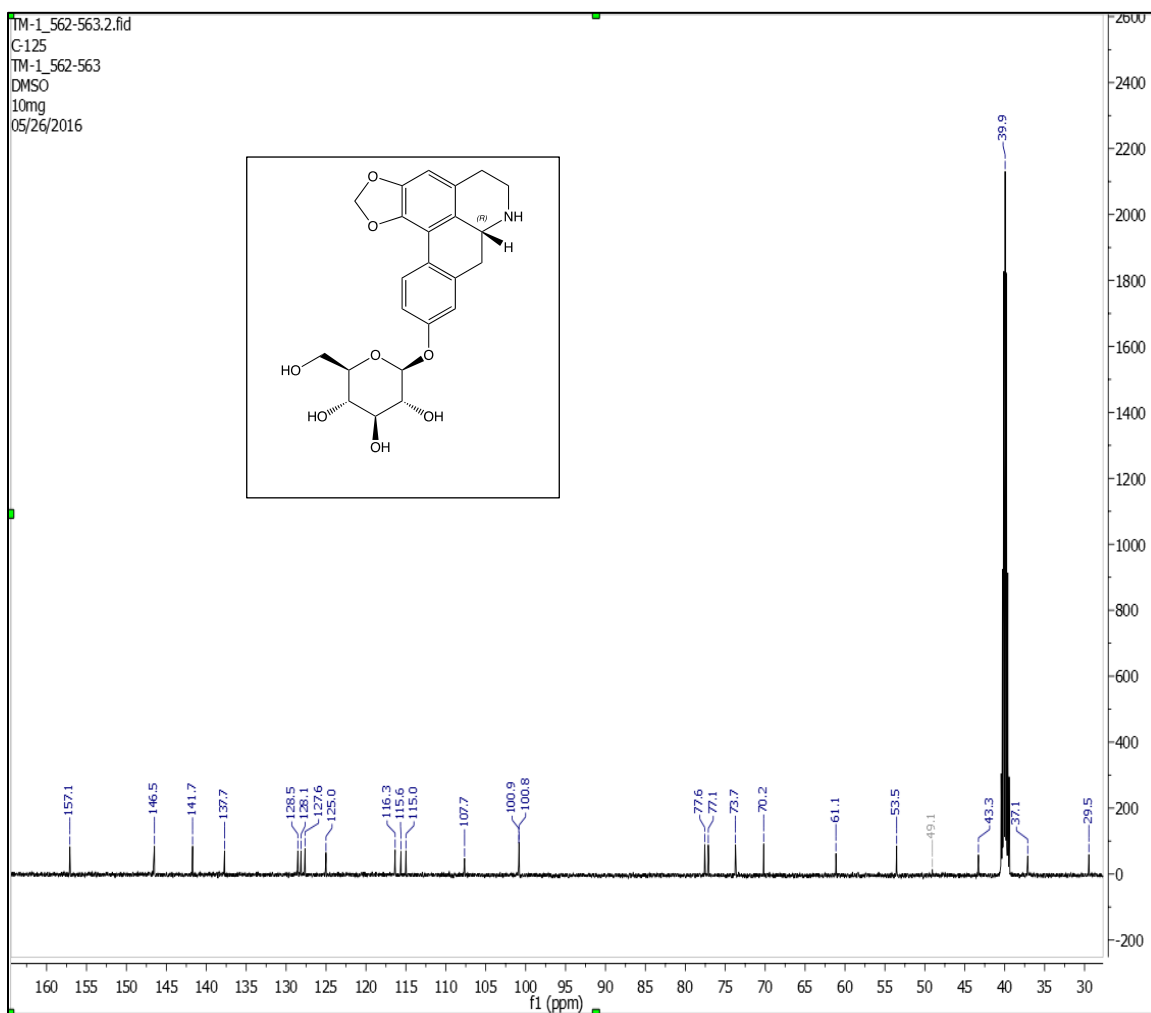
APPENDIX

APPENDIX 1. SUPPLEMENTARY DATA-CHAPTER II

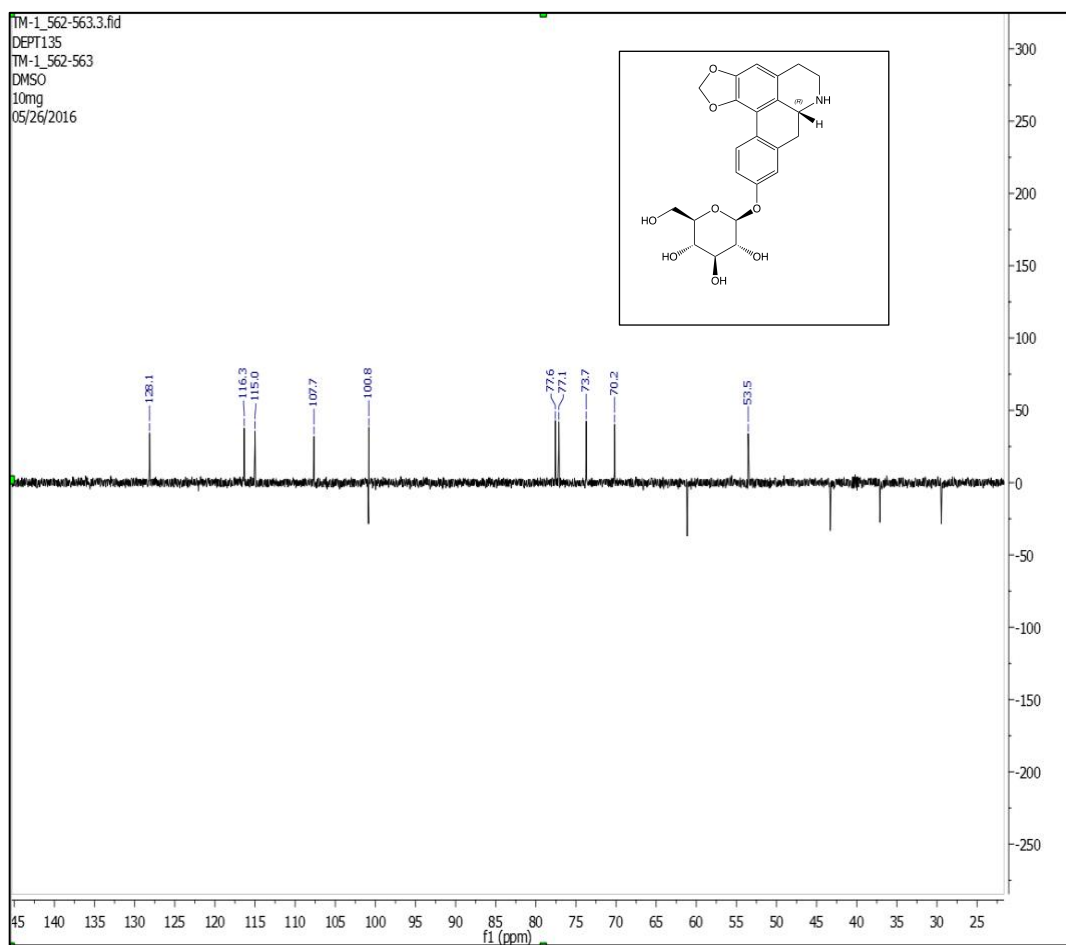
¹H NMR (500 MHz, DMSO-d₆) for (-)-Anolobine-9-*O*-β-D-glucopyranoside (**1**)



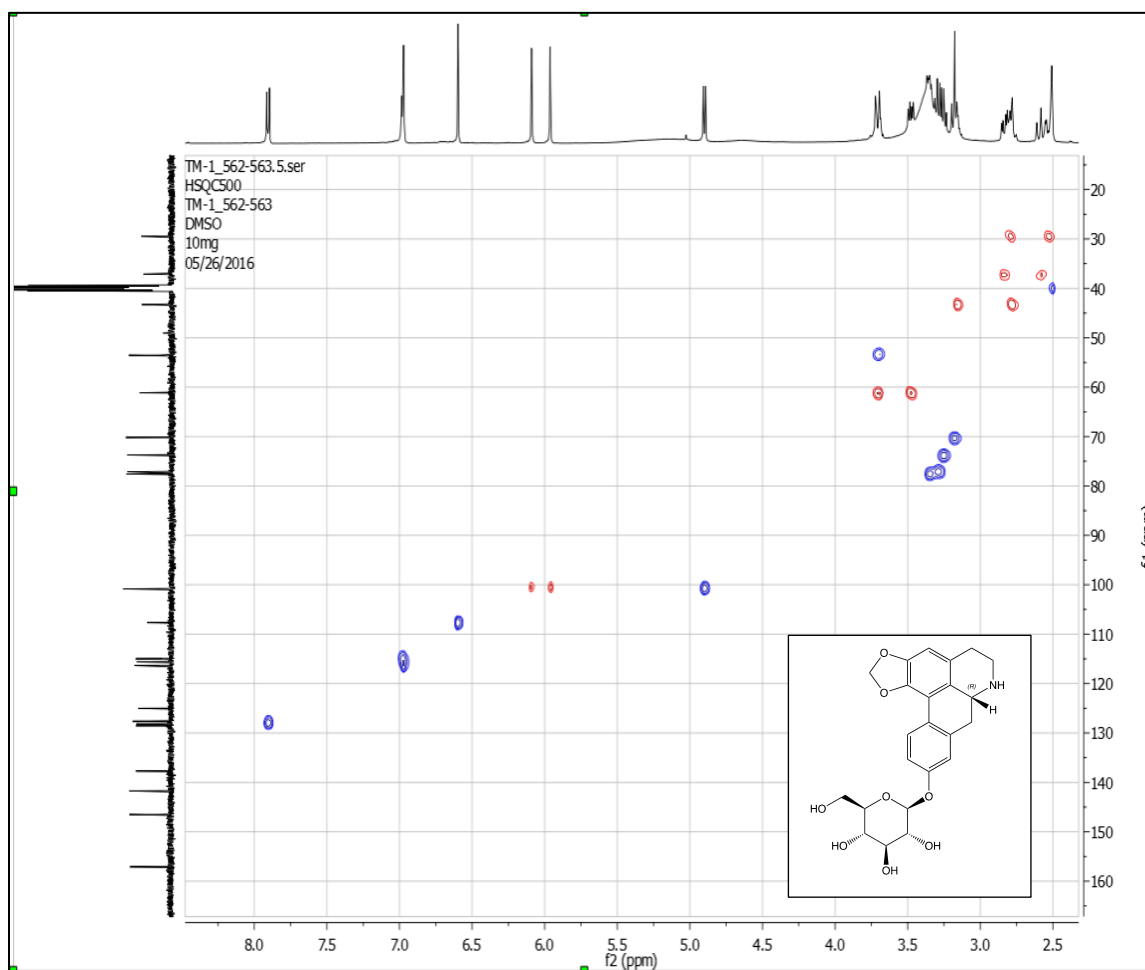
^{13}C NMR (125 MHz, DMSO- d_6) for (-)-Anolobine-9- O - β -D-glucopyranoside (**1**)



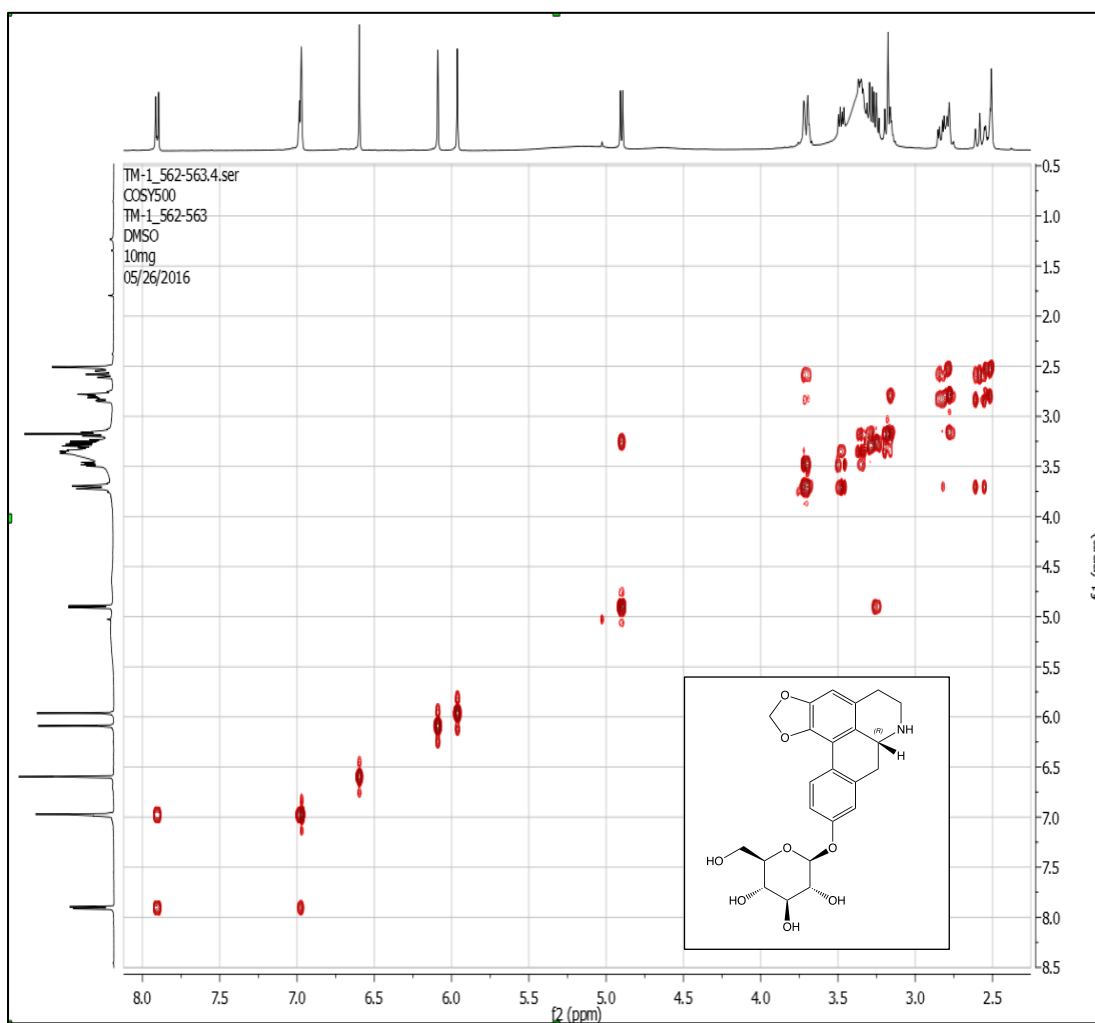
DEPT 135 (DMSO-d₆) for (-)-Anolobine-9-*O*-β-D-glucopyranoside (**1**)



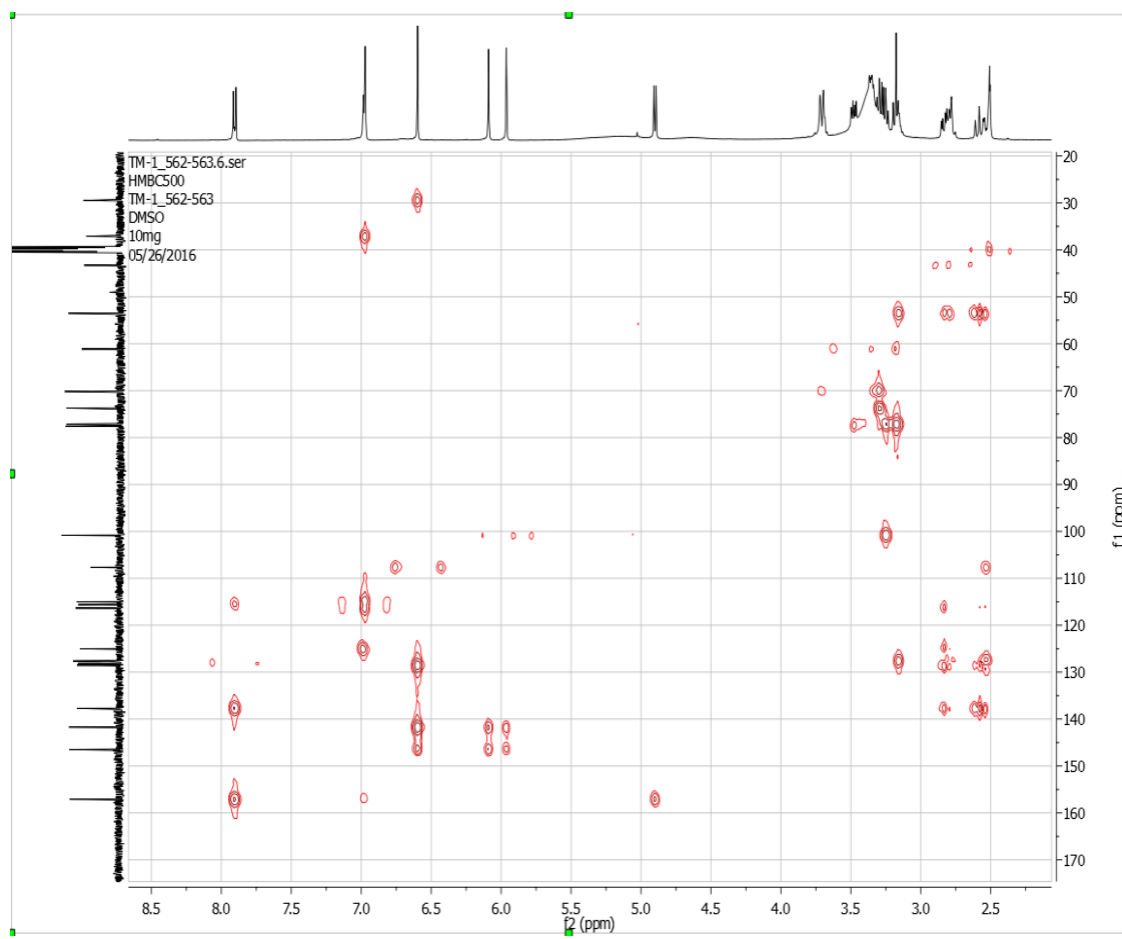
HSQC (DMSO-d₆) for (-)-Anolobine-9-*O*-β-D-glucopyranoside (**1**)



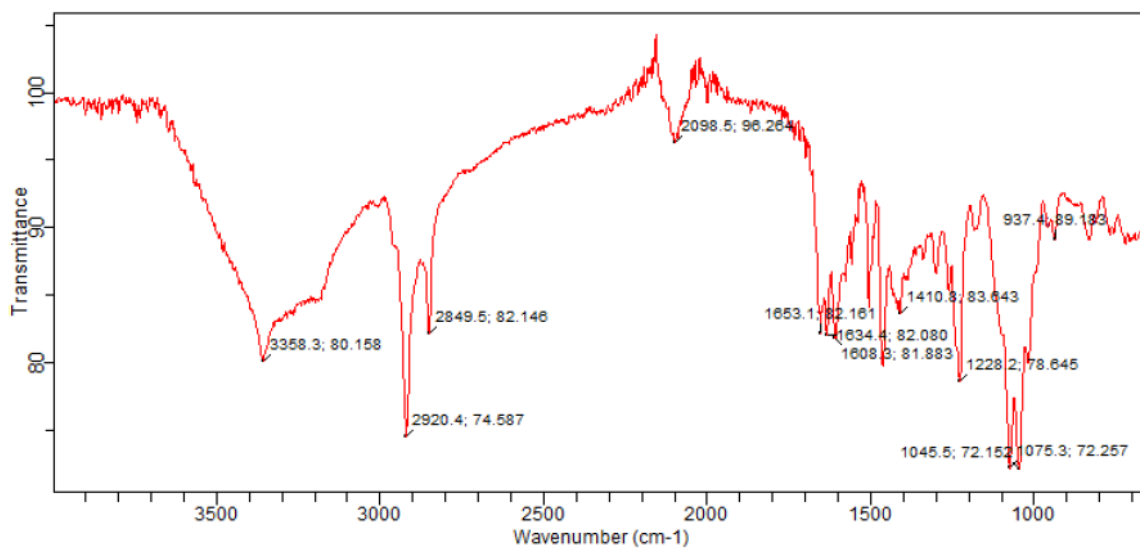
H-H COSY (DMSO-d₆) for (-)-Anolobine-9-*O*-β-D-glucopyranoside (**1**)



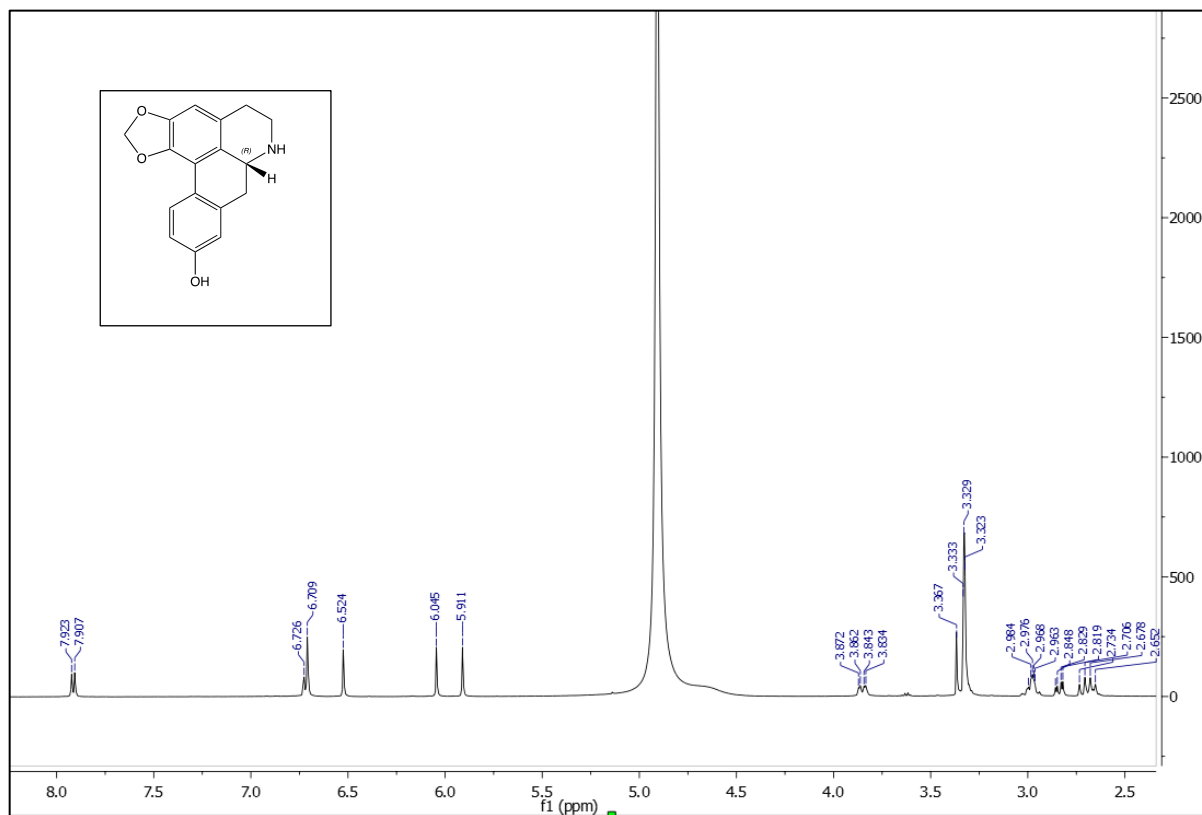
HMBC (DMSO-d₆) for (-)-Anolobine-9-*O*-β-D-glucopyranoside (**1**)



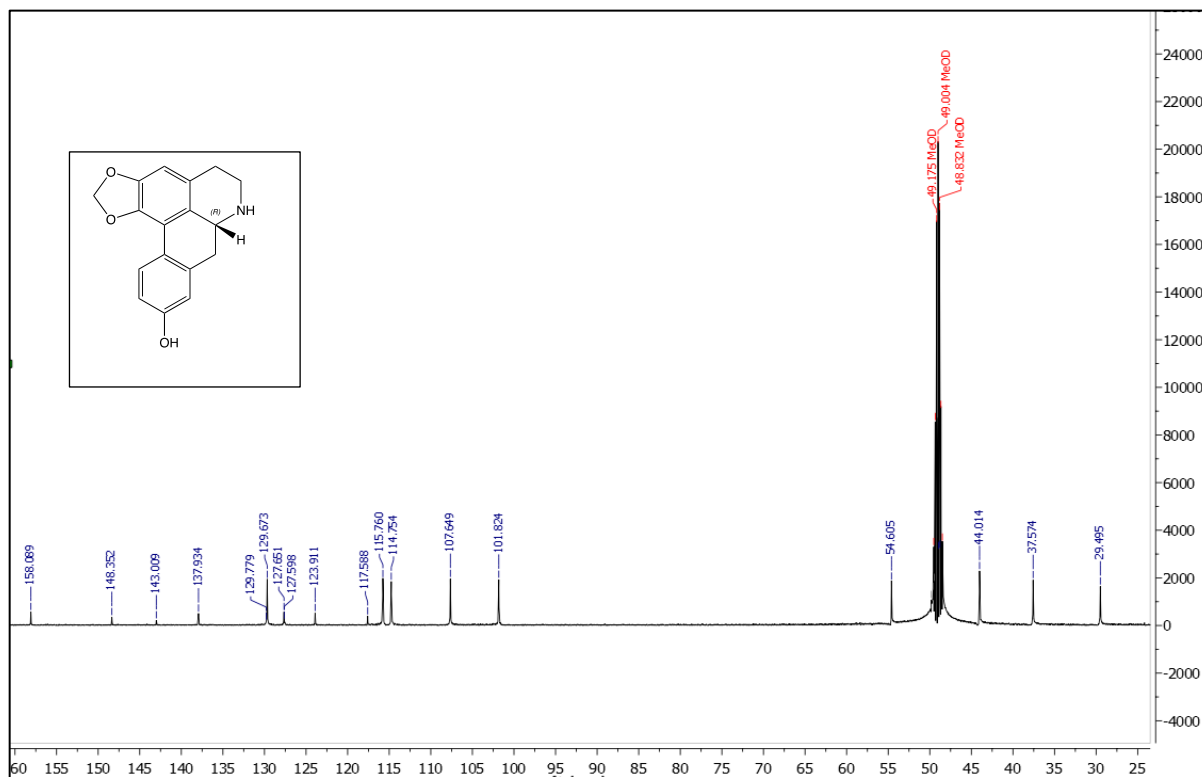
IR (KBr) for (-)-Anolobine-9-*O*- β -D-glucopyranoside (**1**)



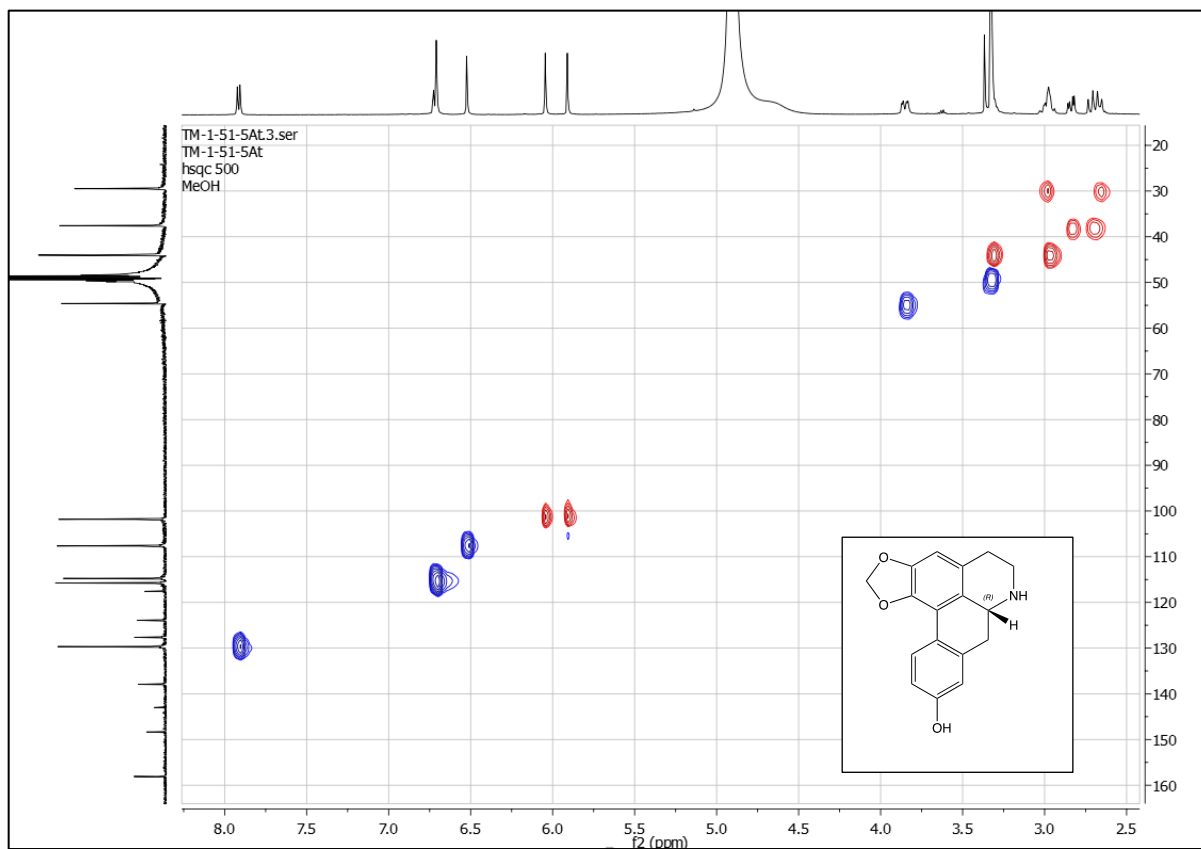
^1H NMR (500 MHz, CD_3OD) for (-)-Anolobine (**2**)



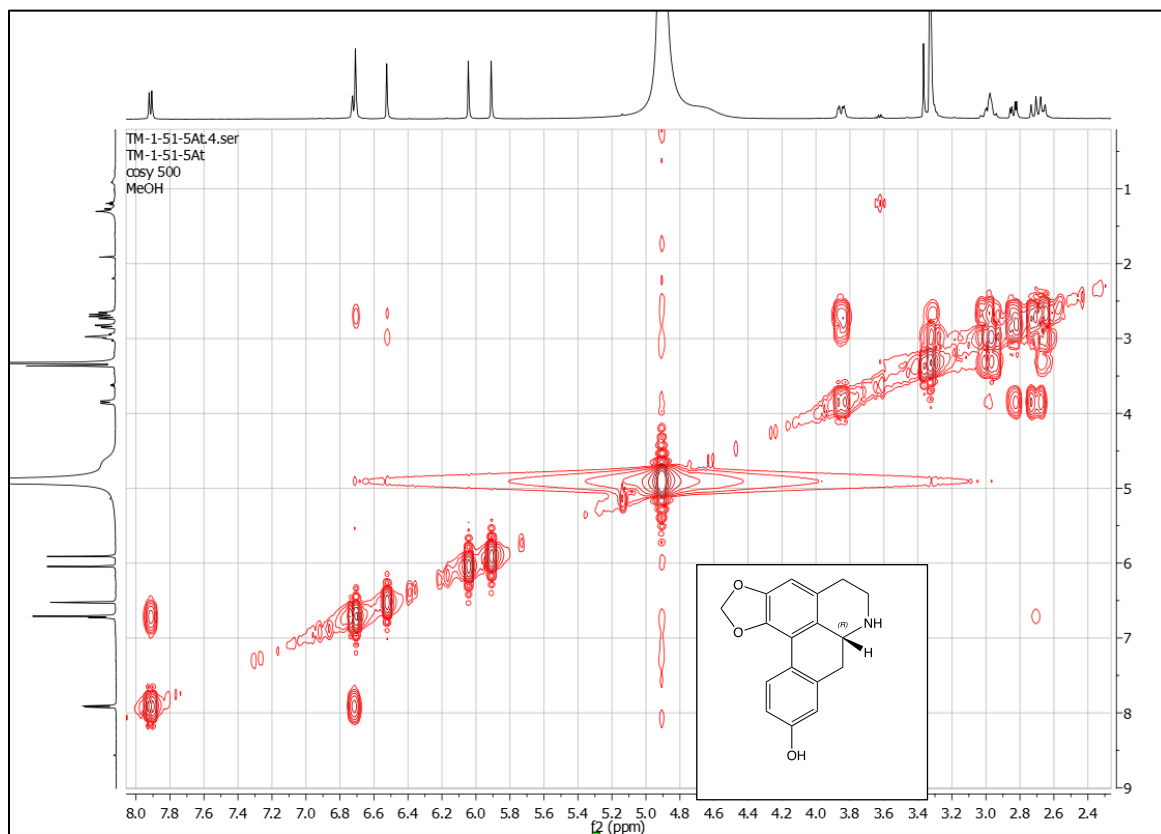
^{13}C NMR (125 MHz, CD_3OD) for (-)-Anolobine (**2**)



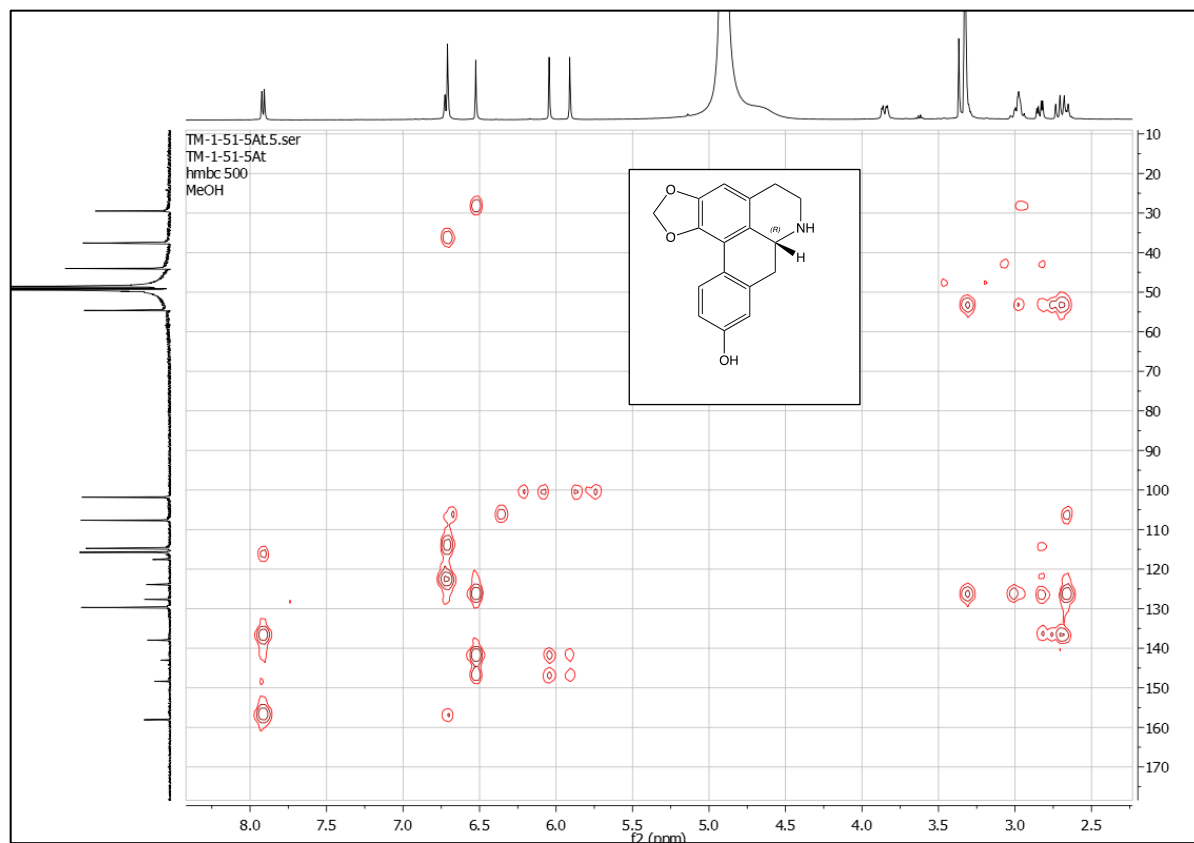
HSQC (CD₃OD) for (-)-Anolobine (2)



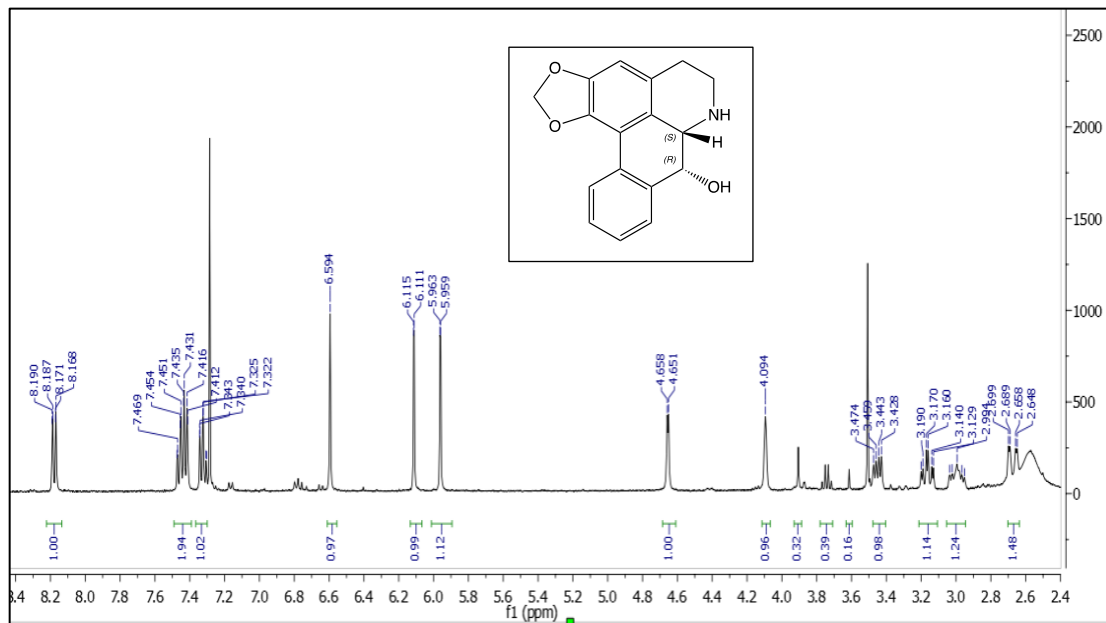
COSY (CD₃OD) for (-)-Anolobine (2)



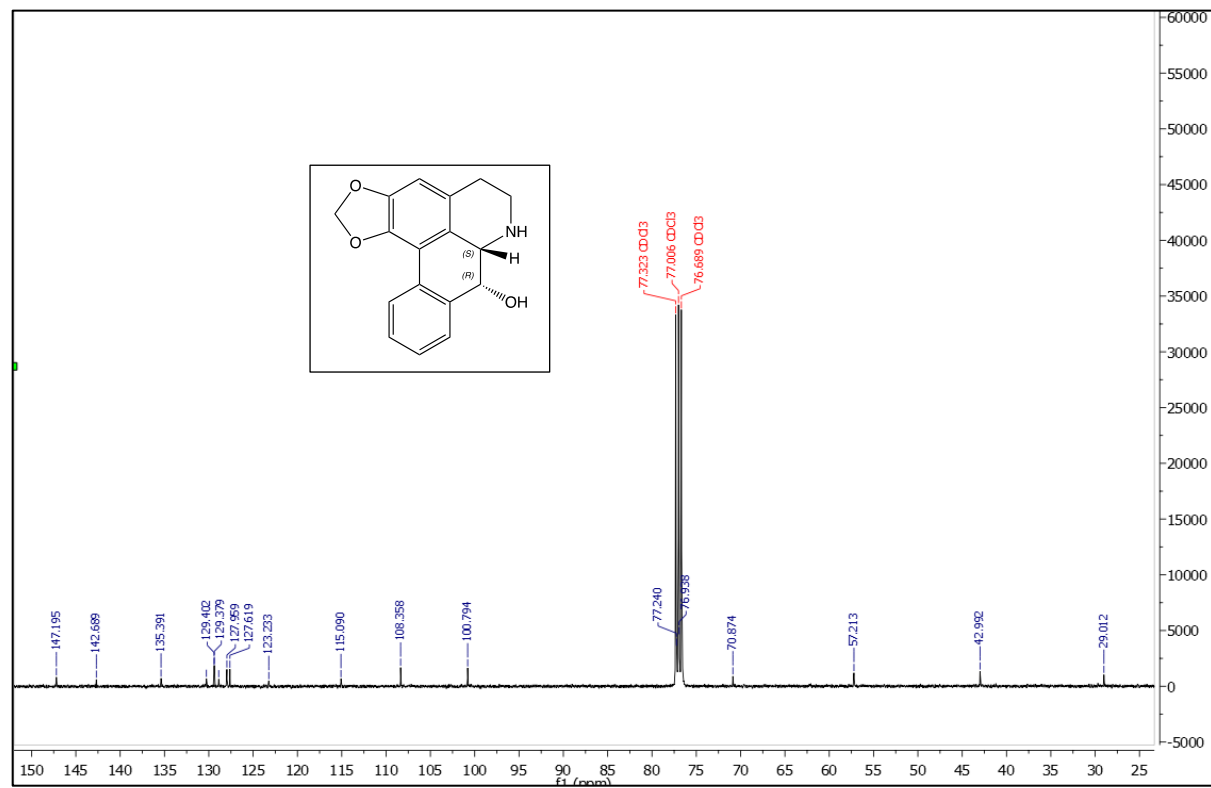
HMBC (CD₃OD) for (-)-Anolobine (2)



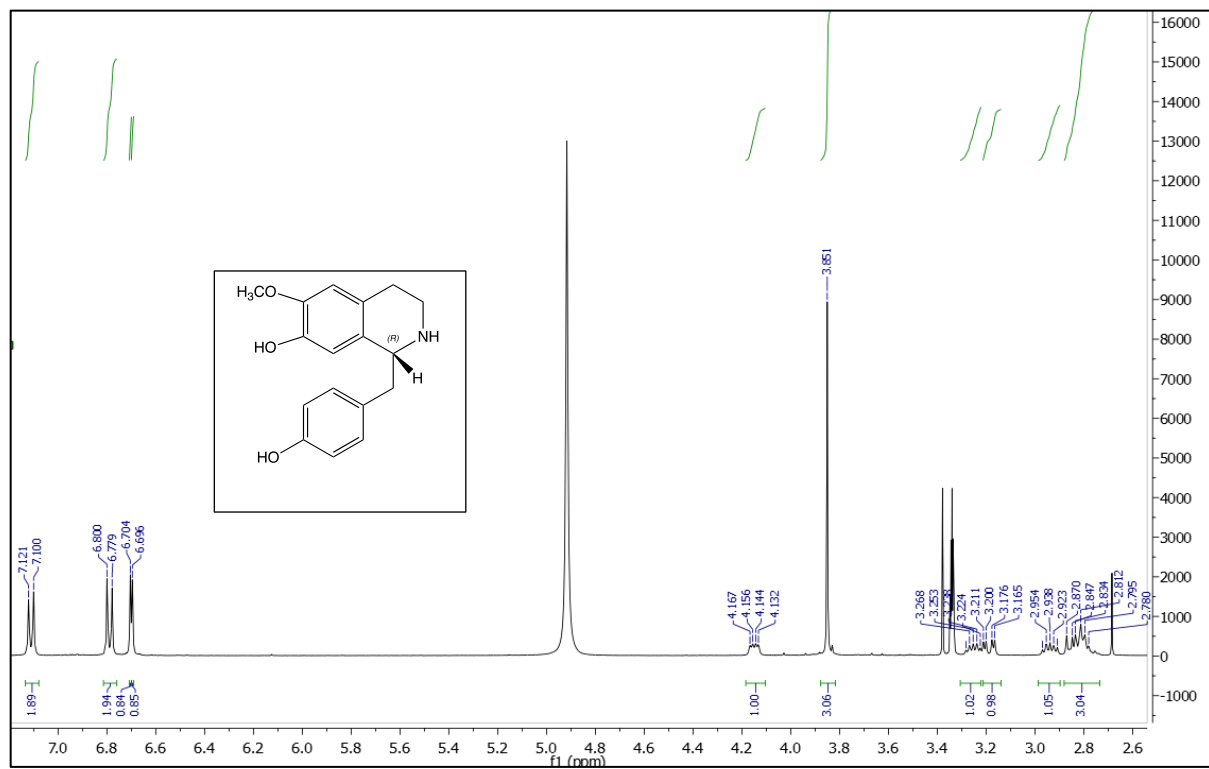
¹H NMR (400 MHz, CDCl₃) for (-)-Norushinsunine (**4**)



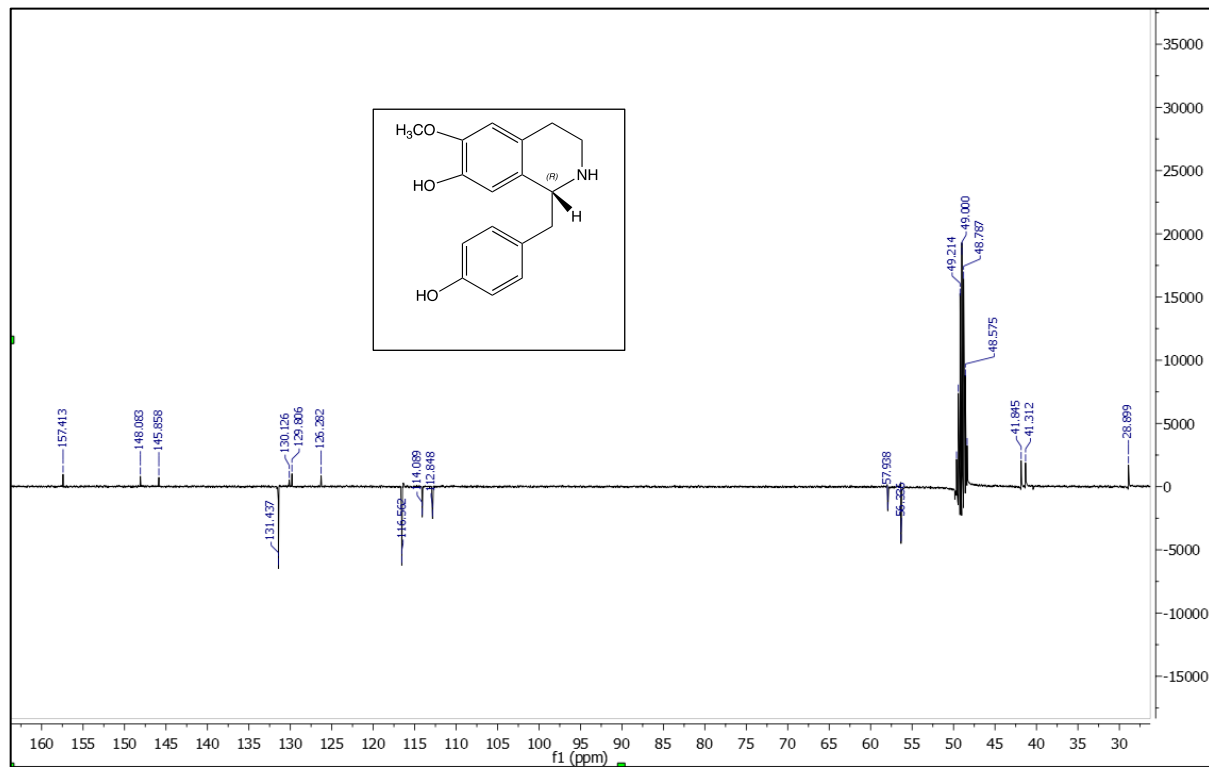
^{13}C NMR (100 MHz, CDCl_3) for (-)-Norushinsunine (**4**)



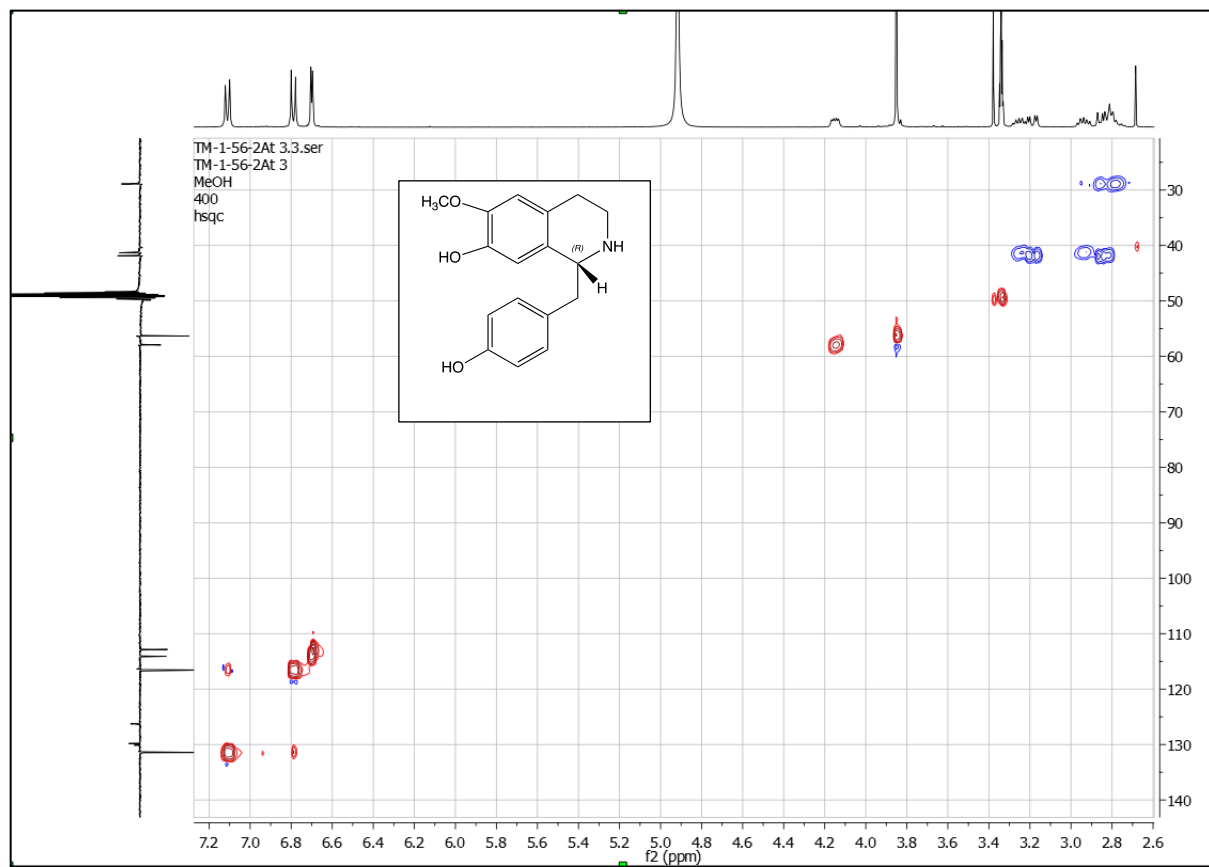
¹H NMR (400 MHz, CD₃OD) for (+)-Coclaurine (**8**)



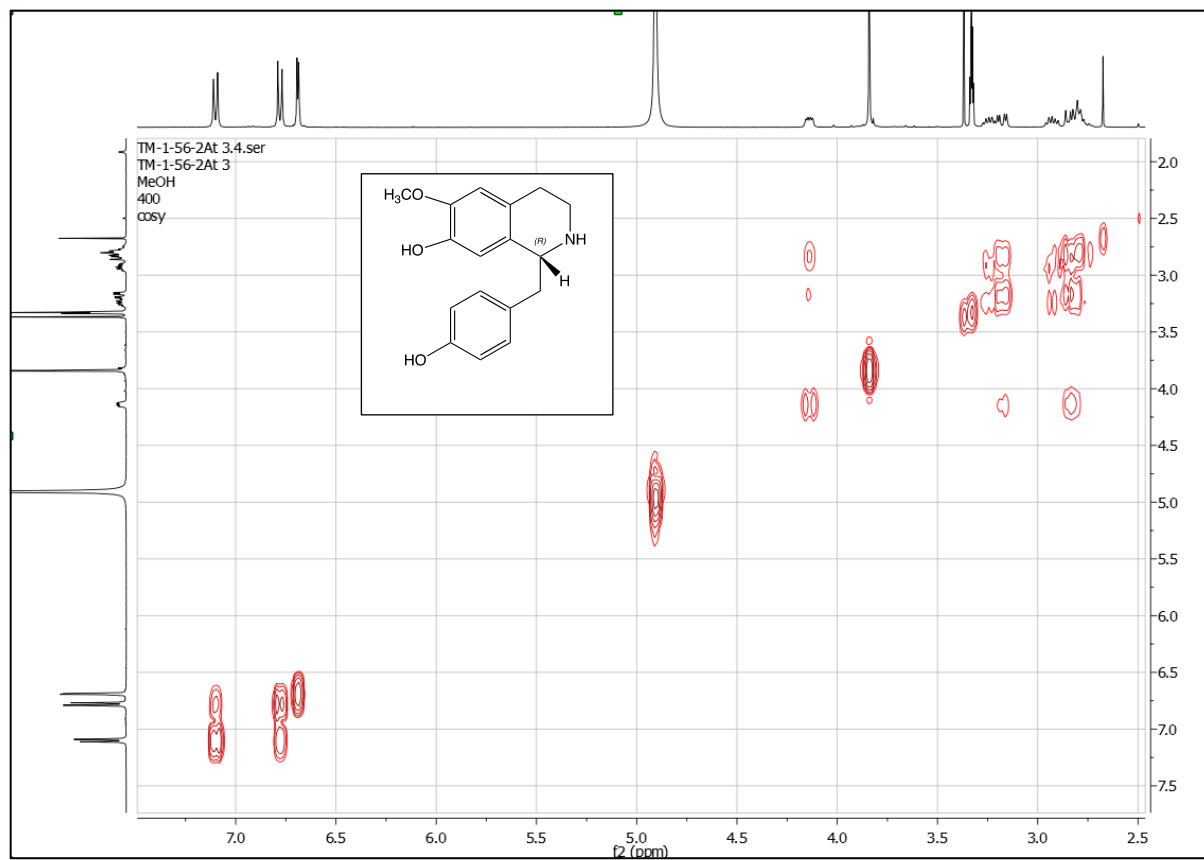
^{13}C NMR (100 MHz, CD_3OD) for (+)-Coclaurine (**8**)



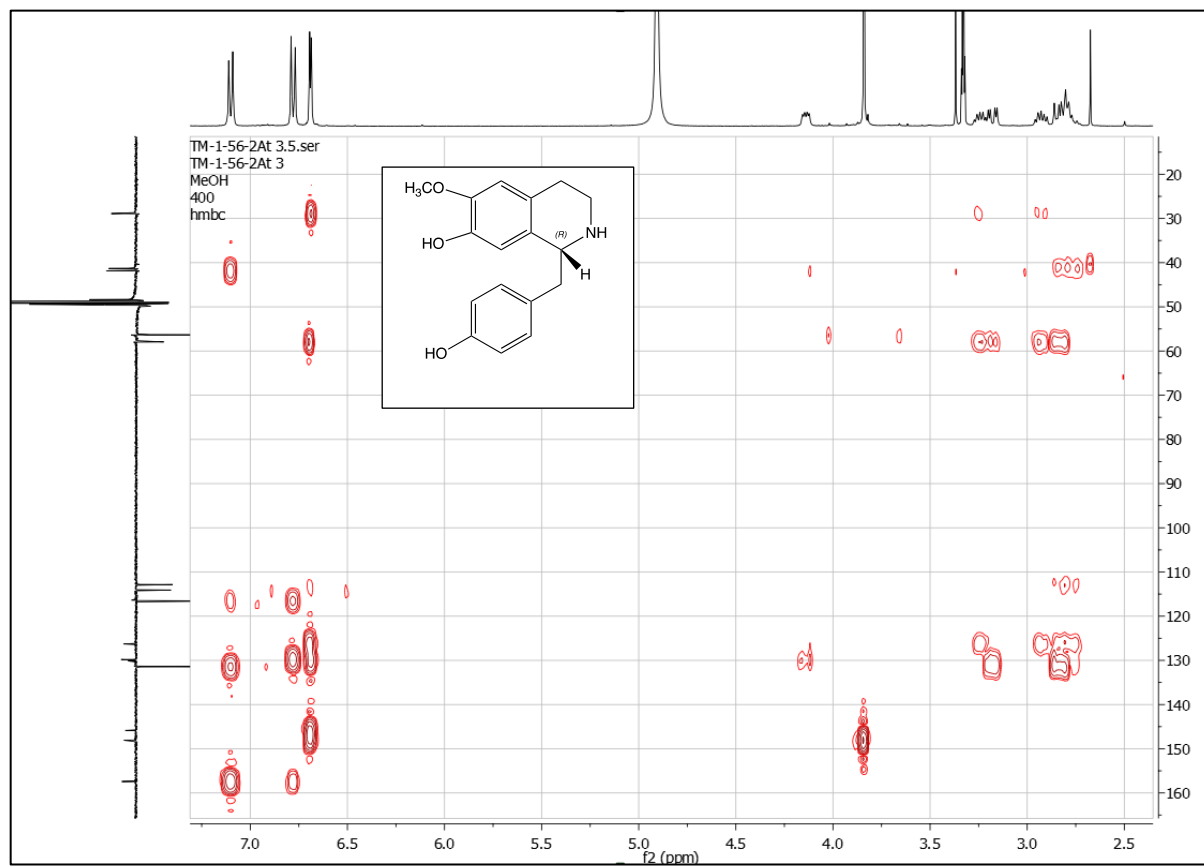
HSQC (CD₃OD) for (+)-Coclaurine (**8**)



COSY (CD₃OD) for (+)-Coclaurine (**8**)



HMBC (CD₃OD) for (+)-Coclaurine (**8**)

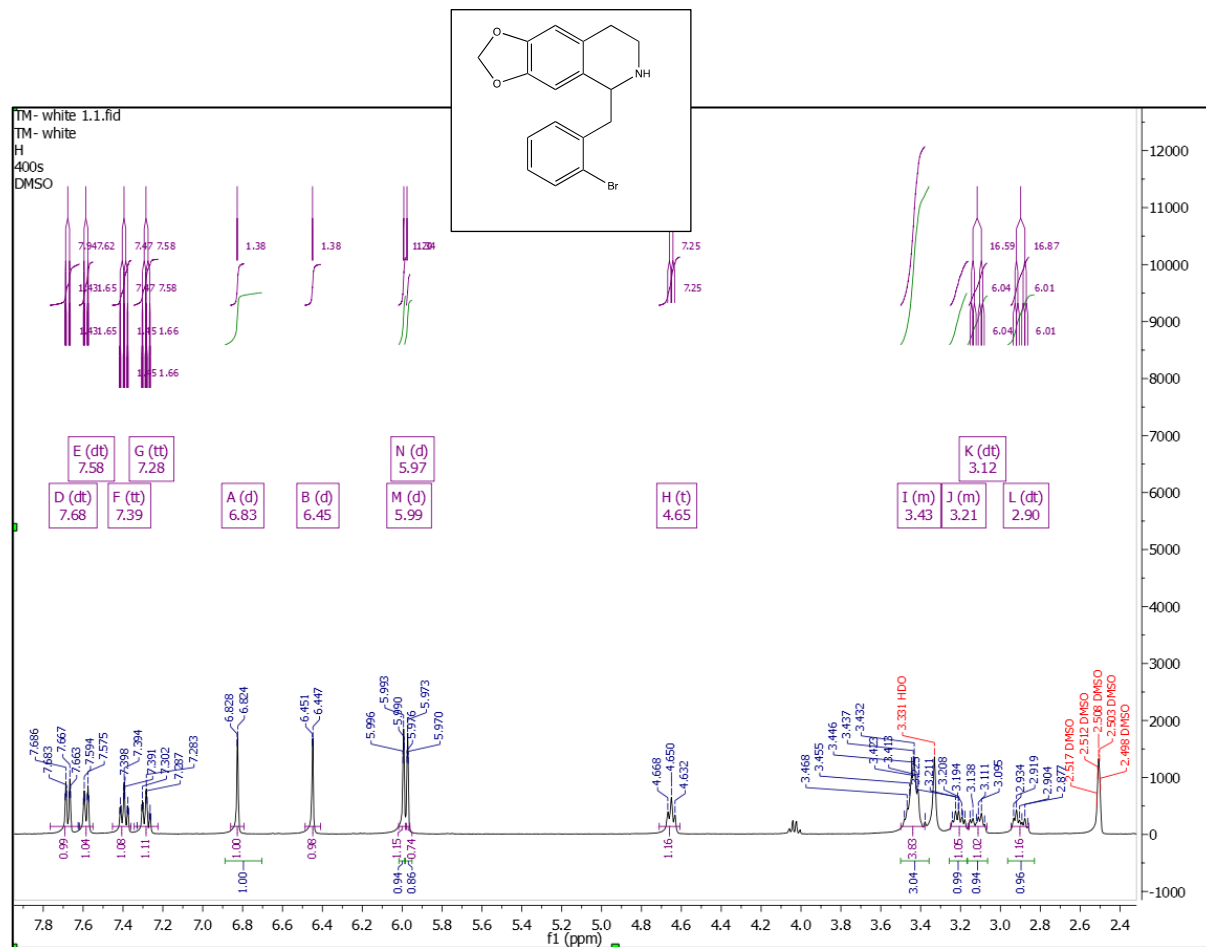


NOESY (CD₃OD) for (+)-Coclaurine (**8**)

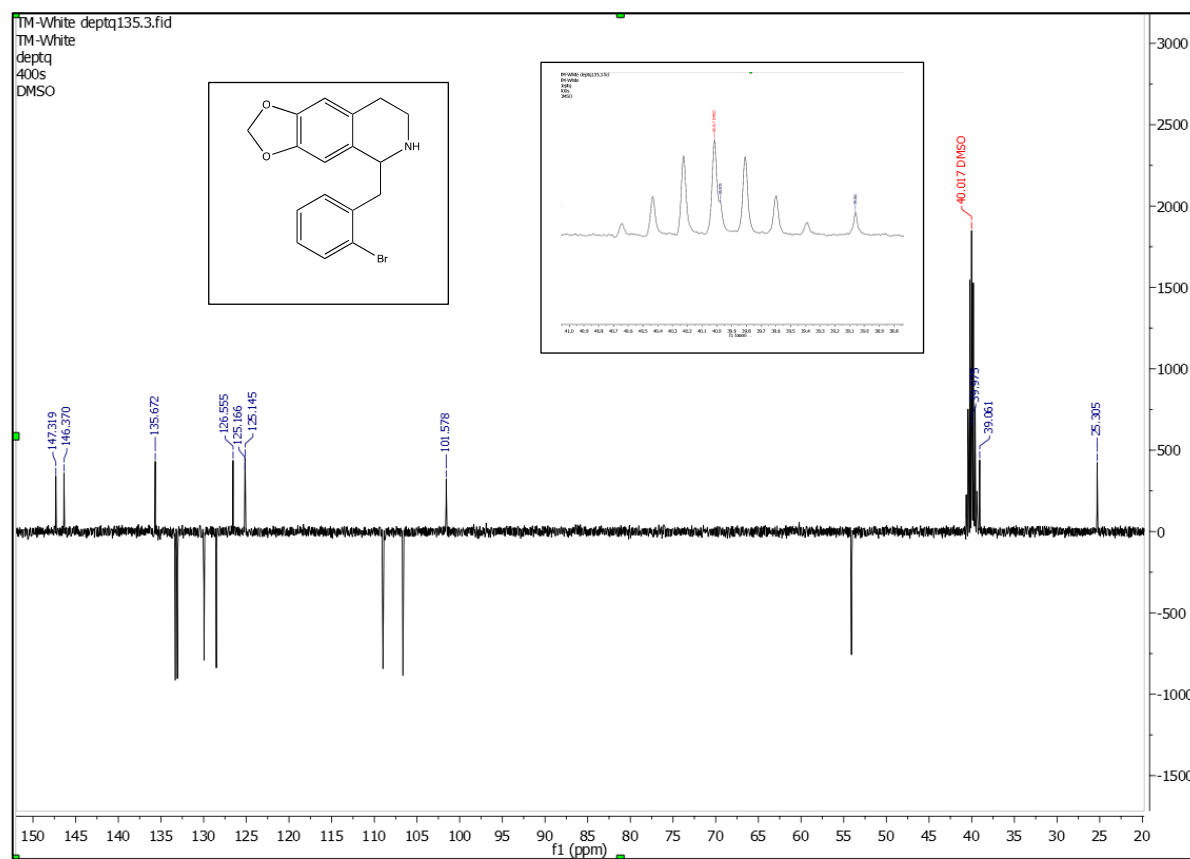


APPENDIX 2. SUPPLEMENTARY DATA-CHAPTER V

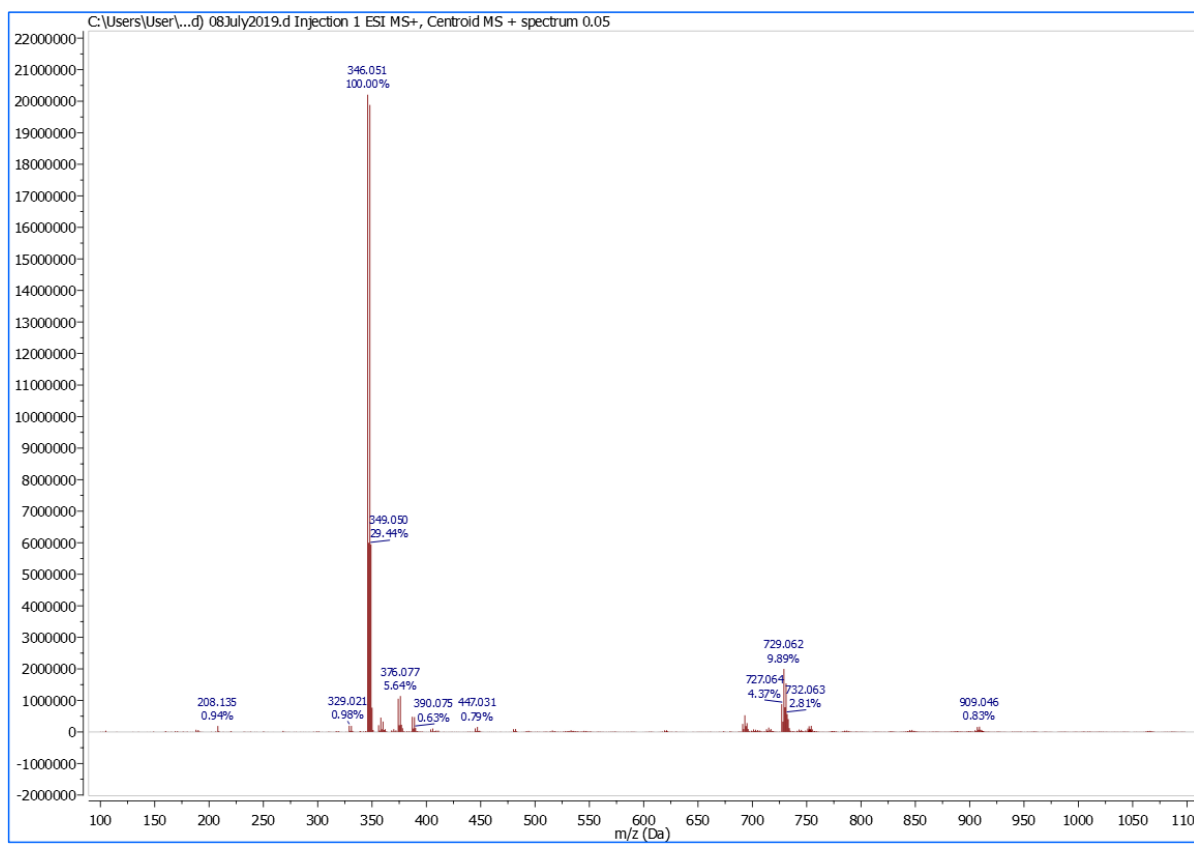
Compound (3) (400 MHz, DMSO-d₆) ¹H NMR:



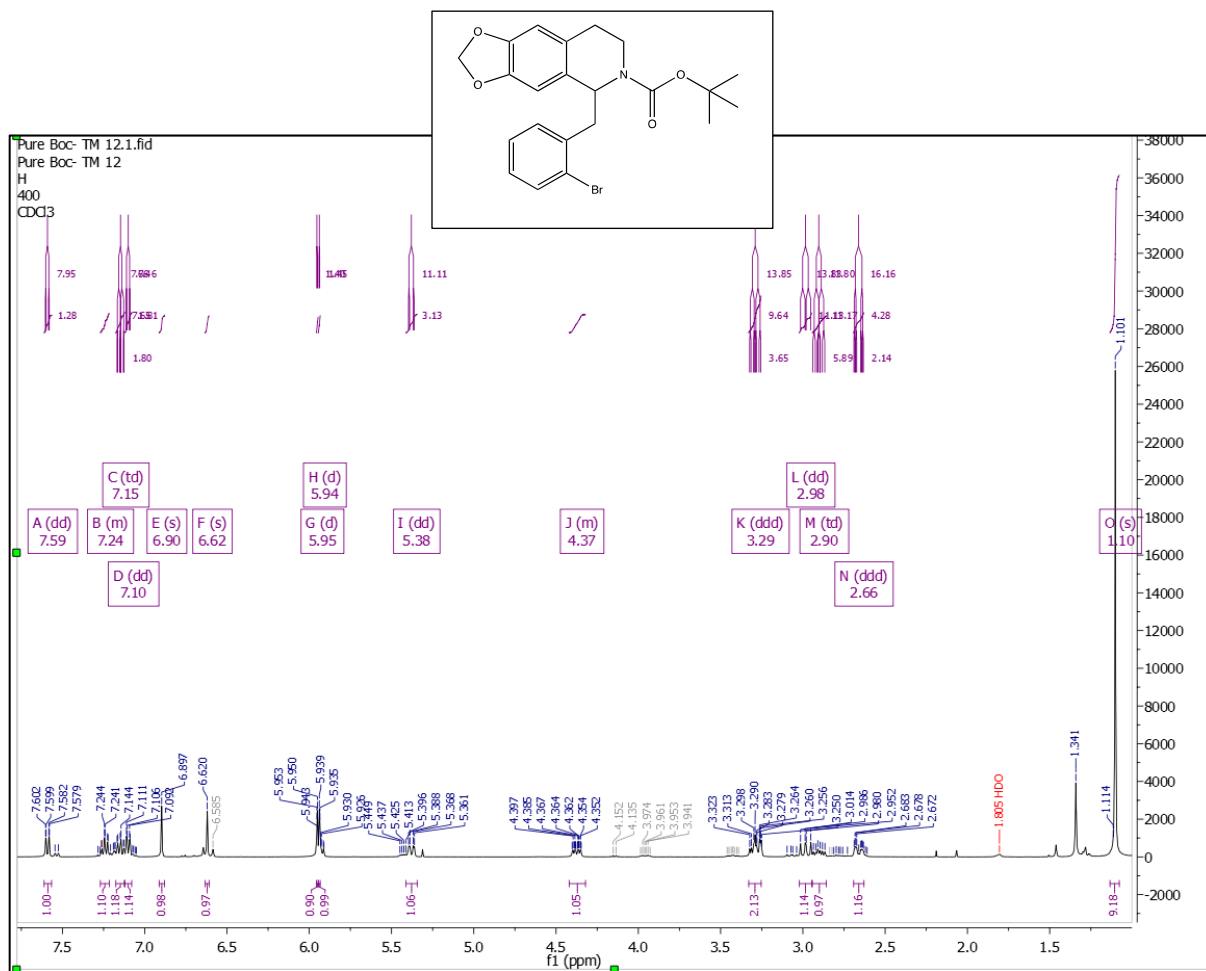
Compound (3) (DMSO-d₆) DeptQ135 NMR:



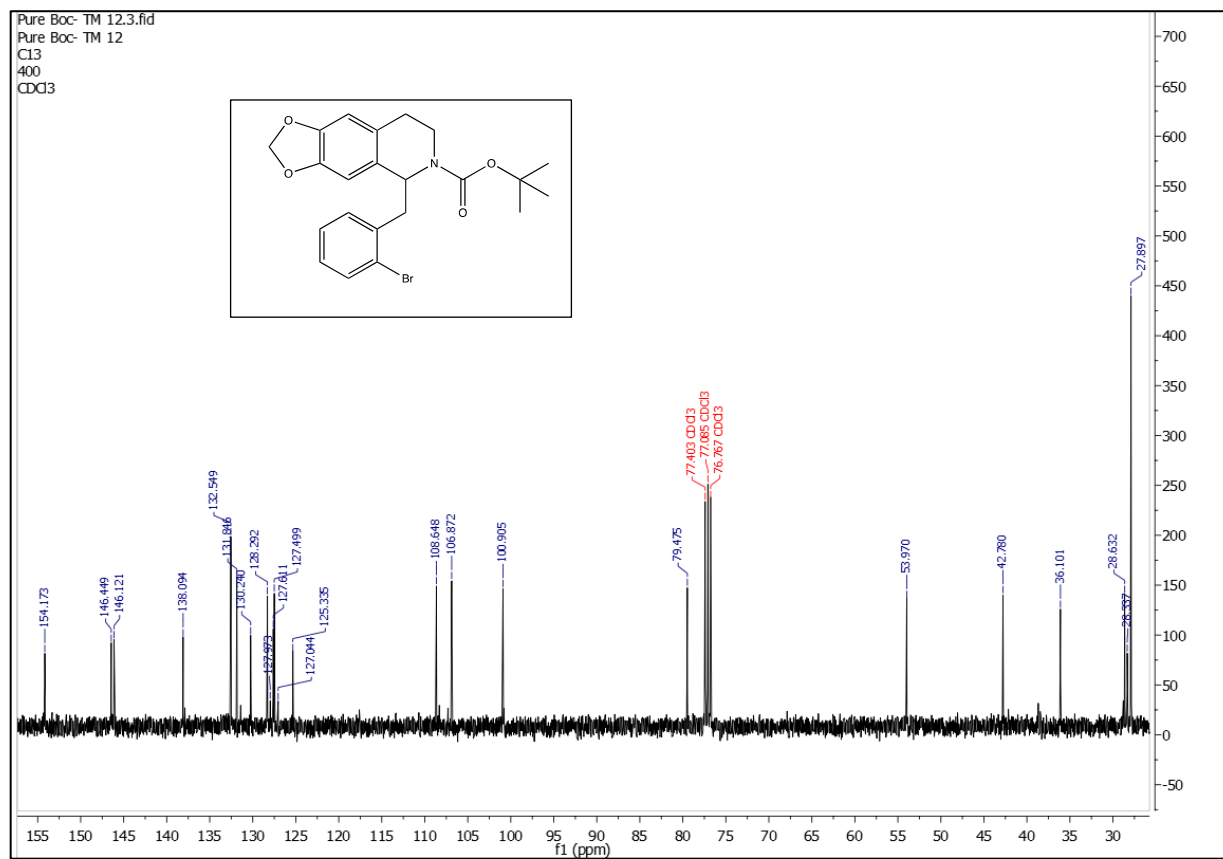
Compound (3) HRESI-MS:



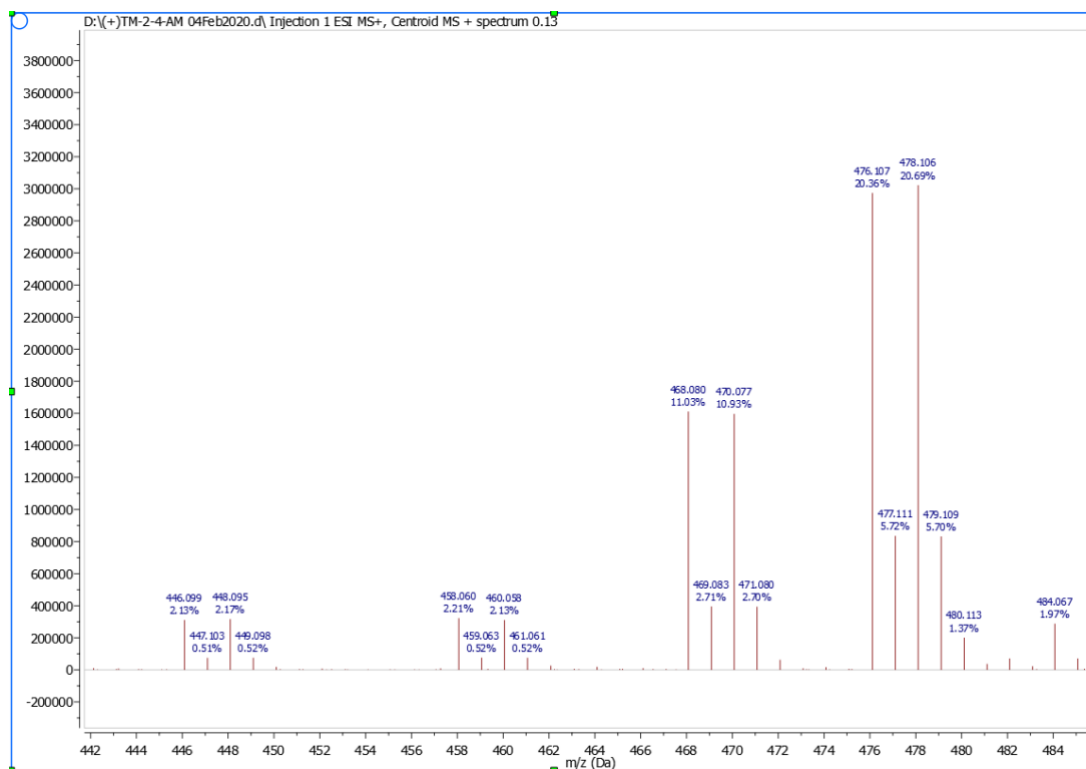
Compound (4) (400 MHz, CDCl₃) ¹H NMR:



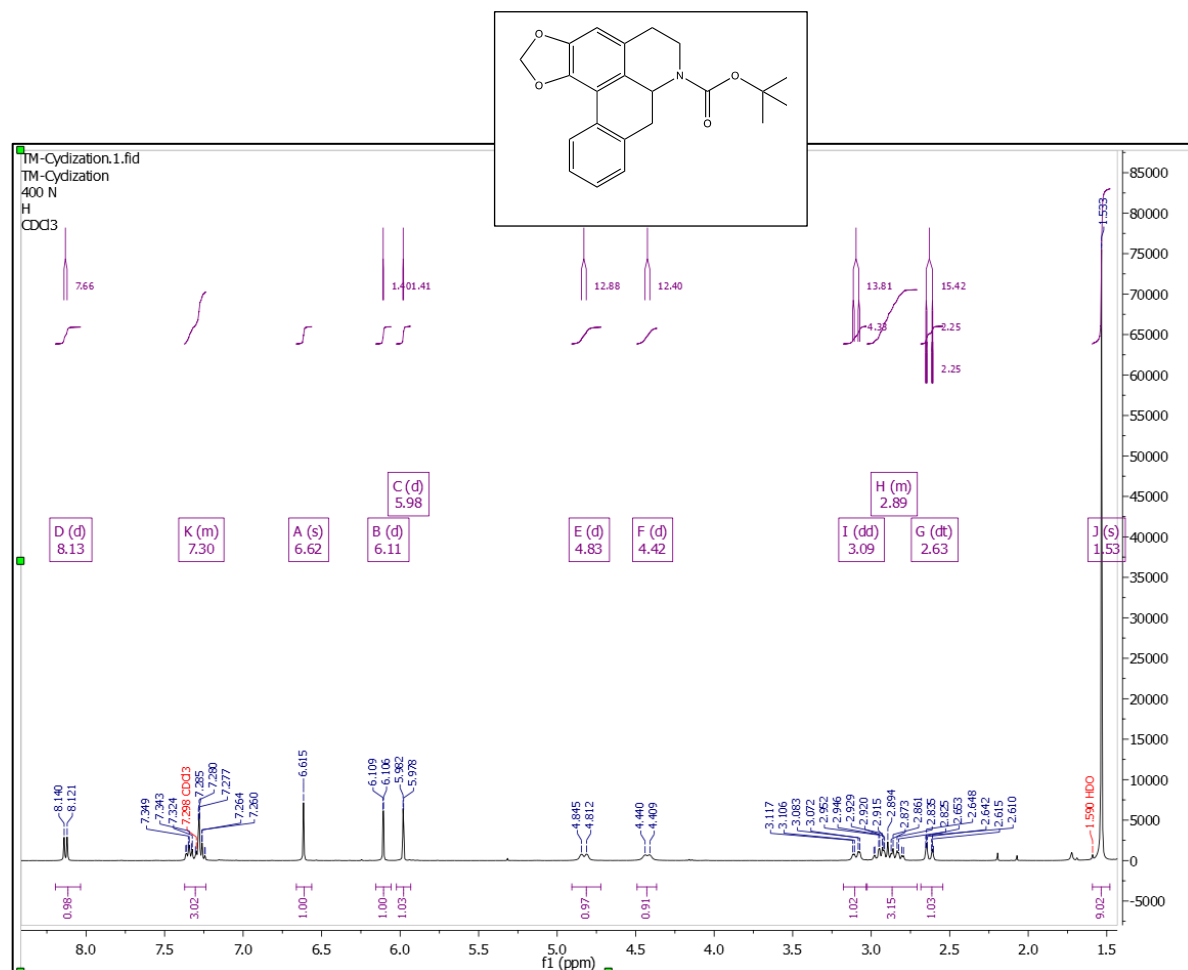
Compound (4) (100 MHz, CDCl₃) ¹³C NMR:



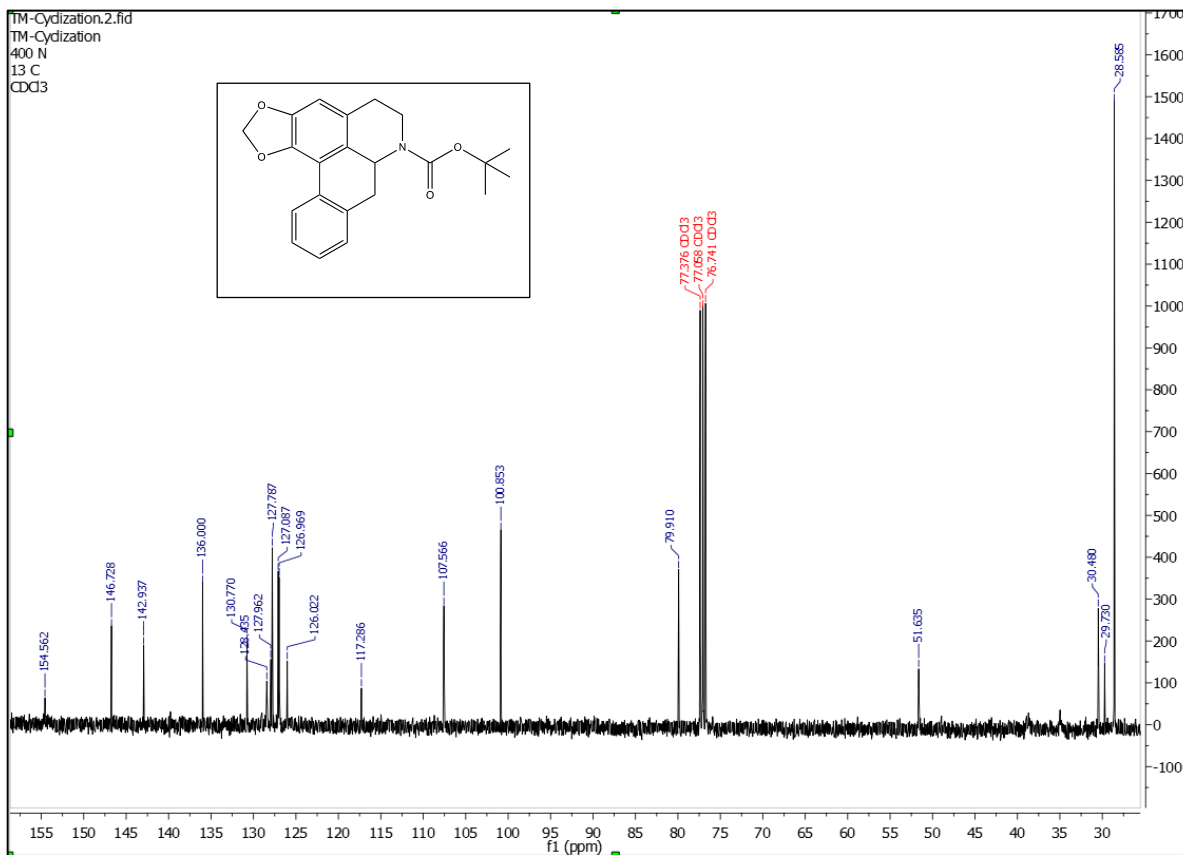
Compound (4) HRESI-MS:



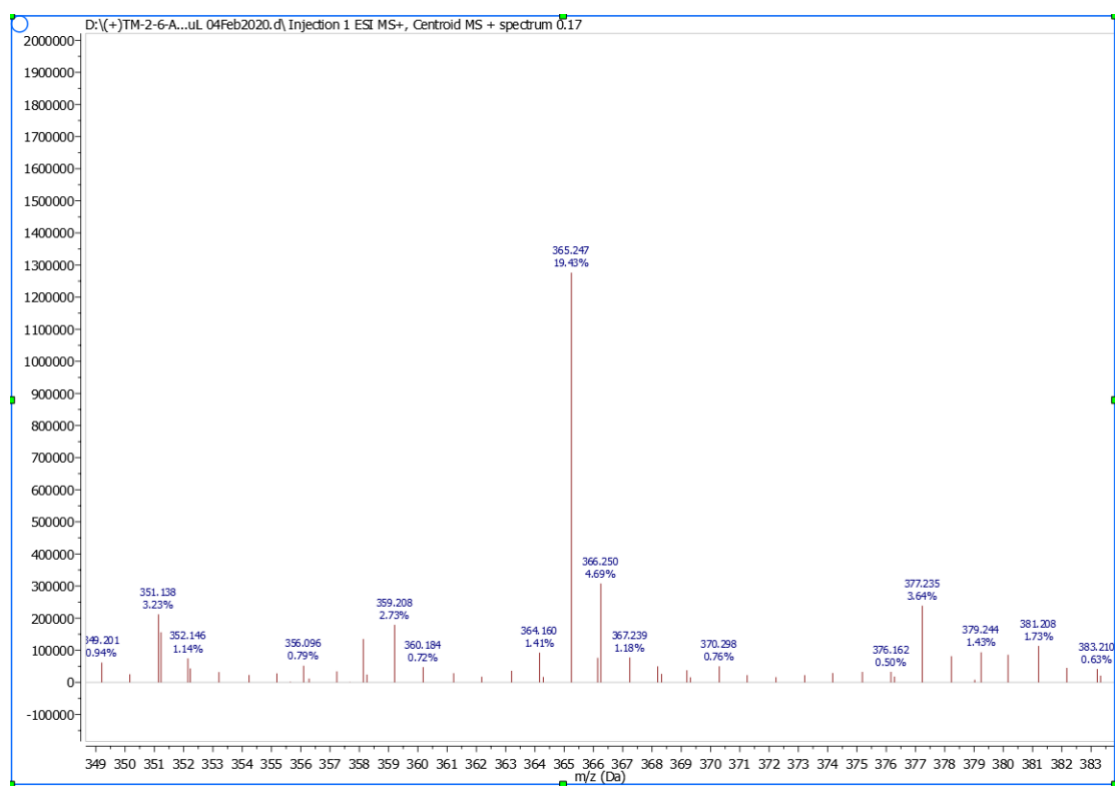
Compound **(5)** (400 MHz, CDCl₃) ¹H NMR:



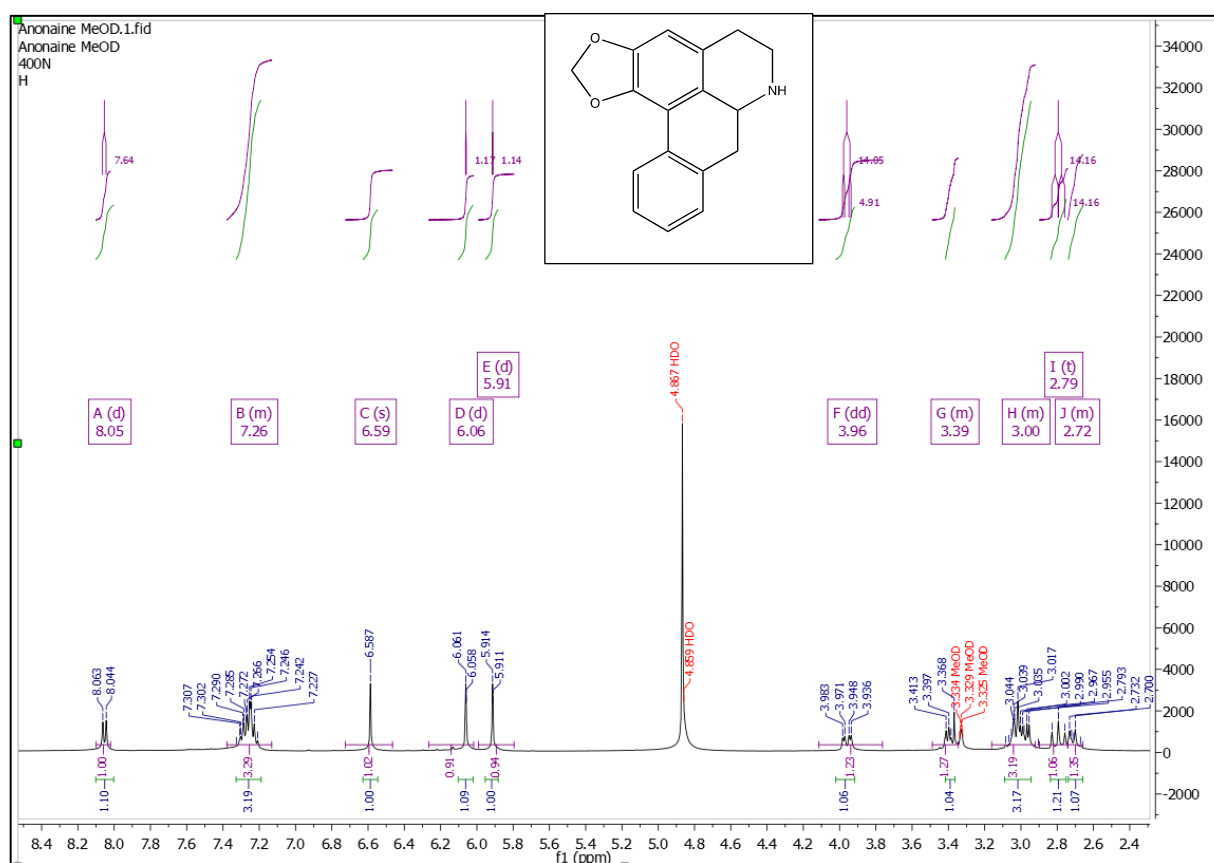
Compound (5) (100 MHz, CDCl₃) ¹³C NMR:



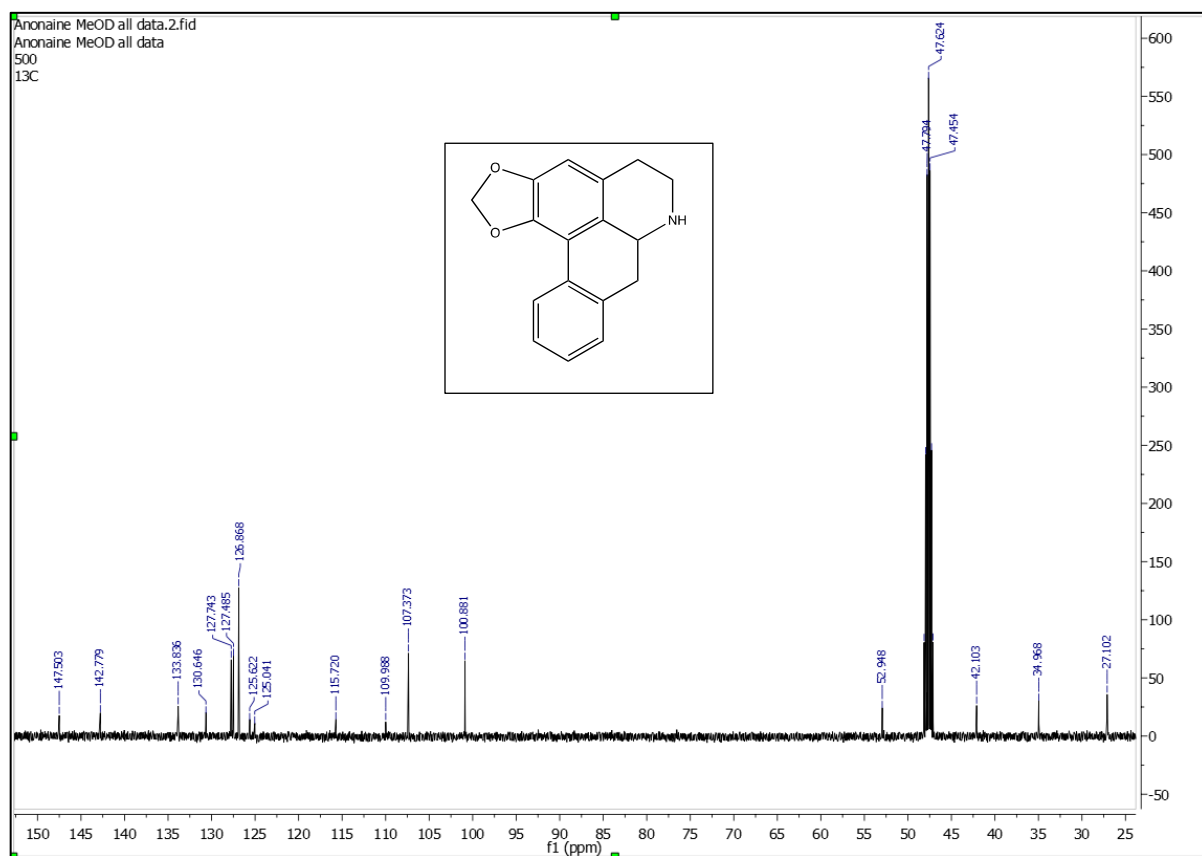
Compound (5) HRESI-MS:



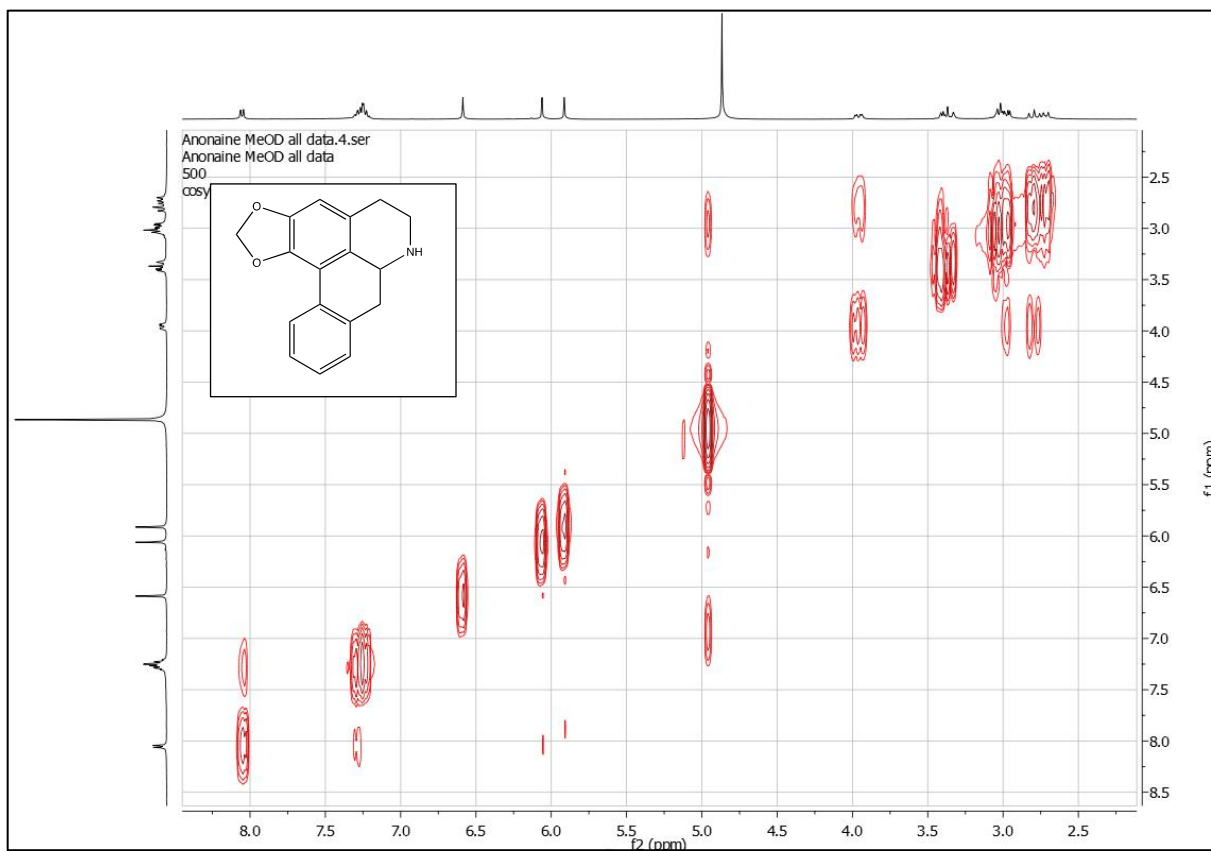
Compound (6) (400 MHz, CD₃OD) ¹H NMR:



Compound (6) (100 MHz, CD₃OD) ¹³C NMR:



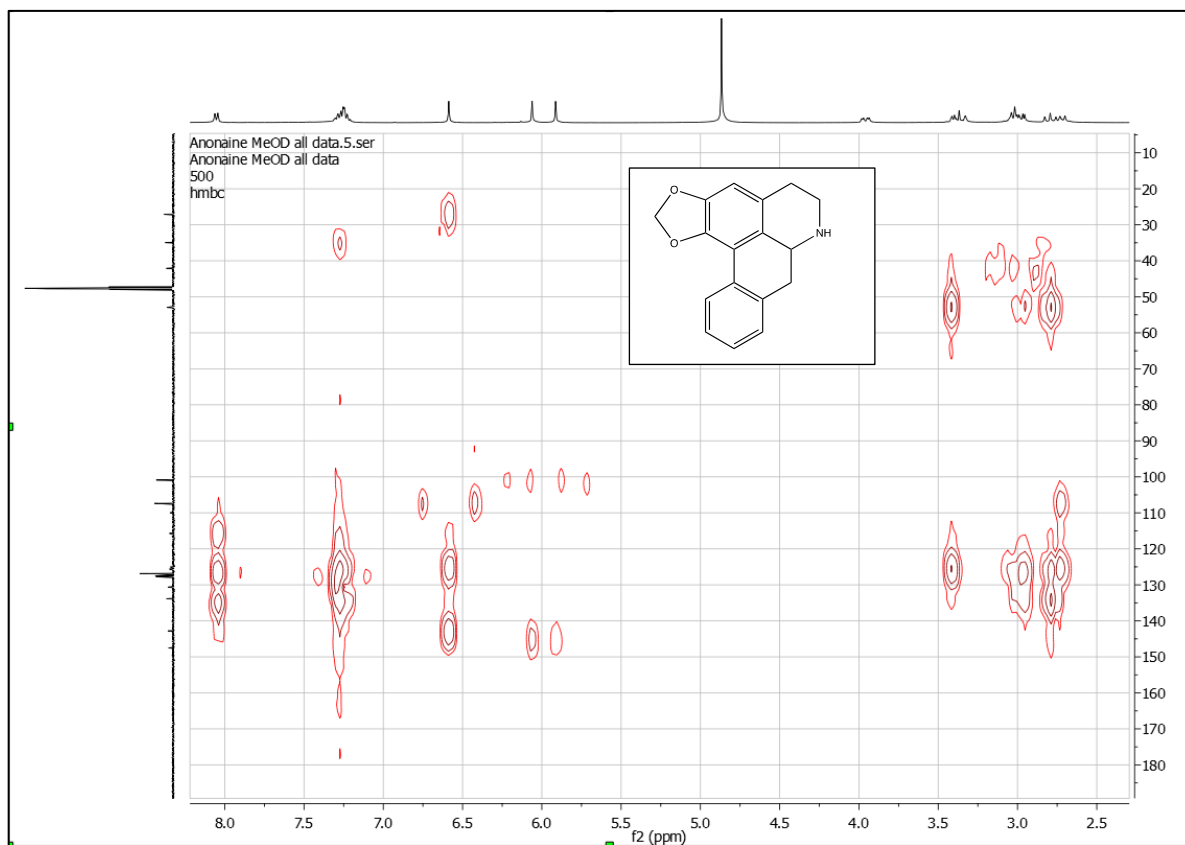
Compound (6) (CD₃OD) COSY NMR:



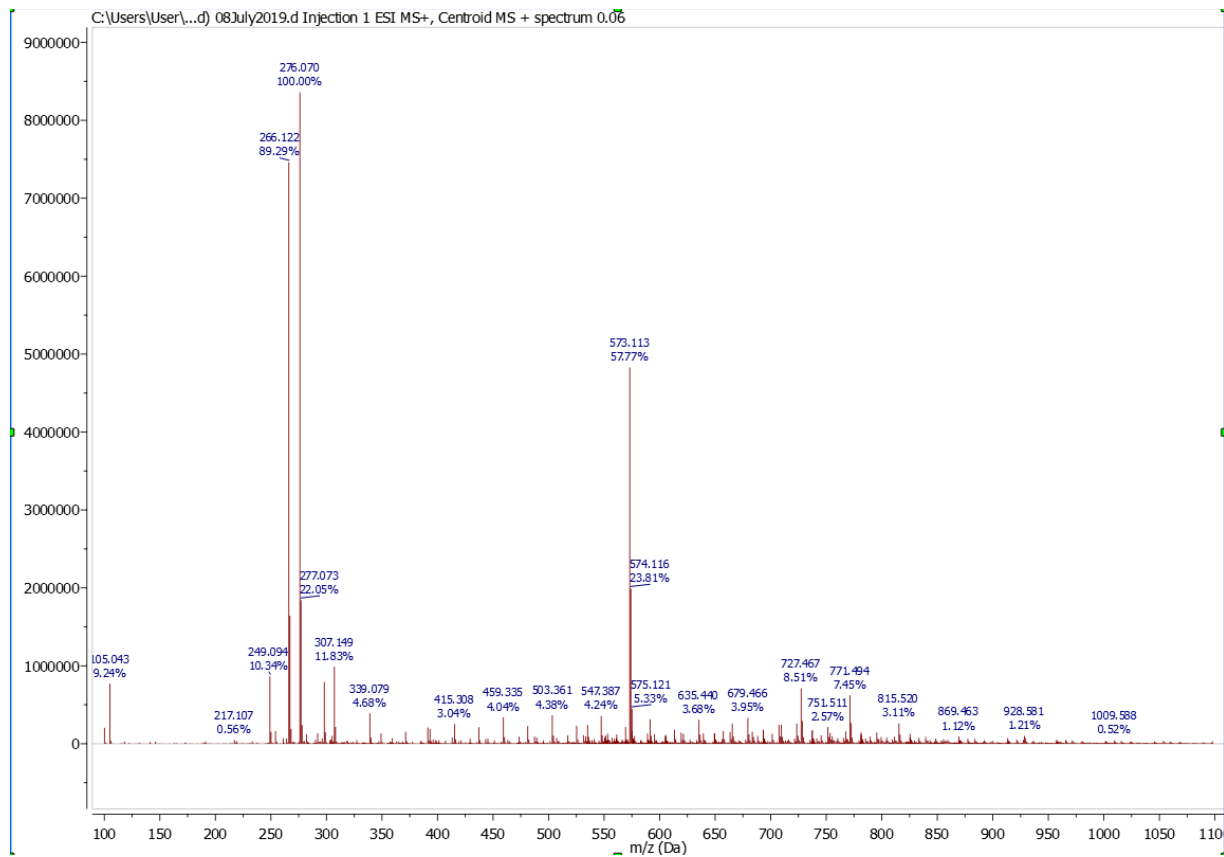
Compound (6) (CD₃OD) HSQC NMR:



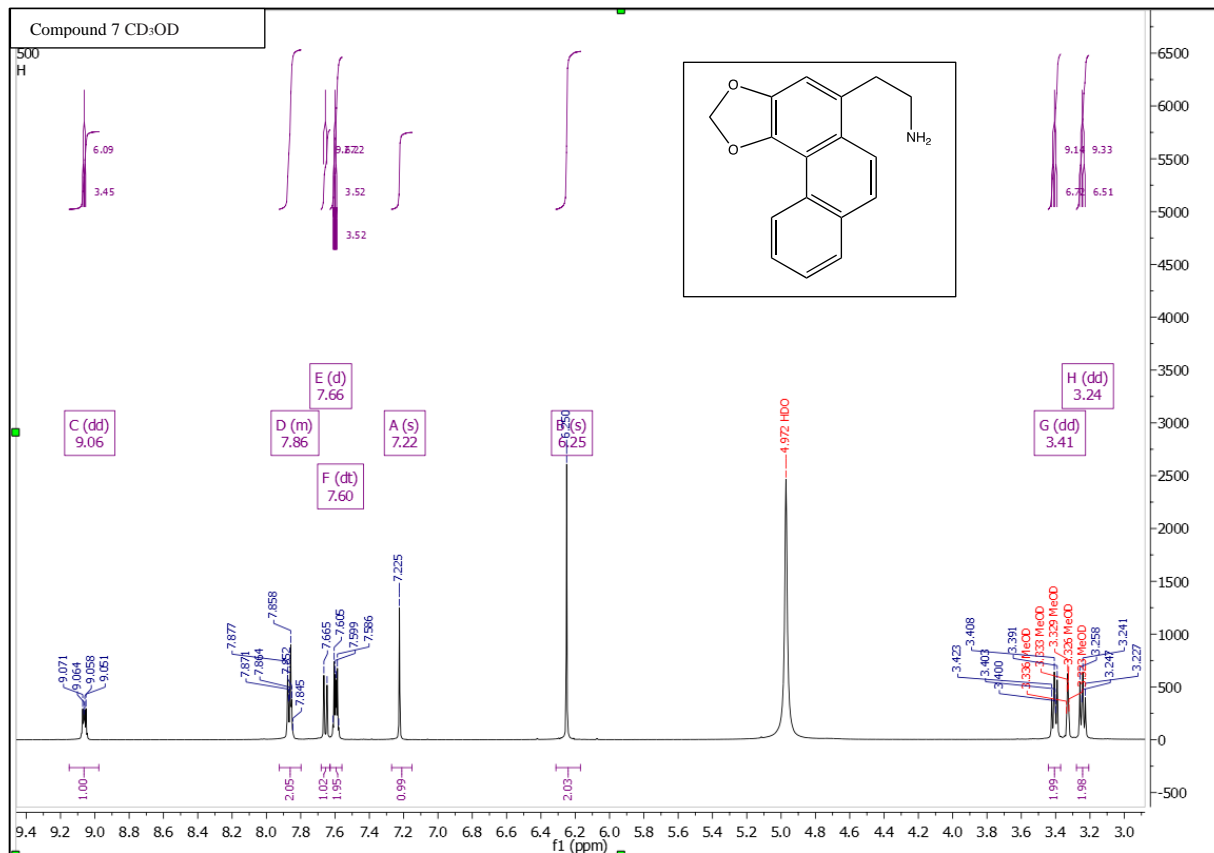
Compound (6) (CD₃OD) HMBC NMR:



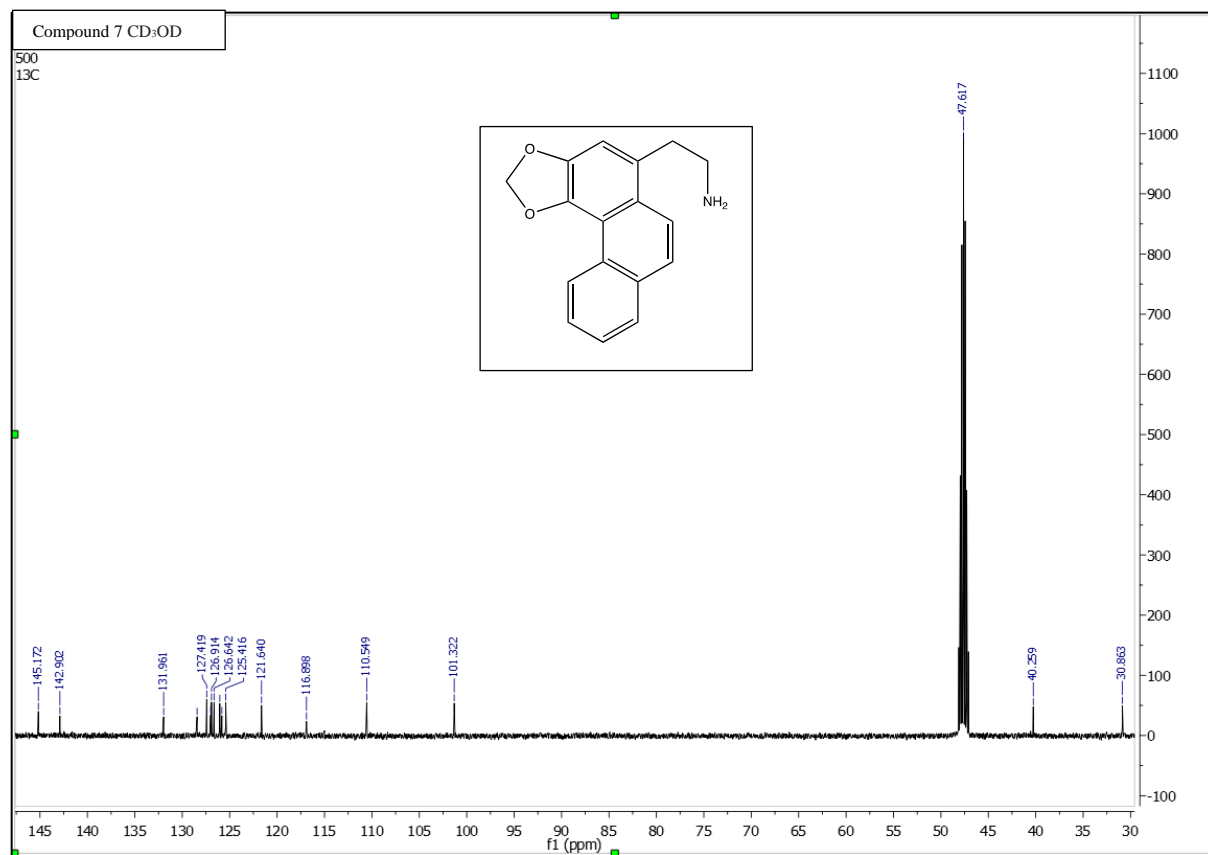
Compound (6) HRESI-MS:



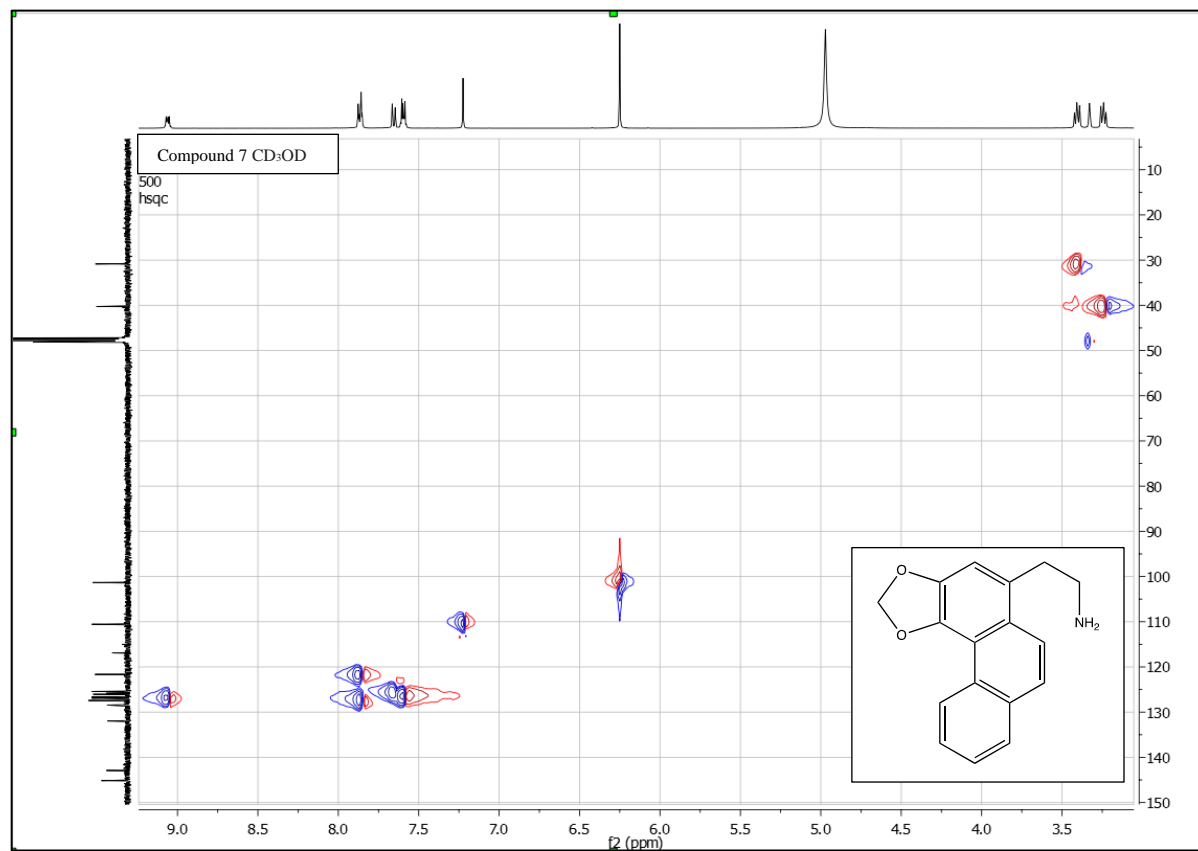
Compound (7) (500 MHz, CD₃OD) ¹H NMR:



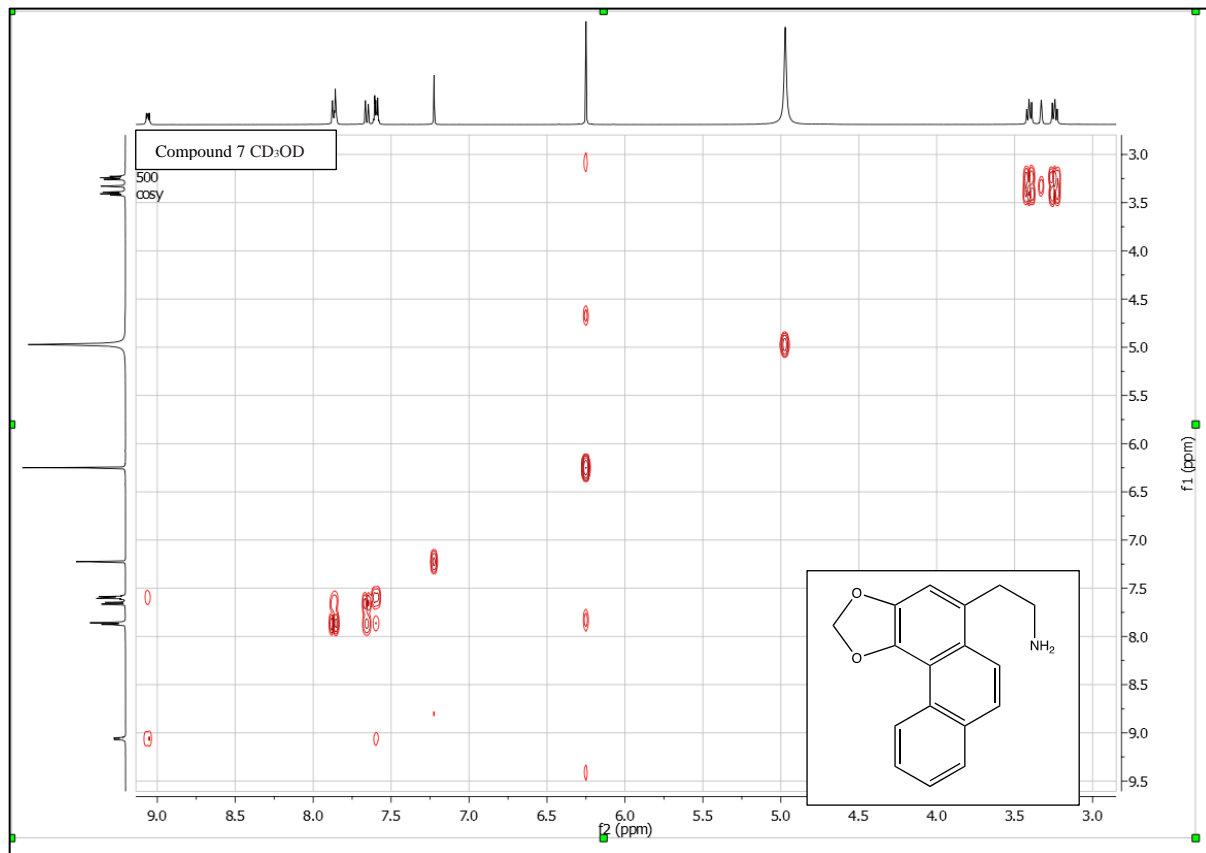
Compound (7) (125 MHz, CD₃OD) ¹³C NMR:



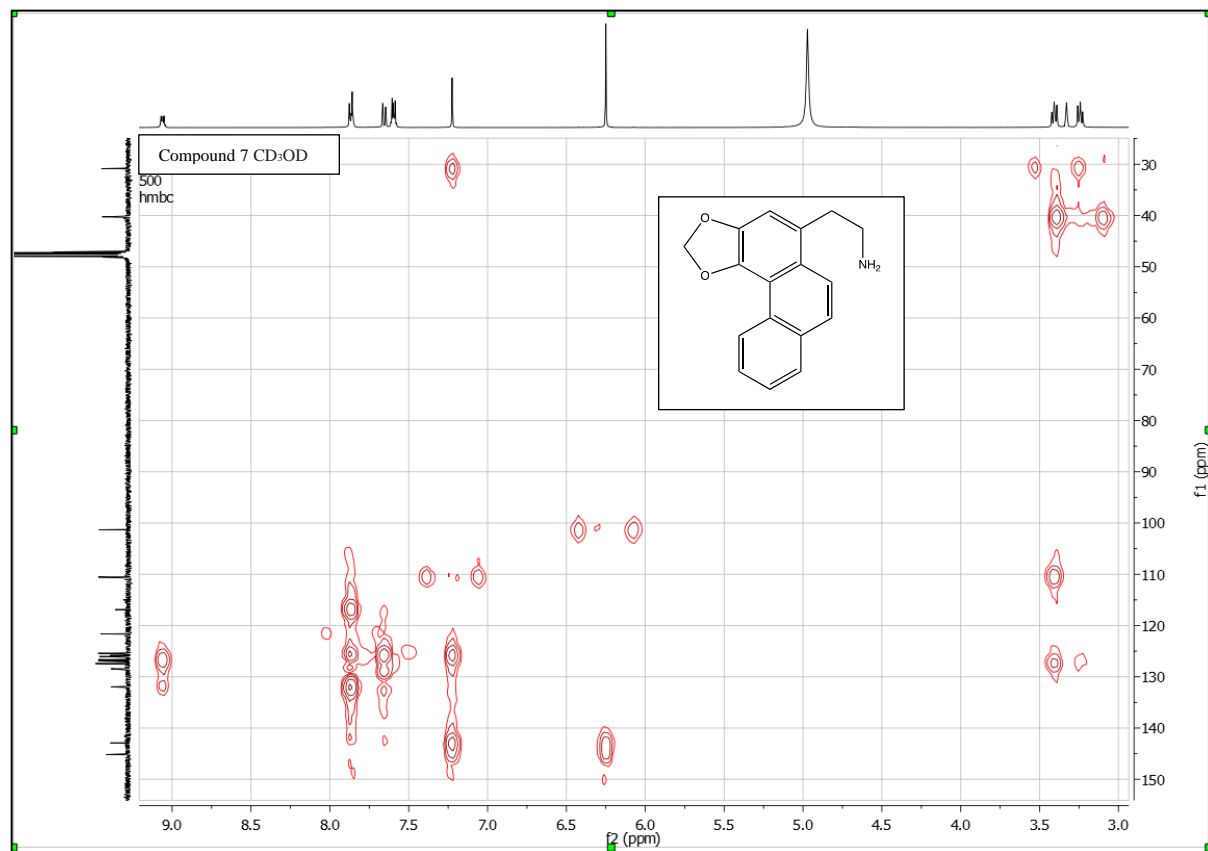
Compound (7) (CD₃OD) HSQC NMR:



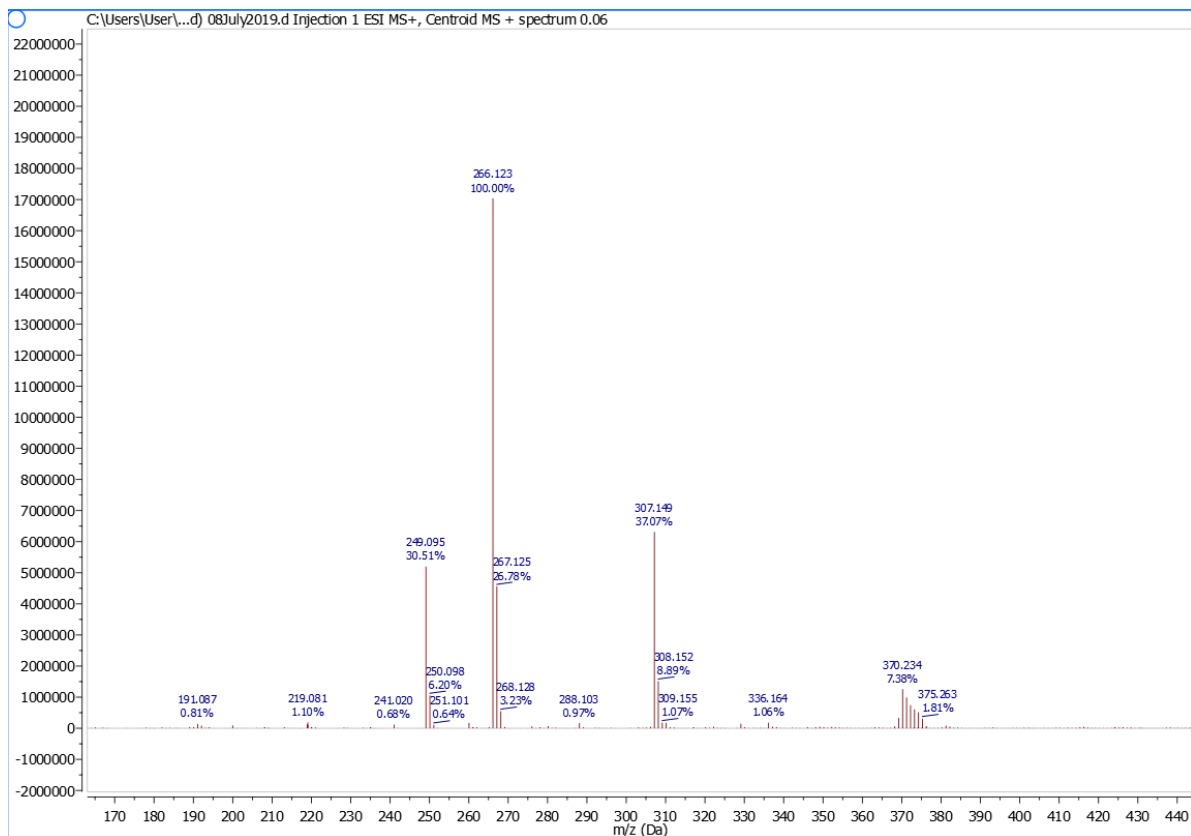
Compound (7) (CD₃OD) COSY NMR:



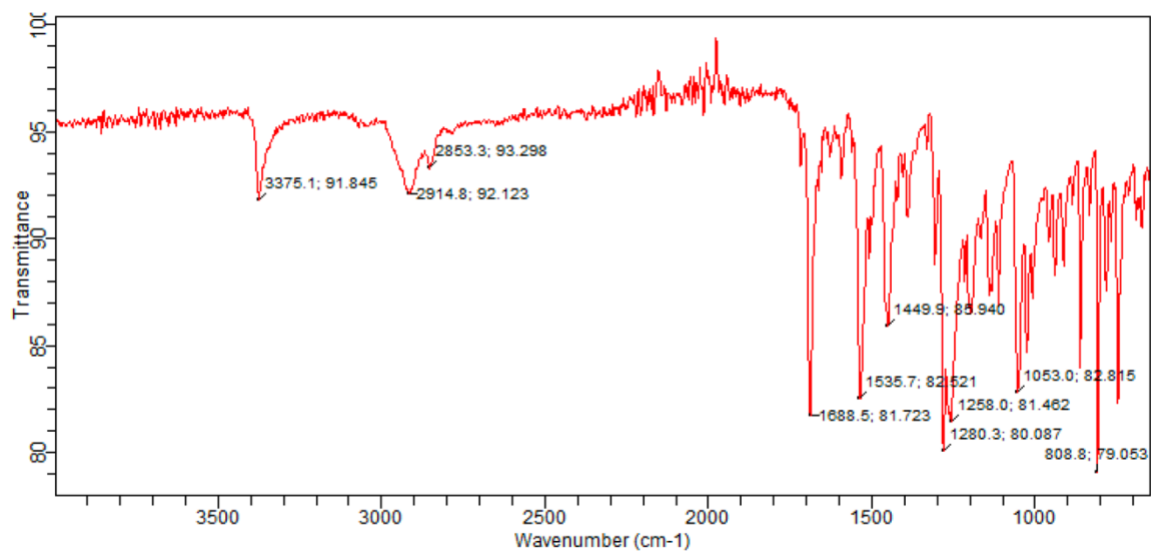
Compound (7) (CD₃OD) HMBC NMR:



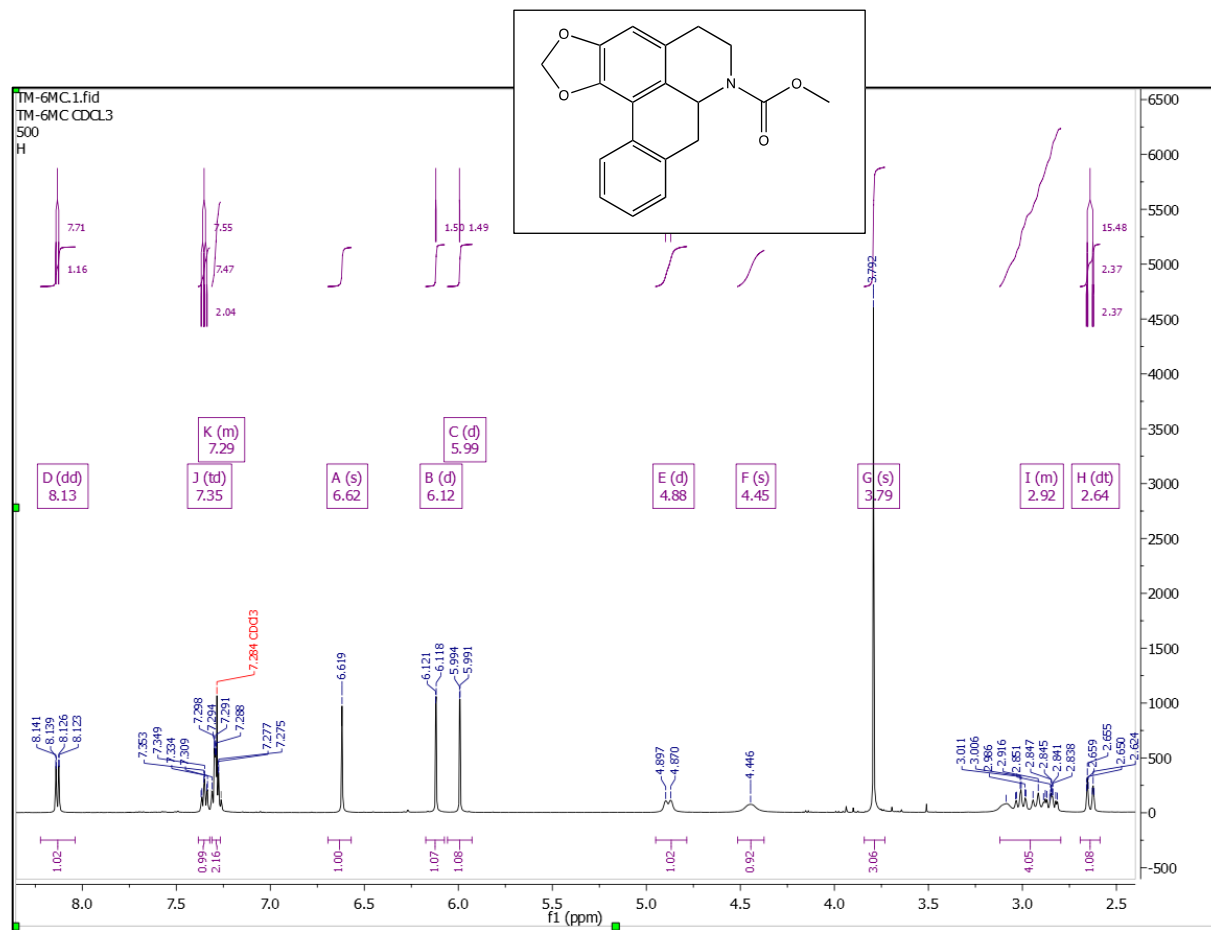
Compound (7) HRESI-MS:



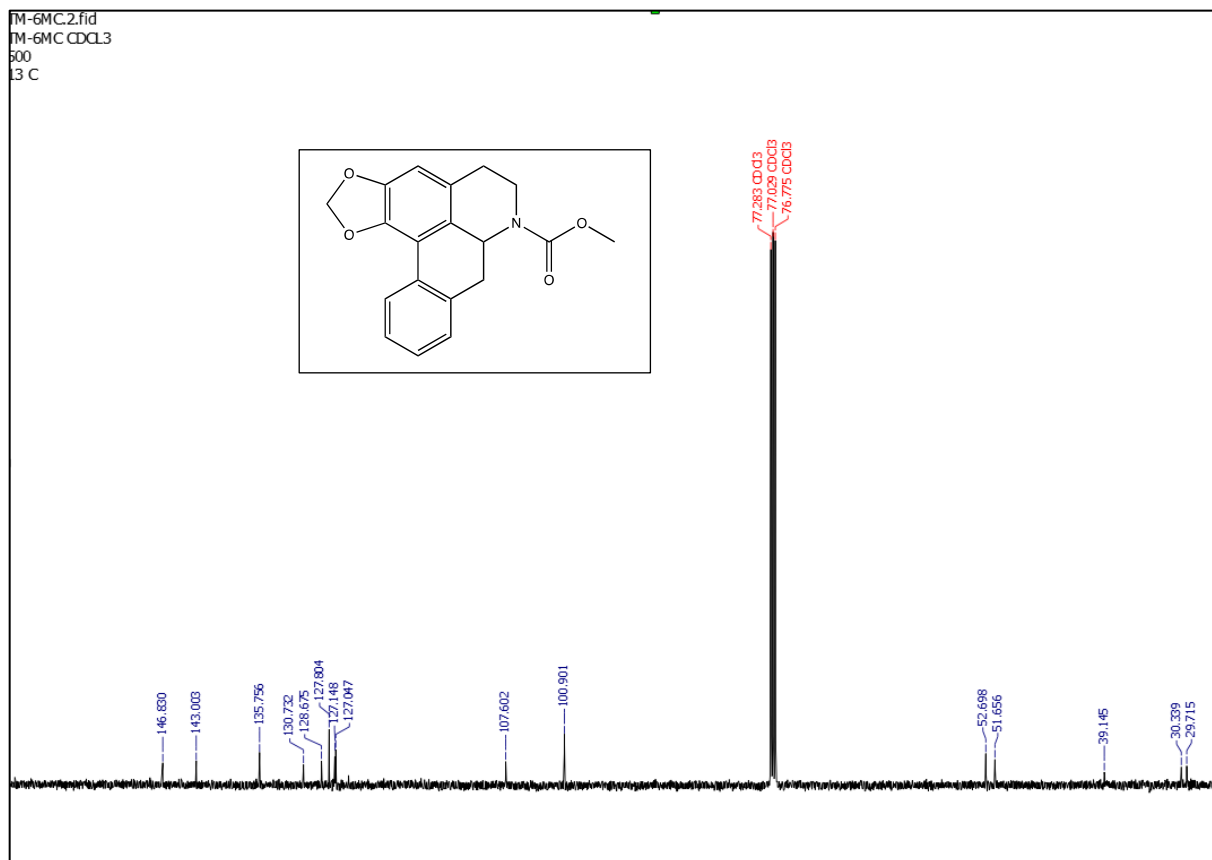
IR (KBr) for compound 7:



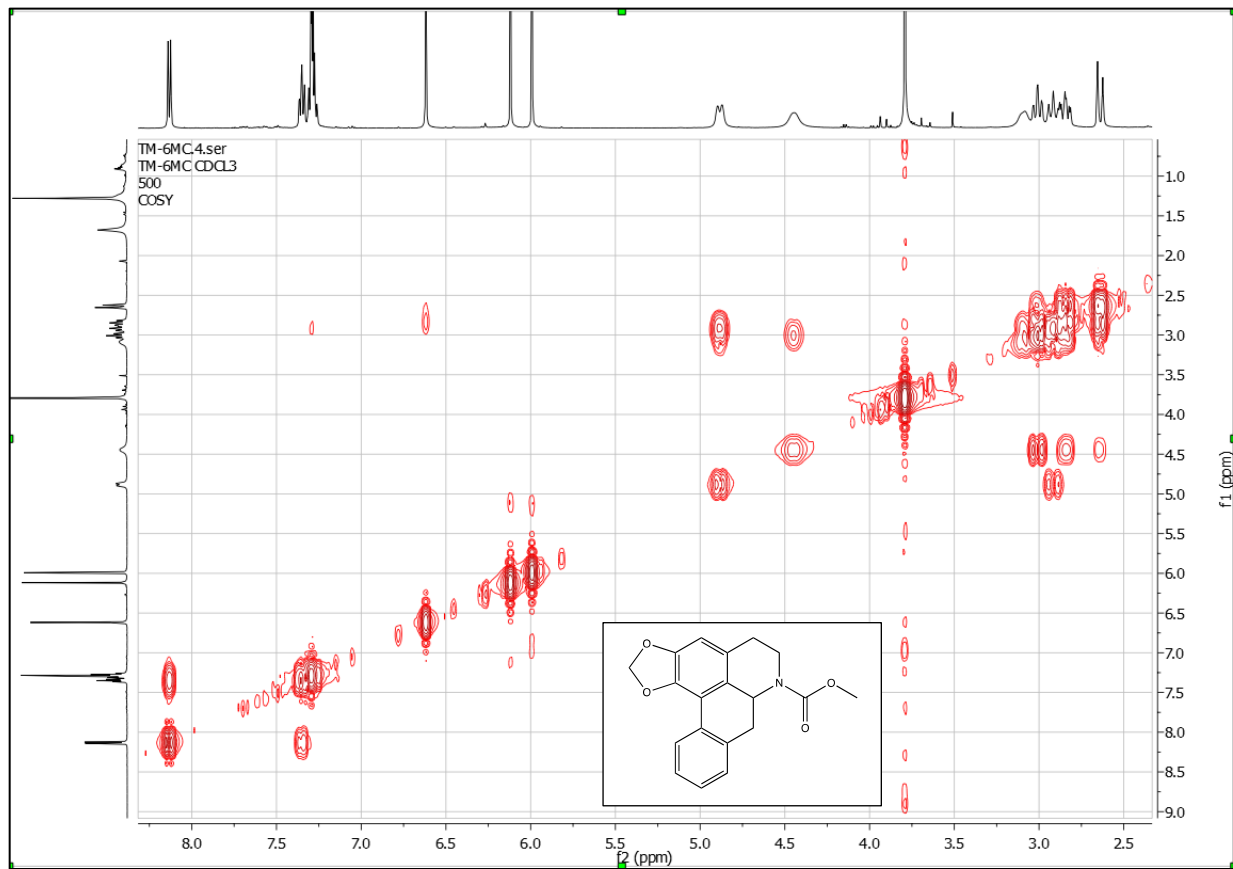
Compound (8) (400 MHz, CDCl₃) ¹H NMR:



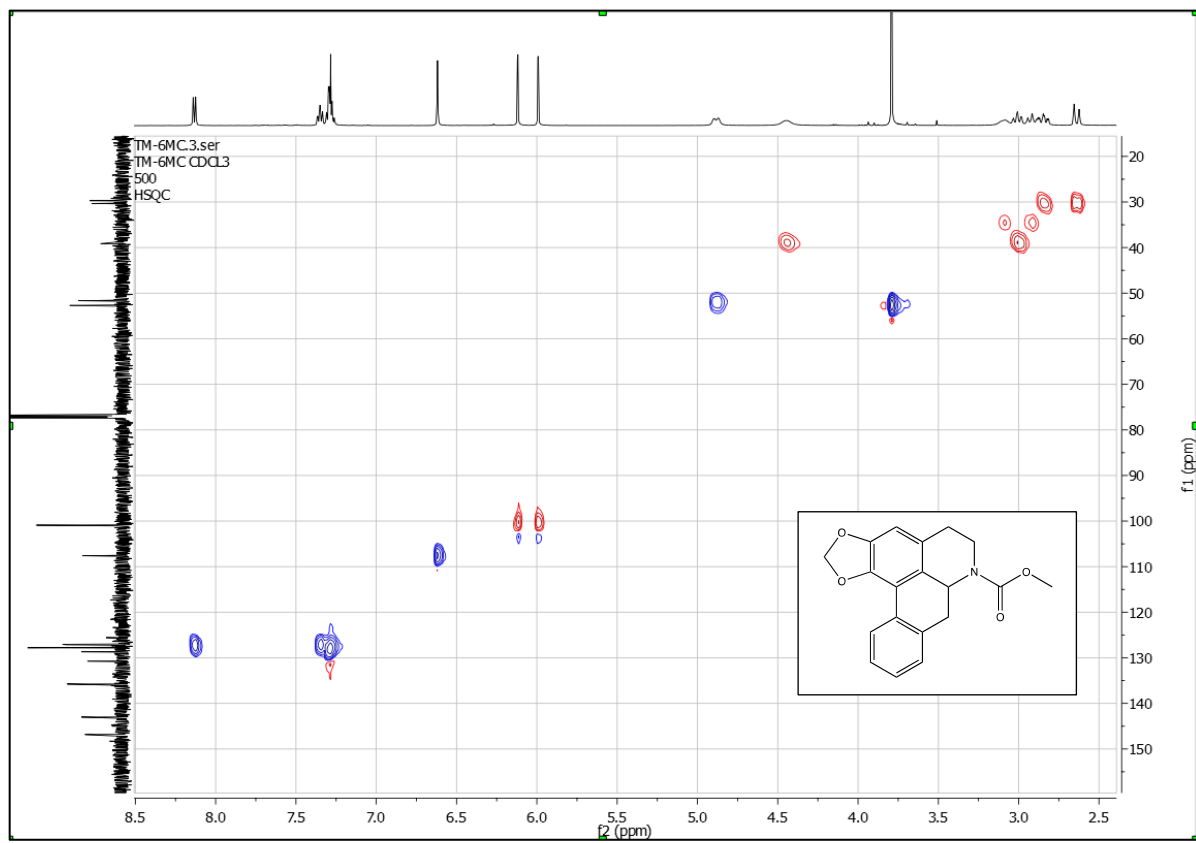
Compound (8) (500 MHz, CDCl₃) ¹³C NMR:



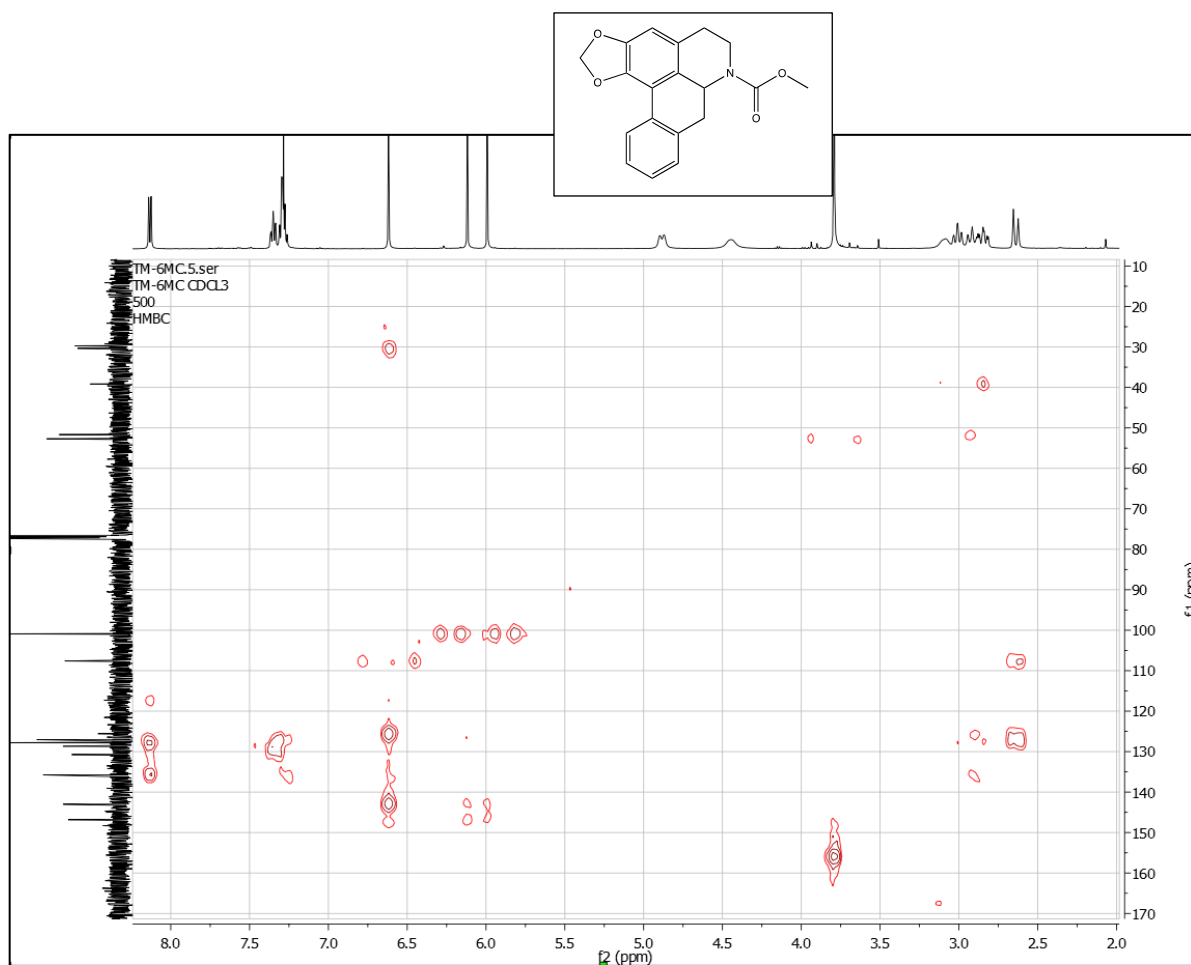
Compound **(8)** (CDCl₃) COSY NMR:



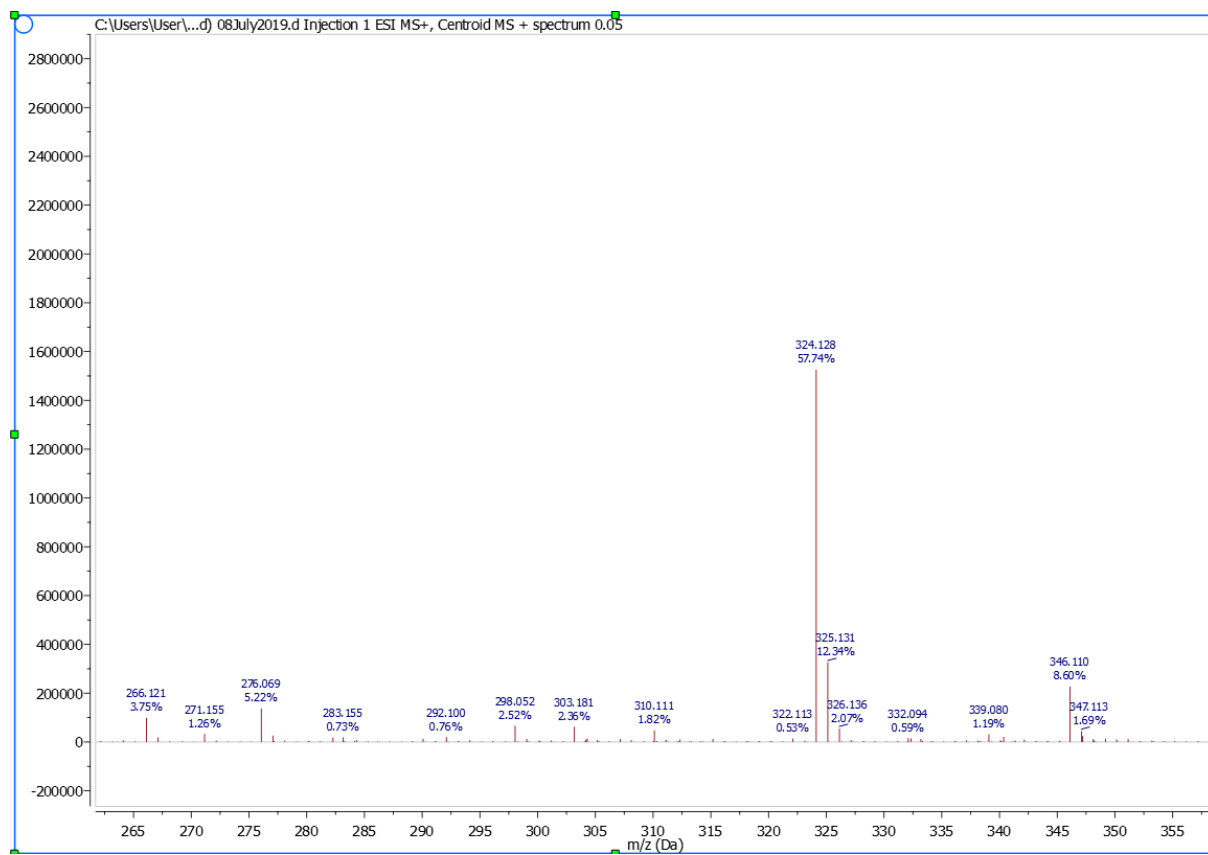
Compound **(8)** (CDCl₃) HSQC NMR:



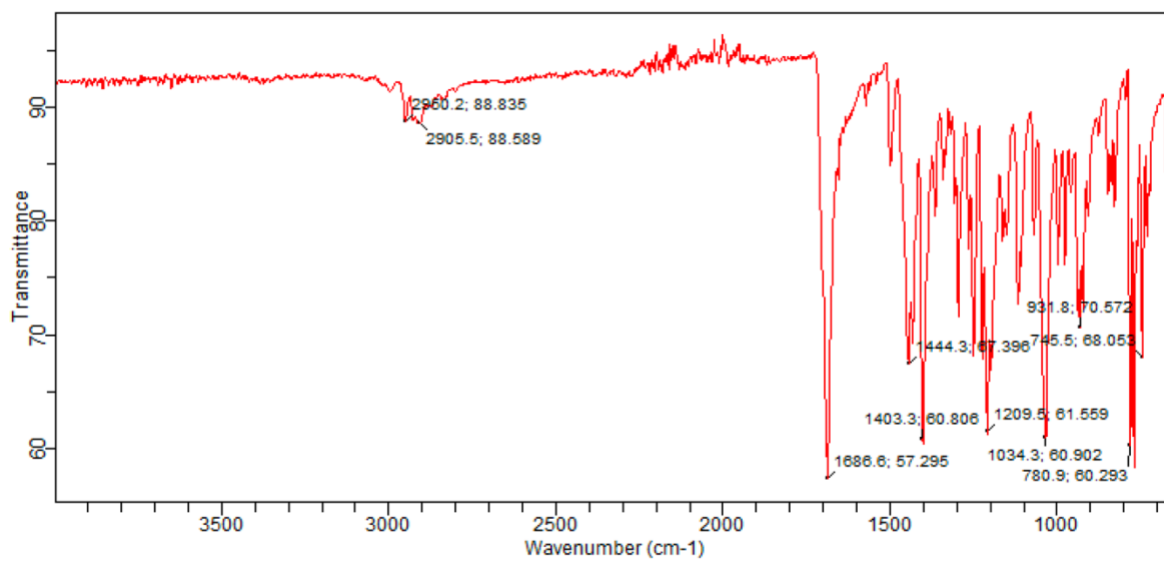
Compound **(8)** (CDCl₃) HMBC NMR:



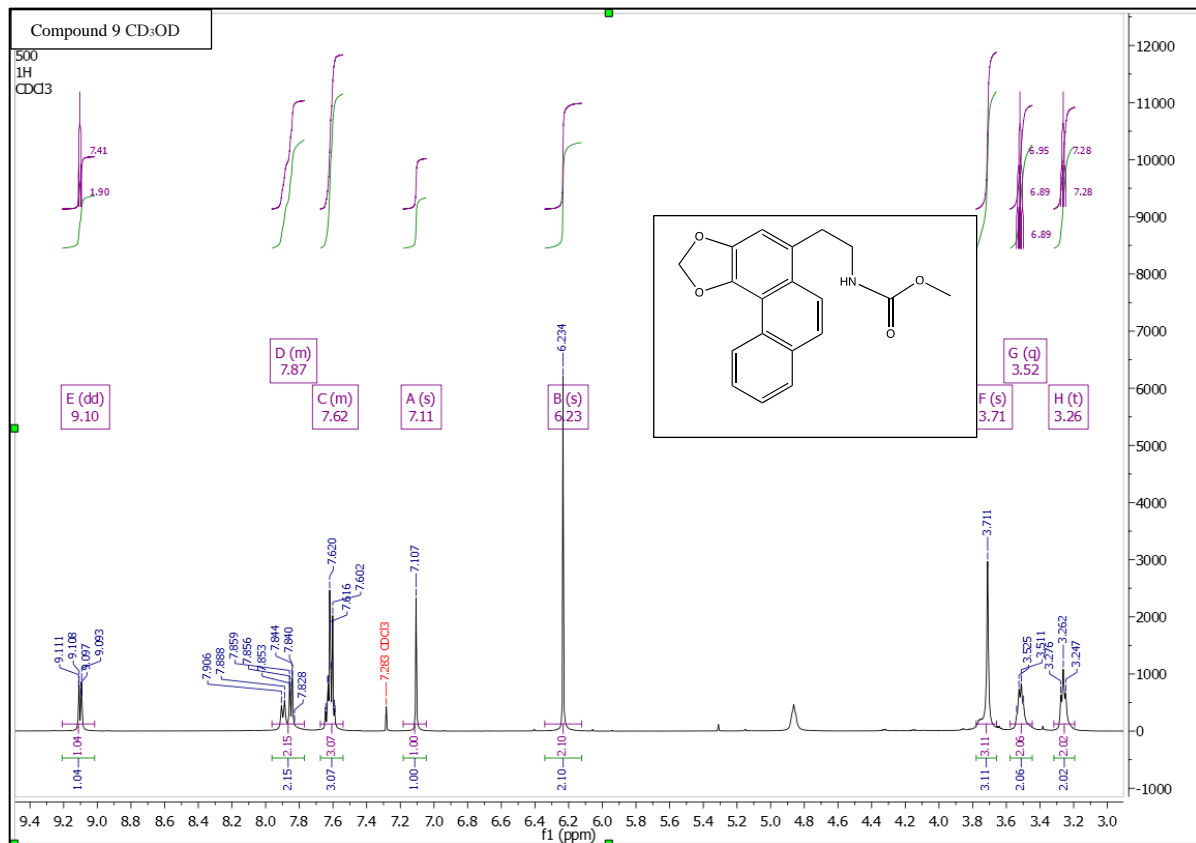
Compound (8) HRESI-MS:



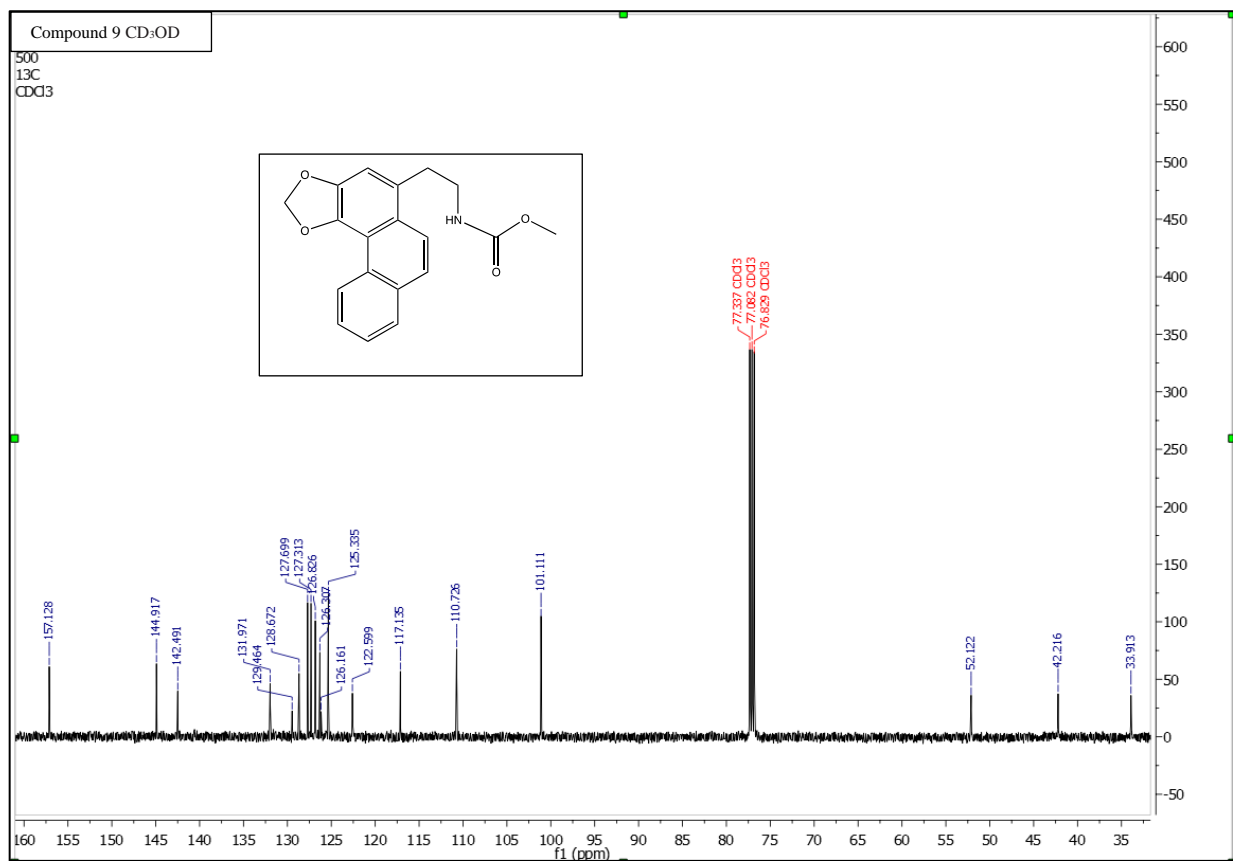
IR (KBr) for compound **8**:



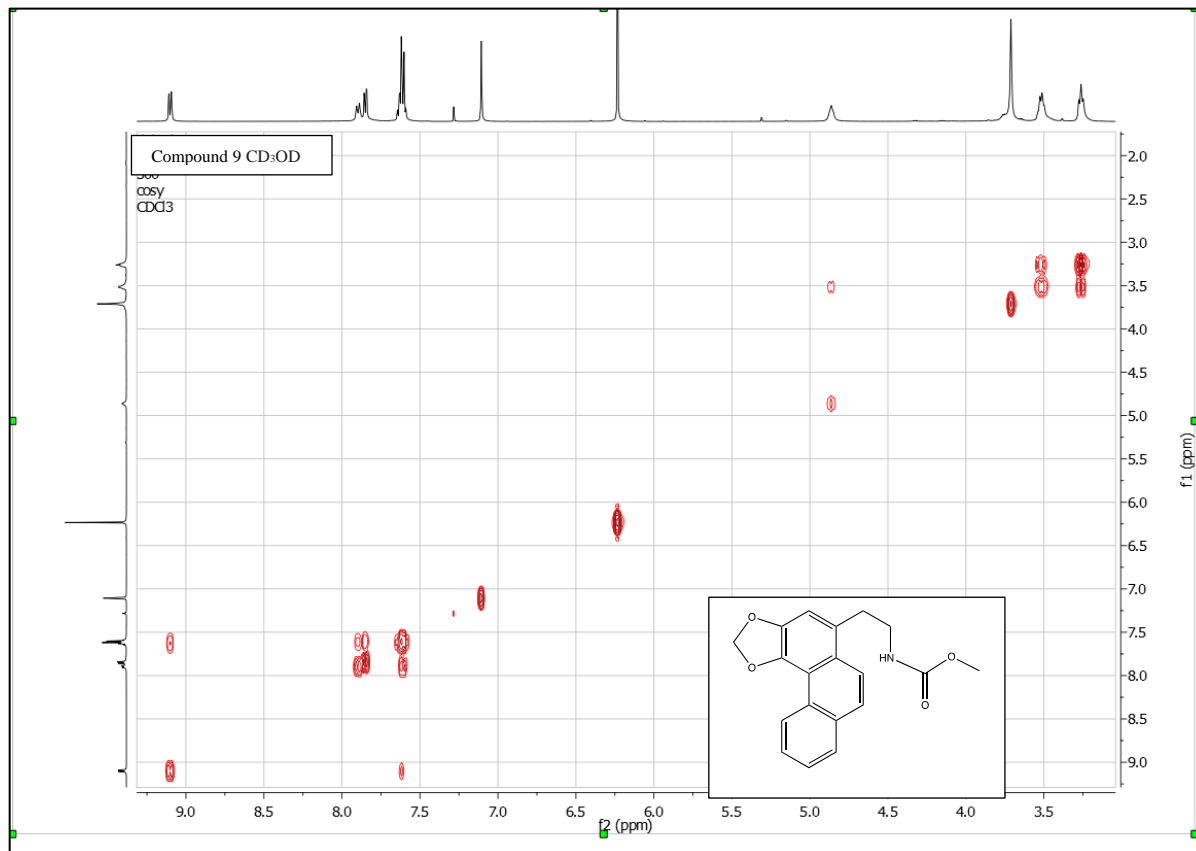
Compound (9) (500 MHz, CDCl₃) ¹H NMR:



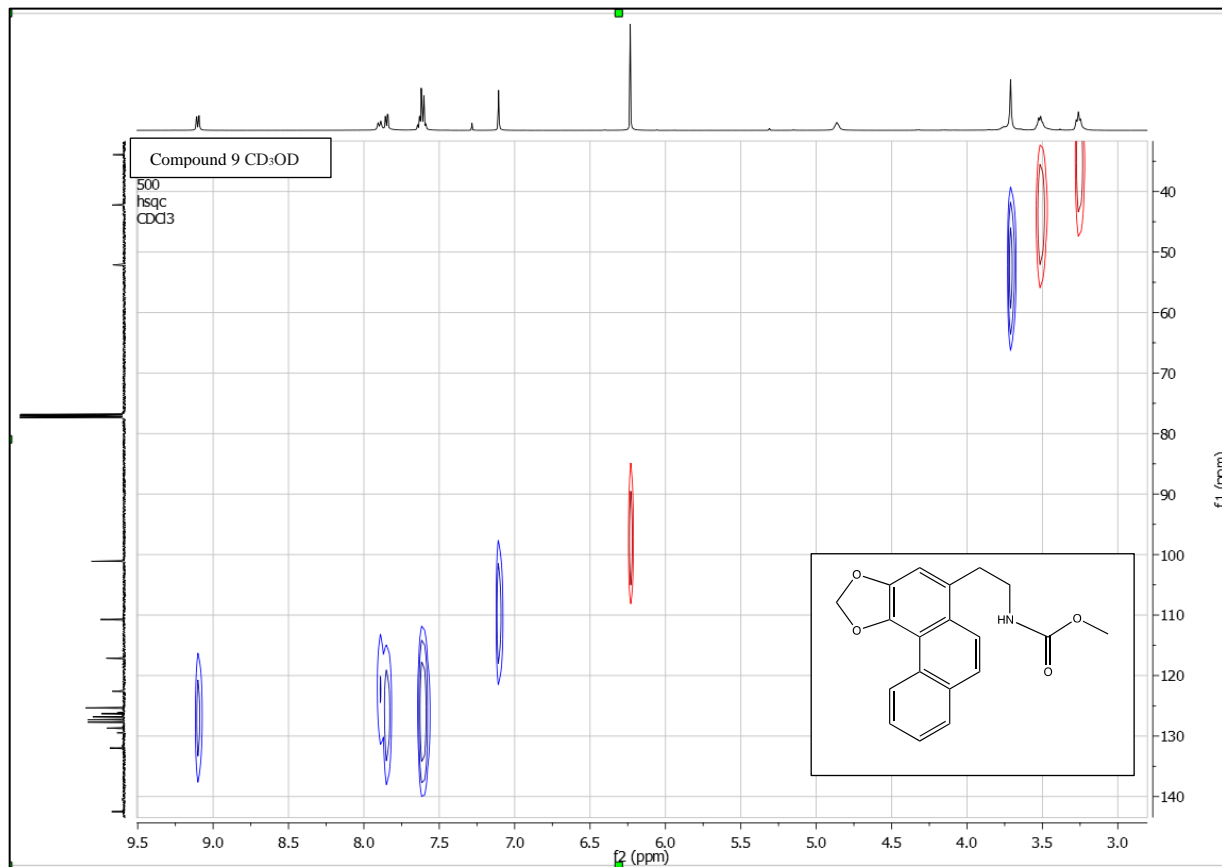
Compound (9) (100 MHz, CDCl₃) ¹³C NMR:



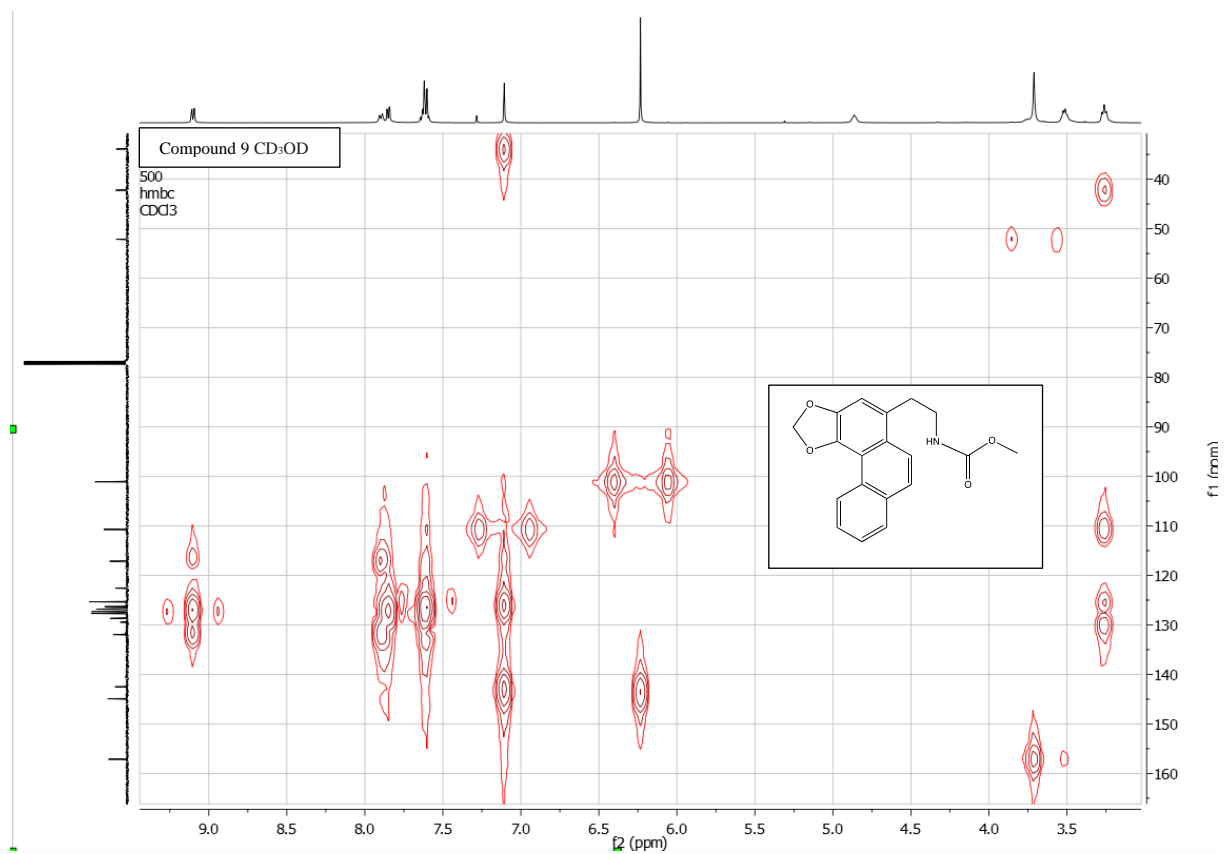
Compound (9) (CDCl₃) COSY NMR:



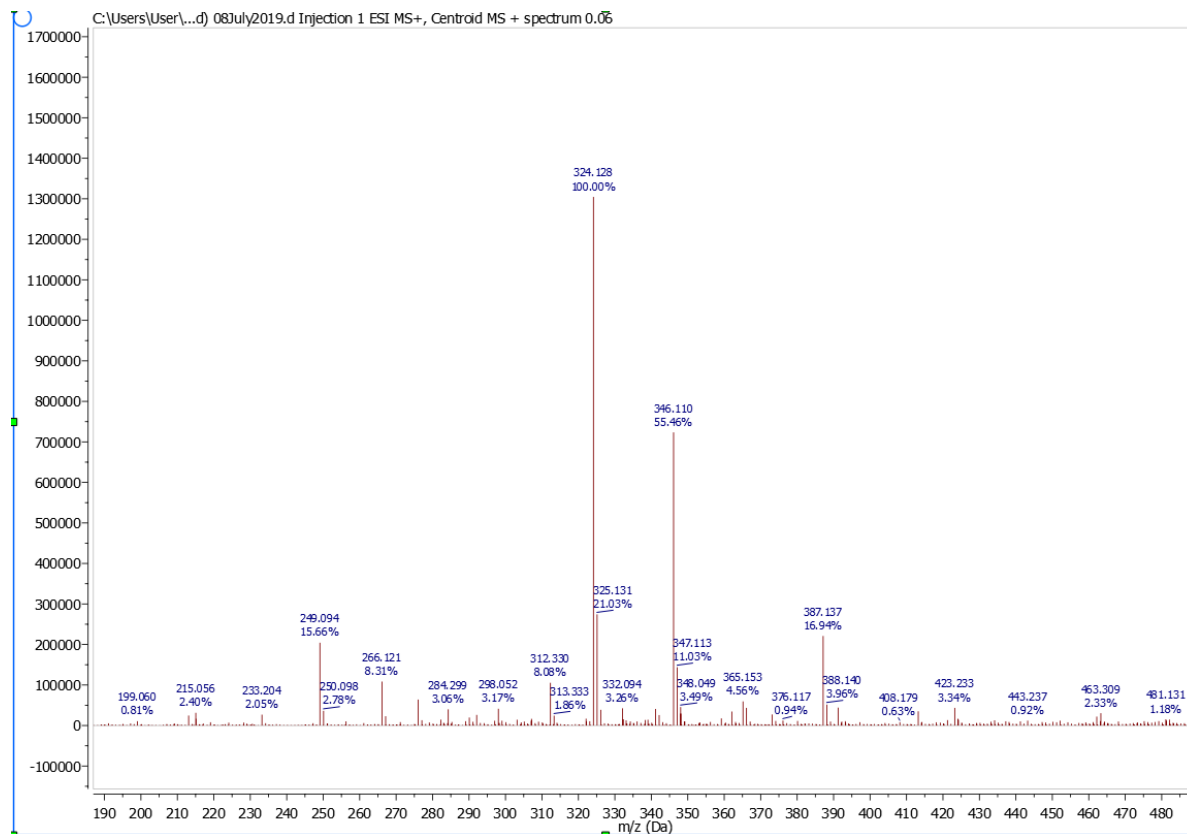
Compound **(9)** (CDCl₃) HSQC NMR:



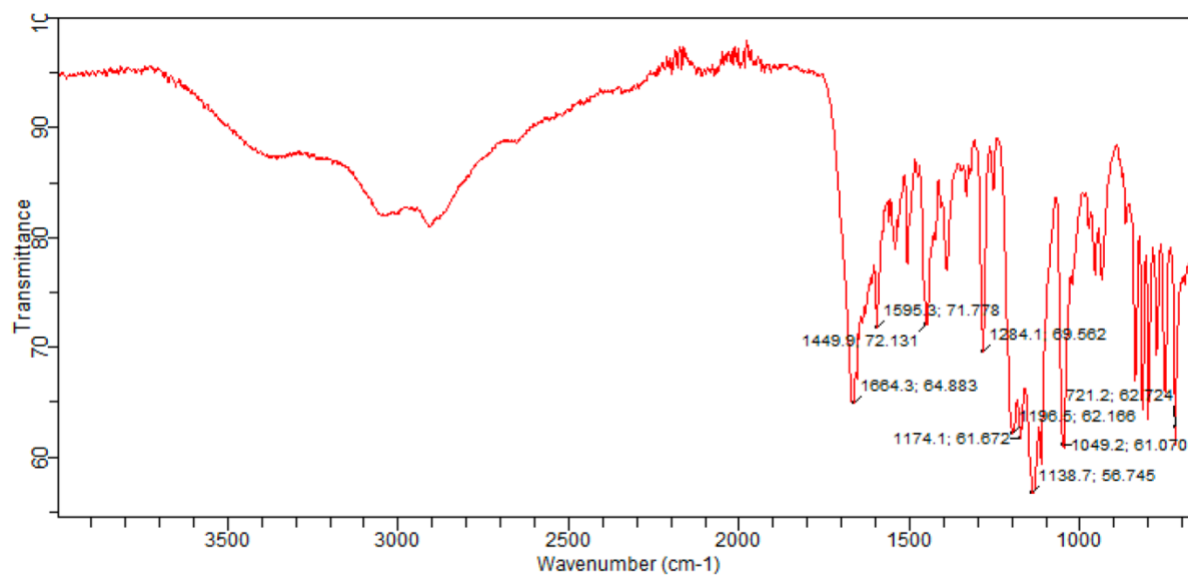
Compound **(9)** (CDCl₃) HMBC NMR:



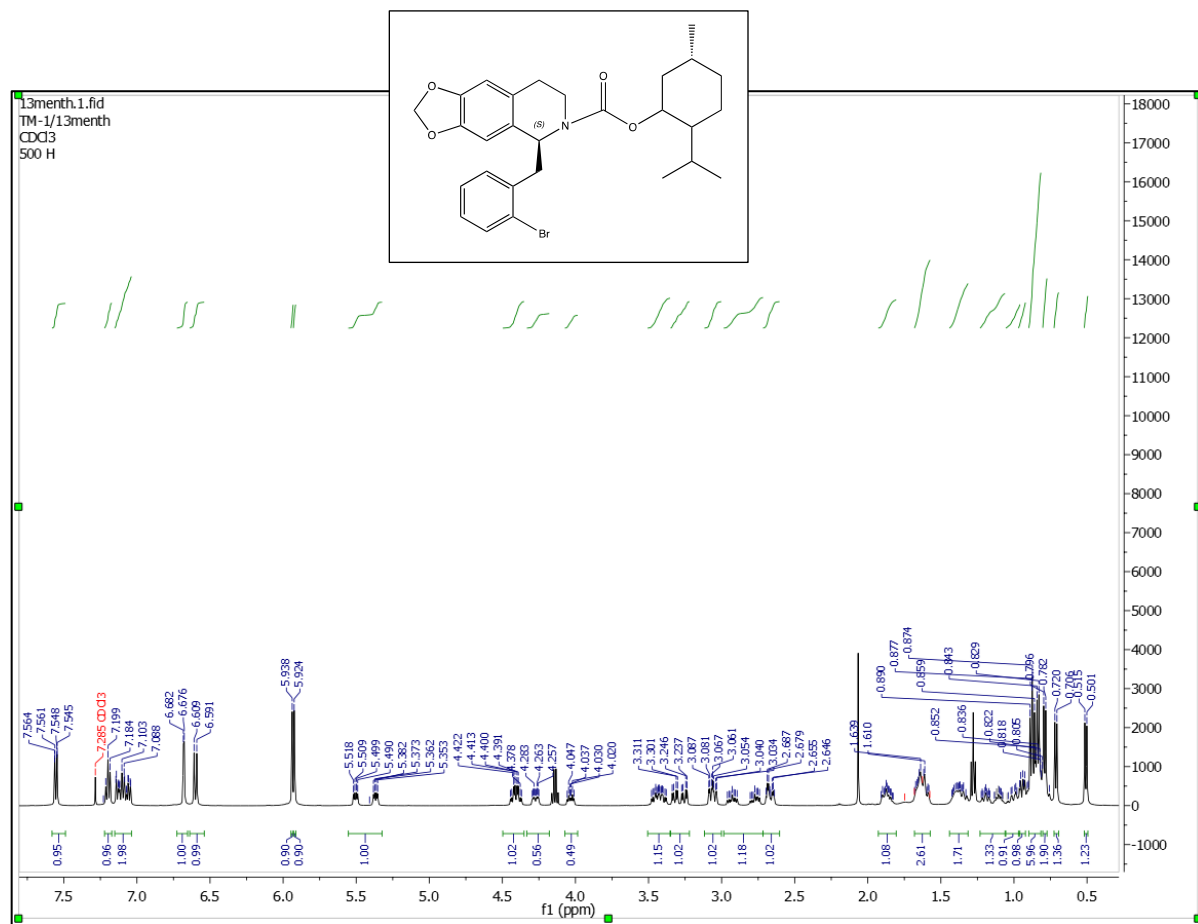
Compound (9) HRESI-MS:



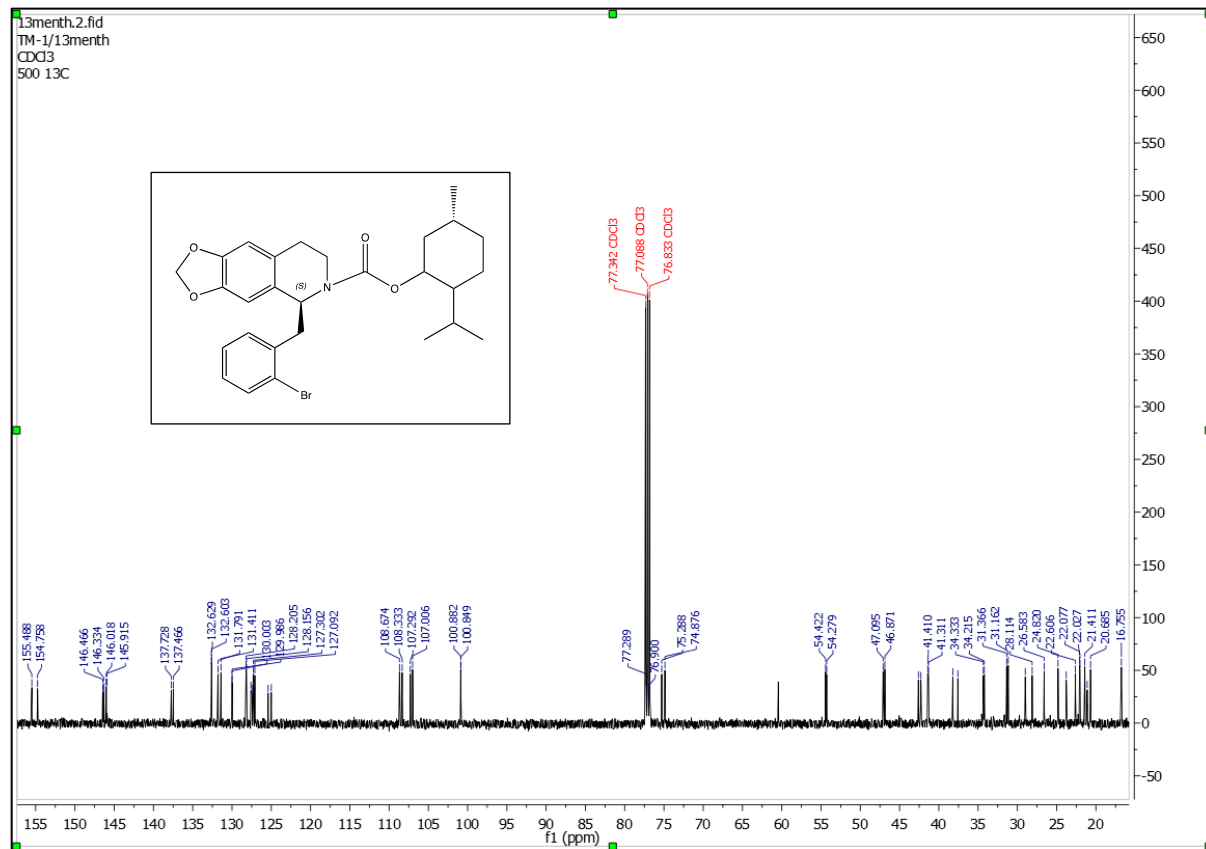
IR (KBr) for compound **9**:



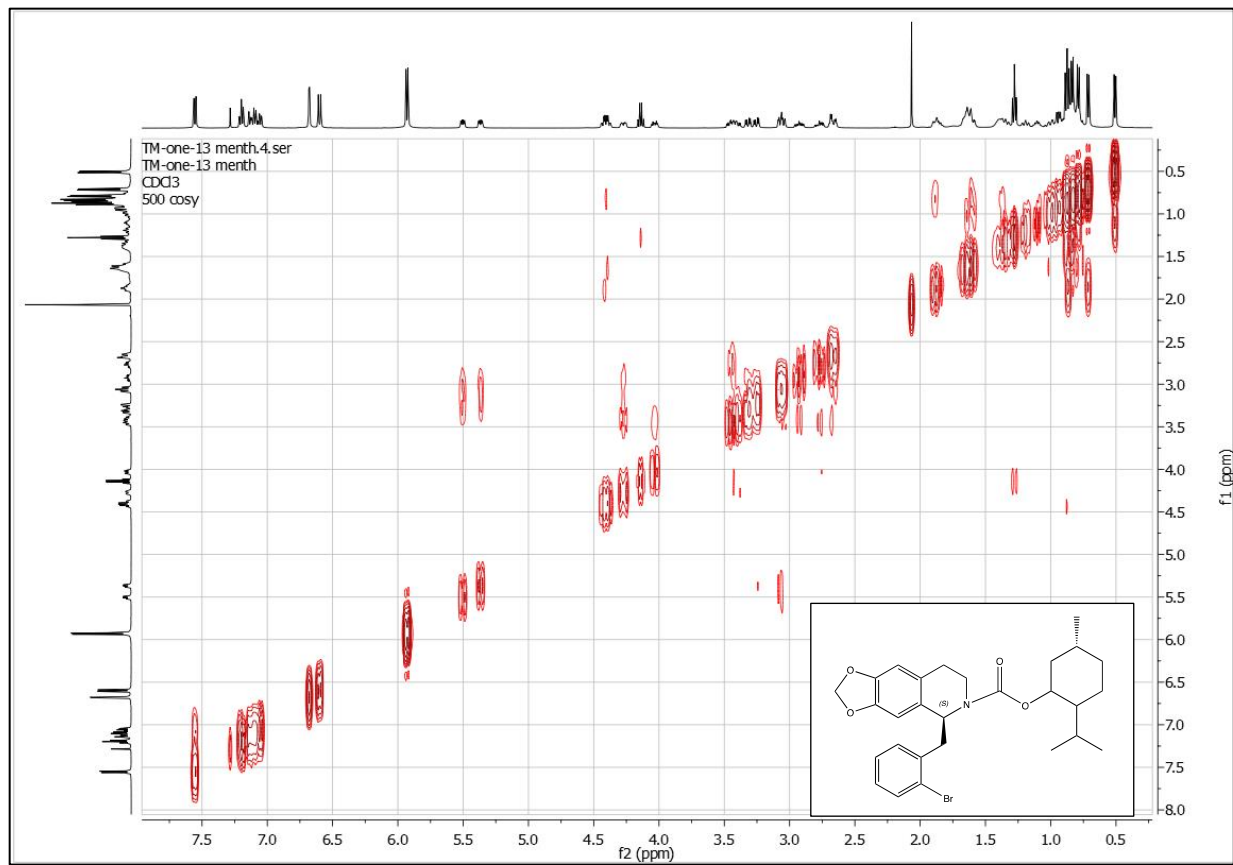
Compound (10) (500 MHz, CDCl₃) ¹H NMR:



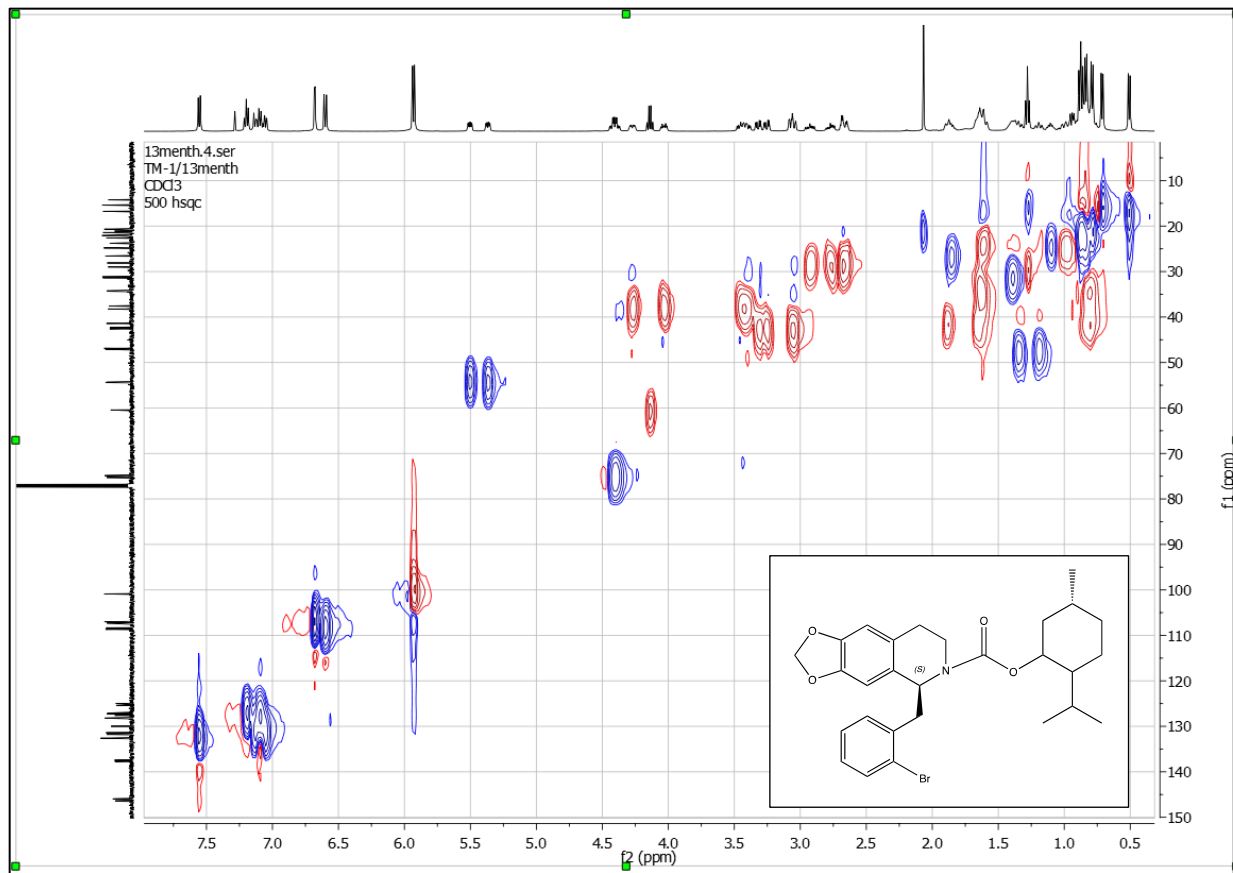
Compound (10) (125 MHz, CDCl₃) ¹³C NMR:



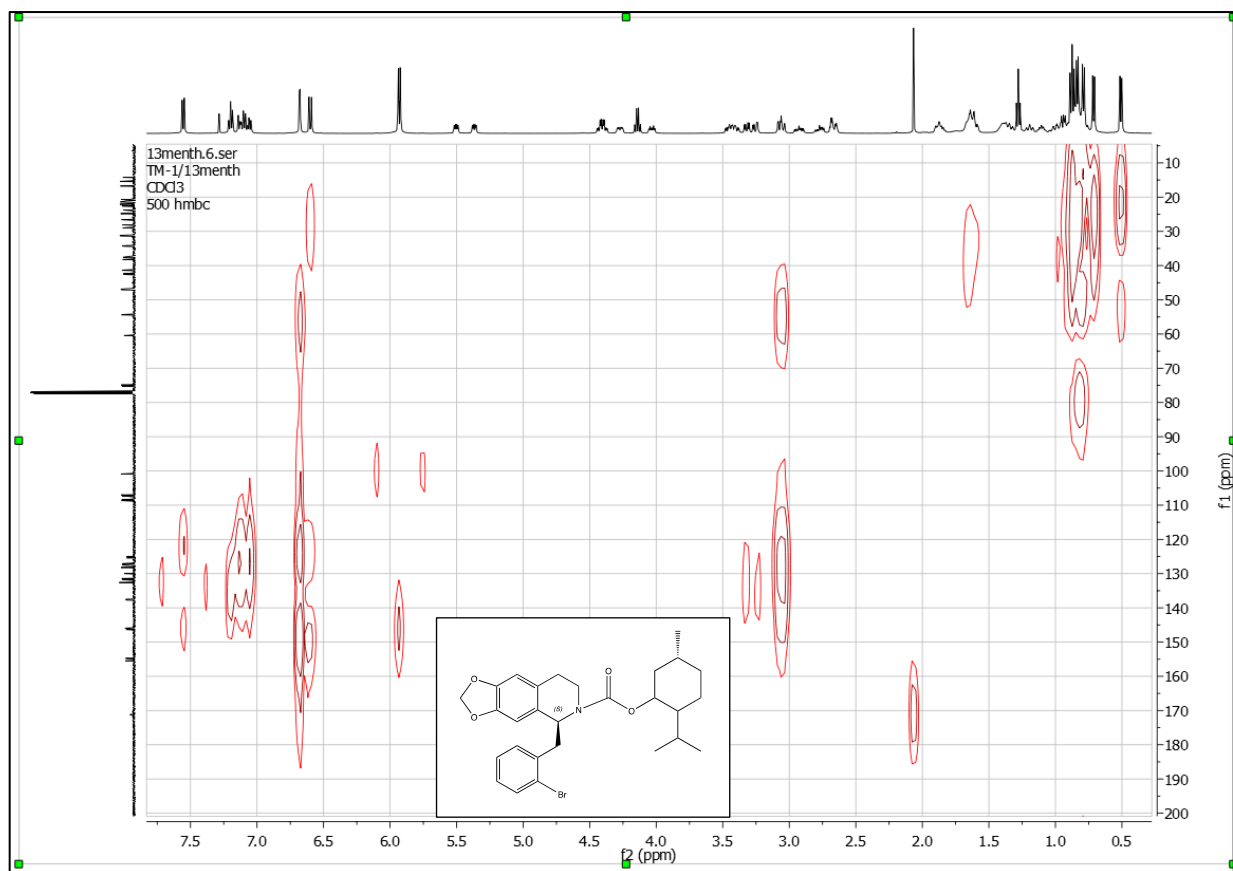
Compound **(10)** (CDCl₃) COSY NMR:



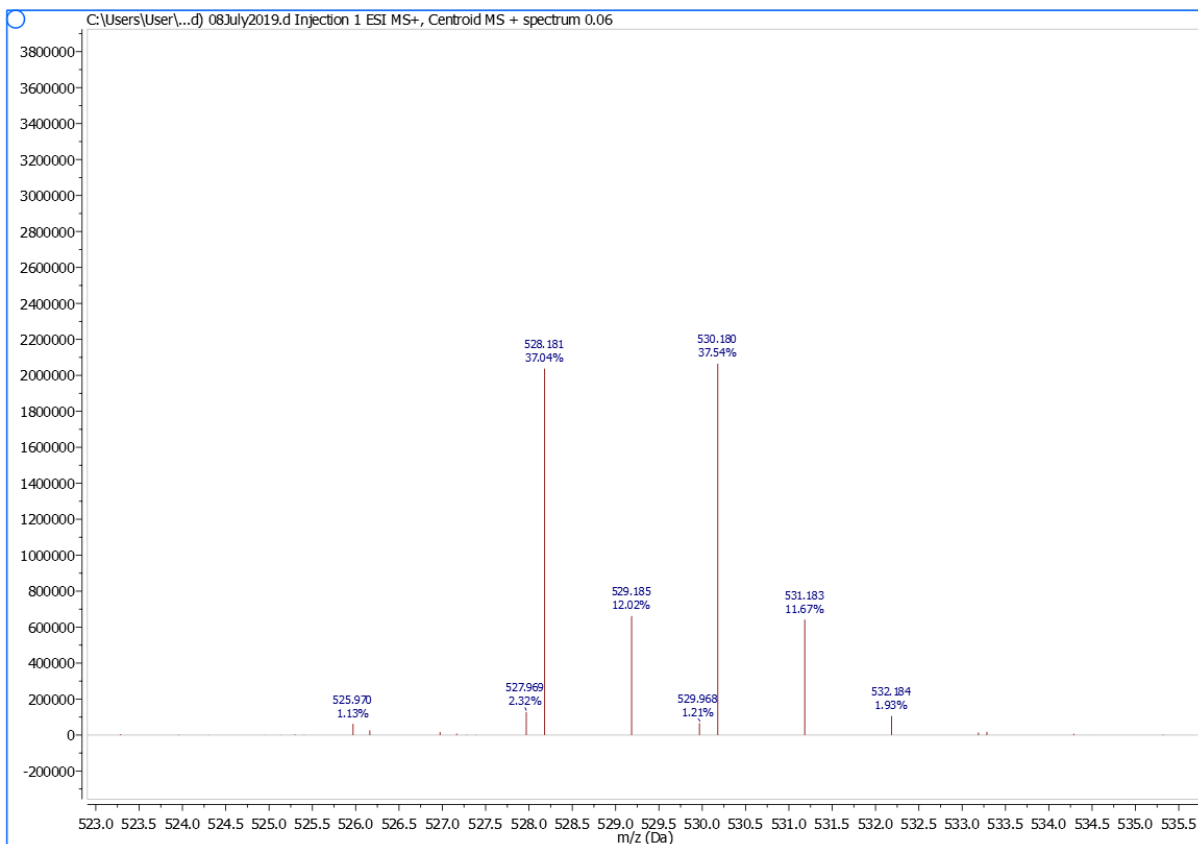
Compound **(10)** (CDCl₃) HSQC NMR:



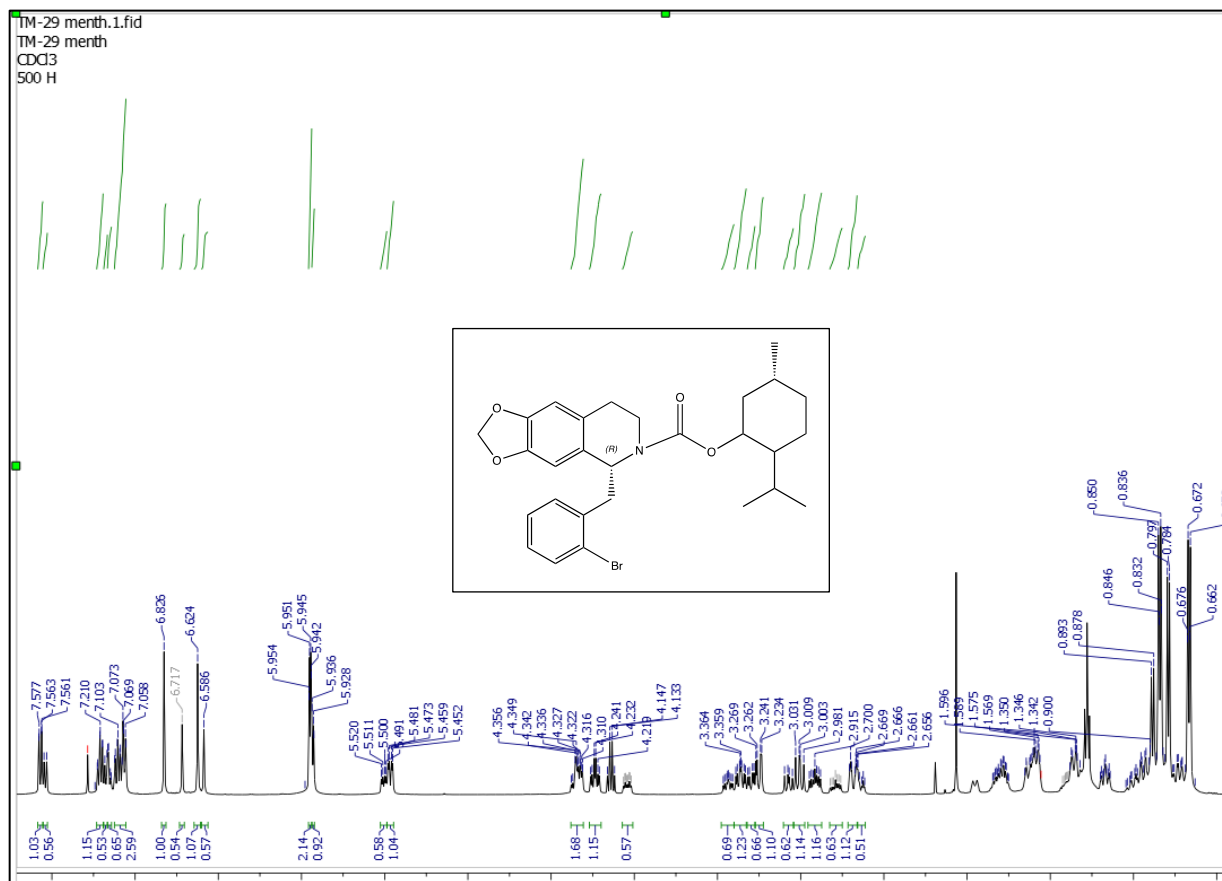
Compound **(10)** (CDCl₃) HMBC NMR:



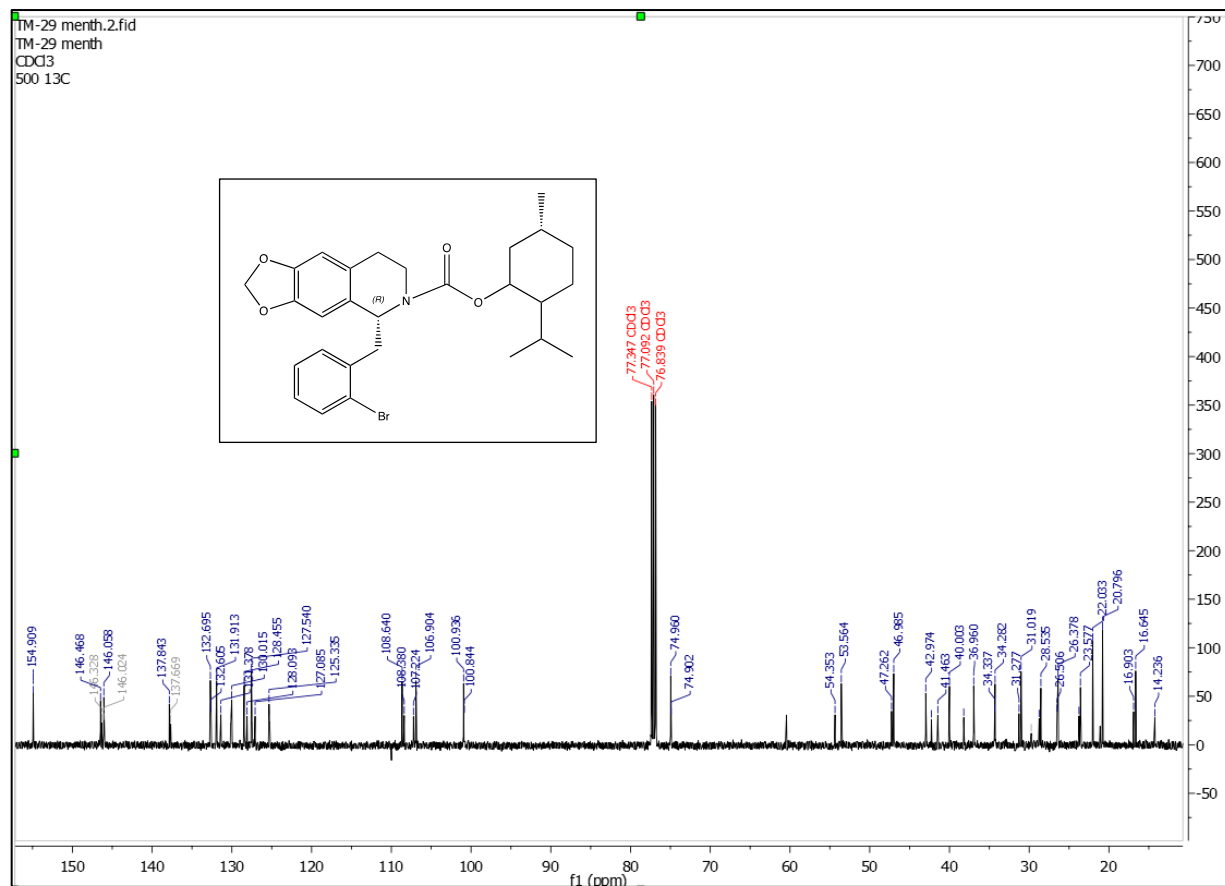
Compound (10) HRESI-MS:



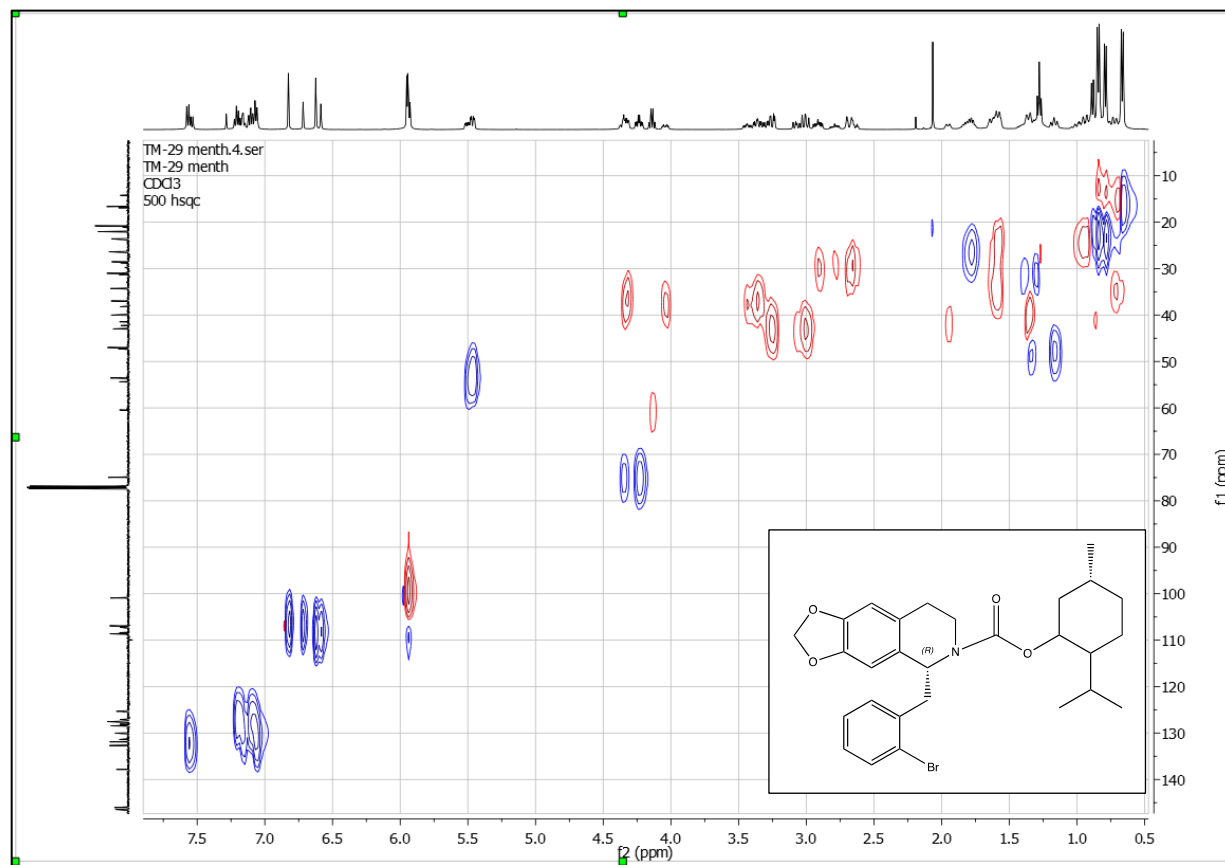
Compound (11) (500 MHz, CDCl₃) ¹H NMR:



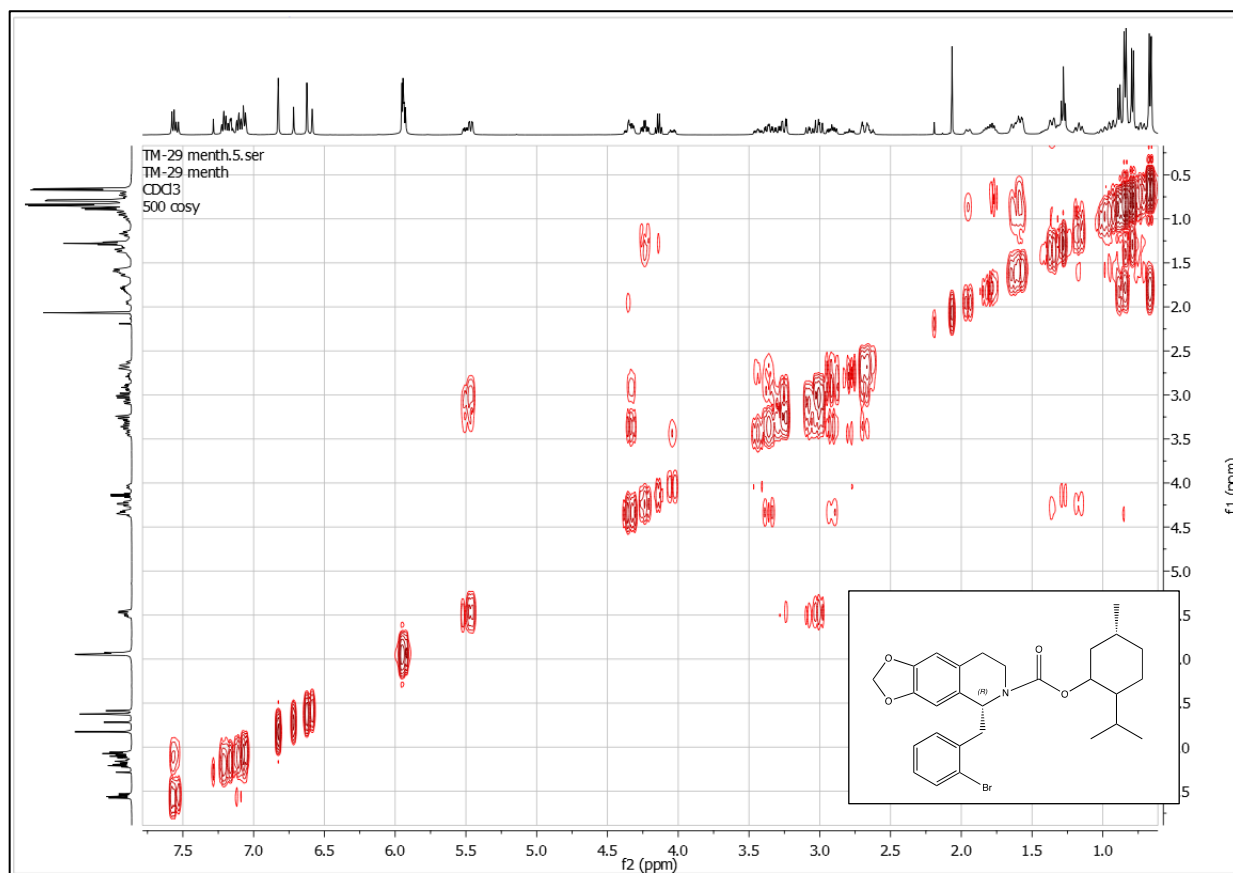
Compound (11) (125 MHz, CDCl₃) ¹³C NMR:



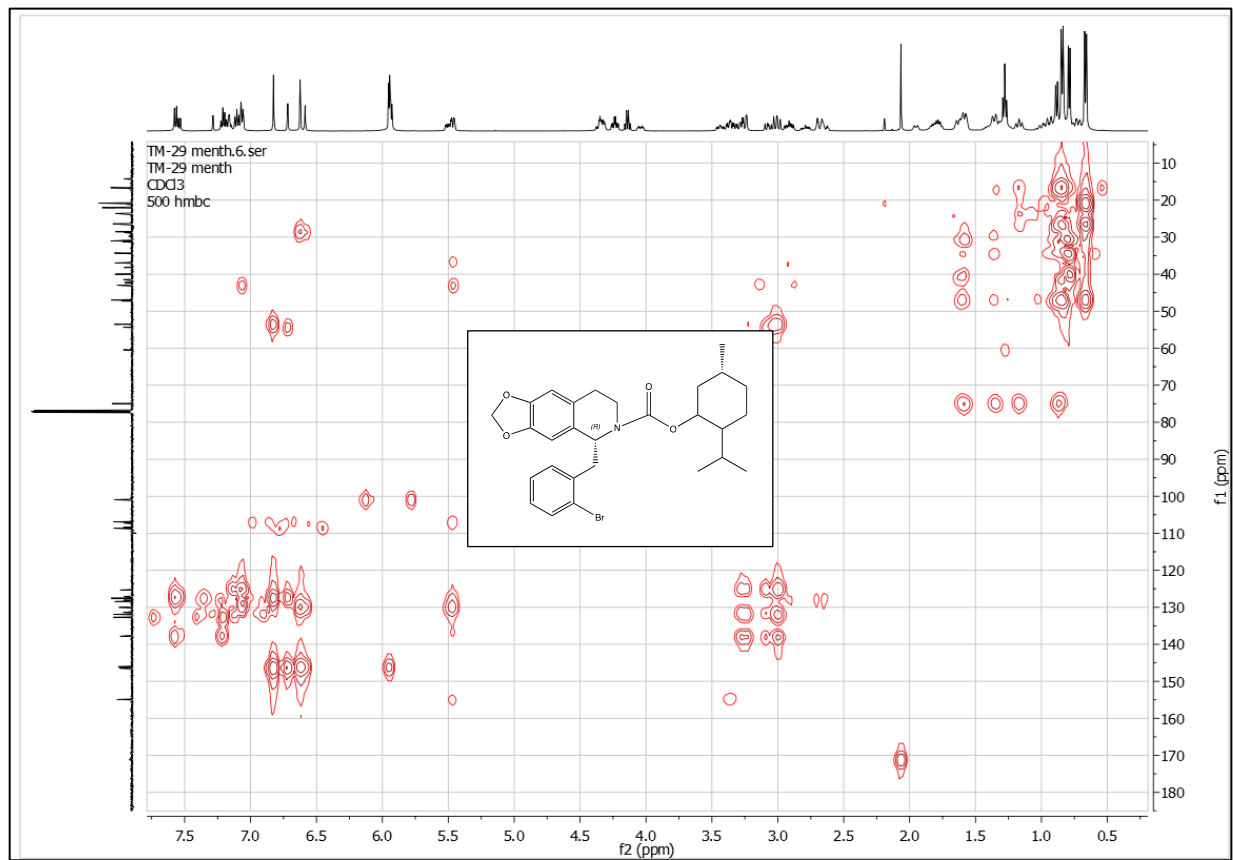
Compound **(11)** (CDCl₃) HSQC NMR:



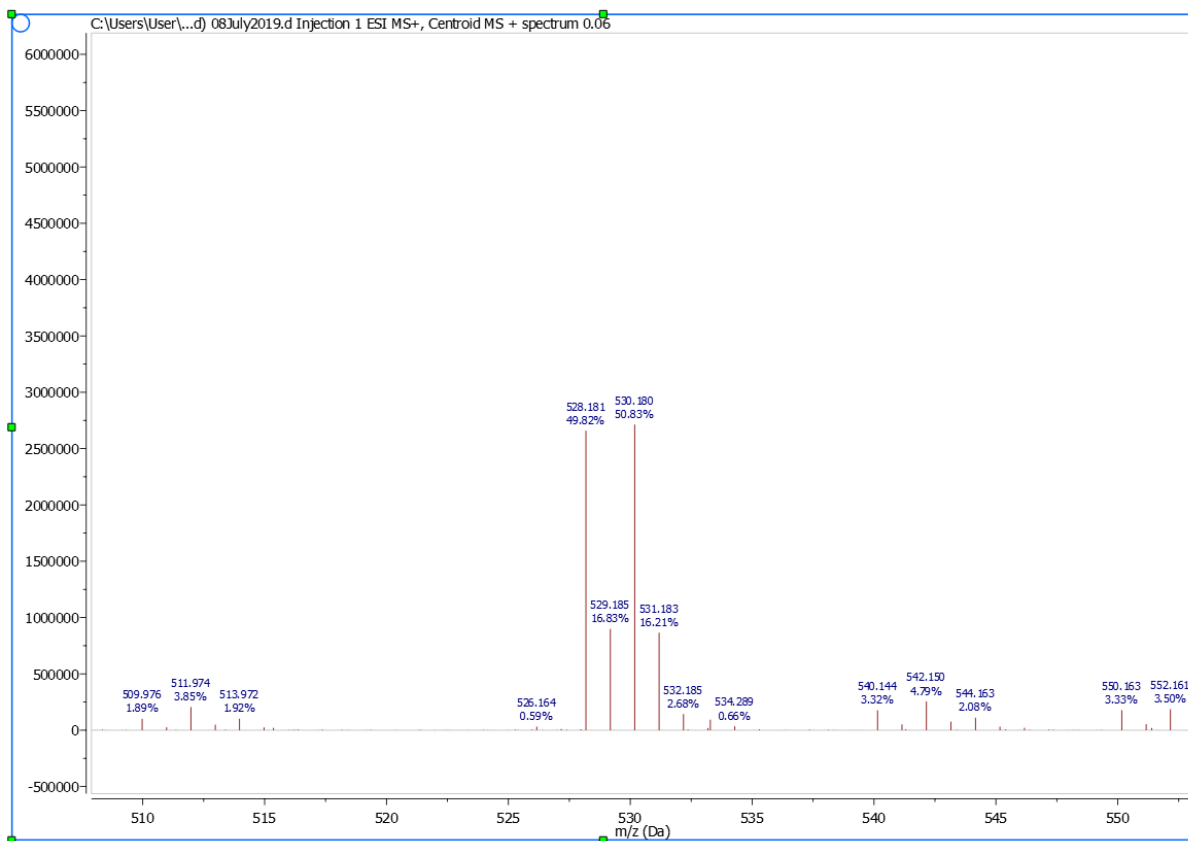
Compound (11) (CDCl₃) COSY NMR:



Compound (11) (CDCl₃) HMBC NMR:



Compound (11) HRESI-MS:



VITA

Taghreed Majrashi was born and raised in Saudi Arabia. In 2007, she joined the School of Pharmacy at King Khalid University, Abha, Saudi Arabia, and received her bachelor's degree with 2nd class honor in 2012. After graduation, she was selected for the faculty of the Department of Pharmaceutics in the School of Pharmacy at King Khalid University, and awarded a full scholarship to pursue her Ph.D. degree in the United States of America as a result of her outstanding work and academic performance. Thereafter, she joined the Department of BioMolecular Sciences, Pharmacognosy division at The University of Mississippi in Fall 2015. During her time as a graduate student, she received the outstanding graduate student award in pharmacognosy for 2019, which is to honor exceptional students for their significant contributions in research and academic field. She has published one paper as a first author, and she is a co-author in two different papers. She has also one more manuscript under preparation for publication. Taghreed is a member of the Golden Key International Honor Society. She received her Doctor of Philosophy in Pharmaceutical Sciences (pharmacognosy emphasis) in May of 2020 under the supervision of Dr. IKhlas Khan.

Publications

- 1) Avula B, Bae J, **Majrashi T**, Wu Y, Wu T, Wang Y, Wang M, Ali Z, Khan, I. A.

Targeted and non-targeted analysis of annonaceous alkaloids and acetogenins from

- Asimina* and *Annona* species using UHPLC-QToF-MS. *Journal of Pharmaceutical and Biomedical Analysis*. 2018;159:548-566.
- 2) **Majrashi AT**, Zulifqar F, Chittiboyina A, Ali Z, Khan I. Isoquinoline Alkaloids from *Asimina triloba*. *Natural Product Research*. 2018;33:2823-2829.
- 3) Fantoukh OI, Albadry MA, Parveen A, Hawwal, MF, **Majrashi T**, Ali Z, Khan SI, Chittiboyina AG, Khan IA. Isolation, synthesis, and drug interaction potential of secondary metabolites derived from the leaves of miracle tree (*Moringa oleifera*) against CYP3A4 and CYP2D6 isozymes. *Phytomedicine*. 2019;60:153010.
- 4) **Majrashi AT**, Ashpole NM, Khan SI, Sanders M, Fantoukh OI, Khan IA. Cytotoxic and neurotoxic potential of alkaloidal constituents of *Asimina triloba*. *NeuroToxicology*. 2020. (forthcoming).